Predicting the Microbial Risk in Flooded London Dwellings Using Microbial, Hygrothermal, and GIS Modelling

Jonathon Taylor

The Bartlett School of Graduate Studies
Department of Civil, Environmental, and Geomatic Engineering
University College London

A thesis submitted for the degree of
Doctor of Philosophy

August 2012

University College London

Gower Street

London, UK

WC1E 6BT

Statement of Originality

'I, Jonathon Greig Taylor confirm that the work presented in this thesis is a result of my own work. Where information has been derived from other sources, I confirm that this has been indicated in the thesis. The work for this thesis has not been and will not be, in part or wholly, submitted for another degree, diploma, or similar qualification. This dissertation does not exceed 100,000 words in length, excluding the bibliography'.

To Anna and Sara

Acknowledgements

This research would not have been possible without the contributions of a number of individuals and organisations. I am incredibly grateful for their untiring help, guidance, and support.

First, I am greatly indebted to my co-supervisors Professor Michael Davies and Dr Ka man Lai. They have given me endless and enthusiastic support, limitless patience, the freedom to make this research my own, and the guidance to help me back on course when I was off-track. Throughout my PhD, I have always enjoyed my meetings and conversations with them and looked forward to their feedback on my work, which I believe is testament to their skill as supervisors. Without their help and friendship, this work would not have been possible.

I am also thankful to the Engineering and Physical Sciences Research Council (EPSRC) for their funding of the research programme (Grant Reference EP/G029881/1), and the assistance of the EPSRC funded "Intrawise" project (PE/F007132/1) in producing this work.

A number of individuals and organisations have provided advice, insight, data, or technical assistance during the research project. For the microbiological work, I am indebted to Drs Melissa Canales, Louise Pankhurst, and Hector Altamirano-Medina and Mr Ian Sturtevant for their advice and technical assistance. David Clifton from the Polygon Group has provided a great deal of insight into the professional restoration methods used when drying out flooded properties. Advice on housing stock modelling has been provided by Anna Mavrogianni and Eleni Oikonomou, whose research on the London housing stock provided a critical foundation for this work. Advice on the geospatial component of the research has been kindly provided by Dr Muki Haklay, Dietmar Backes, and Ed Manley, while flood maps were courtesy of the Environment Agency (EA). Assistance with modelling came from Drs Ian Ridley and Zaid Chalabi. I am extremely grateful to Dr Phillip Biddulph for his help and guidance on building simulation, his adaptation of the UCL-HAMT model to suit my specific needs, and without whom this work could not have been completed.

I would be remiss if I did not acknowledge the huge contribution of my family in producing this research. I am grateful to my Mum, Dad, brother, and sister, who admit they don't have a clue what it is that I actually do, but have been supportive anyway. Finally, and most importantly, I am indebted to my wife Anna and new daughter Sara. Anna has made this work possible with her patient support, love, and constant encouragement. But, to say she has been my rock understates her importance: her intelligence and insight have helped me to solve problems and find new ways of looking at my research. Without her, I would be lost. And to my beautiful baby daughter Sara, your impending arrival provided me with a clear deadline for completing the first draft of this thesis, and your presence has made me smile like an idiot through the subsequent revisions. You've been a sounding board during early morning and night conversations, a welcome distraction from my work, and a reminder to me of what is truly important in life.

Abstract

With a changing climate, London is expected to experience more frequent periods of intense rainfall and tidal surges, which will lead to an increase in the risk of flooding. Floodwater may deposit harmful microorganisms on building surfaces, while damp indoor environments in flooded dwellings can support the growth of microorganisms including mould, bacteria, and protozoa. This thesis investigates possible flood-borne and damp-related pathogens in flooded London dwellings, and the potential duration of microbial contamination risk following a flood event. Microbiological laboratory work and models are used to characterise microbial risk within flooded dwellings. Dwelling archetypes representative of the London housing stock are developed and hygrothermal simulation techniques used to model the flooding and drying behaviour of the archetypes under different scenarios in order to predict the duration of damp and microbial risk inside typical dwellings. The results of the combined biological and hygrothermal models are mapped alongside existing flood risk maps in order to predict areas in London susceptible to long-term microbial risk or prolonged displacement following a flood. Highlights of the research findings include the following (i) The persistence of bacterial contaminants on flooded materials is related to the type of floodwater, the drying conditions including temperature and drying rate, and the material drying characteristics, ii) Different dwellings in London have different drying behaviours due to their built form and dominant wall types, with modern purpose-built flats the most prone to long-term damp and microbial risk following a flood event, (iii) The flood height, external weather, and internal conditions including heating and ventilation can have a major impact on the length of time a dwelling will remain at risk of microbial contamination, and (iv) The concentration of properties vulnerable to long-term microbial exposure following major flood events is highest in areas of South and East London, particularly Southwark.

Contents

List of Figures

List of Tables

Abbreviations and Acronyms

AAC	Autoclaved Aerated Concrete
ABPA	Allergic bronchopulmonary aspergillosis
ach	Air Changes Per Hour
AFS	Allergic Fungal Sinusitis
ANOVA	Analysis of Variance
ASHRAE	American Society of Heating, Refrigerating and Air Conditioning Engineers
ATP	Adenosine Triphosphate
BDMA	British Damage Management Association
BESTEST	Building Energy Simulation Test
BHPS	British Household Panel Survey
BRE	Building Research Establishment
BREDEM	Building Research Establishment's Domestic Energy Model
BS	British Standard
CDC	Centers for Disease Control
CFD	Computation Fluid Dynamics
CFU	Colony Forming Units
CHEF	Cultural Heritage Protection Against Flood
CIBSE	Chartered Institution of Building Services Engineers
CIRIA	Construction Industry Research and Information Association
CLEA	Contaminated Land Exposure Assessment

COA	Census Output Area
CR	Cities Revealed
CSO	Combined Sewer Overflows
DALY	Disability-Adjusted Life Years
DCLG	Department of Communities and Local Government
DEFRA	Department for Environment, Food, and Rural Affairs
DEM	Digital Elevation Models
DSA	Differential Sensitivity Analysis
DTM	Digital Terrain Model
EA	Environment Agency
EHCS	English House Condition Survey
EHS	English Housing Survey
EMPD	Effective Moisture Penetration Depth
EPA	Environmental Protection Agency
ERH	Equilibrium Relative Humidity
EST	Energy Saving Trust
FDM	Finite Difference Methods
FEM	Finite Element Methods
FEMA	Federal Emergency Management Agency
FHRC	Flood Hazard Research Centre
GIS	Geographic Information System
HAM	Heat, Air, and Moisture
HAMSTAD	Heat, Air and Moisture Standards Development
HDAT	High Drying Ambient Temperature
HDLT	High Drying Low Temperature

HEED	Homes Energy Efficiency Database
HP	Hypersensitivity Pneumonitis
HPA	Health Protection Agency
HVAC	Heating Ventilation and Air Conditioning
IbM	Individual-based models
IDW	Inverse Distance Weighting
IEA	International Energy Agency
IPCC	Intergovernmental Panel on Climate Change
ISO	International Standards Organisation
LDAT	Low Drying Ambient Temperature
LDLT	Low Drying Low Temperature
LiDAR	Light Detection and Ranging
LIM	Lowest Isopleths for Mould
LPS	Lipopolysaccharide
MAUP	Modifiable Areal Unit Problem
MVOC	Microbial Volatile Organic Compounds
NHS	National Health Service
ORNL	Oak Ridge National Laboratory
OS	Ordnance Survey
PBS	Phosphate Buffered Saline
RFM	Response Factor Methods
RH	Relative Humidity
RMSE	Root Mean Square Error
SAP	Standard Assessment Protocol
SEH	Survey of English Housing

SEM	Standard Error of the Mean
SFVI	Social Flood Vulnerability Index
TOID	Topographic Identifiers
TOW	Time-of-Wetness
TRY	Test Reference Year
TSA	Tryptic Soy Agar
UCL-HAMT	University College London Heat And Moisture Transport
UKCP09	UK Climate Projections 2009
USAACE	United States of America Army Corps of Engineers
UV	Ultraviolet
VOA	Valuation Office Agency
VOC	Volatile Organic Compounds
WHO	World Health Organisation
WME	Wood Moisture Equivalent
WRc	Water Research Centre
WUFI	Wärme Und Feuchte Instationär

Symbols and Definitions

Microbiological Modelling Parameters

Symbol	Description	Units
N_t	Bacterial Population at Time T	#, CFU
N_0	Bacterial Population at Time 0	#, CFU
a_w	Water Activity	-
k	Rate of bacterial population change	hr^{-1}
k_{max}	Maximum specific rate	hr^{-1}

Environmental Parameters

Symbol	Description	Units
E	Energy	J
h	Specific enthalpy	J/kg
h_v	Evaporation enthalpy of water (= 2, 489, 000J/kg)	J/kg
m	Mass flux	kg/s
t	Time	s
T	Temperature	ºC
RH,φ	Relative humidity	%, fraction
w	Moisture Content	kg/m^3
P	Absolute Pressure	Pa
$p_{WaterVapour}$	Water Vapour Pressure	Pa
p_s	Saturation vapour pressure	Pa
v	Water vapour concentration	kg/m^3
ρ_w	Density of water (= $1000kg/m^3$)	kg/m^3
σ	Surface tension of water	N/m
R_{H_2O}	Specific gas constant for water (461.5 J/kgK)	J/kgC
L_v	Latent heat of vapourisation of water at 0ºC	J/mol
$P_{ambient}$	Ambient air pressure	Pa
δ	Water Vapour diffusion coefficient in air	kg/msPa
C_s	Air flow coefficient	
c_{DryAir}	Specific heat capacity of dry air (=1.006J/kgºC@ 20ºC)	J/KgC
$c_{WaterVapour}$	Specific heat capacity of water (=4,180J/kgºC@ 20ºC)	J/KgC
g	Gravitational Constant	m/s^2
l_v	Incident Solar Radiation	W/m^2
h_f	Flood Height	m

Hygrothermal Material Parameters

Symbol	Description	Units
ϱ	Material Density	kg/m^3
c	Specific heat capacity of dry material	J/kgC
λ	Thermal conductivity	W/mC
P	Material Porosity	m^3/m^3
r_k	Pore radius	m
i,j	Cell indices	-
x	Distance between cell centres	m
A	Contact Surface area	m^2
h_r, h_c	Heat transfer coefficient for radiation and conduction	$W/(m^2C)$
K	Water Permeability	kg/msPa
q_c, q_r	Convective and radiation heat flow	W
P_h	Hydraulic pressure of water inside the material pores	Pa
P_{suc}	Suction pressure of water inside the material pores	Pa
g_{vapour}	Water vapour transport	kg/m^2s
g_{liquid}	Liquid water transport	kg/m^2s
ϑ	Contact angle between the water & pore wall in a capillary	Deg
D_{ws}	Liquid Transport Coefficient (suction)	m^2/s
D_{ww}	Liquid Transport Coefficient (redistribution)	m^2/s
$\frac{\partial H}{\partial T}$	Moisture dependent heat storage capacity	J/m^3C
$\frac{\partial w}{\partial \varphi}$	Moisture dependent moisture storage capacity	kg/m^3
K^w	Moisture dependent thermal conductivity	W/mC
μ	Moisture dependent vapour diffusion resistance factor	-
a_s	Shortwave Radiation Absorptivity	-
β	Moisture Transfer Coefficient	m/s
K_l	Liquid Water Conductivity	s

Thesis Associated Publications

Refereed Journal Papers

Taylor, J., Lai, K.M., Davies, M., Clifton, D., Ridley, I., and Biddulph, P. (2011). *Flood Management: Prediction of microbial contamination in large-scale floods in urban environments.* Environment International. 37: 1019-1029.
Contributed as lead author; the paper reviews the microbiological risks inside damp and flooded dwellings and proposes hygrothermal modelling and mapping as a means of predicting the extent and duration of post-flood contamination.
[Chapters 2,3, and 4]

Taylor, J., Davies, M., Canales, M., and Lai, K.M. (2012). *The persistence of flood-borne pathogens on building surfaces under drying conditions.* International Journal of Hygiene and Environmental Health. DOI:10.1016/j.ijheh.2012.03.010
Contributed as lead author and researcher; performed experiments on the persistence of bacteria on drying building material surfaces.
[Chapter 5]

Taylor, J., Biddulph, P., Davies, M., Ridley, I., Mavrogianni, A., Oikonomou, E., and Lai, K-M. (2012). *Using building simulation to model the drying of flooded building archetypes.* Journal of Building Performance Simulation. DOI:10.1080/19401493.2012.703243
Contributed as lead author and researcher; described the development of building archetypes and carried out building simulations of drying dwellings using hygrothermal models.
[Chapter 7, 8 and 10]

Taylor, J., Biddulph, P., Davies, M., Lai, K-M. (2012). *Predicting the microbial exposure risks in urban floods using GIS, building simulation, and microbial models.* Environment International. In Press
Contributed as lead author and researcher; used GIS techniques to map the building simulation results across the research area, both in terms of the relative drying capability of different areas, their drying response to specific flood events, and the human impact and vulnerability.
[Chapter 11]

Refereed Conference Papers

Taylor, J., Davies, M. Lai, K.M. (2010), *The Simulation of the Post Flood Drying of Dwellings in London.* In: Rameezdeen, R. and Senaratne, S. and Sandanayake, Y.G., (eds.) Proceedings of the International Conference on Sustainable Built Environments. University of Moratuwa: Sri Lanka.
Contributed as lead author and researcher; described the development of dwelling archetypes for flood modelling, and how the archetypes may be integrated with flood and GIS models to predict damp following flooding. ***[Chapter 7]***

Presentations

Dampness, Flooding, and the Effect on Occupant Health, British Aerobiology Federation (BAF) Meeting, 19/11/2009, Rothamsted, UK

GIS, Building Simulation and Microbes in Flood Impact Studies, Poster Presentation, Infectious Disease Research Network Meeting, 4/11/2009. London, UK

GIS in Flooding, December 2010, Health Protection Agency, Didcot, UK

The Simulation of the Post Flood Drying of Dwellings in London, International Conference on Sustainable Built Environments, December 2010, Kandy, Sri Lanka

Part I

Background

Chapter 1

Introduction

Flooding can have a major impact on its victims, from physical damage to property, to health consequences stemming from direct or secondary flood-related illnesses and trauma. Floods have affected more people than any other natural disaster worldwide in recent years, with an estimated 99 million victims a year between 2000 and 2008 [152]. Flooding in the UK is currently a significant problem, with 2.79 million properties located in areas at risk of flooding [74]. Current annual flood damage in England and Wales costs around £1.2 billion, a figure which, according to the Department for Environment, Food and Rural Affairs (DEFRA), could rise as high as £12 billion by 2080 if adaptive action is not taken [75]. Flooding has been described by the UK government's former Chief Scientific Advisor Sir David King as the biggest climate change threat to the UK [164].

London is particularly vulnerable to tidal floods from the Thames, and fluvial and surface water floods from heavy precipitation. During the summer floods of 2007, 1,108 London households were flooded following heavy rainfall [87]. It has been estimated that a 1-in-50 year rainfall event would lead to the flooding of 1-in-7 London buildings and damages of tens of billions of pounds [112]. In addition to floods caused by climatic events, small, localised floods caused by water mains are also a common occurrence. Flooding is expected to become more frequent due to rising sea levels and the increased frequency of rain storms predicted to occur with climate change.

A good understanding of the effects of floods on population health is necessary in order to minimise potential health impacts. Floodwater can enter sub-floors and wall cavities, and can be absorbed into building materials. Flooding can impact on buildings in different ways, with some materials and building assemblies prone to long drying out periods. One secondary effect of flooding is the presence of microorganisms in buildings due to dampness, as well as human and opportunistic pathogens transported into the building structure by floodwater. Mould, bacteria, and protozoa have all been identified in damp and flooded buildings, and are thought to lead to health problems through direct contact and inhalation of bioaerosols. The environmental conditions that influence microorganism survival include the heat and moisture transport properties of the envelope design, the restoration methods that will determine internal and external climate conditions which affect

how fast and the extent to which the building dries, and the available nutrients or growth inhibitors in the construction materials, contaminating water, and sediment. Therefore, an understanding of the drying behaviour of dwellings following flooding can help to reduce the risk to humans from microbial contamination.

1.1 Basis for Research

With the majority of the population spending most of their time indoors, the impact of microorganisms on indoor climate and health is significant and has been a topic of considerable research interest. However, there is little information available on how flooding may impact the microbial ecology of indoor environments, and a lack of clear information regarding the drying behaviour of different types of residential property following flooding. Furthermore, with no specific industry definitions of what constitutes 'dry', and a lack of data on the microbial hazards inside a drying flood-damaged building, there is significant confusion about when a building is suitable to be reoccupied and what hazards remediation workers encounter in the built environment. Due to insufficient information about the drying behaviour of different dwellings and the risks that may be present at different stages of the drying process, the response to a flood event by residents, health officials, emergency planners, and government officials is inconsistent and may place individuals at risk.

There are a number of specific questions regarding the impact of floods in London, such as:

- How long can a flooded dwelling expect to remain contaminated by microorganisms following specific flood events?
- How does the built form and envelope properties of a dwelling influence its ability to dry following a flood event?
- What are the more flood-vulnerable dwelling types found in London?
- How do drying conditions and flood height impact on the drying behaviour of a dwelling?
- What are the best techniques for drying flooded properties?
- Where are the locations of the most vulnerable dwellings and people in London?

Understanding the answers to these questions would lead to:

- A better understanding of the risks present inside flooded dwellings following a flood.
- A better allocation of remediation resources after a flood.
- An understanding of how long the resident population may be affected or displaced.
- A more informed conclusion about the trade-off between drying a dwelling well and returning residents to their homes as soon as possible.

This thesis examines how building simulation and biological modelling can be used in conjunction with information on local housing stock to estimate the risk of microbial growth and survival following flooding, with a particular focus on London. By combining a number of existing and adapted modelling techniques, this research aims to answer the main questions related to the health of occupants in dwellings following flood events and the duration of risk following a flood under different conditions, and ultimately to produce an exposure assessment for a large scale flood in London.

Research Question

The growth or survival of microorganisms on building surfaces will be dependent on how long environmental conditions on surfaces remain hospitable. Different microbial contaminants will survive for differing lengths of time on drying building surfaces, depending on the rate of drying, the surrounding environmental conditions, and the contaminating species. Drying rates and environmental conditions on building surfaces are likely to vary due to the heat and moisture characteristics of building materials, and the building design will affect the ability of the envelope to dry by determining the potential for airflow and exposure to heat sources. This research examines the question of how microbial survival inside flooded dwellings is related to the drying behaviour of building materials, and how this drying behaviour will vary in relation to built form, building fabric, and prevalent drying conditions. This research will also examine the question of whether the geographic distribution of certain dwelling types and a variation in flood risk within London means that some locations will be more prone to long-term microbial risk following a flood event.

1.2 Objectives

The aim of this research is to predict the microbial risk in flooded dwellings, from the individual dwelling to city-wide level, and in doing so, produce an original contribution to research. The work carried out as part of this research proposes to achieve the following objectives:

- Part I
  - To review the historical, present, and future flood risks to London, and to describe the current opinions in flood prevention, response, and remediation [Chapter 2].
  - To review the existing knowledge of health risks to building occupants associated with microbial contamination in flooded and damp indoor environments [Chapters 3 and 4].
- Part II
  - To describe the survival of contaminating microbial species in flooded indoor environments by using microbiological laboratory techniques to show how drying conditions, water quality, and material drying characteristics affect decay rates of contaminating bacteria [Chapter 5].

  - To create a model describing how transient temperature and water conditions can influence the survival of contaminating species [Chapter 6].

- Part III
  - To create dwelling archetypes for typical London dwellings with the appropriate information to allow for the simulation of their heat and moisture performance of dwellings during and after flooding, and develop a housing stock model that will allow results to be mapped spatially [Chapter 7].
  - To assess the suitability of different building simulation models for flood modelling, and perform an initial validation of a model for this purpose [Chapter 9].
  - To simulate the drying of typical London dwelling archetypes using building simulation models in order to examine the drying behaviour of these dwellings under different flooding and drying scenarios [Chapter 10].
  - To use the simulation results alongside existing and novel microbial models to describe the duration of microbial risk inside dwelling archetypes [Chapter 10].

- Part IV
  - To use maps to visualise the geospatial variation of dwelling archetypes throughout the London research area in terms of their drying characteristics, and to use this data to predict areas most at-risk from long-term health issues, displacement, or social vulnerability following a flood event [Chapter 11].

1.3 Research Tools

To achieve these research objectives, a number of interdisciplinary models and techniques are combined to demonstrate the microbial risk to dwelling occupants following a major flood event in London.

The survival of bacteria on flooded surfaces is investigated using microbiological laboratory investigations to examine how drying rate, materials, bacteria species, and water quality impact on the microbial risk present. Microbiological modelling techniques are then used to describe the decay of contaminating bacteria under transient drying conditions in order to help identify the amount of time dwellings will be at risk of microbial growth and persistence following a flood, based on the temperature and Relative Humidity (RH) conditions. Existing mould models are also used to predict the duration of risk of microbial contamination on flooded surfaces.

Research into the drying behaviour of flooded dwellings is based on dwelling archetypes and housing stock models. The dwelling archetypes model is composed of notional dwelling types which

are intended to represent average dwellings within the housing stock. Existing dwelling archetype models are assigned building fabric data on the basis of survey data analysis and hygrothermal materials data. The dwelling archetypes are used for Heat, Air, and Moisture (HAM) building simulation of the drying of flooded dwellings under different environmental scenarios.

HAM computer models simulate the transport of heat, air and moisture within building assemblies. HAM models vary widely in their complexity, from simple steady-state models unable to account for changing external and internal conditions, to complex whole-building simulation models that can calculate air and heat flow throughout the building and account for transient heat, air, and moisture levels (e.g. EnergyPlus) [275]. By considering the hygrothermal properties of the materials in the assembly and the internal and external environmental conditions, whole-building HAM models are used to estimate the moisture content and temperature at various locations in the dwelling and building fabric, which can then be used to predict the risk of bacteria survival and mould growth using novel and pre-existing models.

The outputs from this research inform the drying behaviour of different dwelling archetypes in terms of their potential for lingering damp and contamination, which can in turn be mapped using Geographic Information System (GIS) software. Geospatial data on population density, social vulnerability to flooding, and flood heights are also incorporated into the GIS study. The result is a prediction of the long-term microbial risk due to damp following a flood and population vulnerability to flooding in London, thus providing important information for flood remediation organisations, health agencies, insurance organisations, and social housing providers so they can better prepare and respond to flooding. Figure 1.1 depicts the integration of the different modelling levels used in this thesis.

1.4 Thesis Outline

An outline of the thesis is illustrated in Figure 1.2. A review of flooding and health will be carried out in Part I which discusses the flood risk to London, the current understanding of the what constitutes a safe, 'dry' dwelling, and a description of the microbial risks and potential health consequences that can arise following a flood. Part II describes microbiological experimentation of bacterial decay on flooded building materials, and describes the development of models that can be used to predict their decay under transient drying conditions. Part III reviews existing UK housing stock models and describes the development of a domestic housing stock model representative of London dwellings. The concept of hygrothermal modelling and the process for modelling the flooding and drying of dwellings under different scenarios is also introduced in this section. Part IV incorporates the results of the previous sections with established flood maps into GIS to illustrate the risk to London following flood scenarios. Part V discusses the conclusions drawn from the research, proposes changes to UK policy, and suggests future research on the topic.

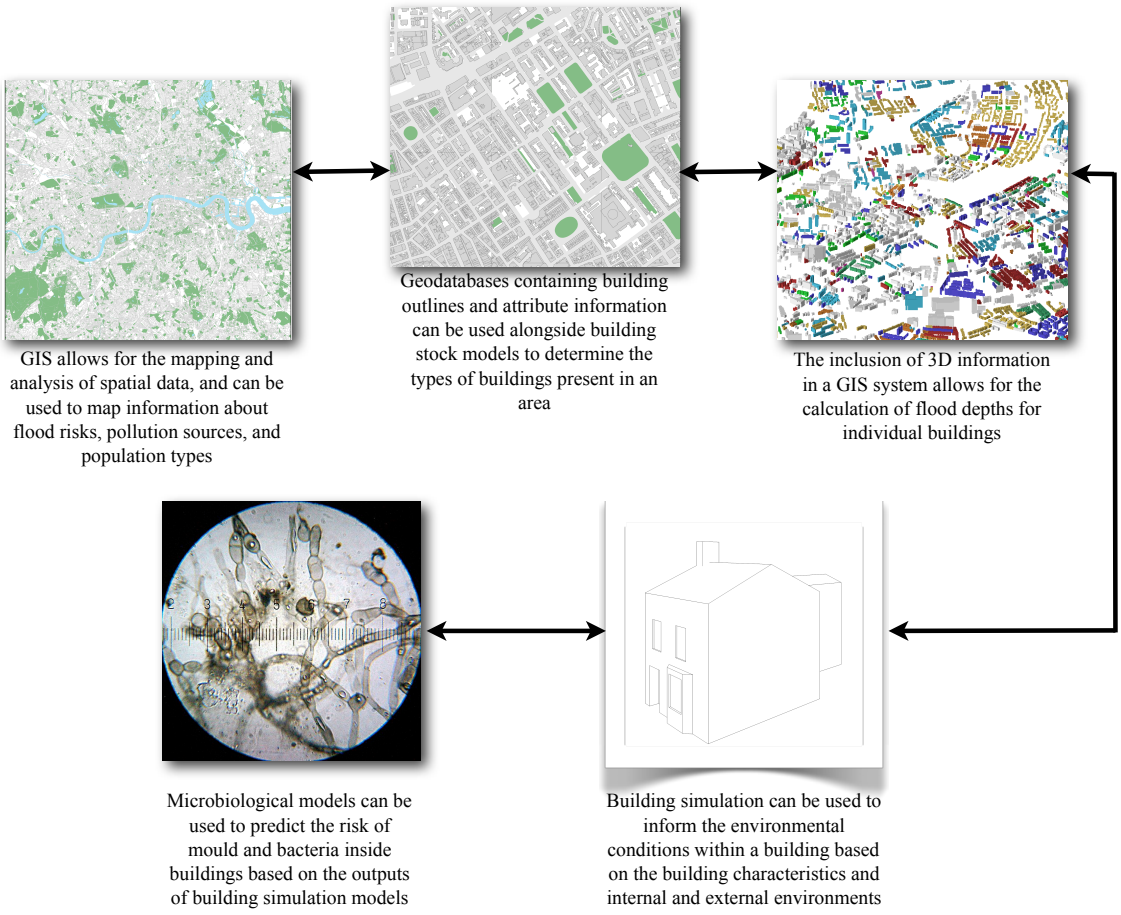

Figure 1.1: The inter-relation of the different levels of detail within the research plan.

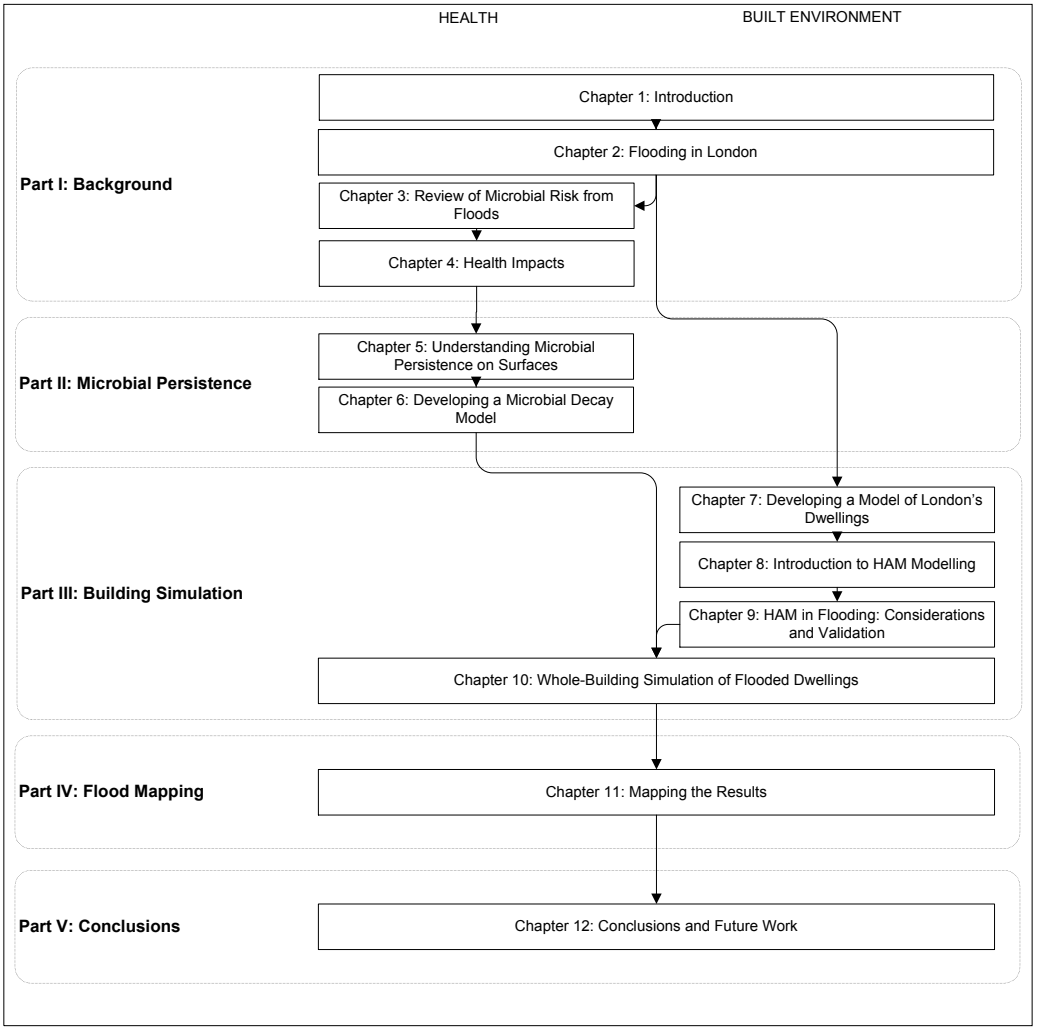

Figure 1.2: Thesis map.

Chapter 2

Flooding in London

2.1 Types of Flooding

The UK Flood and Water Management Act of 2010 defines a flood as being any case where land not normally covered by water becomes covered by water [213]. Floods can be divided into five different types based on the source of the water– coastal, fluvial, surface water, foul water, and groundwater flooding. These floods can have different water qualities, velocities, and durations, which can lead to unique health risks following a flood event.

Coastal floods occur when sea water is driven inland, which in the UK typically occurs due to storm surges. Storm surges happen for various reasons. High winds can cause offshore water to build up to a height above normal sea level. Low atmospheric pressure during stormy weather can also lead to a temporary increase in sea level. As the storm surge moves closer to land, the bathymetry of the land can compound the problem – areas with a steep shelf produce powerful waves, but a lower surge, while gradual drops can produce a large surge.

Fluvial, or riverine flooding occurs when catchment rivers overflow. There are a variety of causes of fluvial floods. Flow paths of rivers can often become restricted due to ice, litter or debris, which can instigate slow flooding upstream. Heavy rains or snow melt can also cause rivers to flood due to a high amount water entering the river directly through surface water instead of draining naturally through an organic surface down to the groundwater. As such, rivers can respond very quickly to high rainfall levels, and can offer little warning as to their potential for flood. The sudden release of a blockage or very intense or prolonged precipitation can bring about flash flooding of a river. Since fluvial floods can occur during heavy rainfalls, they may coincide with storm surges to produce a combined tidal/fluvial event.

Foul sewer floods occur when a sewer system overflows. Properties at or below the hydraulic level of a sewer can become flooded when sewers are blocked or overloaded. Often these are basement flats or premises in low lying areas. Foul sewer flood locations do not follow any discernible pattern, but tend to be small, discrete sub-catchments on the sewer network.

In some areas groundwater flooding is a potential risk. Groundwater is water located beneath the surface of the ground, which flows out of the ground where the water table meets the surface. Groundwater can be affected by heavy rainfall, as it slowly saturates the ground and leads to eventual flooding.

Surface, or pluvial flooding is found primarily in areas of dense development, or large roofed areas such as railway stations, and can occur as a result of intense rainfall, when the drainage network can be overloaded or when the drainage system is blocked. These flood events appear and disappear quickly, meaning predicting and recording surface water floods are problematic. Urban flood events can originate from coastal, riverine, sewer, or groundwater sources, but are exacerbated by a lack of water drainage capacity. As a result, urban floods are often considered to be a separate type of flood.

Flooding can also occur as a result of infrastructure failure, such as a burst pipe or a breach in a reservoir. In cases where there is a sudden release of water, such as a reservoir failure, or the release of a blockage in a river, then flash flooding can occur. The structural damage caused by a flash flood is increased due to the high velocity of water.

The water quality in floods can depend on the source of the water. Floodwater is often classified as cleanwater, greywater, or blackwater. Cleanwater is not considered to be directly harmful, and can occur from broken supply lines, and sink overflows. Greywater is water containing chemical, biological, or physical contaminants that can be harmful if consumed, and may originate from water discharge from domestic appliances. Greywater may contain microorganisms, but does not contain human waste and is not considered to be highly pathogenic. Blackwater is highly unsanitary water containing high levels of microorganisms and is contaminated with human and/or animal waste. Included in blackwater is water derived from sewage, sea water, fluvial water, groundwater and surface water floods. Greywater, if left standing for 48-72 hours after a flood, is reclassified as blackwater [77]. Understanding the nature of contaminant activity in water is important when assessing the health risks to occupants following flooding due to the potential for microbial and chemical contamination.

2.2 Impact of Projected Climate Change

The world is currently experiencing a change in climate, which is predicted to instigate changes in climate variability and extreme events, such as more frequent heat waves, less frequent cold spells, and a greater intensity during rainfall events [156].

Climate change is defined by the Intergovernmental Panel on Climate Change (IPCC) as “a statistically significant variation in either the mean state of the climate or in its variability, persisting for an extended period (typically decades or longer)” [156]. The impacts of climate change on the UK have been studied in the UK Climate Projections 2009 (UKCPO9) climate change scenarios [273],

(a) High emission scenario, summer 2080.

(b) High emission scenario, winter 2080.

Figure 2.1: Impact of climate change on precipitation levels in London (courtesy of the UKCP09).

with projections indicating an increased risk for flooding in the South East of England. Summers are expected to be drier, and winters wetter, and throughout the UK, average annual precipitation may decrease slightly by the 2080s. While actual rainfall may decrease overall, the intensity of precipitation is likely to increase, with the kind of rainfall intensities experienced only once every two years on average becoming between 5% and 20% heavier during the winter season. London and the South-East will experience the largest relative change to precipitation levels. By 2080 precipitation during the winter may increase by 15% (low) to 30% (high) (Figure 2.1).

Intense periods of precipitation increase the risk of fluvial, reservoir, surface, foul, and groundwater flooding. Both extreme high and extreme low levels of water flow in rivers are expected to become more commonplace [226]. High flow events could lead to fluvial flooding, placing reservoirs in particular at risk of failure. Under the UKCP09 Medium-high emissions scenario, reservoir water levels in the UK could increase by 5% above normal retention level during storms by the 2050s [111]. More than half of Britain's reservoirs are over 100 years old and made of earth embankments [178], suggesting that they may be at an increased risk of failure. Dams are also prone to subsidence, landslip into reservoirs, or overtopping, and heavy rainfall and flooding may cause the silting up of reservoirs, pumping stations, and boreholes [111]. An increase in surface flooding is likely to occur with the rise in heavy rainfall events, with drainage systems overwhelmed and surface runoff increasing, while sewerage systems may struggle with the increased levels causing foul water floods. Groundwater flooding may increase if heavy rainfall raises the water table.

Climate change is predicted moreover to lead to an increased risk of tidal flooding and a reduction in the amount of protection offered by flood defences [111]. London and the South East of the UK

is expected to experience greater warming than the North West, with the annual average daily temperature increasing by 3°C by 2080 under the low emissions scenario, and 5°C in the high emissions scenario. A warming climate will lead to high sea surface temperatures, causing an expansion in the size of the ocean and a rise in sea levels, thereby leading to a greater risk of tidal flooding [273]. The melting of polar ice sheets and glaciers will also lead to a rise in sea levels.

In the South East, the land is sinking at between 1 and 1.5mm per year [111], prompting a greater relative sea level rise in southern Britain than in the north. The result is that the projected sea rise around London is estimated at between 20cm and 70cm by 2095 [273]. In addition, for the East coast of the UK extreme sea levels could occur between 10 and 20 times more frequently with levels up to 1.2m higher than current extremes [273]. The average annual sea levels at Sheerness, in the Thames Estuary, have shown a gradual yearly increase over the past 180 years.

The combination of climatic factors suggest that flooding is expected to become a major issue for London in the future. Indeed, flooding is considered by the UK insurance industry to be the biggest threat to the UK from climate change [63]. In fact, flooding during the recent heavy rainfall events in London and across the UK illustrates its vulnerability to flooding from extreme rainfall events. Understanding the risks due to flooding in London is therefore critical for maintaining a healthy, resilient city.

2.3 Flooding and London

Flood risk is classified according to the likelihood of a flood occurring during a given time period. A 1-in-100 year flood represents the type of flood that would be expected to happen once every 100 years – or with a yearly probability of 1% risk. Flood maps are widely used by emergency planners and insurance agencies to show the areas at risk of flooding from different flood scenarios.

London is at risk from tidal, fluvial, reservoir, and surface flooding. Tidal floods can occur along the River Thames and up several tributary rivers. The Thames experiences tides twice a day from the coast up to Richmond Lock, with a range as high as 7 metres on spring tides [211]. The normal river walls prevent daily flooding, while the Thames Barrier and smaller barriers further towards the coast help to deal with storm surges that are caused by high tides, easterly winds, and weather system depressions over the North Sea. Figure 2.2 shows the Environment Agency (EA) flood risk map for Central London for a 1-in-200 year tidal flood event.

The Thames Barrier, which became operational in 1982, was built to defend London from storm surges. Located near Woolwich, the Barrier consists of 10 steel gates which can be raised when storm surges are forecast. If the flow of water down the Thames is unusually high, for example from heavy rains or snowmelt, the Barrier can also be closed during low tide, allowing the Thames to act as a reservoir for fluvial water, and protect against elevated levels of combined fluvial/tidal flood waters. Since completion of the Thames Barrier in 1982 to May 2011, the Thames Barrier has closed

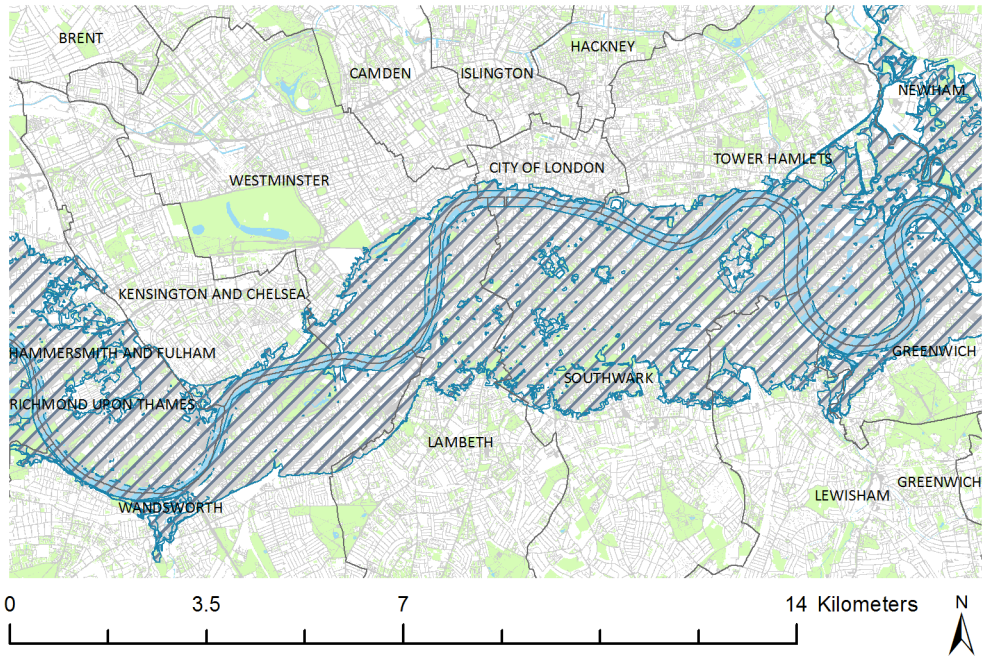

Figure 2.2: 1-in-200 year tidal flood risk map of London (courtesy of the EA).

119 times to prevent London from flooding. Seventy-eight of these closures have been due to tidal surges , while 41 closures have been to prevent rainfall/fluvial flooding. There appears to be a trend towards increasing numbers of yearly closures.

The issue of fluvial flooding in London has been addressed in the Thames Catchment Flood Management Plan [85]. There are 12 major tidal tributaries discharging water into the tidal section of the Thames. As London has developed, many other rivers became culverted, and water is discharged into the Thames through tidal flaps. Figure 2.3 shows the EA flood map for Central London for a 1-in-100 year fluvial flood event. While the surface area at risk of flooding from fluvial sources is small compared to the area at risk from the Thames, a joint tidal/fluvial event combining a tidal surge and fluvial flooding caused, for example, by a storm surge and heavy rainfall, could cover a significant area of London, causing huge amounts of damage (Figure 2.4).

London has not traditionally had a problem with groundwater flooding. Historically, this is because a significant amount of its groundwater was directed towards use in industry. As industry demand decreased, a steady rise in the groundwater levels resumed, which began to threaten London's underground infrastructure. Increased abstraction of the groundwater prevented further increase, and levels are currently monitored regularly by the EA. Climate change is not expected to have an effect on the total amount of rainfall [273] (just on intensity of rainfall), so groundwater flooding in London should not increase under current climate projections.

The EA maintains publicly available maps which show areas at risk of flooding due to a failure of a large reservoir (Figure 2.5). Although many of the UKs reservoirs are over 100 years old, the

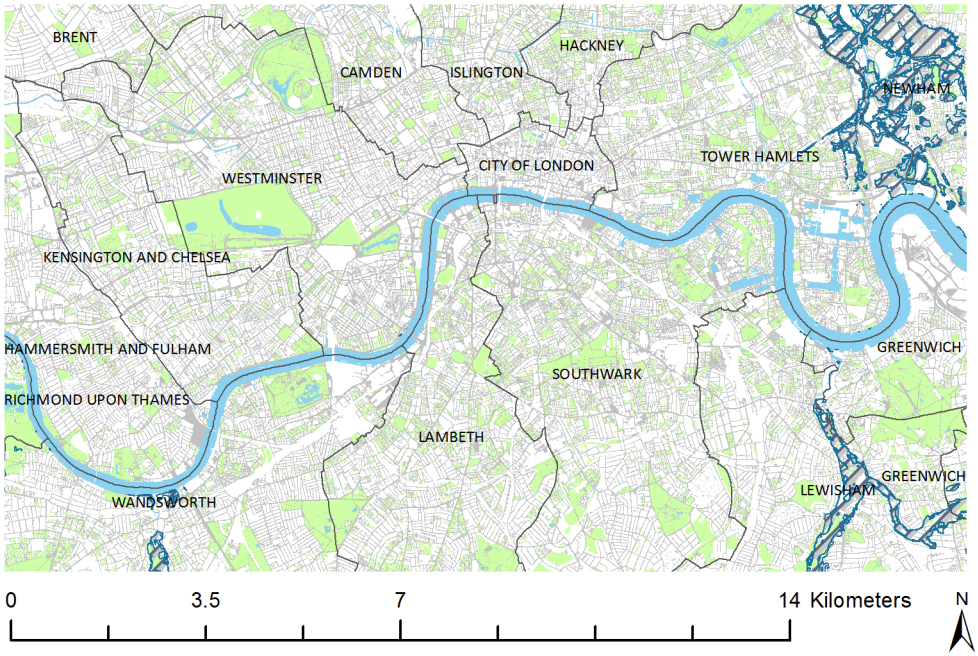

Figure 2.3: 1-in-100 year fluvial flood risk map (courtesy of the EA).

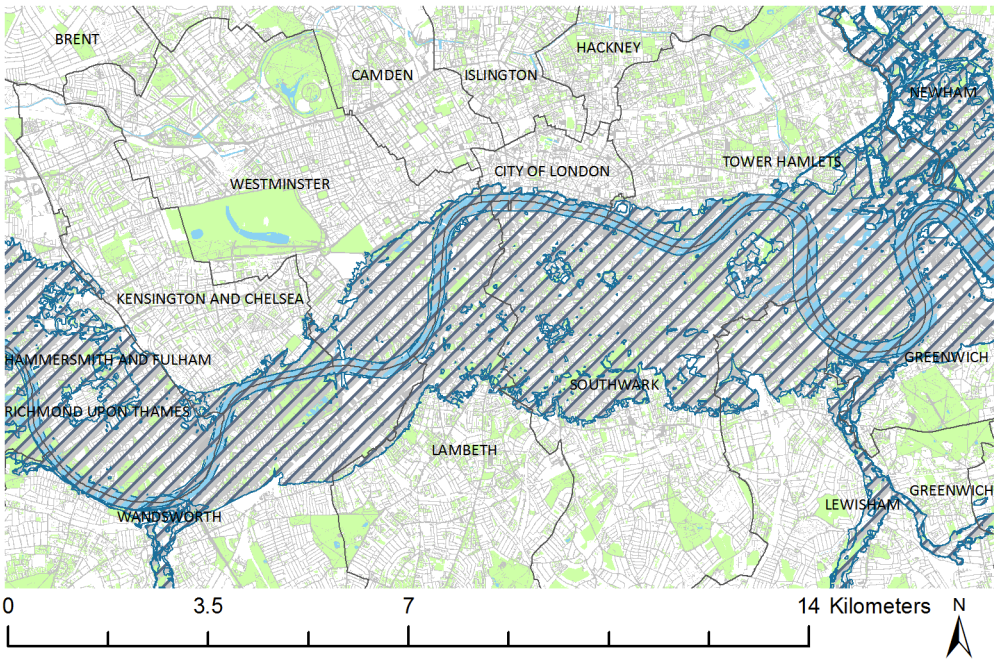

Figure 2.4: 1-in-1000 year tidal/fluvial flood risk map of London (courtesy of the EA).

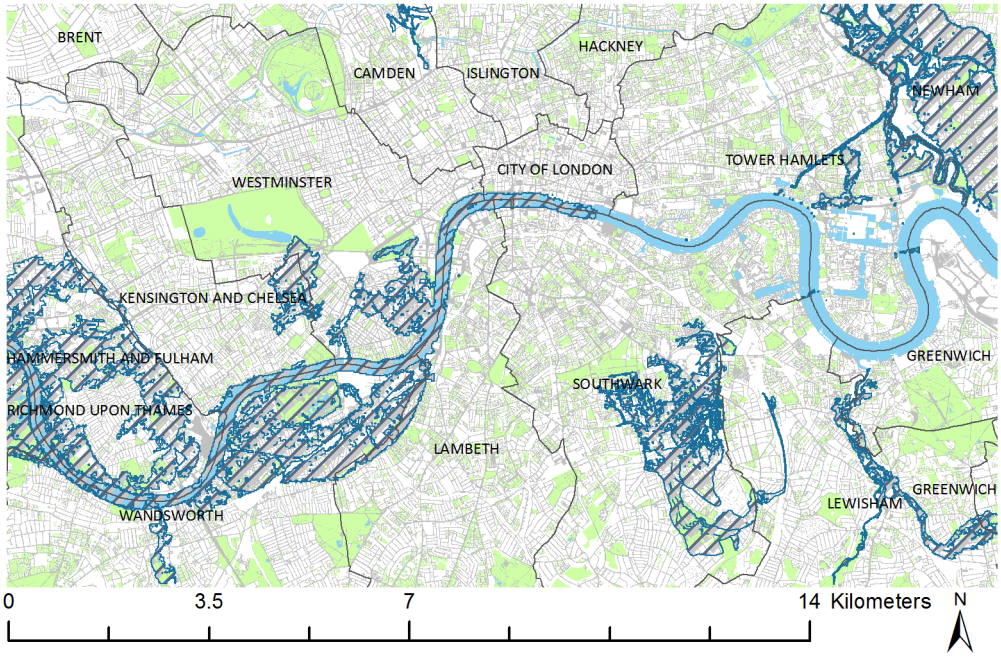

Figure 2.5: Areas at risk of flooding from a reservoir failure (courtesy EA).

failure of one of the major London reservoirs is considered to be unlikely. Reservoir flood maps show the maximum extent that might be covered should a reservoir fail. They are indicative of a worst-case scenario so do not have yearly probabilities-of-occurrence associated with them like tidal or fluvial flood maps.

In urban environments extreme weather effects will be particularly significant due to concentrated populations and high property values [111]. In England, the majority of housing development is in the South East [208]. Government targets aim to have 60% of all new homes built on brownfield sites [67]. While this strategy helps to reduce urban sprawl, it also lowers the built environment to greenspace ratio in urban areas [111] and puts pressure on urban surface temperatures, storm water runoff, carbon storage, and biodiversity [289]. Storm water runoff is fundamental in order to avoid surface flooding, therefore a reduction of the potential land available to absorb rainwater will raise the incidents of flooding.

Surface water in London is drained by a sewerage outfall system and treated at Becton and Crossness sewage treatment plants. Moreover, during heavy rainfall the drainage system can become overwhelmed, and treatment works are compelled to discharge raw sewage directly into the tidal section of the Thames. Approximately 32 million cubic metres of raw sewage is discharged into the Thames annually [286] therefore plans to improve London's Victorian sewerage system through the Thames Tideway Scheme are underway. High levels of development coupled with a lack of storm water runoff and drainage, means that surface flooding is an increasingly serious issue in London. To further complicate the issue, surface water flooding is difficult to predict because there is little

data on drainage in different locations.

Flood plain development is also a consequence of urban growth in London. A larger population living on flood plains as a result of planning decisions may mean that the consequences of a flood event are more severe [273]. There have been 350,000 residential properties built on flood plains in the UK over the past 20 years, with 20,000 of these built between 1997 and 2000 [12]. In London, there will be substantial growth in the Thames Estuary as part of the Thames Gateway project of development.

While the Thames Gateway project will lead to significant development on flood plains, much of the existing London housing stock will remain unchanged over the next 100 years. Existing dwellings represent around 99% of the housing stock at any one time, with new construction taking place at a rate of less than 1% of the total stock per year [248]. Under the most ambitious demolition scenario, 70% of homes in 2050 already exist [89]. This low turnover means that the effects of a changing climate and floodwater on the domestic housing stock needs to be considered for existing dwelling types as well as those being built in the future.

2.4 History of Floods in London and the UK

The history of flooding in the Thames has been summarised by the EA [88], who describe how London has been at threat from floods for much of its history (Table 2.1). The Thames was originally a much smaller river which flowed through marshland on which London was originally built. The Romans settled in London around AD43 and were responsible for building some of the first flood defences for the new city.

Historical records provide noteworthy accounts of major flood events to hit London. The Anglo Saxon Chronicle describes a spring tide that occurred on the Festival of St Martin, where "... the sea flood sprang up to such a height and did so much harm as no man remembered that it did before". In 1242, the Survey of London records a flood that hit Lambeth and Westminster and "...drowned houses and fields by the space of six miles". On December 7^{th}, 1663, Samuel Pepys wrote in his diary of a flood that was ".. the greatest tide that ever was remembered in England to have been in this river, all Whitehall having been drowned".

The famous Dagenham breach of 1707 was the result of an extremely high tide, which washed away an embankment and flooded approximately 1000 acres, leaving behind a seven hectare lake now known as Dagenham Breach. Henry Hunter describes a flood from the Thames into Westminster in 1762, while floods in Stratford and Bow have been recorded as occurring in 1763 and twice in 1764. In 1874, a high tide caused a flood that inundated the south bank of the Thames in Lambeth, Bankside, and Rotherhithe killing at least one person. Due to the high number of floods and the damage caused, the Flood Act was drafted in 1879 to allow for the construction of stronger flood defences for the city.

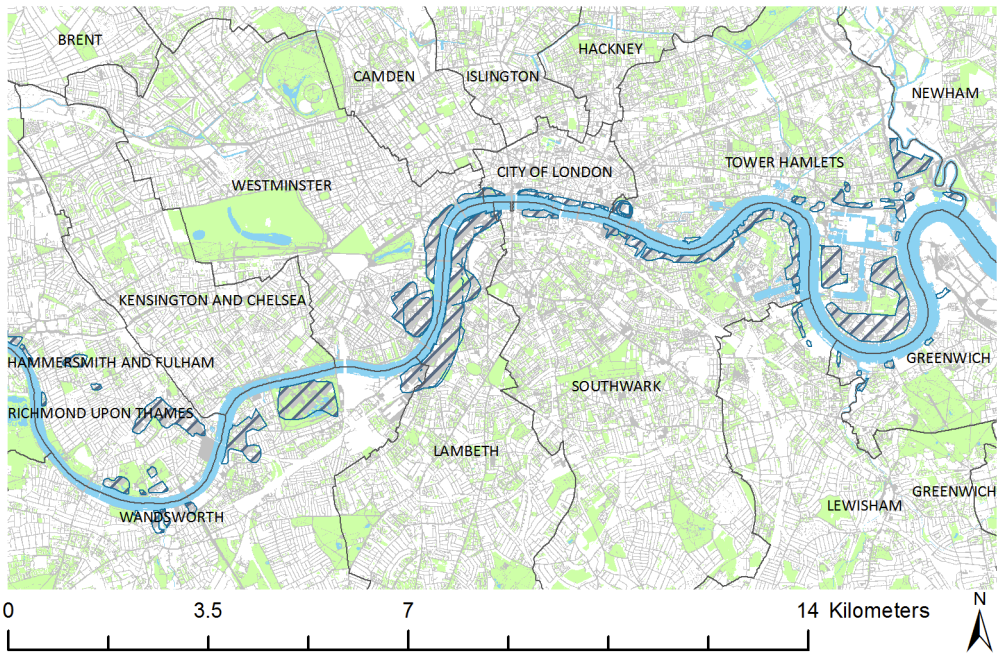

Figure 2.6: Locations in central London affected by the 1928 flood (courtesy EA).

One of the major flood events in London during the 20th century occurred in January 1928. Heavy snowfall farther up the Thames in the Cotswolds thawed rapidly. The melting snow, along with heavy rainfall, nearly doubled the volume of water flowing down the Thames. A high spring tide and storm surge on January 7th raised the water in the Thames, which spread throughout the centre of the city (Figure 2.6). The flood killed 14 people and made 4,000 people homeless.

On January 31st and February 1st 1953, a major storm surge hit the East Coast of the UK, flooding parts of London (Figure 2.7). This surge killed over 300 people, displaced over 32,000, and damaged 24,000 houses [260]. In the Thames Estuary, Canvey Island was flooded resulting in the deaths of 58 people. However, the severity of this particular surge led to the improvement of flood defences, including the construction of the Thames Barrier, which was completed in 1982.

More recently in the summer of 2007, London experienced flooding caused by a wetter than average May and June, and heavy rain in early July. This rainfall led to surface water flooding that impacted on around 400 properties in London. Across the UK, the floods of 2007 caused 13 fatalities and £6 billion worth of damage [228]. Had London experienced the amount of rainfall that other parts of the UK experienced, a major civil emergency would have occurred [211].

A few significant flood events elsewhere in the UK are worth mentioning. The worst flood in UK history occurred in Sheffield when the Dale Dyke Reservoir failed in 1864, leaving 270 people dead and destroying 800 homes. In 1952, a severe flood at Lynmouth in Devon killed 34 people and destroyed 100 buildings when severe rainfall caused surface runoff into rivers. These rivers became clogged with debris, causing overflows and flash flooding when one obstruction came loose. In the

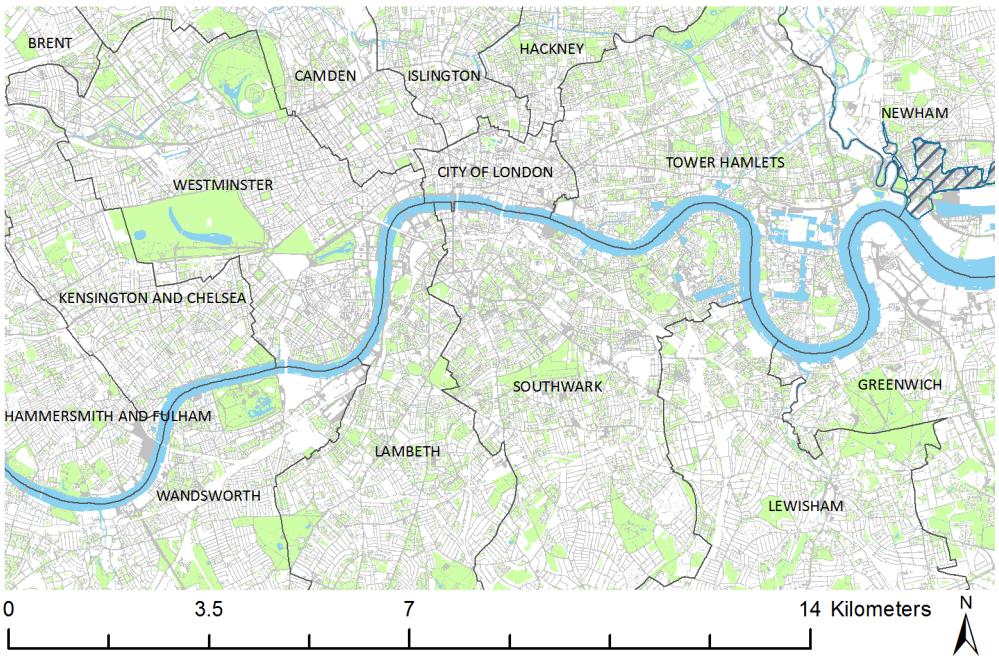

Figure 2.7: Locations in central London affected by the 1953 flood (courtesy EA).

summer of 1968 heavy rainfall in Bristol flooded about 3,000 properties.

Floods in 2002 in Glasgow were caused by heavy rainfall and a drainage network unable to cope with surface runoff. The Boscastle flood of 2004 in Cornwall due to heavy rainfall and subsequent rise in riverine water levels and surface runoff destroyed 100 buildings. In Cumbria in 2005, several rivers flooded after heavy rainfall causing damage to around 2,000 properties, and killing three people. Flooding recurred in Cumbria in 2009, again due to heavy rainfall – that November was the wettest month across the UK since records began in 1914. More than 200 people had to be rescued from their homes in Cockermouth, where the water in the town centre was reported as high as 2.5m. As we have demonstrated using historical records, flooding is the most common natural disaster in the UK, and recent flood events in London and throughout the UK confirms the potential for floods to generate significant damage and loss of life.

2.5 The Impact of Floods on Buildings

Floods have a critical impact on buildings, producing both direct and indirect damages. Direct damages are caused by the physical effects of water on the flooded area and is related to the physical properties of the flooded area, for example, the land-use, land-cover, and susceptibility, area covered, depth and duration of the flood, water velocity, and sediment and effluent content. Secondary direct damages are damages which have a physical impact, but which are not caused by direct contact with water. Examples of secondary direct damages are gas explosions caused by flood damage to

Year	Description	Casualties
1236	A high storm surge caused flooding in Woolwich, drowning many people and cattle	Unknown
1242	A heavy rain storm caused the Thames to flood at Westminster and Lambeth	Unknown
1663	A 200-year high tide, combined with heavy wind, caused flooding in Whitehall	Unknown
1703	A tidal flood caused by a storm surge hit the Thames, the Severn, and the Dutch coast. Most shipping was destroyed in London causing an estimated £2 million in damage.	43 fatalities
1809	Tidal flood hit as far as Windsor, destroying bridges at Eton, Deptford, and Lewisham	Unknown
1928	Westminster, Lambeth, Southwark, Isle of Dogs, Hammersmith	14
1947	Severe flooding in the Thames Valley due to heavy rains.	None
1953	A storm surge inundated the English coast, and caused flooding in England, Belgium, and the Netherlands. Canvey Island in the Thames Estuary was particularly hit, with 58 deaths.	307 in the UK
2000	230 properties along the River Roding, 75 in Edmonton, and 15 in Teddington were flooded due to high volume river flow.	None

Table 2.1: Flooding history in London (Adapted from [88]).

infrastructure, or a collision with floating debris [220]. Indirect damages are disruptions to the physical and economic linkages of the economy. The large number of site-specific variables means that it is not possible to have a standardised relationship between direct and indirect damages.

Flood damage may be immediate or consequential, depending on the stage of flooding in which the damage occurs. Immediate damage is considered to be fairly superficial damage to the contents of a dwelling due to the immersion and the force of water flows. Consequential damage arises from water staying in the structure for a prolonged period of time, or through the process of cleaning and drying. The impact of flooding may also be tangible or intangible [220]. Tangible flood damage includes the costs of repairing damage, while intangible consequences may include anxiety, inconvenience, and ill health.

The damages caused by floods to buildings has been described as being physical or non-physical. Kelman [162] describes the physical actions of floods as:

1. Hydrostatic Actions, which include the lateral hydrostatic pressure on a wall from floodwater and the capillary rise of the water up the flooded wall.

2. Hydrodynamic actions, including lateral pressures on a wall due to water moving past the residence, localised velocity changes, and turbulence, as well as breaking and non-breaking waves exerting pressures against the side of a building. Slow-rising floods will pose a reduced risk of hydrodynamic actions on buildings when compared to flash floods.

3. Erosion of soil from slopes around buildings, causing localized land slips, and destabilizing the dwellings.

4. Buoyancy is a force related to the volume of water that the residence displaces, and can result in the residence, or parts of the residence, floating. For lighter structures (e.g. sheds) or structures that are not securely anchored to the ground (e.g. caravans) the structures can float and become displaced.

5. Debris in the floodwater can lead to static, dynamic, and erosion actions on dwellings. Static issues include sediment accumulation in and around the residence and the pressures they exert on the built form. Dynamic forces include the collision of floating debris with the dwelling, causing damage from a sudden impact. Debris can also facilitate the erosion of soil leading to destabilisation of the property.

The non-physical impacts of a flood on buildings can include:

- Chemical actions, such as those caused by floodwater, such as rusting, warping of wood, and damage due to water vapour, and damage caused by chemical contaminants in floodwater. The presence of salt water will accelerate rusting of some materials, and can cause damage to porous building materials [288].

- Nuclear, in the event nuclear fuel contaminates the floodwater.
- Biological, in which flood-borne and ubiquitous microorganisms are deposited on damp surfaces, or left in standing water, allowing them to grow or persist, potentially degrading building materials and causing health problems for building occupants.

This thesis will address the impact of hydrostatic water movement into the building envelope, potential biological risk, and secondary health impacts which may arise from being inside a flooded dwelling in London.

2.6 UK Flood Guidelines

2.6.1 Living with Floods

UK Government policy on flooding appears to be shifting from flood prevention to flood resilience. Recent publications such as 'Living with floods' [150], 'Preparing for floods' [208], 'Making space for water' [72] and 'Living with risk' [274] show an increasing professional and policy emphasis on adaptability rather than traditional flood defences [221]. This implies that current difficulties in flood risk reduction, as well as the potentially higher flood risks in the future, are better mitigated through land use management, accurate warning systems, awareness of the social costs of floods, and improved emergency planning. Indeed, these strategies are being addressed in government departments responsible for flood strategy [71, 72, 209]. The increased focus on flood resilience rather than prevention indicates that a deeper understanding of the drying behaviour of buildings will be necessary in order to sufficiently manage future flood events.

2.6.2 Recovery and Remediation

Recent flood events in the UK have highlighted the difficulty in managing and restoring flooded homes. During the 2007 floods in the UK there were indications of prolonged displacement from homes due to drying. In Hull City, 3,247 households were forced to move into temporary accommodation. One year later 1,476 households, or 45% of the displaced were still living in temporary accommodation. Even 18 months after the flood, 551 households remained in temporary accommodation, and after two years over 10% of households in Hull had not yet returned home [144]. This led to significant dissatisfaction about the length of time needed to dry homes, with 66% dissatisfied about the length of time taken to repair their homes.

The Pitt Review [228] undertook to examine the lessons learned from the summer floods of 2007 in the UK. It found that the health information provided to affected individuals following the floods of 2007 was inconsistent. Health advisers gave conflicting advice on whether it was safe to stay in flooded properties. Builders also had difficulty obtaining clear advice about the health risks associated with remediation or renovation of a flooded building. Different advice regarding

the removal and disposal of water-damaged and mouldy items from flooded homes, and the health threat from working inside a damp building envelope, was given to the building industry by public authorities and insurance agencies [228].

The Pitt Review also highlighted that a range of guides on how to dry a building were available from different sources, but no definitive guide on best practice in building drying was available, nor is there a widely accepted definition of 'dry' [17, 18, 19, 30, 31, 32, 33, 38, 84, 104, 106, 107, 163, 208]. Advice in these guides to residents returning to flooded dwellings suggests that reoccupation does not occur until the property is 'dry'; however with no clear, measurable threshold for 'dry' and no official advice given on the persistence of microbial hazards on drying surfaces, the potential exists for residents to return to unfit housing. Pitt states that 'publicly available advice on factors to consider when deciding whether to re-occupy a damp property is neither extensive nor definitive and it is found in a confusing variety of locations'. There is not any advice available on the potential health impacts of living inside a building that remains damp after flooding.

Some basic advice is available as to when it is suitable to re-occupy a flooded home, with the Construction Industry Research and Information Association (CIRIA) recommending that reoccupation not occur until the dwelling is 'sufficiently dry' [55], and the Health Protection Agency (HPA) recommending that one must only fully re-occupy their home after cleaning has been carried out [143]. UK standards do exist [38, 107], but these are considered to be general guidelines [203].

More information on flood remediation and the health risks for those entering flooded buildings is available from sources in the U.S. Factsheets and remediation and health information is available from the Environmental Protection Agency (EPA) [96], the American Red Cross [9], Centers for Disease Control (CDC) [29, 47, 48, 49, 50, 251, 252], the Institute of Inspection, Cleaning and Restoration Certification [154, 155], National Center for Healthy Housing and Enterprise Community Partners [200], and the Federal Emergency Management Agency (FEMA) [100].

As part of the post-flood drying process, many companies offer a drying certificate as proof of having remediated the property. Drying certificates are available according to the British Damage Management Association (BDMA) [18], which defines dry as being a state in which:

- Internal conditions are at, or better than, normal room conditions.
- Moisture on and in the building materials themselves will not support active growth of mould and mildew.
- Building materials and contents will return to equilibrium within normal room conditions by themselves, without suffering further damage.

However, determining whether the house qualifies as 'dry' remains at the discretion of remediators or loss adjustors, and can be subjective and carry caveats for pre-existing damp conditions.

It has been suggested that an indoor Relative Humidity (RH) target of 40% or less should be attained as quickly as possible following a flood in order to minimise microbial health threats [60], however, there is scant research to back up this figure. Many guides and standards suggest minimising the number of rooms needing repair by comparing surface moisture levels in a dry room or neighbouring property to those in a flooded room, and then using that number as a reference [107]. This does not consider the fact that the RH of the air will be greater in flooded rooms, and can circulate causing damp on surfaces throughout the property, nor does it take into account capillary action that can cause damp to potentially rise above the flooded ground floor to higher levels. Guides also suggest a threshold water content or RH for building surfaces, but this threshold does not reflect inaccuracies in measuring equipment or specifications on where measurements should be taken in different wall types. Furthermore, static moisture measurements neither indicate the ability of certain microorganisms to grow in transient temperature and humidity conditions, nor the ability of some microorganisms to persist under dry conditions and to recur when normal building operation resumes. Finally, some flood repair guides advise removing plasterboard to a height above the flood line rather than the entire wall in order to save time and cost [9]. However, capillary action and damp air circulation can allow for the entire wall to be capable of supporting mould growth, particularly in cavities where air circulation is minimal.

The responsibility for repairing flooded dwellings is complex, potentially involving owners, insurance companies, landlords, and local authorities. While the published guidelines and standards for drying flooded properties may vary, actions taken to repair the home also depend on decisions made by these parties. Residents in rented or public housing must depend on the landlord or housing agency to arrange for repair of the property. Owners of properties may or may not have insurance coverage, as properties at risk of flood may have expensive premiums or be uninsurable. Those who do have coverage may be unwilling to claim on their insurance fearing that their property may be labelled as flood-prone and therefore made uninsurable [13]. Those who have been flooded may also choose to simply re-locate within their dwelling; Tapsell and Tunstall noted following the floods in 1998 that many flood victims in Banbury and Kidlington who lived in multi-story accommodation opted to relocate upstairs rather than move out of the flooded property [267]. Finally, insurance companies are increasingly offering to pay the claim, leaving the victim to arrange for their own remediation using one-off insurance payments that may be less than optimally utilised. The decisions of the involved parties can mean that some flooded properties remain damp for an extended period of time after a flood.

There is an obvious trade-off between wanting to ensure that homes are safe and will not impact on the health of occupants, and acknowledging the problems associated with displacement. As a result, the Pitt Review made two recommendations based on remediation and health: that the Department of Health and other relevant bodies should develop a single set of flood-related health

advice for householders; and that local response and recovery coordinating groups should ensure that health and wellbeing support is readily available to those affected by flooding based on advice developed by the Department of Health. In response to the Pitt Review, CIRIA has developed up-to-date guidance on flooded property drying [56] and the construction of flood-resilient dwellings [263], and the EA is improving its dissemination of flood information to the public [86]. In addition, the Department of Health is preparing advice on the physical and mental health impacts of floods [73].

Despite the recent push towards providing consistent health information regarding flooded properties and clear guidelines for building repair, a number of unanswered questions remain on the drying of flooded properties and the potential for microbial growth. Furthermore, much advice is only accessible to professional restorers, not to the general population, who may continue to inhabit flooded dwellings by choice or through necessity. Information about the amount of time taken to dry flooded homes is a topic of interest to insurance companies, health officials, and restoration companies, in order to plan and allocate their resources appropriately after a flood event. It is therefore important to understand how different built forms respond to floods, and to investigate how their drying behaviour can influence microbial growth.

2.7 Remediation in Practice

The difficulty in drying out different types of buildings and the risk from microbial contaminants following floods pose practical issues for flood remediation organisations. There are no specific guidelines available for the choice of equipment used for flood remediation; use of recovery methodologies depend on available resources and type of building. Commonly used techniques for drying out a building include:

- Pumps: Standing water can be removed from the inside of a property using a pump. Absorbent material can also be used to help remove surface water.
- Fans and Air Movers: Forcing air to move around a property increases the drying rate through convection. It is important that sufficient ventilation be provided for the moving air. Injection drying involves directing air flows through drilled holes into voids, for instance, into cavity walls.
- Dehumidifiers: Refrigerant dehumidifiers cool down the air and remove water through condensation, while desiccant dehumidifiers use chemicals to absorb moisture from the air. Dehumidifiers should be used in a closed environment.
- Heaters: Heaters are often used in conjunction with fans to ensure ventilation and air movement, because the warm damp air needs to be removed from the building. Heaters differ in

terms of output, from domestic fan heaters located throughout the building, to high-powered heaters capable of heating multiple rooms to over 60^{o}C. With high-heat systems it is important to understand the construction of the building – timber-framed buildings, for example, may experience warping if they are dried too quickly. The central heating system of buildings can also be used, as long as ventilation is provided and electrical safety assured.

- Combined Equipment: Some equipment is capable of heating and dehumidifying simultaneously.

These different remediation techniques are discussed in [231], with experts selecting one or more of the drying methods they would deem appropriate. Using the existing heating system was agreed to be the most popular method, with natural ventilation also commonly used. Sealing off unflooded sections of the buildings was also used to accelerate drying by two-thirds of experts.

Remediation in Practice: Case Study

The practice of a major UK flood remediation company, Polygon (formerly Munters) [229], makes a useful case study to compare theoretical concerns with real-world recovery efforts.

A major issue in the process of managing flood recovery for Polygon is the many different types and ages of properties affected by contaminated water, and the different ways in which they are dried. The threat of microbial contamination affecting health is always considered by professional remediators, but it has now become an overriding factor in the decision making process. Testing for initial contamination is performed using an Adenosine Triphosphate (ATP) test kit, which allows for the instant screening of surfaces and water for microbial and biological residues. If left empty for even a short period of time, water-logged properties can easily become susceptible to outbreaks of mould, depending on the scale of the event, time of year and level of flooding. This poses an additional hazard for remediation workers and occupants. Agar settle plates are used by Polygon to perform spore counts in contaminated buildings.

A number of issues determine the Polygon drying strategy. There may be pressure to focus initially on the restoration of commercial properties rather than dwellings. Such a focus on economic recovery after flooding may have a particular impact on those who may be unable to leave their properties, such as the elderly, infirm, and those in social housing.

Restoration methods may differ, depending on building type and need to quickly restore them to their original condition whilst at the same time looking at the long term impacts on the properties themselves. Issues with the occupants also need to be considered – for example, whether the householder can be moved to alternative accommodation. Before the initial clean up and drying operation takes place, Polygon disinfects contaminated building surfaces by spraying the room with an antimicrobial solution. A drying regime is then introduced that effectively brings the building back to the conditions that prevailed prior to the flood within a reasonable period of time. All aspects of the make-up and design of the property have to be taken into account when putting a plan together.

A fast dry system is sometimes utilised by Polygon, injecting large volumes of very warm very dry air into the building. Drying times in these situations can be reduced by weeks allowing the re-build process to start much sooner. This process tends to be more effective for certain types of buildings, for example smaller domestic properties, and is not advisable for older buildings. Properties with certain floor and wall types, with cavity wall insulation and cellars are considered to take much longer to dry.

Throughout the drying program, measurements are taken to ensure that moisture content in the different materials is returning to 'normal' levels. Moisture measurement through the profile of the walls or floors is considered essential to ensure that the material is drying through its whole thickness. Material water content is typically measured using an electrical resistance meter and temperature and RH in the air is recorded, allowing for an overall picture of building moisture load to be constructed. When the property is 'deemed as dry' a certificate is supplied, although this can perhaps contain some caveats with issues revealed during the drying process such as inherent damp problems. The water content and humidity levels used to define a property as 'dry' are therefore relative to the property, and no limit conditions for mould or bacterial survival are considered.

Thus, understanding the drying behaviour of different property types, the survival and growth of microbes in flooded buildings, and how this influences the microbial safety of a building is an important part of the process to define when a building is in a habitable condition and is highly valuable information to flood remediation organisations.

2.8 Summary

Flooding is presently a major issue for London, and the threat is expected to worsen due to climate change, urban development, and a policy shift towards flood resilience rather than defence. There are a number of guidelines and standards which can be consulted for restoring a flooded dwelling and preventing health issues in flood victims, however, much of this information is based on subjective data, and scant information is given on what constitutes a 'dry' dwelling, and how moisture levels can impact on the microbial risk inside a property. Furthermore, the wide range of responsibilities and remediation practices that exist can lead to confusion, delays, and variations in restoration quality. Understanding what microbial risks may be present in dwellings can help to assess the risks to dwelling occupants, health officials, and restoration workers who enter a dwelling following a flood.

Chapter 3

Review of Microbial Risk from Floods

The World Health Organisation (WHO) recommends that persistent dampness and microbial growth on interior surfaces and in building structures should be avoided or minimised, as it may lead to adverse health effects [292]. Research shows that damp buildings can support the existence of mould, bacteria, protozoa, and algae [292], and may enhance the survival and transmission of aerosolised respiratory viruses [51]. In addition, microorganisms transported into a building by floodwater may pose a risk to human health.

Residents who remain inside flooded dwellings, those who return to inadequately dried properties, and those whose job it is to dry and repair properties are at risk from indoor microbiological contaminants. The potential microorganisms and their modes of transmission are important to understand in order to assess and protect against the possible health risks in flooded dwellings. This section outlines the potential microbial contaminants found in indoor environments following flooding and summarises the environmental pathways through which they may affect occupant health.

3.1 Microorganisms in Floodwater

Floodwater in urban environments can contain a number of microorganisms which may lead to human infection and be deposited on building surfaces. Floodwater and sediment from floodwater are known to host a number of potentially pathogenic bacteria [103], including those resistant to antibiotics [297]. These pathogens can enter the floodwater through, for example, sewage or faecal matter, or may be naturally present in floodwater. Naturally present pathogens are more robust in the environment, and thus may increase in numbers as they grow in floodwaters. Introduced pathogens are less likely to survive for long periods in floodwater.

The levels of microbial contamination in floodwater will depend on the source of the water, with sewage floods composed of blackwater carrying a much higher risk of human pathogens than clean-water floods. Fewtrell [103] reviewed some of the microorganisms from human and animal sources

in floodwater, on the basis of water source. Sources considered were riverine floods, contamination from rural catchments (rural diffuse), foul water (sewage), Combined Sewer Overflows (CSO), urban non-foul floods, and water flooding from leaking roofs. While the review examined only cases where specific microorganisms were found following a flood (a lack of a microorganism in a flood type does not necessarily indicate its absence, but rather a lack of experimental data indicating its presence), it did demonstrate that a diverse group of microorganisms could be found in floodwater. Sewage and CSO floods are highly likely to contain a number of pathogenic microorganisms in the water. For example, samples taken following a CSO in North London found that CSOs are major contributors of microbial contaminants to urban waters [92].

3.2 Microbial Contamination in Flooded and Damp Dwellings

Post-flood microbial contamination can originate from pre-existing and introduced sources. Floodwater can introduce a number of organisms that can be harmful if they persist on building surfaces or when they produce other bio-hazardous materials. Additionally, damp walls can act as a substrate for the growth of opportunistic and human pathogens deposited during a flood as well as prior existing microorganisms in the air and on surfaces. Biological material in the floodwater, such as sewage effluent, can contaminate building surfaces which may lead to growth on surfaces normally inhospitable to microorganisms. Microorganisms on building surfaces can impact on the health of occupants through direct contact with the individual, or through aerosolisation of part or all of the microorganism into the indoor air.

There is a lack of data on the levels and types of microbial contamination inside dwellings following flooding, but there has been significant research into the microbiology of damp indoor spaces. Microbial contaminants in an indoor environment can include mould, bacteria, protozoa, viruses, and the toxins, cell fragments, and metabolic by-products that the contaminating microorganisms can produce.

3.2.1 Mould

Fungi are ubiquitous eukaryotic organisms found throughout the environment. Mould are fungi that grow multicellular filaments known as hyphae. Mould can emerge from a single organism to form a network of interconnected hyphae to create a colony, or a mycelium, visible to the naked eye. A mature mycelium has fruiting bodies that can produce spores either sexually or asexually. These spores are forcibly ejected from the fruiting body into the air, allowing them to travel great distances until they are ultimately deposited. If a spore's landing surface has suitable conditions, it will germinate to form hyphae, and eventually grow into a new mycelium.

Fungal spores appear on the surfaces of every house, and are easily transported into buildings via active or passive ventilation, or are transported by individuals and objects entering into the house.

Moisture Level	Category of Microorganism
High (a_w> 0.90, ERH > 90%)	Tertiary colonizers (hydrophilic)
	Mucor plumbeus
	Alternaria alternata
	Stachyrobotry chartarum
	Ulocladium consortiale
	Yeasts (e.g. *Rhodotorula, sporoblomyces*)
	Actinomyces
Intermediate (a_w= 0.80 - 0.90, ERH 80-90%)	Secondary Colonizers
	Cladosporium cladosporiodes
	C. sphaerosperum
	Aspergillus flavus
	A. versicolor (@ 12ºC)
Low (a_w< 0.80, ERH < 80%)	Primary Colonizers
	A. versicolor (@ 25ºC)
	A. glaucus group
	Penicillium brevicompactum
	P. chrysogenum
	Alemia sebi

Table 3.1: Moisture requirements for microbial growth. Adapted from [292].

However, mould germination and growth on building materials requires certain conditions, of which the predominant requirement is the presence of moisture. The amount of available moisture in a material is generally expressed as Equilibrium Relative Humidity (ERH) or as water activity (a_w)[1]. The RH required for mould growth and mycotoxin production on building surfaces depends on the surface and species being examined [204].

It has been suggested that mould species in the indoor environment can be classified into groups based on their ability to colonise building materials at different moisture levels [114] (Table 3.1). Primary colonisers are able to grow at lower water activities, and so are often the first to appear when dampness occurs in buildings. Secondary colonisers appear at water activities greater than 0.8, while extremely wet buildings can lead to growth of tertiary colonisers at water activities above 0.90.

The nutrients provided by the substrate also influence the ability of fungi to grow on building materials. Organic building materials, such as wallpaper and textiles have nutrients able to support fungal growth, including carbohydrates, proteins and lipids. However, the presence of contaminants, such as dust, cooking oils, and sediment from floodwater can mean that fungi can grow on biologically inert materials, such as concrete and ceramic tiles. Building products found to be most vulnerable to mould growth include water damaged, aged organic materials containing cellulose, such as wood, jute, wallpaper, and cardboard [115]. Linoleum, gypsum, and canvas insulation materials for plumbing fixtures also show a tendency for mould growth. Research into the relative frequency of mould species

[1]More detail on RH, ERH, and a_w is provided in Section 5.2.2.

found in water damaged building materials in Denmark found primary and secondary colonisers to be the most commonly occurring contaminant species [115].

The growth of mould in damp buildings has been a topic of serious research interest due to concerns about indoor air quality [292]. High levels of moisture on building materials can lead to the growth of mould which can produce aerosolised spores, fragments, toxins, and volatile organic compounds. While there is ample research on indoor mould with sustained damp problems, less literature is available on these agents in flooded properties [53]. Flooding can result in extreme surface dampness, and depending on the duration of the event and flood proofing of homes, water is able to penetrate deep into the building fabric. Mould growth associated with damp housing must therefore be considered as a major risk in homes following floods. Briefly, *Cladosporium, Aspergillus, Penicillium, Alternaria*, and *Stachybotrys* species of fungi have all been observed in elevated levels in flooded dwellings [82, 255]. The colonising species may be related to the water levels, with *Alternaria* species and *Stachybotrys chartarum* found in significantly higher levels in flooded dwellings, while *Aspergillus* and *Penicillium* were found more frequently in non-flooded but nevertheless unhealthy houses [82]. Mould in damp indoor houses is well-documented [292]; readers are directed to this reference for more information.

If moisture conditions fall below the levels required for growth, fungi may enter a dormant state that allows them to survive up to 10 years, for example decay fungi in dry wood [45]. If moisture levels in the substrate rise, growth may resume, thereby reintroducing a risk for occupants.

3.2.2 Bacteria

Indoor bacteria in damp spaces seems to be dominated by Gram-positive bacteria [194]. Bacteria growing on building materials have been studied much less than fungi, however, their presence should also be considered for health reasons [181]. For example, *Streptomyces* species have been proposed to be involved in causing respiratory illnesses in individuals who live in damp houses [134].

Abnormally high levels of total bacteria have been found in mouldy indoor environments, while the presence of mesophilic actinomycetes is thought to be indicative of moisture problems [201]. Actinomycetes, mycobacteria, and Gram-negative bacteria have all been found in materials in damp homes [11, 148, 272]. Variations between bacterial ability to grow on different materials have also been observed, denoted by highest counts on wooden and paper products, and lowest counts on mineral insulation, ceramic products, paints, and glues [148].

Streptomycetes have been found to germinate at a low water activity (a_w 0.67, versus values typically above a_w 0.80 for moulds), and low nutrient requirements indicate the possibility that streptomycetes are among the first pioneer species in damp buildings [181] and may be a lingering contaminant in flood-damaged buildings. Streptomycetes can provoke stronger inflammatory responses and cytotoxic effects than those caused by fungi [146], with responses influenced by the

building material, available nutrients, and microbial interactions on the material [181]. Mycobacteria, commonly found in water and soil, have been found on damp building material samples [272].

Gram-negative bacteria, including *Caulobacter* and *Agrobacterium* have also been found in elevated levels on damp building surfaces [11]. Studies show a correlation between the prevalence of Gram negative bacteria in dust and general Sick Building Syndrome (SBS) symptoms (fatigue, heavy-headedness, dizziness, concentration problems) and symptoms in the mucous membranes of the upper respiratory tract [123].

3.2.3 Protozoa

Amoebae, flagellates, and ciliates are groups of protozoa ubiquitous in wet environments and many genera are considered opportunistic or obligate pathogens to humans and animals. Amoebae require a thin film of water in which to transport themselves and engulf food [304], however most species can form cysts that allow them to survive drought. Several bacteria have evolved the ability to survive phagocytosis by amoebae, allowing them to exploit the amoeba as hosts [192]. Pathogenic bacteria found inside amoebae include Legionella, *Chlamydia pneumoniae*, *Burkholderia cepacia*, and *Mycobacterium avium* which have been associated with respiratory symptoms common among occupants in damp buildings, while *M. avium* has been found in air and material samples taken from damp buildings [304]. Cryptosporidium and Giardia are waterborne protozoa that can be found in floodwater and may be deposited within buildings, but have not been observed to survive long (around 2 hours) on dry surfaces [174].

3.2.4 Virus

It is not yet clear whether viruses are a health risk inside damp or flooded properties. The presence of damp may increase the risk of airborne virus transmission between individuals as the survival and transmission of aerosolised respiratory viruses has been correlated to indoor temperature and humidity [51], thereby increasing the risk of person-to-person transmission. It has been proposed that high humidity in the indoor air could lead to an increased risk of respiratory infection and allergies [133]. Enteric viruses such as Norovirus, Rotavirus, and Hepatitis A and E, can be found in floodwaters [103], and could be deposited on building surfaces.

3.2.5 Biofilms

Biofilms are aggregated communities of microorganisms, including bacteria, protozoa, fungi, algae, and archaea, which are attached to living or non-living surfaces. Biofilms have the ability to protect microorganisms from adverse environmental factors allowing microbes to show an increased persistence on environmental surfaces; these are of particular concern in hospitals. Biofilm development on building materials has been researched [109, 141], with material porosity, surface roughness, and

chemistry impacting on materials' ability to support a biofilm. Temperature, humidity, and light intensity can also affect biofilm growth [108].

3.2.6 Toxins

3.2.6.1 Mycotoxins

Fungi can produce a range of secondary metabolites called mycotoxins that can cause a toxic response in exposed humans even in low concentrations. Filamentous fungi are thought to be able to produce over 300 different mycotoxins [122] which can have carcinogenic, immunotoxic, cytotoxic neurotoxic, mutagenic and teratogenic effects. Interactions between microbes and the substrates on which they grow may also effect the toxicity of mycotoxins, making it extremely difficult to predict potential toxins and diagnose the source of mycotoxicosis [147, 223, 224, 303]. A number of common indoor moulds are known to produce mycotoxins. Individual mould species can produce a number of different mycotoxins, although some species produce the same toxin. Additionally, some fungi can produce synergisers which increase the toxicity of mycotoxins.

3.2.6.2 Bacterial Toxins

Endotoxins are produced by certain Gram-negative bacteria from the proteins, lipids, and lipopolysaccharides found in their outer membrane. Of the components of endotoxin, the lipopolysaccharide (LPS) component Lipid A is responsible for the toxicity. LPS is a structural component, so endotoxins can be released when the cell lyses, although release can occasionally occur during bacterial growth as well.

In studies of building surfaces, endotoxin has been found in water-damaged gypsum liner in damp homes [11, 148]. Studies of endotoxin in household dust show a relationship between endotoxin concentration and self-reported damp [80]. Endotoxins have also been reported in the indoor air where they have attached to dust or water particles [292]. A seasonal variation in their presence has also been observed [215].

Gram positive bacteria can also produce toxic metabolites that can be harmful to building occupants. Mitochondriotoxic isolates produced by actinobacteria, including *Streptomyces* and *Nocardiopsis*, *Bacillus pumilus*, and *Bacillus simplex* have been found in damp indoor environments [219]. Variations in equipment, laboratory techniques, and a lack of definitive standards and guidelines for appropriate levels of bioaerosols makes it difficult to compare different studies of aerosolised endotoxin.

3.2.6.3 Protozoan Toxins

Metabolic products produced by protozoa have been suggested as contributors to humidifier fever and hypersensitivity pneumonitis in the indoor environment [90].

3.2.7 MVOC

Microbial Volatile Organic Compounds (MVOCs) are low molecular weight compounds that bacteria and fungi produce during metabolism and include low molecular weight alcohols, ketones, terpenes, esters, lactones, hydrocarbons, aldehydes, and sulphur and nitrogen compounds [173]. MVOCs are considered to be formed during primary and secondary metabolism. MVOC emission rates have been studied for a selection of fungal and bacterial species commonly found in indoor environments [191].

Due to the relationship between microbial metabolism and the surrounding environment, MVOC production can be greatly affected by microbial species, growth phase, nutrients, pH, humidity, and temperature [173]. MVOCs have been linked to fungal and streptomycete growth indoors [244], and have been used as indicators of microbial growth in dwellings, as their vapour form allows them to penetrate walls and damp proof membranes revealing interstitial contamination. MVOCs have been observed to penetrate building moisture barriers, making them a threat to enter the indoor air from wall cavities [170], indicating their health risk potential.

However, the correlation between their presence and indoor damp is questionable [172, 205]. Over 200 MVOCs have been identified in laboratory experiments, although since primary metabolism is similar in all living systems, none of these can be considered to be exclusively produced by microorganisms. Other sources of non-microbial Volatile Organic Compounds (VOCs) include building materials, vegetation, traffic, food, smoking, and mammalian activities including breathing, sweating, and the shedding of skin [173, 216]. In human experimental exposure studies, lung and eye irritation due to MVOCs only occurs at concentrations several orders of magnitude above those found in indoor environments [173]. However, the MVOC toxicological database is poor, and not all MVOCs have been identified or evaluated, meaning MVOCs therefore cannot be discounted from having an impact on occupant health [173]. Studies comparing MVOC levels to indoor mould can be found to support [91] and refute [177, 205, 243] a correlation between the two. As a consequence, MVOCs are not seen as a good indicator of indoor microbial contamination and are not widely used as an indicator of growth in buildings.

3.2.8 (1→3)-β-D-glucans

(1→3)-β-D-glucans are cell wall components found in most fungi, some bacteria, and many types of plants. As cell wall components, they are capable of being aerosolised as fragments from mould colonies, and have been suggested as useful indicators of mould contamination within a building. (1→3)-β-D-glucans have been reported to have an effect on the immune system, and may cause respiratory problems in exposed individuals [79]. A lack of standardisation in sampling methods,

however, means that the comparison of different studies of indoor β-D-glucan concentration is problematic. Interestingly, they have been found in elevated levels in the airborne dust of houses with fungal problems in Sweden and Switzerland [239].

3.2.9 Summary

It is likely that many health problems observed inside damp and flooded properties are due to a combination of the contaminants discussed above, rather than as a result of a single cause. This is evident in the WHO review of health problems associated with damp dwellings, which concluded that there is evidence of an association between damp indoor spaces and poor health, but do not establish a causal role between any single microbial agent and health. The variety of different microbial hazards inside flooded dwellings present health risks to potential returning occupants and remediators. These pathogens are shown to have a range of persistence on building surfaces, with temperature and RH key factors. Understanding the relationship between microbial survival, built form, and population health following a flood requires a series of integrated models, the required elements of which are discussed in this thesis.

3.3 Environmental Pathways

3.3.1 Airborne Pathways

Following a flood event, airborne pathways are one of the most important routes for human exposure to microbial contaminants in indoor environments. Although the airborne pathways are well recognised, understanding of the extent and the reason for the variation of post-flood biological hazards in different homes and flood events is limited. Bioaerosols occur when a microorganism or microbial product is aerosolised, and can include intact cells and spores, toxins, and cell fragments. Air flows through natural ventilation or through heating, ventilation, and air conditioning systems contribute to the movement of biological contaminants through buildings.

A number of studies post-Hurricane Katrina [29, 232, 237] found elevated levels of mould spores, β-D-glucan and endotoxins in the indoor air, indicating mould and Gram negative bacterial growth. Endotoxins and β-D glucans were found on both small (<1.8μm) and large (>1.8μm) particles in comparable levels, meaning these biocontaminants can be inhaled in high levels deeper into the respiratory system [3]. Other studies [245, 255] found that airborne mould spore concentrations in flooded areas of New Orleans in the months following Hurricane Katrina were significantly higher than those in unflooded areas, with the highest spore concentrations indoors. Studies of different flood events report higher indoor bioaerosol concentrations compared with outdoor concentrations more than three months after remediation [98]; other analyses show evidence of an association between asthma severity and levels of total and Gram negative bacteria and mould spores one year after flooding from the Mississippi in Quad Cities. [238].

Different intervention strategies can also change bioaerosol levels. In Illinois, less mould and bacteria were found in flooded homes with dehumidifiers than homes without [65]. It has been suggested that the high airborne endotoxin levels in flooded homes found in the CDC study in New Orleans were due to the recent remediation efforts, including removal of plasterboard [255], which could have led to the reaerosolisation of endotoxin into the indoor air. Aerosols containing mycobacteria were reported in moisture-damaged buildings while being dismantled [233].

The release of contaminants into the indoor air can depend on the surrounding environment. For example, fungal spore release has been found to be dependent on the fungal species, air velocity above the surface, the texture of the surface, and the vibration of the infected material [113]. This has led to recommendations that exposure assessment of fungal spores be carried out by measuring spore release rates in the vicinity of contaminated areas, rather than merely air or surface sampling. In addition, studies indicating that fungal spores are capable of moving through cracks and joints from sub-floors and wall cavities into the indoor air [7, 261], have shown that microbial growth inside the building fabric itself can impact on indoor air quality. Aerosolisation of bacteria and their spores, viruses, protozoa, and protozoan cysts is also possible by different processes [131]. Vesicles containing viable *Legionella pneumophilia* have been produced by protozoa and may act as agents for bioaerosol transmission [22].

Airborne survival of viruses has been studied in laboratory environments [292]. Viruses with lipid envelopes, such as influenza, coronavirus, respiratory syncytial virus, parainfluenza viruses, and febrile rash infections, will survive longer at an RH ranging from 20-30%. Viruses without a lipid envelope, such as adenoviruses and rhinoviruses survive longer in a high RH of 70-90% [265]. However, current knowledge is based on laboratory experiments using animal viruses; there is a lack of real-world data to address the area [292].

3.3.2 Direct Contact and Fomite Pathways

The persistence of flood-borne microorganisms on inanimate objects is dependent on factors such as solar irradiation, presence of organic matter such as dust or sediment, and most importantly, temperature and water activity [189]. For many pathogens deposited on inanimate objects by flood-water, drying will cause inactivation or death, with the rate of the drying dictating the death rate. Experiments on surfaces under a range of conditions show a range of persistence levels (Table 3.2).

As Table 3.2 indicates, microbial contaminants can show a range of survival times. The survival of bacteria on building surfaces following a sewage flood was examined by the UK-based Water Research Centre (WRc), who studied the persistence of *E. coli* on a variety of building materials [301]. This research found that survival was related to humidity, temperature, and sunlight, as well as the building material, but that contaminated houses should only need to be quarantined for 24 hours after a flood for *E. coli* to fall to undetectable levels. However, outbreaks of *E. coli O157*

	Species	Total Survival Time
Bacteria	*Campylobacter jejuni*	Up to 6 days
	Salmonella spp	1 day
	Shigella	2 days – 5 months
	Leptospira	–
	Enterococcus spp.	5 days – 4 months
	E. coli	1.5hrs – 16 months
	Legionella	–
Viruses	Norovirus	8 hours – 7 days
	Hepatitis A	2 hours – 60 days
	Rotavirus	6 – 60 days
	Adenovirus	7 days – 3 months
	Enterovirus	1 day – 8 weeks
	Parvovirus	> 1 year
Fungus	*Candida albicans*	1-120 days
	Candida parapsilosis	14 days
	Torulopsis glabrata	102-150 days

Table 3.2: Survival of flood-borne pathogens on building surfaces. Adapted from Kramer et al. [174].

infection have been attributed to exposure to contaminated building surfaces [280], with the *E. coli* surviving 42 weeks after initial contamination. It is worth noting that DNA from *E. coli 0157* was found in sediments inside a flooded home after the floods in Cumbria in 2009 [293]. It is advised that while some flood-borne pathogens are thought to die out quickly, for example, *Campylobacter*, others may persist for months (e.g. *C. difficile*) [151].

The wide range of results from different studies into the survival of microbial contaminants on building surfaces is due to the differing experimental temperature and humidity conditions, and may also be due to different rates of material drying and bacterial desiccation caused by the variety of sizes of material samples used in experiments. Under the right conditions, microbial contamination associated with flooding can be diverse and long-lasting, particularly in specific ecological niches within the building envelope which may remain damp for prolonged periods. The survival of microbial contamination varies according to multiple factors; the most critical are water availability, temperature, and building material. It is therefore important to understand the drying dynamics of different locations within the building envelope.

Virus survival on a range of surfaces has also been studied [1, 20, 188], with apparent links found between the porosity of the material and viral survival. Viral persistence can also depend on the type of virus, with gastrointestinal viruses persisting for months, blood-borne viruses for weeks, and respiratory viruses for a few days. The impact of humidity and surface types has inconsistent results, while lower temperatures appeared to increase persistence [174].

3.4 Summary

Microbial contamination can occur in flooded properties through contact with contaminated floodwater, or through the subsequent damp which can provide the moisture required for microbial growth. Microorganisms in damp or flooded buildings presents a risk to occupants by means of direct contact with contaminated surfaces, or through bioaerosols in the indoor air. The ability of microorganisms to grow or survive in indoor environments will depend on moisture and temperature conditions, building materials, and presence of other microbial contaminants; the implication here is that the drying behaviour of a building following a flood can determine the extent of the microbial risk inside the property.

Chapter 4

Health Impacts

Emergency services and disaster planning plays a significant role in reducing the number of injuries due to flooding or deaths due to drowning. Furthermore, planning by the HPA, as well as advances in medical care and a developed infrastructure help to reduce the threat of infectious disease development and spread. However, the long term mental and physical health of the population can depend on the vulnerability of segments of the population, the level and persistence of the damp and contamination within their dwellings, or the length of time in which residents are displaced. The health effects of flooding are difficult to quantify as there is very weak data on the numbers of non-drowning or non-immediate deaths that can be attributed to a flood event [101]. Much of the health data derived following flooding is obtained from opportunistic retrospective studies, which attempt to compare health data before and after an event. These studies often rely on routine surveillance of the health of the resident population, which may increase following a flood and lead to a bias in the numbers reported, further weakening the health-related data. An attempt to predict the health consequences of flooding in terms of physical symptoms (minor injuries, asthma, gastrointestinal illnesses, and earache) and mental health issues have been made by Fewtrell and Kay using Disability-Adjusted Life Years (DALYs) [102].

The next section discusses the potential indirect health impacts caused by microbial contamination following flooding, including exposure to pathogens and mental health issues, and the potential pathways for disease transmission.

4.1 Health Impacts of Microbial Contaminants

Indoor biocontaminants can cause a number of health problems for building occupants. These health problems can be classified as allergic and hypersensitivity reactions, infections, and toxicity.

4.1.1 Allergy and Hypersensitivity Reactions

It is probable that most proteins of non-human origin will cause an allergic reaction in a sensitive subset of the population [287]. Allergic responses to indoor microorganisms and biocontaminants

may be the result of immunoglobulin E (IgE) or immunoglobulin G (IgG) immune response. Of the 21.8 million people reported to have asthma in the U.S., an estimated 4.6 million cases are thought to be attributable to dampness and mould exposure in the home [195]. Sensitisation to fungi has been linked to the presence, persistence, and severity of asthma, while exposure has been linked to asthma symptoms and medication use in children [43, 227, 271]. Hypersensitivity to living bacteria has also been observed, which may lead to exacerbated conditions of bronchial asthma [218]. High levels of endotoxin exposure have been suggested to lead to an increased risk of asthma [182].

The most common form of hypersensitivity, immediate type hypersensitivity, is caused by an IgE-mediated reaction to proteins, and can be initiated by inhaling mould spores or hyphal fragments leading to allergic asthma or allergic rhinitis (irritation or inflammation of the nose). Among indoor allergenic moulds, *Penicillium spp.* and *Aspergillis spp.* are major causes of immediate type hypersensitivity [256]. Immediate type hypersensitivity to bacteria has also been observed in patients with bronchial asthma [218].

Hypersensitivity Pneumonitis (HP) occurs when the normal IgG immune response from inhaled biocontaminants is exaggerated, thereby resulting in an intense local immune reaction. HP is usually induced by high levels of contamination and is therefore most commonly due to occupational exposure, although cases due to humidifiers, air conditioning systems, and pet birds have been noted [129]. Outbreaks of HP have been noted to occur in buildings with Heating, Ventilation, and Air Conditioning (HVAC) systems contaminated with bacteria and mould [105], while the most common cause is thought to be thermophilic actinomycetes.

Less commonly exhibited are Allergic bronchopulmonary aspergillosis (ABPA) and Allergic Fungal Sinusitis (AFS). These IgE-mediated diseases occur when fungi actually grow inside an individual's airway. In ABPA, patients with airway damage from previous illnesses experience fungal colonisation in the airway, but without the fungus invading adjacent tissues. Health consequences arise when the individual is allergic to the specific fungus. *Asperigillus* is the most common fungal species causing this type of disease, although other fungal species can lead to similar conditions. AFS is a similar condition which affects the sinuses. It occurs in individuals who have underlying allergic diseases that provoke poor drainage in the sinus cavity. *Asperigillus spp.* and *Curvularia spp.* are the most common fungal species associated with this condition.

4.1.2 Infection

Fungi are capable of infecting both healthy and immunocompromised individuals. Indoor infections tend to occur only in specific situations.

In normal healthy patients, only a few pathogenic fungi such as Blastomyces, Coccidioides, Cryptococcus, and Histoplasma can cause infection and fatal illness. These incidences are rare, and the majority of serious deep tissue fungal infections occur in severely immunocompromised patients,

for example patients with HIV or on immune-suppressant medications. *Candida albicans* is a fungal species that occurs naturally on the human skin and may become a pathogen in immunocompromised patients.

Superficial fungal infections on the skin of mucosal surfaces are much more common, and include Tinea pedis and Tinea cruris. *Candida albicans* can occur in otherwise healthy individuals when the natural microbial flora at a mucosal site have been removed, for example through antibiotic use. Some superficial infections can also be caused by common mould, for example *Trychophyton rubrum*. Indoor pets can also facilitate the occurrence of fungal infections through the species *Microsprum canis* and *Trichophyton mentagrophytes*.

A wide number of the potential floodwater contaminants discussed in Section 3.3.2 can cause serious infectious diseases. Bacteria and viruses can lead to infections in exposed individuals who are brought into direct contact or exposed to an aerosolised particle. Floodwater can often be contaminated by sewage from flooded sewers, and can contain potentially fatal human pathogens including *Salmonella*, Amoebic Dysentery, *Tetanus*, *Campylobacteria*, Polio, Hepatitis, and Weils Disease [101]. Less serious infectious disease including wound infection, dermatitis, conjunctivitis, gastrointestinal illnesses, and ear, nose, and throat infections may be found in a flooded population. Aerosolised bacteria such as tubercule bacilli, *Bacillus anthracis*, and *Legionella pneumophila* are examples of bacteria that can cause infectivity through inhalation. Viral infection also occurs with direct inhalation of the viral particle.

4.1.3 Toxicity

Disease caused through inhalation of mycotoxins has been a topic of scientific research over the past few years, as a result of the media and legal attention given to Sick Building Syndrome and Toxic Moulds. It is likely that toxins from building-associated fungi and bacteria play a key role in the pattern of disease from building exposures [157].

The relationship between fungal toxins and disease is still unclear. Case studies suggest that individuals exposed to higher levels of indoor mould experience health problems, but in the absence of direct measures of the exposure to mould and mycotoxins it is difficult to assess the role of mycotoxins in these health problems [129]. Bacterial toxicity is due to endotoxins that can be inhaled, and can be transported by blood and lymph from the lungs. It is suggested that bacterial endotoxins may cause rheumatic diseases in individuals living in damp houses [186].

Sick Building Syndrome is an ill-defined, controversial illness. As it is related to indoor air pollution, there are a wide range of possible contributors, including toxic mould, artificial fragrances, poor lighting, microbial infections of HVAC systems, acoustics, and chemical contamination. Consequently, there are a wide range of symptoms associated with the illness, including headache, eye, nose, and throat irritation, dry cough, itchy skin, fatigue, depression, bronchitis, pneumonia, and

symptoms resembling Irritable Bowel Syndrome. Sick Building Syndrome has been tentatively associated with water damaged buildings [253].

4.2 Flood Related Illness

Floods have both direct and indirect impacts on the health of a population. Direct impacts include drowning, heart attacks, and injuries sustained due to the floodwaters or the clean up process, while indirect effects include faecal-oral disease, vector-borne disease, rodent-borne disease, acute asthma, skin rashes, outbreaks of gastroenteritis and respiratory infection, poisoning, and mental health issues [6]. Long-term chronic or secondary, health impacts from flood events can include respiratory problems due to bioaerosols, infections through direct contact, or mental health problems. Comparison of flood events suggest that the risk of death is influenced by the characteristics of the flood (scale, duration, suddenness, velocity, depth, amount of warning) and the population that it impacts [6].

4.2.1 Flood Related Respiratory Illness

Studies into flooded properties have shown an association between respiratory problems and water damaged homes [66, 238]. This suggests that microbial growth is a significant environmental health challenge in the aftermath of major floods in populated urban areas. While no clear increase in the occurrence of respiratory health problems was observed in those living in mould contaminated properties in New Orleans following hurricanes Katrina and Rita, this may be due to limitations of the studies [16]. An increase in respiratory symptoms was observed in those living in damp properties [64], which is consistent with the WHO report that indicates an association between dampness and respiratory health rather than exposure to mould [292].

4.2.2 Flood Related Direct Contact Illness

The WHO suggests that there is little evidence of an association between flooding and infectious diseases in Europe, although there is a surprising lack of data in the literature on this issue [291].

In the UK, an association between an increase in gastroenteritis was observed following flooding in Lewes in 2000 [234], with an increased risk, depending on the depth of the flood in the household. Elsewhere in Europe, flood-related outbreaks of leptospirosis were reported in Portugal, the Czech Republic, and Russia [6, 291, 306].

Worldwide, infection levels increase following floods in countries without access to clean water and sanitation. Post-flood increases in cholera, cryptosporidiosis, rotavirus, nonspecific diarrhoea, poliomyelitis, and typhoid and paratyphoid have been observed in low-income countries [6].

4.2.3 Mental Illness and Vulnerability

Flooding is recognised by WHO as taking a 'heavy toll on the mental health of the people involved' [290]. A literature review on the mental health of disaster victims [207] identifies chronic mental health problems, with Post Traumatic Stress Disorder the most commonly observed, followed by cases of depression, anxiety, stress, and somatic concerns. The mental health of flood victims is recognised as a problem by the UK National Health Service (NHS) [202] and the HPA [142]. The Pitt Review [228] also noted a clear link between people who had to move out due to flood damage and consequent physical and mental health problems, with individuals who had to move out twice as likely to have physical health problems as those able to stay in their dry homes (50% versus 24%). This suggests that displacement due to damp can lead to health problems as well.

It is suggested that death can be hastened by the experience of flooding, rather than caused by it [268]. Following the 1968 floods in Bristol, there were reports of significantly increased mortality rates in the homes that were flooded [21]. There was a significant, observed increase from 6% to 18% between flooded and non-flooded areas of new psychiatric cases in women who showed signs of anxiety, depression, irritability, and sleeplessness. Furthermore, a 50% increase in deaths in the flooded population was reported in the year following the flood. A study of the impacts of the flood on Canvey Island recorded a similar delayed increase in deaths [187]. Tapsell et al. [268] reported that interviewed victims of the floods in year 2000 in the North East of England reported feeling generally unwell, although they could not give any specific symptoms. A study in Banbury and Kidlington following the 1998 flooding in the Thames Region indicated that the psychological effects of a flood can continue for years after the actual flood, and often are more pronounced than physical health effects [266].

In order to predict health impacts from flooding on a population, Tapsell and colleagues [268] developed a Social Flood Vulnerability Index (SFVI) used to assess a populations' vulnerability to flooding based on three social characteristics (long-term sick, single parents, and the elderly) and four financial-deprivation indicators (unemployment, overcrowding, non-car ownership, and non-home ownership). The index is able to predict populations that will have an increased risk of health issues following a flood event.

4.3 Microbial Impact on Building Materials

In addition to the health implications for occupants or damp or flooded dwellings, the presence of microorganisms in buildings can cause structural and aesthetic problems. It has been suggested that about 90% of all damage in dwellings results from temperature and moisture effects on building materials [305]. The presence of microorganisms due to damp is a major cause of this damage, with microorganisms affecting the building material either by using the material as a nutrient substrate

(assimilative process), or via the metabolites produced by the microbe (non-assimilative). Microbial growth can lead to discolouration, corrosion and degradation, and weakening of building materials, leading to aesthetic and structural damages.

Wood is particularly vulnerable to microbiological growth; damage due to biological activity is the main mechanism that affects wood durability [206]. Fungal growth on wood building materials is a major problem in temperate climates such as the UK due to the temperature and moisture requirements of the fungi, and the relatively wide use of wood as a building material.

Fungi that live in wood are generally classified as being mould, mildew, and wood-decay fungi. While mould and mildew are generally restricted to causing only surface damage to wood and other building materials, wood-decay fungi can cause significant reduction in the strength of wood materials used in construction. Brown rot fungi (also known as dry rot) release hydrogen peroxide as they digest the hemicellulose in the wood substrate, while species of soft rot fungi release enzymes which degrade cellulose directly, and white rot fungi break down the lignin component of the wood. All types of rot lead to the weakening of the wood structure, which can lead to structural and cosmetic issues. Wood-decay fungi is a major issue in the UK, with the annual cost of damages caused by wood-decay fungi estimated at £400 million in 1994 [254]. While the focus of this thesis is on the health impacts of indoor microorganisms, damp-related microbial growth can lead to costly structural damage in buildings, and is another critical reason why flooded properties should be dried appropriately.

4.4 Summary

Flooding has the potential to cause health problems to individuals through direct and indirect means. Microbial growth and persistence on building surfaces is a result of flooding, and can indirectly influence the health of building occupants and those entering flooded properties by causing illness after the flood has ended. Fungi, bacteria, viruses, and protozoa can grow and survive on damp surfaces, and produce bioaerosols, meaning exposure can be through direct contact or through respiratory pathways. Mental illness following flooding is also a major risk in developed countries, and can be associated with an individual's vulnerability and potential displacement.

Understanding the ability of dwellings to dry following flooding can help to predict the ability of pathogens to grow and persist within these dwellings, and can be used to evaluate the risk to building occupants and repair workers. Building drying data may also help estimate the duration of displacement for flood victims who opt to leave their properties. Finally, socioeconomic data can be used to assess the vulnerability of the resident population, further helping to understand the chronic health problems which may impact a population.

Part II

Microbial Persistence

Chapter 5

Understanding Microbial Persistence on Surfaces

5.1 Introduction

As discussed in Chapter 3, floodwater and the sediment carried by floodwater can contain a number of potentially pathogenic bacteria, with their persistence on contaminated surfaces generally considered to be dependent on factors such as solar radiation, the presence of organic matter, and most importantly, temperature and moisture content. Therefore, the ability of a material or envelope design to dry quickly is an important consideration in understanding the contamination persistence following a flood. Furthermore, the drying regime to which property is subjected to will also impact on the ability of a contaminant to survive on building surfaces and the risk to occupants through direct contact. Understanding the persistence of opportunistic pathogens on flooded surfaces is crucial to recognising the risk to occupants and remediators entering flooded properties.

5.2 Microbial Contamination of Surfaces

Microorganisms in floodwater may be absorbed in liquid phase into pore spaces of building materials, while microorganisms may adhere to the solid/liquid interfaces between the water and the building surfaces. This solid/liquid interface can include the interface on the boundary of the material, as well as within the pore spaces. The change in the number of bacteria on a contaminated surface is related to the attachment rate, the movement of bacteria away from the surface (emigration), predation, growth, death, inter-colony interactions, and the modification of the microenvironment within the colonies [44]. In young colonies the attachment rate and growth rate are the most important factors in bacterial population growth.

In cases of flooding, the amount of attachment to a surface will depend on the level of contamination within the floodwater and the colonising ability of the contaminating bacteria. Floods with standing water present a higher risk of microbial contamination since stagnant water can have a

higher rate of microbial growth; therefore in standing water floods the duration of the flood will effect the total colonisation of the building surface. The primary colonisation may be followed by a secondary colonisation of bacteria that are able to utilise the protection or nutrients provided by the primary colonisers to grow. Colonisation can lead to modification of the substrate microstructure and RH – roughness is increased, leading to more favourable conditions for attachment and growth [81]. Biofilm development can occur as the colonising bacteria grow and new colonisers join the colony. The susceptibility of a substrate to microbial colonisation is called bioreceptivity [120].

Bacteria also need not attach to the substrate in order to present a contamination risk. Contaminated water that is absorbed in to the pore spaces of the building material may contain pathogens able to survive within the saturated pores. The movement of pathogens into materials will depend on the physiochemical processes of advection, diffusion, dispersion, exclusion, straining, and physical filtration, and the biological processes of growth and decay, chemotaxis, predation, adaptation, adhesion, and detachment. The physiochemical processes above are related to the flow rate of the water, itself dependent on the water pressure and the material pore size; hydrodynamic dispersion, relating to the tortuosity of the convective paths; and the physical filtration and straining, where physical filtration refers to the removal of species by collision and deposition in the porous media and straining refers to the trapping of microbes in pores which are too small to allow for the passage of the species [198].

5.2.1 Microbial Survival Strategies

Microbial contaminants deposited on indoor surfaces during a flood will experience a number of environmental stresses that affect their survival. Temperature and water availability, discussed in Chapter 3, are critical factors affecting the survival of contaminants. Other factors include:

- Ultraviolet (UV) Radiation
- Lack of Nutrients
- Predation
- Competition with other species

Microorganisms have developed a number of strategies for survival, including cooperative behaviour, sporulation, and transformation into a dormant state.

Cooperative behaviour amongst microorganisms allows for recipient microorganisms to benefit from the behaviour of an acting individual. In microbial ecology this can include, for example, the production of siderophores, enzymes which can sequester iron in the natural environment for the entire microbial population, and quorum sensing, where signalling molecules released by microorganisms can help a population communicate and collectively respond to a changing environment.

Spores are reproductive structures that are adapted for the dispersal and survival of species in adverse conditions, and can be observed in bacteria (endospores), fungi, plants, algae, and some protozoa. *Clostridium* and *Bacillus* are bacteria genera noted for their ability to survive long periods by producing spores.

Dormancy is a low metabolic state which allows microorganisms to survive unfavourable conditions. After adhesion or after an external stress such as osmotic shock, thermal shock, or disinfection, microorganisms may enter a viable but non-culturable state [46]. This dormant state can make detection of pathogenic bacteria on contaminated surfaces problematic . Some bacteria attach themselves to surfaces as a means of surviving in the external environment, and can show a decreased susceptibility to disinfectant [240]. As a result of these survival strategies, some microorganisms are capable of surviving in inhospitable conditions for extended periods of time, which may impact the duration of microbial risk on flood-contaminated surfaces.

5.2.2 Water Content of Porous Materials

Material water content is often described using the terms RH and water activity (a_w). RH describes the amount of water vapour in any mixture of water vapour and air. Specifically, it refers to the partial pressure of the water vapour in the air as a percentage of the saturated vapour pressure under the same absolute humidity, temperature, and pressure conditions. In terms of the water content of materials, it refers to the air within the pore spaces, which above a certain RH can lead to liquid water accumulation within the pores. RH is commonly used to describe the moisture levels in building science. ERH can be described as being the RH of a material at equilibrium with the surrounding air [62].

Water activity (a_w) is generally used in microbiological studies to describe the water content of a material available for microorganisms. It is defined as being the ratio of a liquid's vapour pressure to the vapour pressure of pure water at the same temperature [35]. The relationship between water activity and RH can be described by the equation:

$$ERH = a_w \times 100 \tag{5.1}$$

For the purposes of this study, RH will be used in order to remain consistent with previous building science work.

5.3 Objectives

It is widely recognised that the range of results from different studies into the survival of microbial contaminants on building surfaces is due in part to the differing experimental conditions, including the temperature and humidity conditions of the experimental material and/or surrounding air [174].

However, investigations to identify and quantify the factors involved and their links to the hygrothermal properties of building materials and the transient environmental conditions during remediation are rarely reported. Differences in death rates on material types in previous studies (for example, those summarised in Table 3.2) are likely to depend on the ability of materials to dry as well as the environmental conditions.

The objective of this work is to examine the decay of bacteria on the wet surfaces of different building materials under different drying conditions. *E. coli* and *E. faecalis* are inoculated on the surface of wood, plaster, and brick coupons following immersion in synthetic sewage, and then allowed to dry at different rates and at different temperatures. To compare the effects of nutrients within the floodwater, the experiment is repeated using *E. coli* and deionised water. The hypothesis of the experiment is that the behaviour of bacteria deposited on surfaces over time will depend on the type of water, drying rate, temperature, material, and species. An emphasis on the impact of the hygrothermal behaviour of the materials is included by examining the surface RH of material samples as they dry, thus accounting for the relative drying abilities of materials under similar conditions. By relating bacterial population size to the changing RH of the materials, it is possible to develop models to integrate into building simulation software in order to predict the persistence of pathogens within flooded dwellings under different drying scenarios.

5.4 Methodology

5.4.1 Building Materials

Coupons were cut from wood (kiln-dried spruce softwood) and brick (Mayfield yellow multibrick) to approximately 15mm x 15mm x 15mm. Plaster samples were obtained by pouring mixed gypsum plaster (Thistle MultiFinish) into a similar sized mould and allowing it to dry for 14 days. These materials were chosen due to their common occurrence on exposed internal building surfaces, and because of their different hygrothermal characteristics: plaster and brick are porous, hygroscopic inorganic materials, while wood is organic, porous, and highly hygroscopic.

In order to understand the impact of nutrient content in the floodwater, coupons were immersed in filtered water with mineral ions removed (deionised water) or nutrient-rich synthetic sewage for a period of 48 hours. Synthetic sewage was prepared according to the guidelines used in ISO 8192:2007 (Table 5.1) [39]. Following soaking, the coupons were placed inside the individual drying chambers and sterilised at 121^{o}C for 15 minutes in an autoclave. Three coupons were prepared for each drying temperature, drying treatment, material, and water type in order to allow for experimental repetition.

16g peptone
11g meat extract
3g urea
0.7g NaCl
0.4g $CaCl_2 2H_2O$
0.2g $MgSO_4 7H_2O$
2.8g K_2HPO_4

Table 5.1: Synthetic sewage components added to 1L water.

5.4.2 Microbial Indicators

E. coli and *E. faecalis* were chosen as representative species of flood-borne bacteria. *E. coli* and *E. faecalis* are considered to be appropriate model organisms for *Shigella*, enterotoxigenic *E. coli*, *Campylobacter*, and *Vibrio cholerae* [225]. The U.S. EPA recommends the use of *E. coli* as an indicator species in freshwater and *Enterococcus* spp. for both freshwater and saltwater [95].

E. faecalis (American Type Culture Collection 29212) and *E. coli K12* were stored in 10% glycerol at -80 °C. Bacterial cultures used in this experiment were prepared by inoculating a loopful of cell solution on Tryptic Soy Agar (TSA) agar (Difco Laboratories, Detroit, MI) and incubated at 37 °C for 18 hrs in order to obtain the cultures during growth phase.

Bacterial colonies on TSA agar were then suspended in Phosphate Buffered Saline (PBS), (NaCl 0.8%, KH_2PO_4 0.02%, Na_2HPO_4 0.115%, KCl 0.02%, pH 7.4). To ensure that the bacterial concentration in the inoculant for separate experiments were similar, the absorbance of the prepared bacterial suspension was measured at 620 nm (OD620). Serial dilutions of the inoculants from 10^{-1} to 10^{-10} were performed in 0.1 % Tween and plated onto MacConkey (Oxoid Ltd, Hampshire, UK) (*E. coli K12* only) and Bile esculine agar (Sigma-Aldrich, Fluka BioChemika, UK) (*E. faecalis* only) in order to count inoculant concentration. Colony Forming Units (CFU) exhibiting typical *E. coli K12* (characteristic pink colour) and *E. faecalis* (characteristic blackening colonies) morphology were counted following incubation at 37°C for 24 h. This revealed a final inoculant concentration of approximately 5 x10^{11} CFUml^{-1} *E. faecalis* and 3 x 10^{12} CFUml^{-1} *E. coli K12*. The sterile, sewage-soaked coupons were inoculated with 10 µL of bacterial suspension, with *E. coli* and *E. faecalis* inoculated on opposite sides of individual coupons, while the water-soaked materials were inoculated with 10 µL of *E. coli* suspension only. Wood was inoculated on the with-grain face.

5.4.3 Drying

Magnesium nitrate $Mg(NO_3)_2$ and sodium hydroxide (NaOH) were used to remove moisture from the air inside the chambers, allowing the materials to dry at different rates. Both salts are hygroscopic, with $Mg(NO_3)_2$ capable of maintaining RH of 54.38 (±0.23)% at 20ºC and NaOH 8.91 (±2.4)% RH at 20ºC at equilibrium [116]. A petri dish containing granulated salts of $Mg(NO_3)_2$ (70g) was used to provide a low drying rate, while a dish with NaOH (90g) was used to provide a high drying rate.

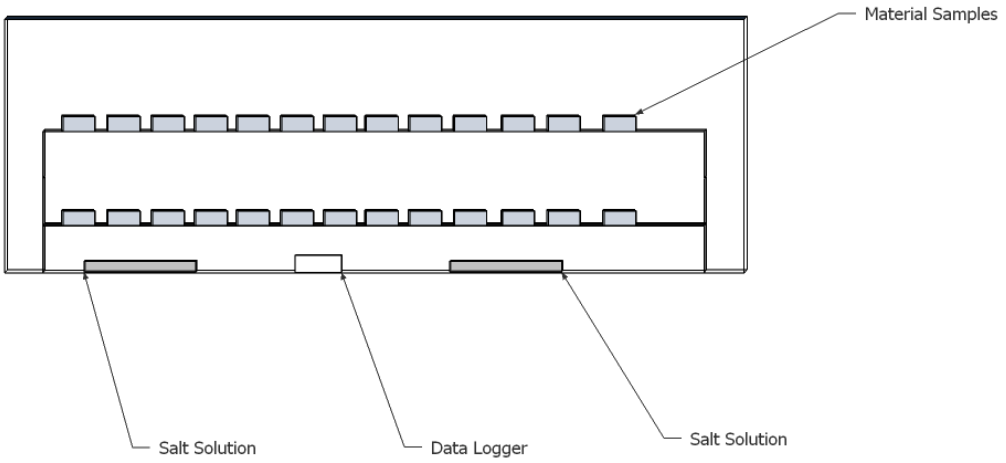

Figure 5.1: Drying chamber design and experimental setup.

The following experiments were carried out:

- Low drying rate at ambient temperature (21-23^{o}C) in chamber **(LDAT)**.
- High drying rate at ambient temperature (21-23^{o}C) in chamber **(HDAT)**.
- Low drying rate at low temperature (8^{o}C) in chamber **(LDLT)**.
- High drying rate at low temperature (8^{o}C) in chamber **(HDLT)**.
- Optimal conditions for E. coli growth (37^{o}C and >97% air RH) in a sealed incubated chamber (wood and brick only) **(OPT)**.

The petri dishes containing the granulated salts were placed inside a sterile chamber containing the 16 coupons of each material type for the desiccating experiments, while no salts were used for the heat treatment. The airtight chamber was then sealed and exposed to the appropriate temperature conditions. A data logger (HOBO U10) recorded the temperature (-20^{o}C to 70^{o}C, +/- 0.54^{o}C) and RH (25% to 95%, +/- 5%) inside the boxes for the duration of the experiment. The experimental setup can be seen in Figure 5.1.

5.4.4 Microbial Sampling and Counting

Sampling was performed immediately after inoculation, and then at 24, 48, 72, and 144 hours. Individual coupon samples were removed from each chamber and placed into sterile 250ml polypropylene vials containing 40ml of 0.1% Tween. Three coupons were taken for each material type, temperature and drying rate to ensure repetition. The vials were vortexed for 20 seconds, and then dilutions in

0.1% Tween solution performed. Dilutions were plated on McConkney and Bile Esculin agar. Plates were inoculated at 37^{o}C for 24-48 hours before counting.

At sampling times a designated reference coupon was removed and the surface RH measured using a Rotronic Hygrolab 3 humidity and water activity analyser (0-100%, +/- 1.5%) until the measurement value stabilised. The surface RH of the material was recorded, and the material returned to the desiccating box.

5.4.5 Material Parameters and Statistical Analysis

Statistical tests were performed to examine the differences in surface drying rates between water and material types, and the differences in bacterial behaviour depending on the water, material, drying type, temperature, time, and the transient RH conditions on the surface and in the air. To test the effects of the drying conditions on the surface water activity, a univariate Analysis of Variance (ANOVA) was performed in SPSS with the surface RH as the dependent variable, the drying type, water, and material type as fixed independent factors, and time and the RH of the air as covariates. To understand the changes in microbial population, the values of Log_{10} CFU material^{-1} and the standard error of the mean (SEM) were calculated for each series of samples using Microsoft Excel. A univariate ANOVA analysis was performed in SPSS for the dependent Log_{10} CFU material^{-1} data with temperature, type of water, and type of material as fixed factors, and time and air and surface RH as covariates. The level of significance was 95% ($P<.05$). Results were examined for both between-subjects effects and interactions between factors.

Finally, decay curves were fit to the experimental data using the online Combase toolkit [61], and the linear inactivation rate and standard error of the curve calculated.

5.5 Results

5.5.1 Drying Rates

Figure 5.2 shows the change in the RH of the air and the material surfaces as the materials dry. As expected, the air and material coupons in the chambers containing the more hygroscopic salts dried much more rapidly that those with less hygroscopic salts. The RH on the surface of the coupons dried at the same rate as the air inside the boxes, with a slight lag. A significant difference between the drying rates of brick versus the other materials could be observed ($P = 0.007$), with brick tending to dry slower than the other materials, particularly under high drying rate and ambient temperature conditions. Water type did not appear to make a significant difference to the drying rate ($p = 0.207$).

5.5.2 Survival of *E. coli* and *E. faecalis* on Material Surfaces

Physical recovery of bacteria from building materials immediately after inoculation showed recovery of viable bacteria varied from 0.04% to 86.7%. A decline could be observed in all bacterial populations

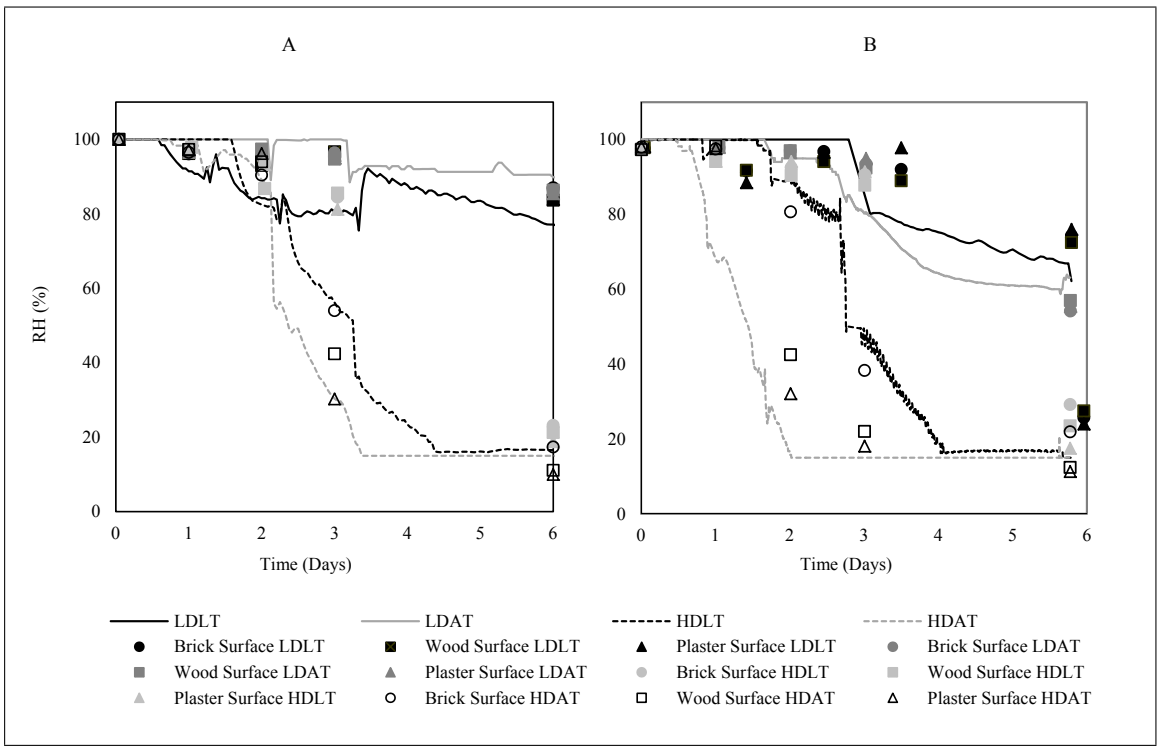

Figure 5.2: Air and surface RH of A) Water soaked materials, and B) Sewage soaked material for Low Drying Ambient Temperature (**LDAT**) Low Drying Low Temp (**LDLT**), High Drying Ambient Temp. (**HDAT**), and High Drying Low Temp (**HDLT**).

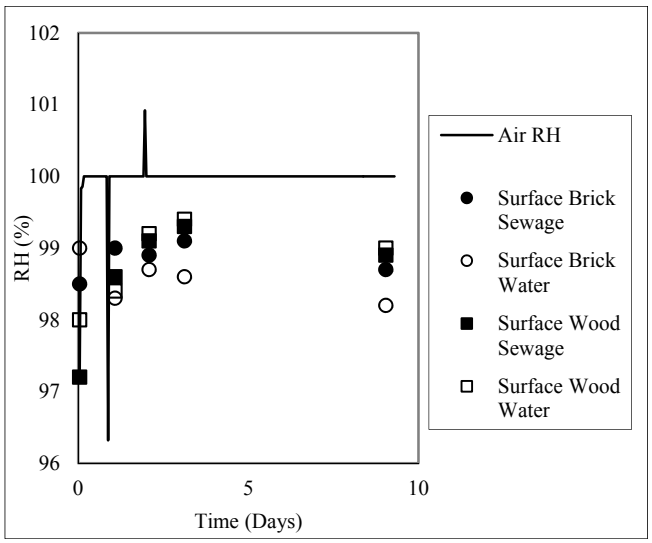

Figure 5.3: Air and surface RH of water and sewage soaked materials under optimal conditions (**OPT**) (37ºC and >97% air RH).

over time, with the exception of the experiment under optimal conditions for microbial growth (**OPT**), which showed an average of 0.9Log_{10} (*E. faecalis*) and 0.7Log_{10} (*E. coli*) increase in bacteria counts per coupon over the initial four days before a subsequent population decline (Figure 5.4 and Figure 5.5).

5.5.3 Effect of Water Types

Different decay curves could be observed depending on the treatment of the inoculated coupons (Figure 5.4 and Figure 5.5). The deionised water treated materials tended to show a rapid initial decline in the population, followed by a tail, while sewage treatments tended to show slower, more linear death rates after an initial stationary phase. There was a significant difference ($p = 0.000$) between the population decline of *E. coli* on drying samples, depending on whether the material had been immersed in sewage or water, with the bacteria on sewage-contaminated materials exhibiting a slower decline. The impact of water type did not make a difference to the amount of growth observed during the optimal treatment ($p = 0.078$).

5.5.4 Effect of Drying Conditions

There was a significant difference between the population declines of *E. coli* subjected to different drying treatments when the coupon had been immersed in sewage ($p = 0.043$), while no significant difference could be observed in any of the treatments following soaking in water ($p = 0.145$). Average microbial decay rates for the treatments based on the fitted curves varied from -0.0249 Log_{10}CFU per day (Low Drying Ambient Temperature Plaster) to -0.6321 Log_{10}CFU per day (Low Drying Low Temperature, Plaster) for sewage and -0.4431 Log_{10}CFU per day (High Drying Ambient Temperature Plaster) to -1.7481 Log_{10}CFU per day (High Drying Ambient Temperature, Wood) for water per coupon (Table 5.2). The impact of temperature in the drying experiments was not significant by itself ($p=0.174$). For *E. faecalis*, there was no significant difference between decay rates based on drying method used ($p = 0.327$).

A significant correlation between the air RH and the *E. coli* bacterial population inactivation was observed ($p = 0.000$). The relationship between the surface RH of the materials and the bacterial decline was significant ($p = 0.004$), although not as strong as the relationship with the air RH, which may be a factor of inaccuracies in the surface water measurements – for materials with high surface RH, the measurement did not always stabilise. No significant difference between the surface and air RH and the inactivation of *E. faecalis* was found ($p = 0.127$).

5.5.5 Effect of Materials

There was no significant difference between the building materials when examining the decline of the *E. coli* population in water soaked materials ($p=0.902$). A significant difference between brick and

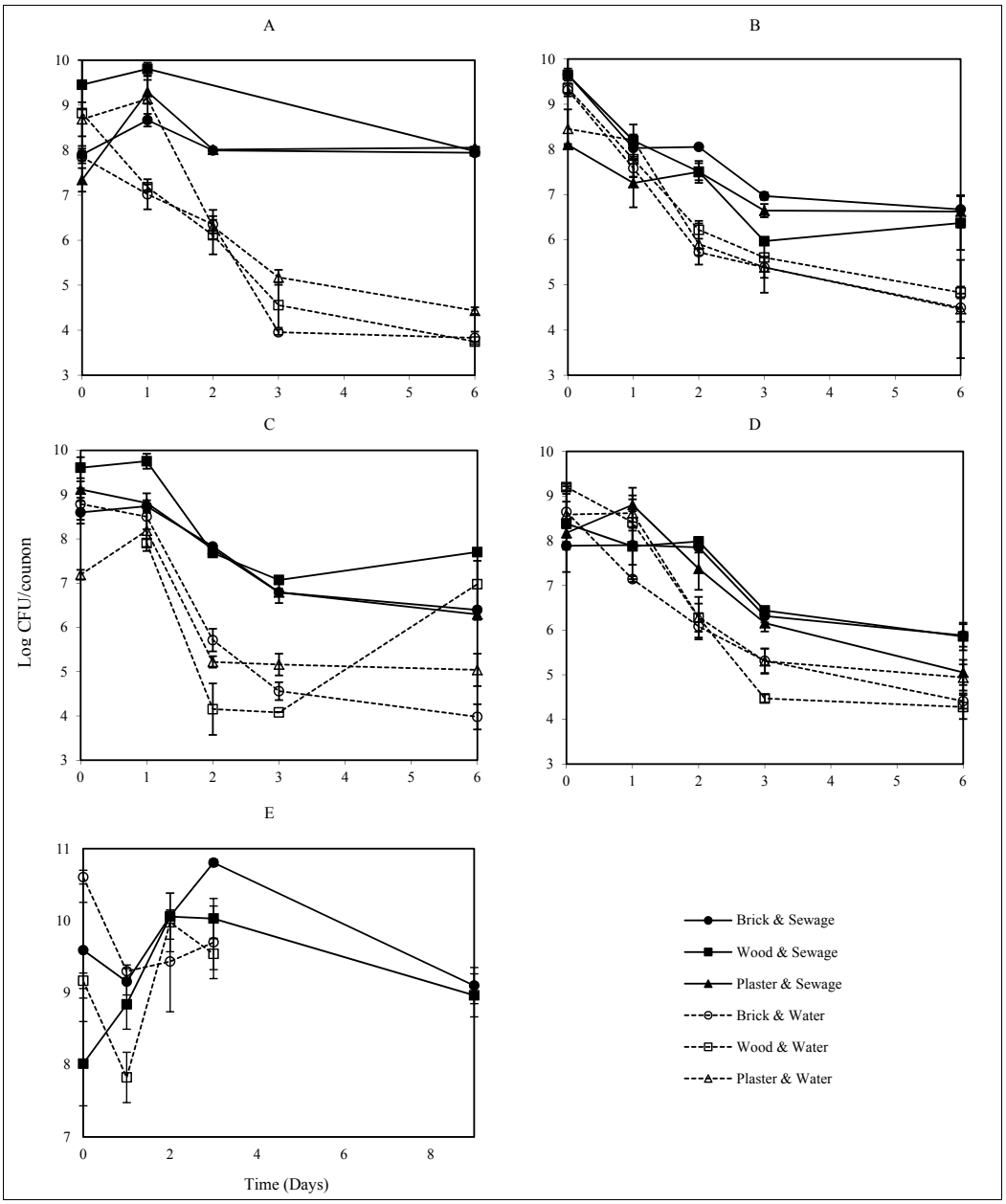

Figure 5.4: *E. coli* population counts at A) Low Drying Ambient Temp. (**LDAT**).; B) Low Drying Low Temp. (**LDLT**); C) High Drying Ambient Temp. (**HDAT**); D) High Drying Low Temp. (**HDLT**); E) Optimal (**OPT**). Error bars represent standard error of the mean (SEM).

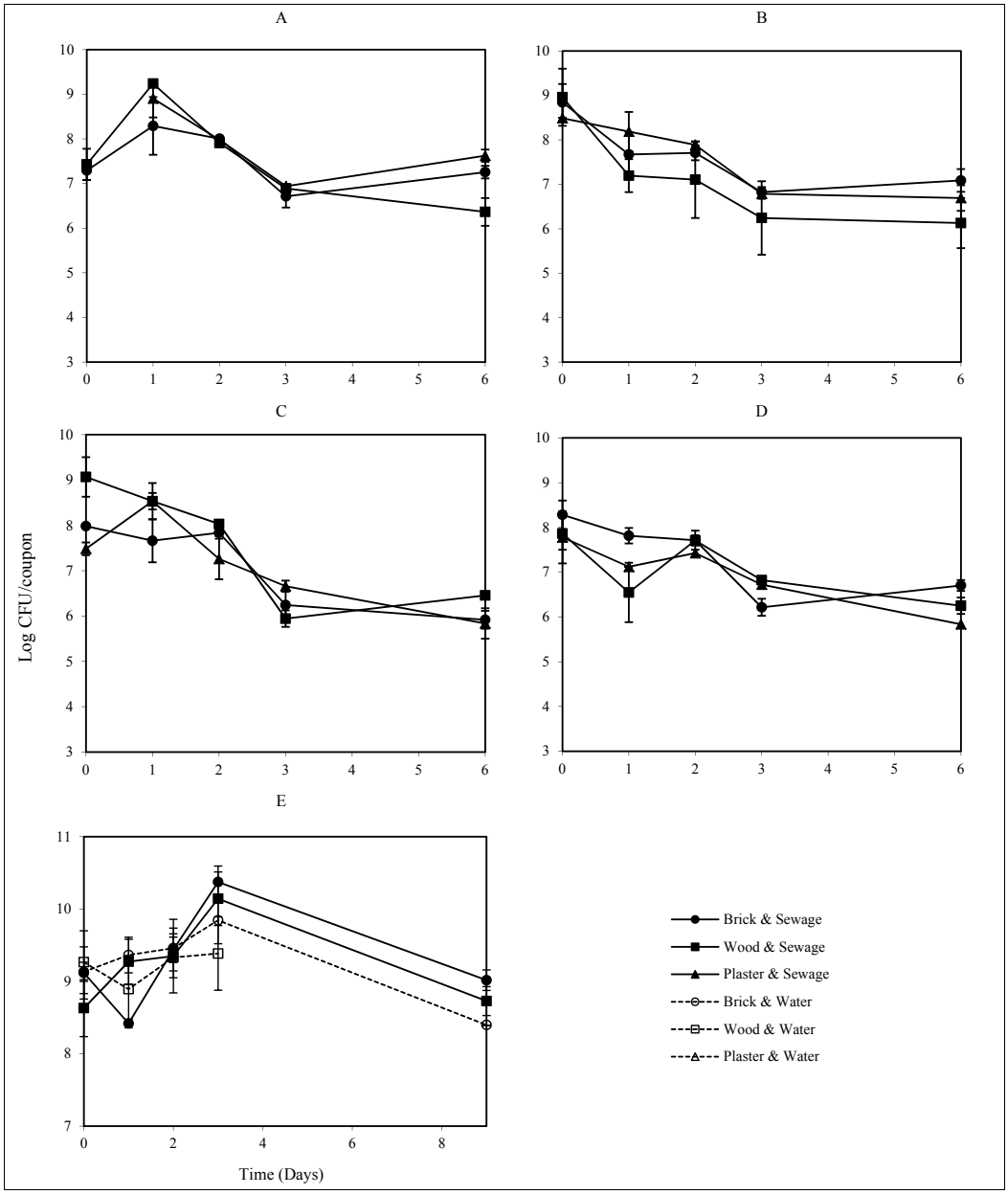

Figure 5.5: *E. faecalis* population changes at A) Low Drying Ambient Temp. (**LDAT**).; B) Low Drying Low Temp. (**LDLT**); C) High Drying Ambient Temp. (**HDAT**); D) High Drying Low Temp. (**HDLT**); E) Optimal (**OPT**). Error bars represent standard error of the mean (SEM).

		Water			Sewage		
		Wood	Brick	Plaster	Wood	Brick	Plaster
E. coli	Low Drying Low Temperature	-0.6949 *(0.1025)*	-0.7531 *(0.1190)*	-0.5306 *(0.2328)*	-0.4395 *(0.0661)*	-0.3855 *(0.0878)*	-0.6321 *(0.1072)*
	High Drying Low Temperature	-0.7597 *(0.2078)*	-0.6683 *(0.0996)*	-0.6712 *(0.1223)*	-0.5138 *(0.1254)*	-0.4452 *(0.0780)*	-0.2099 *(0.0786)*
	Low Drying Ambient Temperature	-0.9770 *(0.1685)*	-0.6967 *(0.0849)*	-0.8063 *(0.1296)*	-0.2724 *(0.1010)*	-0.0362 *(0.0619)*	-0.0249 *(0.1292)*
	High Drying Ambient Temperature	-1.7481 *(1.7835)*	-0.8593 *(0.1339)*	-0.4431 *(0.1451)*	-0.3698 *(0.1047)*	-0.4201 *(0.0621)*	-0.4993 *(0.0594)*
	Optimal Conditions	0.2345 *(0.1787)*	-0.3190 *(0.2040)*	-	0.7447 *(0.1702)*	0.4551 *(0.1800)*	-
E. faecalis							
	Low Drying Low Temperature	-	-	-	-0.3629 *(0.1441)*	-0.2864 *(0.0988)*	-0.3101 *(0.0767)*
	High Drying Low Temperature	-	-	-	-0.2298 *(0.0827)*	-0.2738 (0.0807)	-0.3032 *(0.0679)*
	Low Drying Ambient Temperature	-	-	-	-0.3655 *(0.1056)*	-0.1229 *(0.1007)*	-0.2081 *(0.0999)*
	High Drying Ambient Temperature	-	-	-	-0.4768 *(0.1036)*	-0.3812 *(0.0925)*	-0.3680 *(0.0883)*
	Optimal Conditions	0.0799 *(0.1784)*	0.2398 *(0.0835)*	-	0.4614 *(0.1662)*	0.4792 *(0.1656)*	-

Table 5.2: Calculated linear inactivation and growth rates for treatments in Log_{10}CFU per day, with standard error of the fit (). Results for the Optimal treatment calculated during the growth period (first three days only).

the other materials was observed for the sewage treatment for *E. coli* (p=0.04), with brick having a slower population decline. This is most likely related to the observable difference between the drying of the surface RH of the brick when compared to the other materials, with the brick material drying rate being slower. No significant difference between the materials and material properties and the death of *E. faecalis* in sewage was observed (p=0.453).

5.5.6 Differences Between Bacteria

No significant differences were observed between the population changes of the two bacteria species on sewage in either the drying or the optimal treatment experiments (p=0.699).

5.6 Discussion

Different bacterial decay rates were observed for experiments with differing water types and drying treatments (Figure 5.4). Many of the population curves in this study indicate an initial or final stationary phase, suggesting that a linear assumption of inactivation rates may not be appropriate, and that low-level contamination may linger, regardless of drying treatment. The observable growth over the first few days during the optimal conditions suggests that under certain remediation techniques or climate conditions, growth may be a possibility. The decay following the initial growth period suggests that the growth of the population on the material is limited by factors such as lack of nutrients or population competition.

5.6.1 Water Quality

The difference between the bacterial population change observed for materials soaked in water and in sewage indicates that the content of the water can affect the survival time of the microbial contaminants. While mould, another post-flood contaminant, is capable of utilising the nutrient content of organic and many man-made building materials, bacteria will be more dependent on the nutrient levels of the contaminating floodwater. There was no significant difference between the drying rates of the water-soaked and sewage-soaked materials, however previous studies [171] indicate that materials soaked with salt-containing water dry slower, and it has been suggested that sediment in the water can also delay drying [203]. Therefore, the presence of sediment and salts inside the contaminating water can influence microbial survival by providing nutrients while potentially slowing the reduction in the surface RH.

5.6.2 Drying Regimes

Different decay rates in the *E. coli* populations for the sewage soaked materials with different drying treatments suggest that the environmental conditions have a significant impact on the persistence of microorganisms. Decay rate was closely related to the drying conditions and the reduction of the

air and surface RH conditions. Surfaces with limited ventilation, such as spaces behind furniture, may be prone to longer periods of contamination than others.

While understanding microbial persistence can help inform those entering flooded properties, it can also help advise the best remediation technique. As discussed in Section 2.7, flooded properties can be remediated using a number of techniques such as natural ventilation, dehumidification, or heating. High temperatures are commonly used when treating flooded properties, often by installing a temporary heater capable of injecting large volumes of very warm very dry air into the building. This heat can be transferred into cavities and unventilated spaces, where trapped moisture may remain for extended periods. Growth was observed in the bacterial population over the first three days when the material was treated at a high temperature, and with no ventilation or drying. This suggests that in certain situations, heat treatment of a building may actually increase the growth of human pathogen bacteria.

5.6.3 Materials

The effect of materials on the decay of bacteria was examined. It was expected that the materials would dry at different rates; however a large difference was not observed (Figure 5.2). Only sewage-treated brick exhibited a reduced rate of decline for *E. coli*, which was likely due to the brick drying slower than wood or plaster following immersion in synthetic sewage. The absence of further significant differences in decay rates for bacteria inoculated on the materials is likely due to the lack of significant differences between the drying rates of the materials. This may be because of the small size of the material coupons used, which resulted in a large surface area to volume ratio and an increased ability for the materials to dry. Space restrictions and the need to keep the materials sterile meant it was unrealistic to use larger coupons.

The drying ability of materials vary, with the moisture transport behaviour and the vapour diffusion resistance factor of the materials being the most influential hygrothermal parameters [138], while the porosity and water content of the materials at effective saturation dictates the ability of the material to absorb floodwater. Brick was found to have a reduced decline in the material drying and bacterial decay rate (Figures 5.2 and 5.4); however this could not be significantly correlated to any individual hygrothermal parameter. Hygrothermal parameters have a major influence on the ability of a material to dry, and so will influence the surface RH. Further work should examine the impact of strongly hygroscopic materials such as a wider range of wood products, or materials which are not considered to be hygroscopic but can potentially soak and retain water, such as vermiculite and glass fibre insulation. Those entering flooded properties should be wary of materials that are prone to retaining contaminated water.

The drying behaviour of a flooded surface will depend on the hygrothermal characteristics of the surface material, as well as other materials used in the building fabric, the surface area exposed to

the surrounding air relative to the volume of the material, and boundary environmental conditions including temperature, RH, radiation, and rate of air change and air movement around the material. The differences in drying behaviour between hygroscopic inorganic, hygroscopic organic, and non-hygroscopic materials needs to be considered. Hygroscopic materials can absorb water from the surrounding environment, which in turn can change their thermal and moisture behaviour. At high moisture contents, wood can undergo structural changes due to swelling, causing pore sizes to increase and reducing the hygroscopic effects [57], and can exhibit strong non-linear changes to its water vapour permeability with water content. These effects are difficult to model due to a lack of available material information, and may lead to an overestimate of drying time when using hygrothermal models. Uncertainties, structural changes, and a lack of data in material databases can make modelling the drying of flooded dwellings problematic, particularly with the unique drying behaviour of wood and other organic porous materials. Material and environmental factors can alter significantly between dwellings, and should be considered when evaluating a flooded property.

5.6.4 Bacteria

While no difference was observed between the two types of bacteria tested, this may be due to *E. faecalis* having only been inoculated on sewage-treated materials, reducing the amount of comparable data. Different bacteria may persist for longer periods on surfaces for a variety of reasons, such as a resistance to desiccation and the ability to form spores. Bacteria can also produce endotoxins which can become aerosolised into the indoor air as the population grows and dies off, meaning the threat to occupants from biological particles may not be eliminated through bacterial death. Interactions with other flood-borne bacteria may enhance or restrict bacterial survival. Further work into the persistence of different pathogens following a flood can help to inform about the risks relative to changing conditions inside a flooded property.

5.6.5 Implications for Building Safety

As discussed in Section 2.6.2, there is no consensus on what constitutes a safe 'dry' building. Flooded dwellings should be dried as quickly as possible to minimise microbial contamination, however this is often not possible; occupants and remediators may have to enter properties that have been flooded and left standing, sealed and without drying actions having been taken. While professional flood remediators often use ATP Bioluminescence test kits to search for contamination (refer to case study on page 26), this only identifies the presence of ATP-producing microorganisms within the area tested, and neither the pathogenicity nor the presence of any viral contaminants (which do not produce ATP). Therefore, a better understanding of building damp following flooding developed through building simulation will help to identify the risk of microbial contamination in areas prone to

lingering damp under different post-flood scenarios, and to indicate areas to susceptible to microbial persistence.

The experimental results indicate the importance of water type, drying regime, and material type on the bacterial decay rate. Individuals entering flooded properties should be aware of the type of floodwater present, the ability of different material types to dry, and the potential for microbiological niches to develop in areas where drying is restricted due to construction materials, poor ventilation, and built form. This study has shown that, under certain conditions, growth of bacteria in a flooded property may be possible. In cases where a flood contains highly contaminated blackwater, an understanding of the origin of the contamination, the potential pathogens present in the floodwater, and their abilities to survive on surfaces can help minimise further risks.

Previous research of bacterial contaminants on material surfaces shows a range of different survival times under different conditions. This research confirms the impacts of different drying rates and water types on bacterial survival. However, defining a fixed duration for microbial risk on a flooded surface that applies to all scenarios, such as those suggested by the WRc [302], may not be appropriate, given that the amount of viable bacteria remaining at any one time will depend on initial contamination levels, drying ability of the material in question, and surrounding environmental conditions. The levels and species of bacteria found in floods will vary, depending on the type of flood event. As an example, concentrations of *E. coli* and *E. faecalis* levels in floodwater following an urban sewer flood in the Hague were found to range from 8.7 x 10^1 to 1x10^3 CFU/ml in floodwater and 1.1x 10^5CFU/ml in sediment [269]. The inoculated levels of bacteria in the experiments described in this chapter were intentionally high in order to ensure countable levels throughout the experiments. The risk to occupants will depend on the amount of a pathogen deposited on the wall during the flood, the decay rate, and the infectious dose.

This experiment has assessed the survival of bacteria deposited on building surfaces. The method of recovery was intended to extract the highest number of viable cells possible. While much research has been done on fomite-to-human transfer rates of bacteria through direct contact (e.g. fingers), further research is required to understand how flood-borne pathogens may impact on human health through direct contact with contaminated surfaces or airborne pathways.

5.7 Conclusion

This chapter has examined the implications of drying conditions commonly found in domestic dwellings following a flood event on the survival of flood-borne microorganisms. Previous studies have examined the survival on surfaces relative to different material types and surrounding environmental conditions, but have not related it to the transient drying abilities of individual building materials. By monitoring the surface RH and temperature, a better understanding of the persistence of pathogens on a flooded surface has been developed through the experimentation. The results will

be used in subsequent chapters to test a bacterial model designed to be used alongside building simulation software in order to predict the risk on drying flooded surfaces within the building envelope. The outcomes of this research, as well as the tool developed in the next chapter, will help to better inform on the risks inside flooded properties based on building construction and internal and external drying conditions. By combining an understanding of the persistence of flood-borne pathogens on building surfaces relative to the materials temperature and moisture levels with the ability to simulate the drying out of a flooded property under different remediation regimes using building simulation, we can develop a model of the microbial risk to occupant health.

Chapter 6

Developing a Microbial Decay Model

6.1 Introduction

Understanding the growth, survival, and persistence of microorganisms on surfaces following flooding is important in order to assess the health risks inside the dwelling. Experimental work in the previous chapter demonstrates how microbial growth and survival in dwellings relates to the temperature and RH of the environment, in addition to the properties of the water. To know the relationship between these variables allows for the development of models which can predict the behaviour of microorganisms within the environment in damp indoor spaces. This chapter discusses the existing models for predicting microbial growth in the indoor environment, and develops a simple model for the survival of flood-borne microorganisms on a building surface.

6.2 Common Modelling Methodologies

Modelling methodologies for microbial species can take various different forms, and can vary according to type of microorganism. Mould growth is based on filament spread, and so mould growth tends to be described in terms of radial spread (in distance), or by using an index to describe the degree of coverage of contamination on a surface.

Bacterial and some fungal growth occurs when a single cell divides into two daughter cells through binary fission, and is commonly described in terms of population change over time. Under appropriate conditions, the rate of binary fission in a population exceeds the rate of death, leading to exponential population growth. Some bacteria, such as mycobacteria, can display mycelial growth like that of mould fungi.

Bacterial growth in a closed system with a fixed amount of nutrients and under specific conditions conducive to growth (i.e. batch culture) is often referred to as having four different phases. These are:

- A lag phase, where the bacteria adapt to the surrounding conditions and the individual cells mature.
- An exponential phase, where the population grows at an exponential rate due to cell doubling.
- A stationary phase, where the growth rate slows as the population begins to run out of nutrients and toxic by-products inhibit growth.
- A death phase, where the nutrients run out and the bacteria population dies.

Under poor conditions, death of the bacterial population can occur. Bacterial populations can show different death rates depending on the species and conditions, but can often display population curves with:

- A shoulder, equivalent to a lag phase, where the population is neither increasing or decreasing.
- A death phase, where the population is in decline.
- A tail, where the death rate decreases and can halt, leaving a small persistent population.

A range of modelling techniques are available to describe the different growth and death behaviours of a bacterial population or individual cell in response to its environmental conditions. These modelling techniques can predict bacterial population change during specific phases of growth or death, or through multiple phases. Predictive microbiology is the mathematical modelling of the rate of growth and decline of a microbial population under specified environmental conditions. There are different approaches to modelling the behaviour of a microbial population, including modelling population change under static or transient environmental and nutrient conditions, stochastic growth probability models, growth/no growth interface models, and individual mechanistic models. Predictive microbiology is widely used to model food, soil, and water systems, and predictive mould models have been developed for building science research.

6.2.0.1 Kinetic Models

Kinetic microbial models describe the change in population over time under given environmental conditions. Kinetic bacterial models are often described in terms of primary and secondary models. The primary models describe the population over time in terms of parameters, such as growth rate and initial population size. Using primary models as a basis, secondary models can be developed to describe the factors that affect growth, such as temperature, water activity, and pH. Combining primary and secondary models produces a tertiary model which can be used to predict the behaviour of a population under transient environmental conditions.

Bacterial growth in an unrestricted environment is commonly described using an exponential equation:

$$N_t = N_0 e^{kt} \tag{6.1}$$

Where N_0 is initial population density, k is growth rate, t is time, and N_t is population density at time t. In situations where $k < 0$, the same formula can be used to describe the exponential decay of a bacterial species. With the large number of bacteria typically observed in experiments and in nature, the growth or death of a population of bacteria is often described in terms of logarithms.

$$\ln\left(\frac{N_t}{N_0}\right) = kt \tag{6.2}$$

The growth rate of a population, k, is assumed to be constant in primary microbial models, however previous work, including that in the previous chapter, indicates that growth and survival rates are dependent on surrounding environmental conditions. Secondary and tertiary microbial models are therefore valuable tools in predictive microbiology.

Kinetic models describing changes to the growth rate of a population may also be developed for nutrient limitation scenarios. One of the first microbial models was that of Monod, who described the hyperbolic relationship between microbial growth rate and a limited nutrient concentration, using Michaelis-Menten kinetics, which can be used to describe changes to the growth rate.

$$k = \frac{k_{max} S}{K_s + S} \tag{6.3}$$

Where k is specific growth rate (1/time), k_{max} is maximum specific growth rate in the culture, S is substrate concentration, and K_s is half saturation constant.

The Monod model accounts for the fact that growth of a bacterial population is typically restricted by the amount of available resources, competition from other species, the maximum population density of the supporting substrate, toxin production, and other limiting factors.

6.2.0.2 Deterministic vs Stochastic Models

A deterministic model is a model whereby the variable states are determined by the parameters and previous states. For the same conditions, deterministic models will provide the same result. However, real-world systems contain a myriad of factors that can influence the behaviour of a microbial system. Stochastic models take into account random influences on systems by including random fluctuations, for example, through a Monte Carlo analysis. These stochastic models can be used to show the variation between growth data and predictions from deterministic models due to environmental fluctuations.

6.2.0.3 Growth vs No Growth Models

Models that describe the interface between the growth and no growth of bacterial species have been developed in order to predict the risk of bacterial contamination under specific environmental conditions. These models take the form of an isopleth which indicate the boundary in the environmental conditions that determine whether growth can occur. Often the growth/no growth models have a value applied to the interface, indicating the probability of growth occurring under the specified conditions, and thus enabling the modeller to predict the risk of growth under certain conditions.

6.2.0.4 Individual-based Modelling

Individual-based Models (IbM) use a bottom-up approach to microbial modelling that focuses on global patterns and collective behaviour of the microbial population based on the behaviour of individual particles. These models are well established in ecological models and are becoming more widely used in quantitative microbial ecology.

IbM models the behaviour of individual cells, and can take into account issues such as substrate uptake, cellular morphology, and metabolism. Variability can be added to the system to account for microbial heterogeneity, uncertainty in the cellular processes (e.g.. cellular regulation due to changing substrate conditions), and material heterogeneity. By considering the behaviour of individual cells, a mechanistic model can be created to consider the cellular behaviour in order to predict the behaviour of the population as a whole. An example of an IbM for bacterial population change in response to the surrounding conditions is the BacSim model, which is able to model bacterial colony growth based on the behaviour of individual cells [175].

6.3 Review of Existing Models

6.3.1 Mould Risk Models

Modelling mould germination and growth on building materials is complex, due to the biological nature of the fungal species, the differences between the ability of various building substrates to support growth, and the transient nature of temperature and RH conditions suitable for the species. Several models have been developed to help predict the risk of mould on the basis of the species, substrate, and surrounding conditions. That these models predict the risk of mould growth rather than actual growth means that these models can be used to examine potential mould growth within a building envelope under certain weather conditions, and as a comparison between different wall types. These models are currently limited by a lack of information about different building materials, the ability of mould species to grow on these materials under certain conditions, and a lack of model verification.

6.3.1.1 Adan

Adan [2] describes the growth lag, acceleration phase, and log-growth phase of *Penicillium chrysogenum* on gypsum board material using sigmoidal curves fit to experimental data using non-linear regression. In order to assess the impact of the transient humidity conditions on mould growth, Adan proposes the use of Time-of-Wetness (TOW) as an indicator. The TOW describes the ratio of the duration of the wet periods (>80% RH) to the dry periods in the fluctuating humidity conditions over a 24 hour period, and acts as a measure of the overall water availability for fungal growth. The model assumes that mould growth will take place if a limit value is exceeded, although the inclusion of a lag phase accounts for the delay in growth. Mould growth is calculated in terms of the growth rate per day using a numerical scale of growth coverage.

The model developed by Adan is one of the original transient mould growth models, however it was developed based on data derived from experiments on a single substrate and species. It does not predict mould growth in response to any individual time series of temperature and RH, nor is it capable of predicting species death or decline.

6.3.1.2 Clarke

Clarke and colleagues [58] determine minimum combinations of surface RH and temperature for six mould species by reviewing existing data in the literature. These combinations are used to develop mould growth limitation curves (isopleths), showing the minimum conditions required for mould growth. The species under analysis are prevalent in UK houses and range from hydrophilic to xerophylic species. These species can, in turn, be used as representatives for the behaviour of different physiological groups of moulds, allowing the model to be applied to a broader range of species. The limiting equations for some of the species modelled can be seen in Table 6.1.

The isopleths developed by Clarke and colleagues were based on experiments using laboratory media, which has higher nutrient content than building materials. The mould model was developed using steady-state temperature and humidity experiments, and does not consider the effects of transient temperature and humidity on mould germination. The result of this is that not all points that lie above the mould growth curve will result in mould growth. The model also does not take into account the amount of time that conditions remain suitable for mould growth, nor does it quantify mould growth. The outcome is an 'all-or-none' assessment of mould growth potential. Therefore, this model is best treated as being a worst-case scenario for mould germination risk.

The application of an interface to describe the boundary conditions for mould growth allows the Clarke model to be classified as a growth/no growth model. Probabilities for growth are not included in the Clarke model.

The growth limitation curves were used in conjunction with a building energy simulation program (ESP-r) to predict the likelihood and extent of mould infestation, given the temperature and RH in

Species	Growth Limit Equation
S. chartarum	$RH(\%) = 0.0008(T)^3 - 0.0363(T)^2 + 0.28T + 97.823$
A. versicolor	$RH(\%) = -7E5(T)^3 + 0.0401(T)^2 - 1.6572T + 97.086$
E. herbariorum	$RH(\%) = -0.0011(T)^3 + 0.1005(T)^2 - 2.6876T + 98.171$

Table 6.1: Third-order equation describing the growth limits for different mould species in the Clarke model.

Index	Growth Rate	Description
0	No growth	Spores not activated
1	Small amounts of mould on surface (microscope)	Initial stages of growth
2	<10% coverage of mould on surface (microscope)	-
3	10-30% coverage of mould on the surface (visual)	New spores produced
4	30-70% coverage of mould on the surface (visual)	Moderate growth
5	>70% coverage of mould on the surface (visual)	Plenty of growth
6	Very heavy and tight growth	Coverage around 100%

Table 6.2: Mould growth index (from [281]).

simulated walls. ESP-r allows for the simulation of temperature and moisture flow within porous building materials, thus providing the information necessary for predicting the conditions beneficial to mould growth. The Clarke mould models have also been used with building simulation programs to examine mould growth in building corners [78].

6.3.1.3 Viitanen

A kinetic-type mould model was developed by Viitanen [281] to model mould growth under indoor and outdoor conditions. This model is based on laboratory work [283], which examined the growth of mixed mould species on spruce and pine wood under steady state and alternating conditions of temperature and humidity. This mathematical model includes the effects of temperature, RH, and exposure time, and calculates the mould growth based on a mould index (Table 6.2) that can be determined through visual inspection, either by eye or through stereomicroscopy.

A minimum RH is necessary for mould growth to begin. This critical RH (RH_{Crit}) required for the initiation of mould growth is dependent on temperature. A boundary curve, valid for the temperature range 0ºC to 50ºC, was determined experimentally, and can be described using the equation:

$$RH_{Crit} = \begin{cases} -0.00267T^3 + 0.160T^2 - 3.13T + 100.0 & \text{when T} \leq 20^{\text{o}}\text{C} \\ 80\% & \text{when T} > 20^{\text{o}}\text{C} \end{cases} \tag{6.4}$$

The maximum amount of mould growth possible is limited by the conditions, regardless of the amount of time these conditions are present. The maximum mould growth (M_{Max}) according to the

index (Table 6.2) at any one time under specific conditions depends on the difference between the RH and the critical RH.

$$M_{Max} = 1 + 7\frac{RH_{Crit} - RH}{RH_{Crit} - 100} - 2\left(\frac{RH_{Crit} - RH}{RH_{Crit} - 100}\right)^2 \tag{6.5}$$

Mould growth does not occur instantly when conditions become favourable, so the Viitanen model also takes into account a delay in mould growth when conditions become suitable. Experiments performed by Viitanen suggest that the response time for mould growth initiation (t_m) on wooden materials under constant conditions can be shown as:

$$t_m = exp\left(-0.68lnT - 13.9lnRH + 0.14W - 0.33SQ + 66.02\right) \tag{6.6}$$

where W is Wood species (0= pine, 1 = spruce) and SQ is Surface Quality (0= resawn, 1 = original kiln-dried). For growth beyond the initial stage (M=1), a second regression model can be used to describe the response time for the visual appearance of mould growth (M=3).

$$t_v = exp\left(-0.74lnT - 12.72lnRH + 0.06W + 61.50\right) \tag{6.7}$$

Modelling the increase and decline of mould contamination is done using equations that predict behaviour in favourable and unfavourable conditions. During favourable conditions, an equation for the changes in mould growth index can be derived from equations relating the response time required for growth to be initiated and growth beyond the initial stage. By assuming that the mould index increases linearly with time, the equation for initiation of growth (Equation 6.6) can be differentiated to show how, under variable conditions, with RH above the critical value and temperature in the range of 0^{o}C-50^{o}C, the mould index can change over time.

$$\frac{\partial M}{\partial t} = \frac{1}{7exp\left(-0.68lnT - 13.9lnRH + 0.14W - 0.33SQ + 66.02\right)} k_1 k_2 \tag{6.8}$$

The growth coefficients k_1 and k_2 represent correction factors for growth in the complete and upper growth rate range, respectively.

$$k_1 = \begin{cases} 1 & \text{when M<1} \\ \frac{2}{t_v/t_m - 1} & \text{when M>1} \end{cases} \tag{6.9}$$

$$k_2 = 1 - exp\left[2.3\left(M - M_{Max}\right)\right] \tag{6.10}$$

Where M represents mould growth rate at the time-step, and which can be assumed to be 0 immediately after the wood has been kiln-dried.

In fluctuating humidity conditions, unfavourable conditions can lead to the halt of mould growth, and a delay in mould growth when conditions subsequently become more favourable. Unfavourable

Hazardous Class	Description	Example Species
A	Highly Pathogenic	*Aspergillus flavus* *A. funigatus* *A. niger* *A. penicilliodes* *A. versicolor* *Stachybotrys atra*
B	Allergenic	*A. candidus* *A. restrictus* *Alternaria alternaria* *Penicillium chrysogenum* *Cladosporium cladosporioides*
C	Not dangerous	*Chrysosporium fastidium* *P. citrinum* *Ulocladium sp.*

Table 6.3: WUFI-Bio definitions of mould hazardous classes.

conditions are periods when the RH drops below the critical RH, and can be the subsequent delay of mould growth can be categorised based on the length of time the dry period persisted.

$$\frac{\partial M}{\partial t} = \begin{cases} -0.032 & \text{when } t - t_1 \leq 6h \\ 0 & \text{when } 6h \leq t - t_1 \leq 24h \\ -0.016 & \text{when } t - t_1 \succ 24h \end{cases} \tag{6.11}$$

The mould index value calculated with the Viitanen model under fluctuating conditions depends on the time interval used in the calculation, as the mould index rises faster than it falls in these conditions. Six hours is considered to be the minimum calculation interval, while 24 hours has been used in previous research [284]. This model has been used with HAM programs (LATENITE VTT) to predict mould growth in simulated building environments.

The Viitanen model is currently limited by the fact that it was developed for pine and spruce sapwood, which is typically sensitive to mould growth. Furthermore, the model is weak at simulating mould growth in long seasonal cycles with cold, dry conditions. Work in being done to improve this model by accounting for seasonal cycles and the sensitivity classes of different building materials to mould growth [210, 282].

6.3.1.4 WUFI-Bio

The Wärme Und Feuchte Instationär-Bio (WUFI-Bio) model [249] is based on the hygrothermal behaviour of mould spores. The model allows for the prediction of mould germination (in days) and growth (in mm/day) based on species and substrate categories. Different moulds commonly found inside buildings were divided into three hazardous classes. These classes are defined in Table 6.3.

These hazardous classes were simplified further by joining categories B and C into a common group B/C, as groups B and C exhibited similar growth characteristics.

Substrate Category	Description
0	Optimal media culture
I	Biologically recyclable material, such as wall paper, cardboard, and kraft paper
II	Biologically adverse materials including renderings, some wood and insulation products, and mineral building material
III	Non-biodegradable and nutrient free materials

Table 6.4: WUFI-Bio substrate categories.

Isopleth systems were developed for each hazardous class of mould by reviewing existing literature. These isopleths describe the temperature and humidity requirements for germination times and growth rates on optimal culture. Isopleths for hazardous classes were determined from data on individual species within the classes by drawing new hyperbolic curves that intersect with the lowest points of all the curves of individual species. These lines, known as Lowest Isopleths for Mould (LIM) show the limits for germination and growth of each hazardous class. Below the LIM line, germination or growth is not possible, whereas above this line germination and growth can occur with increasing rates.

WUFI-Bio also accounts for the substrate by categorising the surface on which the mould grows into four different groups (Table 6.4). Again, the categories can be simplified by excluding category III, which will not support any microbial growth. The ability of the different hazardous classes of mould to germinate on different substrate categories is also modelled using an isopleth, with the LIMs shifted to a higher RH to represent the requirements for non-optimal cultures. For growth isopleths, the requirements for the B/C class are taken, as they have lower growth requirements.

These isopleths systems are used in conjunction with a biohygrothermal model. The biohygrothermal model accounts for the transient boundary conditions by modelling the moisture transfer between the surrounding environment and the mould spore. The moisture storage function (adapted from those from bacteria) and the vapour diffusion resistance of the mould spore are used to model the movement of water into the spore, where the isopleths are used to predict the critical moisture levels required for germination and growth. WUFI-Bio does not consider the pH of the material, light or oxygen levels, surface quality, or other biological factors such as competing species. The model shows cumulative mould growth, and does not allow the prediction of the declination of mould growth, because the model does not calculate interim drying out of the spores during dry periods.

By taking into account the mechanistic behaviour of mould spores in relation to the surrounding environment, the WUFI-Bio model uses methodologies similar to IbM to predict mould growth.

6.3.1.5 Moon

Moon [193] developed a probabilistic performance indicator for mould growth risk which treats mould as a risk and limit state phenomenon when the building is exposed to simulated moisture loads.

This model tracks the environmental conditions over time by recording the conditions at the previous time step. Like the methods above, this model uses isopleths for mould spore germination, specifically the data used by Krus and Sedlbauer [249] to develop the LIM model. These isopleths for germination are used to create a mould germination graph, with temperature and humidity conditions required for germination to begin, and each isoline representing the number of days before germination will begin under each condition. At each time step, the length of time spent in conditions favourable for mould growth is recorded, and used to adjust the current mould growth risk. By doing so, the model can account for transient environmental conditions and the moisture history of the spore in establishing the mould growth risk (PI).

Moon added to this mould model by proposing a practical mould growth performance indicator. His hypothesis suggests that the unexpected deviations from the building design – imperfections in build, changes in use, and lack of maintenance - are largely responsible for mould growth. The performance indicator accounts for the fact that building design and operation have an impact on mould growth risk. The indicators are:

(a) The building usage factor which takes into account how the building is used, and how this may contribute to the origin of mould spores.

(b) Correction factor for the substrate effects of different building materials.

(c) A maintenance and operation factor, which accounts for building maintenance and HVAC system operations.

(d) A details factor, which accounts for design defects and mistakes in buildings, such as improper insulation installation or thermal bridging.

The mould growth performance indicator can then be calculated using the equation:

$$\text{Mould Growth PI} = a \cdot (b \cdot PI*) \cdot c \cdot d \text{ where } (0 \prec a, b, c, d \prec 1) \tag{6.12}$$

6.3.2 Limitations of Existing Mould Models

As discussed above, each of the mould models described above have a number of limitations which prevent them from being ideally suited to modelling mould growth in a drying flooded property. One of the limitations of existing models relates to the problem that the models have been developed to calculate the minimum conditions required for mould growth, but not death. These models predict the risk of mould growth inside buildings under operating conditions where the conditions on the

internal surfaces may exceed the moisture limits required for mould growth. By using the minimum required temperature and RH values for growth, these models are able to predict situations where growth may occur. Conversely, at the extremely high moisture contents found following flooding, the question is not whether there is a risk of mould growth, but rather at what point does the risk of mould growth cease? The ability of an established mould colony to hydrolyse its own water sources from the substrate material, and the phenomena of anabiosis or sporulation mean that mould can survive on surfaces under conditions in which they might not otherwise grow. The ability to model the decline of mould colonies is a feature of only the Viitanen model.

In addition, the models do not take into account competition with other species of mould, or indeed, microorganisms that may influence the ability of mould to grow on a building surface. Microorganisms may outcompete each other for limited resources, or produce toxins which can inhibit the growth of competitors, impacting the growth of the contaminants. The limitations of the models mean that there is no ideal model to predict the growth of mould inside flooded buildings.

6.3.3 Mould Model Selection

Against this background, the model of Clarke and colleagues was chosen for this research in order to predict the extent of the mould growth within dwellings. The advantage of their model is that:

- It is simple and easy to integrate into building simulation outputs.
- It offers the means for predicting the growth of more than one species of mould independent of each other.
- The model output is not in terms of a spatial distribution (e.g. WUFI-Bio), or a degree of mould growth (Viitanen), but is a yes/no result which can be easily used to determine whether there is a risk of mould growth on an individual surface within a dwelling based on simulation results.
- The isopleths developed for the Clarke growth models are for agar substrates, an ideal substrate which can represent highly contaminated building surfaces such as those found following sewage or sediment-heavy floods.
- The limitations in terms of the anabiosis of species and the upper limits of water activity for mould growth exist for all mould models, however the Clarke model would be the easiest to adapt with additional isopleths for these phenomena as part of future modelling studies.

The results of the model will therefore be the total surface area within the flooded dwellings which is prone to mould growth at any one time, due to the temperature and moisture conditions on its internal surface. The degree of mould contamination on any surface will not be output, but can be inferred from the length of time that the surface is suitable for growth, as surfaces that will remain

wet for long periods of time under suitable temperatures will have a higher density of mould growth, according to all model predictions.

6.4 Non-Mould Models

The literature does not discuss any existing models for understanding the persistence or development of bacteria, protozoa, viruses, or microbiological biproducts in indoor building environments, however there are a number of models from different fields that may be possible to apply in order to further understand potential hazards.

6.4.1 Bacteria

Bacteria have yet to be modelled using hygrothermal simulations in the same way mould has for building-related work, as the current research focus has been on damp due to building design and operation rather than extreme events such as floods. Sedlbauer states that 'to prevent microbial growth in buildings [it is] sufficient to concentrate upon mould fungi and to coordinate the prediction methods accordingly' [250]. This is justified due to mould having a broad range of temperature and RH conditions under which it can grow, making it a primary coloniser on many damp environments. Furthermore, it is argued that fungal myceliums can act as nourishment for other microorganisms, making the presence of mould an important factor in the appearance of additional species.

However, in the event of a flood, building envelopes can achieve levels of damp sufficiently high for bacterial growth to take place. Furthermore, water from floods or broken wastewater pipes can carry high levels of bacteria, allowing these bacteria to colonise the building surfaces, grow while the conditions are suitable, and then gradually die or form spores as the wall dries out. Therefore, under certain damp conditions, bacterial modelling can be relevant to the hygiene of the building. Like with mould, differences between bacterial ability to grow on different materials have been observed, with highest counts on wooden and paper products, and lowest counts on mineral insulation, ceramic products, paints, and glues [148].

Models have been developed for use in predictive microbiology that take into account water transfer within the growth substrate, thus using many of the same principles used in HAM and indoor mould modelling. Lebert [179] developed a water transfer model for the changes in water activity at the surface of gelatine gel which shares many principles with existing mould growth models in building simulations. Models of bacterial growth and coexistence on variably saturated porous surfaces such as soil [185] can also be adapted to work with hygrothermal simulations. Biofilm models exist [279] which can be used to simulate biofilm structure formation.

The WRc has developed a predictive tool for assessing the risk of indoor contamination following sewage floods on surfaces such as furnishings, hard floors, and plaster walls. The model uses information about the size of the sewage flood event, whether the water was standing or flowing, and the

amount of time after the flood receded, and uses persistence information of different microorganisms to generate a count of the microorganism level on the building surface and the subsequent risk to building occupants [302]. However, since this model does not consider the variation in drying rates of different building envelope structures and niches within these structures, the models assumptions about the drying rate of materials may not be appropriate in cases of sustained damp.

6.5 Developing a Bacteria Decay Model

The objective of this research is to develop a bacterial model that can use outputs from building simulation software as a component to predict the longevity of health risk of bacterial pathogens inside flooded dwellings. By borrowing modelling techniques from predictive microbiology and existing mould models, the behaviour of a set of pathogens at different temperatures and RH are modelled using a simple deterministic tertiary model.

6.5.1 Modelling Methodology

A tertiary deterministic kinetic model for bacterial death, based on data on the growth and decay of bacteria on ideal substrates was selected to model the behaviour of bacteria on a flooded surface inside a dwelling. Primary death rates from experimental data at constant temperatures and RH will first be determined. The variations in the death rates with temperature and water activity will be modelled creating a secondary microbial model. The primary and secondary models will then be combined to produce a tertiary microbial model describing the death rates of bacterial species under transient temperature and RH conditions. The predictions of the developed overall (tertiary) model will be compared with the data observations of laboratory-based microbiological work described in the previous chapter for model validation.

6.5.2 Model Theory and Assumptions

6.5.2.1 Reference Data

The impact of water deprivation on bacterial behaviour has been studied previously using liquid cultures with the available water reduced using salts or polyethylene glycol (PEG) to a solution [137]. A wide range of experimental data is available for the growth and death of microbial species on ideal media. The use of culture media also reflects the assumptions of the Clarke model, where ideal media was used as the basis for the mould isopleths. By using ideal media, the model will account for the potential contamination of dwelling surfaces with sewage or sediment which may help prolong the contamination. Therefore, growth within a bacterial culture was used as the basis to develop the model.

6.5.2.2 Model System Assumptions

Model assumptions are based on those of a continuous bacterial culture, where bacteria are grown in a culture continuously supplied with nutrients within a closed system over time. Any death will be assumed to be caused by the temperature and RH conditions of the surface and not due to nutrient limitations or toxin production. The persistence following deposition will depend on the speed with which the temperature and RH conditions on the surface become unfavourable.

This assumption that death is not due to nutrient limitation is necessary since the total amount of nutrients in the substrate will not be known, as it will vary with the type of nutrients in the floodwater, sediment, and substrate. The accessibility of the nutrients to the contaminating species will also be unpredictable, as nutrients may diffuse towards and away from the contaminating bacteria.

6.5.2.3 Bacteria Deposition

The number and type of water-borne pathogens in floodwater will depend on the type of flood event, while the attachment rate of the bacteria to the surfaces of the dwelling will depend on the material and species. The total bacteria in the wall will depend on the amount of time that the water is in contact with the surface, the concentration of bacteria in the water, the ability of the material to absorb floodwater, and the bacterial attachment rate.

Because of the wide range of unknowns in predicting the amount of bacteria deposited on the surfaces, it is unrealistic to predict the initial levels of bacteria following a flood. Therefore, a model of relative bacteria population will be considered, with a nominal initial concentration of bacteria, N_0.

6.5.2.4 Growth

As observed in the previous chapter, under optimal conditions bacteria can show temporary growth on material surfaces. This growth appears to be restricted by either nutrient limitation or toxin production, since the population was observed to decline towards the end of the experiment. The maximum growth rate observed in nutrient-rich sewage for *E. coli* under optimal conditions was Log_{10} 0.6223 to 0.8207 per day, and was found to stop after a few days. The likelihood of exponential growth indoors following a flood is small due to the typical indoor temperatures of a dwelling and the high temperature requirements for human pathogenic bacteria. Growth of any microbial community will also be limited by the number of nutrients available and by competition with other microorganisms. The limitation of growth observed in the previous chapter is likely due to a limit in the number of nutrients and competition between the bacteria.

In addition, combining both growth and death models into a single dynamic microbial model presents a number of problems, including the occurrence of discontinuities as the population rate of change switches from positive to negative or vice versa, and a lack of consideration for lag time

between the two phases. Because of the small likelihood of exponential growth occurring, explicit growth will be ignored, and we will assume that the population will maintain a constant stationary level when conditions are not predicted to lead to death.

6.5.2.5 Death

The behaviour of bacteria on environmental surfaces under transient temperature and RH conditions is difficult to model due to the lack of available experimental data on the temporal changes due to surface conditions. In addition, it is difficult to extrapolate the results of transient experimental results to create a model able to predict bacteria death for all drying scenarios. Therefore, data from experiments performed under constant temperature and RH conditions will be used in developing the model. Adapting such data to create transient (dynamic) models is an established practice in microbial modelling [278].

6.5.2.6 Lower Limit of Risk

Without knowing the initial amount deposited on indoor surfaces, it is impossible to estimate a precise bacterial count at any one time. Furthermore, the risk of infection to an individual will depend on the rate of transfer of the bacteria from the surface to the individual, the amount of surface area touched, and the pathogenicity of the contaminating species itself. Therefore, the surface was considered to be safe when the initial population had declined to 1% of the initial value.

6.5.3 Model Development

6.5.3.1 Primary Death Model

Bacterial information was downloaded from Combase [15], a web-based resource for quantitative and predictive food microbiology that contains downloadable datasets describing the death of bacterial species on specific substrates and under specific constant environmental conditions. Data was downloaded from the Combase online database for three bacteria species considered to be risks in floodwater [103]. These species included:

- *E. coli*: a faecal indicator found in riverine floods and a potential indicator of sewage contamination in the floodwater
- *Salmonella* spp: Found in riverine, sewage, CSO, urban non-foul, and roof floods and has been observed in the UK literature
- *Listeria* spp: found in rivers, sewage, and in the UK literature

The complete dataset was downloaded for each species over all the temperature and water activity (a_w) ranges available, while data only in the neutral pH range of 6-8 was downloaded, comparable to neutral freshwater or the pH of 7-8 typically found in domestic sewage. Water activity was converted

into RH values using Equation 5.1. Only experiments performed in culture medium (i.e. optimal media) was selected in order to demonstrate the behaviour of the bacteria under the worst-possible scenario, where the death of the bacteria is not due to nutrient limitation.

The Combase database contains bacterial records with and without a calculated death rate. For data records without pre-calculated death rates, the death rate of the bacteria population was calculated using the online Combase Toolbox [61] for each downloaded experimental result. The Combase tool fits a log linear, biphasic (stationary phase followed by log linear death, or log linear death followed by tail), or triphasic (stationary phase followed by log linear death and tail) death rate to the bacterial data, providing the maximum death rate (k_{max}) for the experiment. Only experiments with a fit of better than R^2=0.9 were retained for the next step. This was done in order to reduce the uncertainty in the slopes of the primary models and allow for a better fit to the secondary model.

A total of 37 (*E. coli*), 21 (*Salmonella*), and 42 (*Listeria*) experiments at a range of different temperatures and water activities were analysed for each bacterial species to develop the model.

6.5.3.2 Secondary Death Model

The rates determined from the Combase dataset for population declines at constant temperatures and RH were used to create a secondary microbial growth model by modelling the relationship between the death rates and the experimental conditions. The hourly death rates of the primary inactivation model (k_{max}) relative to their respective temperatures and RH were described using a full polynomial, as per [278] using SPSS.

$$k_{max}\left(T,\varphi\right)=\beta_0+\beta_1 T+\beta_2 T^2+\beta_3\varphi+\beta_4\varphi^2+\beta_5 T\varphi \tag{6.13}$$

In cases where any of the model coefficients were found to be statistically insignificant at p=0.05, they were eliminated and the model was re-fitted. The result was an equation describing the relationship between the instantaneous temperature and RH and the maximum death rate.

$$k_{max}=f\left(T,RH\right) \tag{6.14}$$

6.5.3.3 Integrated Dynamic Model

The secondary and primary bacterial model were combined into a single model describing the population change over time in response to changes in temperature and RH.

$$\frac{\partial N_t}{\partial t}=k_{max}N_t$$

where t is time (hours), and N_t is population at time t.

Bacteria	β_0	β_1	β_2	β_3	β_4	β_5	R^2
E. coli	(-)	-2.12E-3 (0.001)	(-)	(-)	(-)	2.01E-3 (0.004)	0.75186
Salmonella	(-)	(-)	(-)	(-)	(-)	-1.92E-3 (0.000)	0.97587
Listeria	(-)	-2.47E-3 (0.000)	(-)	-1.55E-5 (0.000)	(-)	2.97E-3 (0.000)	0.88765

Table 6.5: Model parameters and their significance (). If the results were not significant, it is indicated by (-).

6.5.3.4 Comparison with Lab Work

The results of the model development for *E. coli* were compared to the experimental data obtained in the previous chapter. The average Log_{10}CFU count and standard deviation at each time step was calculated for the sewage-soaked drying experiments, regardless of the material type. The RH and temperature values recorded by the data loggers for the Low Drying Ambient Temperature (LDAT), Low Drying Low Temperature (LDLT), High Drying Ambient Temperature (HDAT), and High Drying Low Temperature (HDLT) experiments (Figure 5.2) were used to calculate the hourly changes to the death rate (k_{max}) over time. The changes to the population N were calculated and compared with the experimental data (Log_{10}CFU) using Microsoft Excel. The fit between the model and the experimental data was assessed using 95% confidence intervals for the experimental data and by calculating the root mean square error (RMSE).

6.5.4 Results

6.5.4.1 Secondary Inactivation Models

The parameters describing the secondary model coefficients can be seen in Table 6.5, along with the model fits. The quality of the data fits varied in relation to the species, with *Salmonella* showing a strong fit to the data, whereas *Listeria* and *E. coli* were less strong. Removing insignificant parameters resulted in a more stable model particularly outside the temperature and RH ranges from which the models were developed.

For all secondary models, temperature, RH, and the interaction between the two were found to be important in determining the death rate of the bacteria.

6.5.4.2 Validation with Lab Work

Comparisons between the tertiary *E. coli* model and the average of the *E. coli* experimental data at each time step and for each experimental drying condition can be seen in Figure 6.1. Comparisons between the model and the experimental data showed that the model provided a conservative

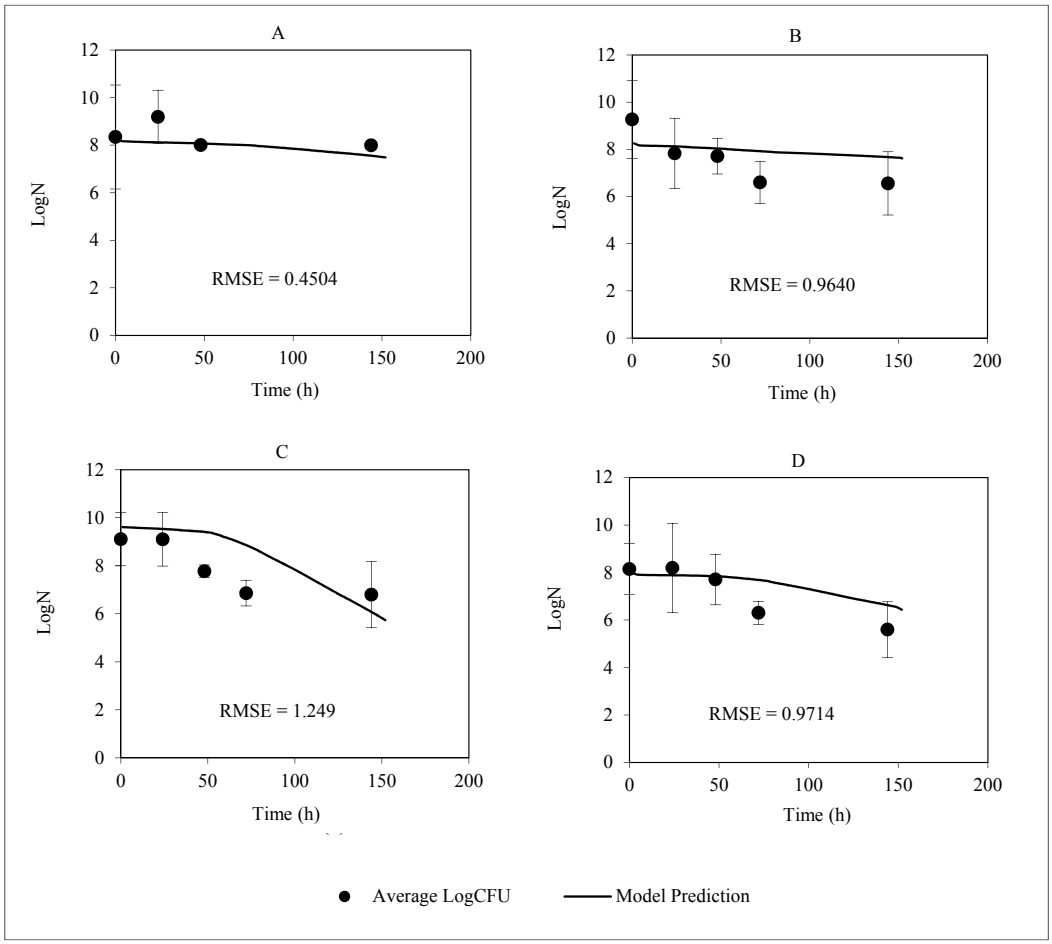

Figure 6.1: Model predictions compared with experimental results for bacteria drying under LDAT, LDLT, HDAT, and HDLT conditions. Error bars indicate the 95% confidence interval of the experimental results.

estimate of the decline of the bacterial population, underestimating the decline that was actually observed, but typically passing through the 95% confidence interval for the Log_{10}CFU count for the experimental data. The calculated RMSE suggests that the model error ranges between 0.45 Log_{10}CFU and 1.25 Log_{10}CFU. By overestimating the population size, the model can be considered 'fail-safe'.

Some of the experimental results (for example HDAT) exhibited a tail towards the end of the experiment, where the decay rate dropped off despite the conditions remaining unfavourable. However, the tails exhibited in the experimental data occurred below the 1% threshold for the model, indicating that they were below the point where the surface would be considered to be 'safe'.

6.5.5 Discussion

The fitting of the model to the Combase data has resulted in a robust and fail-safe model of bacterial decline under transient environmental conditions, meaning that it can be applied to predict microbial decay on flooded dwelling surfaces under drying conditions under worst-case scenario assumptions.

The derived model reflects changes in the rate of population decline observed during the laboratory experimentation of the persistence of bacteria on drying surfaces following contamination with synthetic sewage. The model provides a useful description of bacterial population changes observed in the experimental data, considering that the Combase experimental data was obtained by performing experiments using different media. In comparison with the laboratory experiments, the model provides a conservative estimate of the population size, rarely predicting a smaller population than was actually present. As such, the model produces a fail-safe result that predicts the decline in the population of *E. coli* on a surface over time, drying in transient temperature and RH conditions. By developing a model with data derived from experiments on ideal media and comparing the results with experiments on materials flooded with nutrient-rich synthetic sewage, this model is intended to predict bacterial population decay following a foul-water flood, and so it can be applied with the assumption of the worst-case scenario for floodwater nutrient content.

This model can be used alongside temperature and RH conditions output from building simulation models to estimate the degree of contamination on indoor surfaces in dwelling affected by flooding. The 1% threshold for the surface to be considered as safe is arbitrary, and based on the assumption that the risk of infection through direct contact is insignificant at lower levels of contamination.

6.5.5.1 Model Limitations

There are a number of limitations to this model, particularly given the assumptions made. By excluding situations where microbial growth may occur, the model has ignored the possibility that contaminating human pathogenic bacteria may increase on the surface. However, as experimental work has demonstrated, even under optimal conditions, growth potential is limited, and growth under typical operating conditions of UK houses is considered to be unlikely.

The Combase data used to develop the model was only available for a range of RH values typically found in food (0.7-0.99), and temperature values from 0^{o}C to 50^{o}C. Normal operating conditions inside dwellings are unlikely to go above or below the temperature range found in the Combase data, however under drying normal operating conditions, the RH of a wall may drop below the 0.7 limit of the data. Eliminating insignificant parameters from the model and reducing the terms means that the resultant model is robust and provides stable results outside the range of the Combase dataset. However, due to the lack of available data on bacterial death rate at these low RH values, using the model below an RH of 0.7 is not recommended.

A lack of knowledge about the initial population of bacteria deposited on the surface makes it impossible to calculate a precise estimate of number of bacteria per unit area of flooded surfaces. By calculating the risk on the surface based on a relative amount, the issue of specific population sizes is ignored, but in events where there are extremely high levels of contamination, the remaining 1% threshold deemed to be safe may actually pose a health risk to occupants, and therefore the duration of risk may exceed those predicted by the model.

There are also a number of environmental variables not included in the model which can contribute to the decay of microbes on building surfaces. Like the mould models discussed above, these models do not take into account the UV radiation that external building faces are exposed to, and so the models will not be appropriate for calculating the risk on these surfaces. Competition, predation, and nutrient limitation are also not considered. While not including these factors in the model affects the accuracy of the model, ignoring them allows for the prediction of the 'worst-case scenario', and offers a fail-safe prediction of the relative risk on surfaces.

6.6 Conclusions

A number of mould growth models have been developed to predict the risk of contamination in indoor environments. These models build on established microbiological modelling techniques to predict mould growth (in the form of occurrence, radial growth, or degree of growth coverage) according to surrounding conditions (temperature, RH, and potentially material type) for different species. While no mould growth model is ideally suited to modelling the presence of mould in drying flooded properties, the model proposed by Clarke and colleagues provides a simple growth/no growth threshold that can be applied to the interior of drying dwelling archetypes without requiring knowledge of the internal surface finishes present in the dwelling. Used alongside building simulation data of a drying dwelling, it can indicate the total surface area at risk of mould growth within the dwelling, without considering the actual degree of growth.

While there have been a number of mould models developed to predict growth in indoor environments, other microorganisms found in damp indoor spaces have been ignored. Predictive microbiology is an established technique used in food, medical, and environmental microbiology to predict changes to bacterial populations over time, and in response to different environmental variables. The derived model for the decay of *E. coli*, *Salmonella*, and *Listeria* on surfaces following flooding builds on previous microbiological modelling techniques, using aspects of a kinetic decay model to predict the instantaneous decay rate of a population, and uses this information to predict the decay rates of a bacterial population deposited on a dwelling surface. It is able to provide a useful estimate of the amount of contamination on indoor surfaces, and therefore the risk to dwelling occupants to infection through direct contact pathways. By using temperature and RH as the parameters for

calculation, the resultant model can be applied alongside building simulation models to predict the bacterial threat inside drying flooded dwellings.

Part III

Building Simulation

Chapter 7

Developing a Model of London's Dwellings

7.1 Introduction

Predicting the impact of flooding across the housing stock requires information on the location of dwellings, the exposure of dwellings to potential flood events, the built form and construction methods and materials used, and the surrounding environmental conditions. The information required to develop such a model can be obtained from a range of different sources, including existing models and dwelling archetypes, GIS data, surveys, and material information databases. By combining different data sources the impact of flooding on different property types can be determined using building simulation models, while the results of the simulation can be mapped out across areas of flood risk to identify vulnerable locations.

Any potential housing stock model for flood recovery will be complex due to the variations in the physical form and construction of dwellings. In the UK, the housing stock has been constructed over a long period of time, with a wide range of materials and building techniques used, implying that a range of assumptions are necessary in order to develop a model. Many of these assumptions are already in use - housing stock models are widely used for energy consumption estimation and energy policy development in the UK - and these models can be adapted for hygrothermal simulation. Models of the current housing stock can also offer insights into future scenarios, as the London housing stock is predicted to change slowly. New construction occurs at a rate of less than 1% of the total stock per year [248] and under the most ambitious demolition scenario, 70% of 2050's homes already exist [89].

The objective of this chapter is to develop a housing stock model which will enable the whole-building hygrothermal flood simulation of dwelling archetypes, and make it possible for the results of the simulations to be mapped out across a research area. Existing housing stock modelling methodologies, dwelling classification methods, data requirements to perform whole-building hygrothermal flood simulations, and the geospatial data required to map the results across the research area are

reviewed. The results of the analysis are presented and the integration of the different components is discussed.

7.2 Existing Housing Stock Models

Housing stock models have been developed to describe the types of dwellings present in a research area and can be classified as bottom-up or top-down models. Bottom-up housing stock models are built from a hierarchy of disaggregated components which are then combined according to estimates of their individual impacts. Bottom-up models based on building physics tend to consider dwelling archetypes, which are nominal dwellings representative of the types of dwellings in a housing stock. Building physics calculations are then used to estimate, for example, the energy consumption based on utilisation scenarios. There are a wide number of different bottom-up housing stock models for the UK; these range from 2 to 1,000 dwelling archetypes [161]. Top-down models are built from aggregated data, for example fitting historical energy consumption data, and so do not have the level of constructional detail or historical flood recovery data required for this study. A variety of housing stock models with research topics as diverse as energy, flooding, and health have been developed.

7.2.1 Energy Modelling

Kavgic and colleagues [161] review many of the existing housing stock models used in the UK for energy research. Of the existing housing stock models in the UK, most bottom-up models divide the housing stock into age-type groups and define dwelling archetypes to represent these dwelling types. Dwellings of different ages have different built forms, and can be constructed using different methods and materials. In studies of energy consumption this is reflected, for example, in the differing heat transfer characteristics (U-values) for walls of different ages [34], which are based on assumptions about materials and material thicknesses. In order to calculate heat loss, the structure of the dwelling is used to infer the area of external walls and the internal layout of dwellings. Consequently, housing stock information available for analysis tends to be divided into age brackets and dwelling types that have similar layouts, and wall and floor constructions.

7.2.2 Hazard and Vulnerability Modelling

As discussed in Section 2.5, the impact of flooding on a dwelling can be considered as tangible or intangible [220]. The magnitude of tangible damage on any one property is the cost of repairing the damage, or if it is not repaired, the loss in value of the property. The relationship between the tangible damage following a flood and the flood characteristics is typically described using depth-damage curves, which are considered to be essential for hypothetical damage estimates [220].

The underlying assumption of these curves is that, given the same flood conditions, damages are transferable between dwellings of the same characteristics.

Building on early work by Penning-Rowsell [220], the Flood Hazard Research Centre (FHRC) at Middlesex University has studied flooding in the UK extensively, and produced a series of manuals with depth-damage curves for various land use categories, and for two arbitrary flood durations (Short - less than 12 hours, and long-more than 12 hours) [222]. Nine land use types were examined, including residential properties. The residential properties were classified into:

- five housing types (detached, semi-detached, terrace, bungalow, and flat);
- four housing ages (pre-1918, 1918-1938, 1939-1965, and post-1965);
- four social categories reduced from six social classes;
- the independent housing type category of "pre-fab" which is subdivided by neither age nor social class.

The dwelling types were based on standard dwellings defined by the typical size, construction type, and an estimated inventory inside the property. Depth-damage curves work in conjunction with maps of inundation depth and land use in order to predict the amount of damage. The value of the property and its components, and its susceptibility to flooding is estimated; thereafter a function is fitted, describing the predicted damage according to the calculated depth of the flood. An updated version of the FHRC by Suleman and colleagues [259] added the cost of cleanup to the depth-damage functions.

The Dundee Flood Loss Tables [24] provide a financial damage estimate for flooding in domestic properties based on depth, duration, velocity, contaminating substances, salinity, season, and dwelling type. The dwellings are classified as:

- semi-detached
- detached
- ground-floor flat
- terraced
- bungalow

The financial losses for flooding were calculated as a function of the total insured sum of the property.

GIS and dwelling classifications have been used by Fedeski and Gwilliam [99] to create a methodology for assessing vulnerability and risk to dwellings of damage from floods. This methodology involves estimating the damage likely as a reinstatement cost through an assessment of their exposure, hazard, and vulnerability of individual dwellings. Dwellings are classified by Fedeski and Gwillian in terms of:

- Property type: Nature, Number of storeys, and dwelling type
- Property Age: As an indicator of foundation type, internal and external wall and roof construction, and the use of lime or cement in construction
- Structure type: As an indicator of potential resilience to ground movement
- Property Design: Extensions, bay windows, basements, listed dwelling status
- Openings: Location, type and scale of windows, doors, air bricks
- Context: Conservation area status, trees/vegetation (where swell/shrink soils are present), site slope.

Event severity is discretised into classes (low, moderate, high, intense, devastating), as well as building vulnerability (very resilient, resilient, average, susceptible, very susceptible).

Blong [28] also classifies building types for his study of risk for natural hazards. His classifications include:

- Small House
- Median House
- Large house
- Admin (1-3 Storeys)
- Admin (3-10 storeys)
- Town Hall
- Library/Museum
- Police Station (suburban)
- School
- University

Unlike the other models used to predict damage, Blongs' model does not account for the built form of the property.

Outside of the UK depth-damage curves have been developed for use in the Netherlands, where floodwater velocity is considered [169], Hungary [125], and Germany [153, 165, 197, 235], however, they are not regarded as applicable to UK dwellings due to differences in construction techniques, layouts, and the pattern of durable ownership [220]. Housing stock models have also been developed for research into indoor air quality and health. Jones and colleagues [159] studied cardio-respiratory

disease in relation to the built environment through dwelling classifications and the implementation of a sub-model to identify dwellings with mould and carbon monoxide problems.

While housing stock models are well-established for energy performance simulation, flood damage calculations, and health impacts, there is no appropriate set of dwelling archetypes to simulate the post-flood drying of typical UK dwellings using HAM models. This gap in the literature can be addressed by supplementing existing models with suitable hygrothermal data.

7.3 Definitions of Dwellings

Combining different data sources to develop a dwelling archetype model is complicated by the wide range of definitions and categorisations of dwelling types and age classifications used by data providers. The 2001 Census categorises dwellings as houses and bungalows, flats, maisonettes, apartments, and bedsits. No definitions are provided for these. Houses and bungalows are divided into detached, semi-detached, and terraced. The classifications for flats and houses have changed with each census. The English Housing Survey (EHS) (formerly the English House Condition Survey -EHCS) uses categories similar to those of the 2001 census, but with a finer categorisation with respect to terraced houses and purpose-built flats, and have bungalow as a separate category. The Survey of English Housing (SEH) and the British Household Panel Survey (BHPS) show differences between how dwellings are classified in 1981 (enumerator) and 1991 (householder).

Age classification brackets also differ according to the body providing the information (Figure 7.1). These classifications guide assumptions about the built form and construction of different dwellings, and are meant to reflect periods of design and construction practice. Developing an archetype model using dwelling data with different age classifications can require combining age brackets and matching brackets with slightly offset beginning and ending years.

7.4 Housing Stock Model Development

There is a range of different models and data sources for developing a housing stock model suitable for use in hygrothermal simulation and flood modelling.

Existing Models Housing stock models for hygrothermal simulations require many of the same inputs as energy simulations. Age-structure archetypes can be used to estimate the wall constructions for internal and external walls, and the surface area of the floors and walls exposed to flooding and drying scenarios. The type of wall in a dwelling can also be used to attempt to infer the air change rates due to infiltration, which can be used to model the internal drying of unventilated dwellings. Examples of existing models include: Allen and Pinney [8], who describe standard dwelling dimensions, construction, and occupancy schedules for building simulation modelling; the

<table>
<tr><th>Year</th><th>EHCS</th><th>SAP</th><th>HEED</th><th>Cities Revealed</th></tr>
<tr><td>1800</td><td rowspan="2">Pre 1850</td><td rowspan="5">Pre 1900</td><td rowspan="5">Pre 1900</td><td rowspan="2">Historic to End Georgian</td></tr>
<tr><td>1825</td></tr>
<tr><td>1850</td><td rowspan="2">1850-1899</td><td rowspan="2">Early and Middle Victorian</td></tr>
<tr><td>1875</td></tr>
<tr><td>1900</td><td>1900-1918</td><td rowspan="2">1900-1929</td><td rowspan="2">1900-1929</td><td rowspan="3">Late Victorian/Edwardian</td></tr>
<tr><td>1925</td><td rowspan="2">1919-1944</td></tr>
<tr><td></td><td>1930-1949</td><td>1930-1949</td></tr>
<tr><td>1950</td><td rowspan="2">1945-1964</td><td rowspan="2">1950-1966</td><td rowspan="2">1950-1965</td><td rowspan="2">Post War Regeneration</td></tr>
<tr><td></td></tr>
<tr><td></td><td>1965-1974</td><td>1967-1975</td><td>1966-1976</td><td rowspan="2">Sixties and Seventies</td></tr>
<tr><td>1975</td><td>1975-1980</td><td>1976-1982</td><td>1977-1981</td></tr>
<tr><td></td><td>1981-1990</td><td>1983-1990</td><td>1982-1990</td><td rowspan="4">Recent</td></tr>
<tr><td></td><td rowspan="4">Post 1990</td><td>1991-1995</td><td>1991-1995</td></tr>
<tr><td>2000</td><td>1996-2002</td><td rowspan="3">Post 1995</td></tr>
<tr><td></td><td>2003-2006</td></tr>
<tr><td></td><td>Post 2007</td></tr>
</table>

Figure 7.1: Different age classifications of data providers.

Standard Assessment Protocol (SAP) for energy performance rating of dwellings [34]; and the Building Research Establishment's Domestic Energy Model (BREDEM) [10] that describes a number of building envelope assumptions used in housing stock modelling.

Surveys Many of the assumptions made about building envelope design and construction are based on surveys, such as the EHS [69]. These surveys provide information on building characteristics and conditions for a subset of the housing stock. By analysing the data, researchers are able to make assumptions about the characteristics of different types of dwellings.

Historical Information Information on the history of construction can be gathered through an analysis of historical building regulations and from reviews of architectural and construction history.

Geospatial Data Geospatial databases have been developed in previous studies for energy simulation data at levels ranging from the individual dwelling to administrative area. GIS enables the storing of dwelling information in a spatial database, the mapping and dissemination of the housing stock data, and it can act as a platform for energy simulations. Energy simulation algorithms require a large amount of input data, which is costly and time-consuming to collect via house by house surveys, so GIS can also be used to infer dwelling characteristics using remotely sensed data such as aerial imagery. A range of different sources of geographic data are available which contain housing stock data relevant to hygrothermal simulations. These databases can be used to develop a bottom-up housing stock model that has information suitable for modelling the flooding and drying of geographic areas, such as location within areas at risk of flooding. Cities Revealed (CR) Landuse database [270] and the Ordnance Survey (OS) Mastermap [214] are examples of GIS-based data used in housing stock analysis.

The Homes Energy Efficiency Database (HEED) [130] is a collection of information from energy suppliers, government scheme managers, local landlords, Energy Saving Trust (EST) energy checks, and EST programs on wall types, cavity wall insulation levels, and dwelling ages within areas of the UK. Information is available on the frequency of insulation in aggregated areas down to Census Output Area (COA) level detail, or around 125 households, and can be used for studies into energy performance of local housing stocks. The data within HEED is limited by the number of dwellings within the local areas that have been surveyed or involved in energy reduction programmes, and does not represent a complete dataset for all dwellings. However, it is an effective tool for estimating local housing stock data.

In cases where elevation data is important, such as calculating the flood depths in flood risk models, Light Detection and Ranging (LiDAR) and aerial photogrammetry can be used to develop Digital Elevation Models (DEM) to describe the local heights of the terrain and features including buildings and surface vegetation. The DEM can be processed further to determine the individual

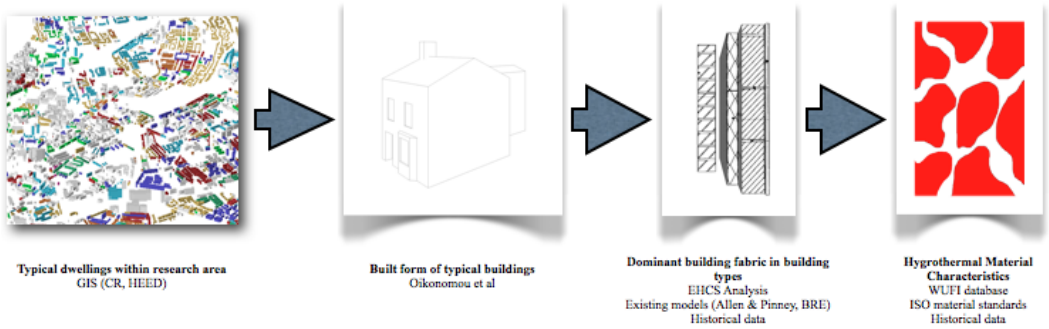

Figure 7.2: Integration of different data sources into a model for simulating and mapping whole-building flood simulations.

heights of buildings, or to create a Digital Terrain Model (DTM) that represents the height of the terrain without the features. Understanding the 3D terrain features is critical for modelling flood events, and GIS software is widely used for flood prediction and planning to inform local flood depths, flow direction, and sinks in which floodwater may accumulate. CR provides a LiDAR-derived DEM for London with 2m resolution.

Hygrothermal Material Information While energy models are concerned with the thermal performance of the building envelope, hygrothermal simulations carried out to evaluate the combined thermal and hygric performance of buildings. Harmonised design values for the hygrothermal properties of building materials in energy studies has previously been determined by statistically analysing existing material data [37]. However, hygrothermal simulations require additional information on the materials within the envelope that are not contained in the harmonised standard hygrothermal design values used for energy simulations, such as porosity and detailed sorption functions. Many of these values can be estimated from the basic material data found in standardised datasets, while complete material data is available from the databases provided with hygrothermal software such as Wärme Und Feuchte Instationär (WUFI) and Delphin.

The integration of all the different data sources required to simulate and map the flooding of typical London dwellings can be seen in Figure 7.2.

7.5 Methods

A variety of different data sources were consulted in the development of a housing stock model to analyse the London housing stock's resilience to flooding. The objective was to develop a model of the most common built forms/age combinations in London which could be used in hygrothermal simulations to model drying times under a variety of conditions following a flood. The housing stock

model was to be mappable in order to use it in conjunction with flood maps to predict risks over a larger area.

7.5.1 Built Forms

The housing stock archetypes used in this study were originally developed for research by Mavrogianni and colleagues (Figure 7.3) [190]. These archetypes consist of 15 of the most commonly occurring built forms and dwelling age combinations in their research area (29% of the Greater London Authority household spaces), as determined from individual dwelling–level data provided by the CR database [270]. Mavrogianni and colleagues used GIS calculations to determine the average dwelling footprints, while internal layouts were taken from floorplans based on the age and form of the dwellings [36, 54, 158, 199, 217, 300]. Window sizes were calculated based on dwelling footprints, as described by Chapman [52].

The built form/age categories of the dwellings are shown in Table 7.1. Combined, these built forms account for 76% of the London domestic stock within the research area. For the purposes of this research, variations of the Mavrogianni archetypes that would not be directly impacted by floodwaters, such as flats above ground level and those with shops underneath, were ignored, although their ground-floor equivalents were considered. Detailed drawings of these archetypes, including facades and floorplans, can be seen in Appendix A.

The floorplans of terrace H02, H05, and H10 were the same, with the exception of different window sizes. Temporary dwellings were not considered, as they represented a minority of dwelling types, and have an increased risk of being destroyed or moved by floodwater [162]. Dwellings converted into flats were considered as whole buildings.

7.5.2 Building Envelope

The types of building fabric found in each built form was estimated using a combination of EHS data [70] and e0xisting housing stock models. The EHS data for 2008 was analysed in SPSS to identify the types of building envelope construction associated with each dwelling archetype based on its age/built form classification. The EHS divides dwellings into 8 types of built form, 14 types of structure, 8 types of building fabric, and 7 types of exterior finish (Table 7.2).

In order to simplify the study, boxwall and crosswall constructions were considered to have the same building fabric, as were in-situ and pre-cast concrete walls. For individual properties recorded in the survey, the wall structure and finishing material was recorded for both front and back of the dwelling. The survey also took into account the fact that individual building surfaces could be composed of various wall types and finishing materials by dividing walls into tenths and describing the wall fabric and finish for each section. For the sake of simplicity, the majority construction type, building fabric, and building surface of the dwelling was assumed to represent that of the entire

Dwelling Code	Description	Age Bracket
H01	Late Victorian or Edwardian terrace with large T	1902-1913
H02	WWI & WWII simple terrace	1914-1945
H03	WWI & WWII large semis	1914-1945
H04	60s & 70s tall purpose shared discrete house	1960-1979
H05	Late Victorian or Edwardian simple terrace	1902-1913
H06	Post-war regeneration tall purpose shared discrete house	1946-1959
H07	Recent years' tall purpose shared discrete house	1980-2008
H08	Late Victorian or Edwardian simple terrace with attic	1902-1913
H09	WWI & WWII bungalow	1914-1945
H10	60s & 70s simple terrace	1960-1979
H11	60s & 70s line built walk up flats	1960-1979
H12	WWI & WWII line built walk up flats	1914-1945
H14	Post-war regeneration step-linked terrace	1946-1959
H15	Post-war regeneration line built walk up flats	1946-1959

Table 7.1: Built form/Age combinations from Mavrogianni et al. [190].

Dwelling Type	Wall Construction Type	Building Fabric	Exterior Finish
End terrace	Solid Masonry Boxwall	Masonry Cavity	Masonry pointing
Mid terrace	Cavity Masonry Boxwall	Masonry Single Leaf	Non-Masonry pointing
Semi detached	Masonry Crosswall	9" solid	Rendered
Detached	In-situ Concrete Boxwall	>9" Solid	Shiplap timber
Temporary	PreCast Concrete Boxwall <1m wide	in-situ concrete	Tile hung
Purpose built	PreCast Concrete Boxwall >1m wide	Concrete panels	Slip/tile faced
Converted	in-situ Concrete Crosswall	Timber panels	Wood/metal/plastic panels
Non-residential plus flat	PreCast Concrete Crosswall	Metal Sheet	
	In-situ concrete frame		
	PreCast Concrete frame		
	Timber Frame Pre 1919		
	Timber Frame Post 1919		
	Metal Frame		
	Other		

Table 7.2: EHS classifications of dwelling type and wall construction.

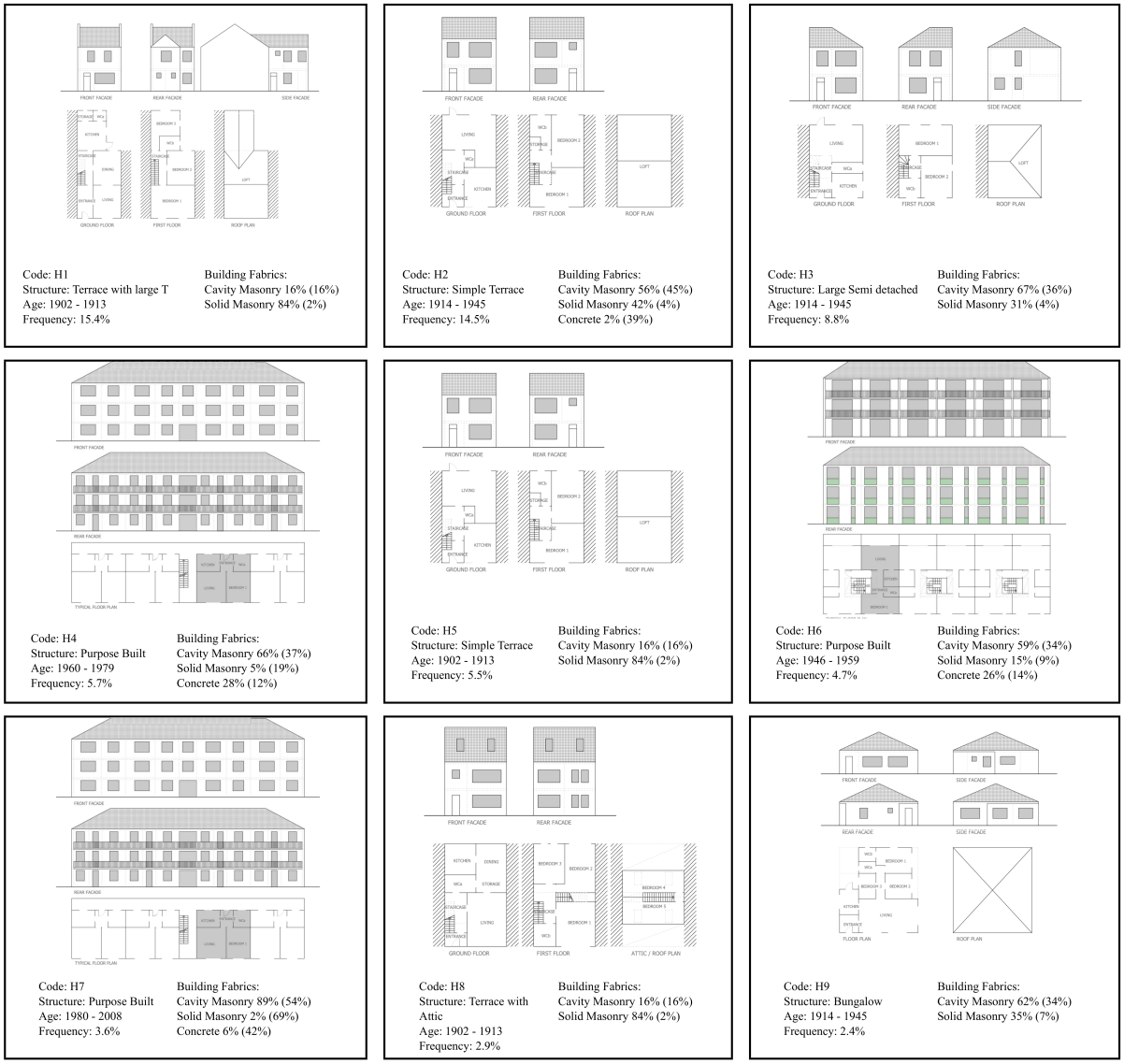

Figure 7.3: Built forms and the EHS-derived frequency of their building fabrics. Archetypes can be seen in greater detail in Appendix A.

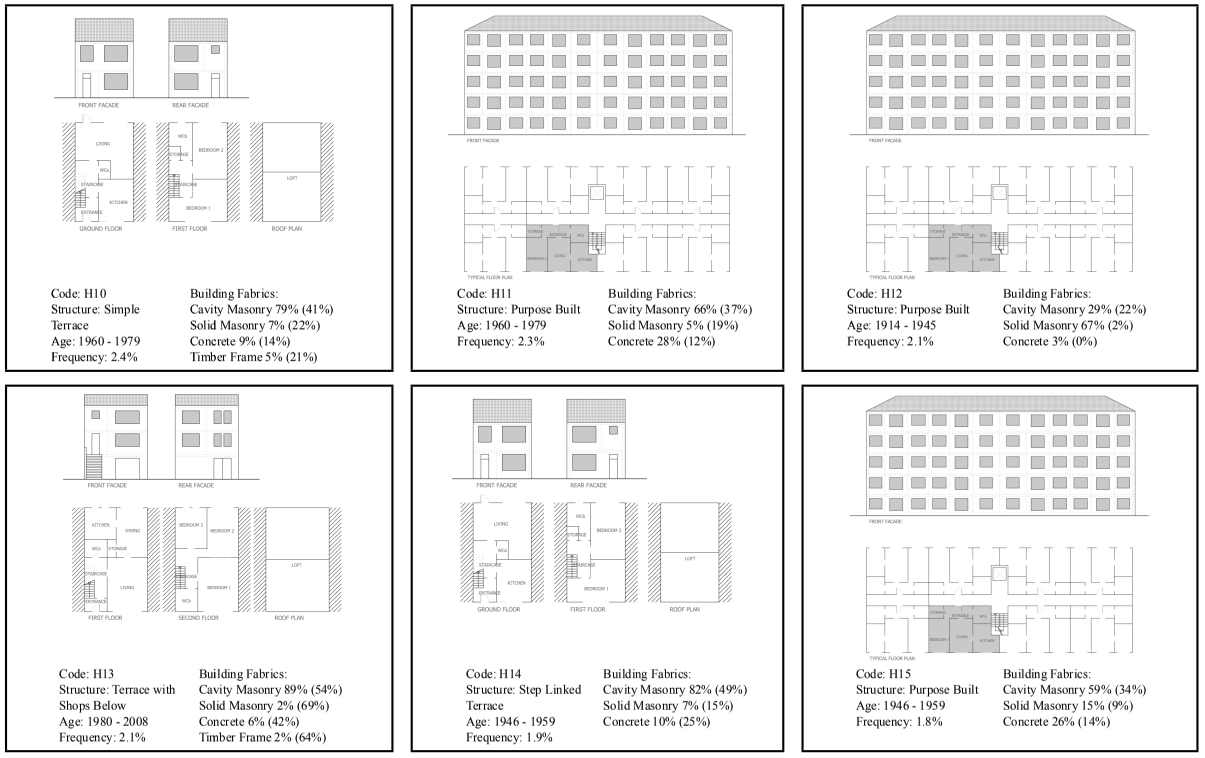

Code: H10
Structure: Simple Terrace
Age: 1960 - 1979
Frequency: 2.4%

Building Fabrics:
Cavity Masonry 79% (41%)
Solid Masonry 7% (22%)
Concrete 9% (14%)
Timber Frame 5% (21%)

Code: H11
Structure: Purpose Built
Age: 1960 - 1979
Frequency: 2.3%

Building Fabrics:
Cavity Masonry 66% (37%)
Solid Masonry 5% (19%)
Concrete 28% (12%)

Code: H12
Structure: Purpose Built
Age: 1914 - 1945
Frequency: 2.1%

Building Fabrics:
Cavity Masonry 29% (22%)
Solid Masonry 67% (2%)
Concrete 3% (0%)

Code: H13
Structure: Terrace with Shops Below
Age: 1980 - 2008
Frequency: 2.1%

Building Fabrics:
Cavity Masonry 89% (54%)
Solid Masonry 2% (69%)
Concrete 6% (42%)
Timber Frame 2% (64%)

Code: H14
Structure: Step Linked Terrace
Age: 1946 - 1959
Frequency: 1.9%

Building Fabrics:
Cavity Masonry 82% (49%)
Solid Masonry 7% (15%)
Concrete 10% (25%)

Code: H15
Structure: Purpose Built
Age: 1946 - 1959
Frequency: 1.8%

Building Fabrics:
Cavity Masonry 59% (34%)
Solid Masonry 15% (9%)
Concrete 26% (14%)

Figure 7.3: Built forms and the EHS-derived frequency of their building fabrics (cont.)

dwelling. The frequency of occurrence of each type of construction/building envelope/finishing type in the proposed archetypes was determined using the SPSS Custom Tables feature.

Evolution of UK Building Envelope Construction

Age classifications are used in UK housing stock models to represent changing building trends and building standards over time. The history of UK built forms shows an evolution towards more energy-efficient building envelopes.
Prior to 1930 the majority of dwellings in the UK had 9 inch (228mm) thick solid brick walls with a coat of plaster on the inside. In taller dwellings, for example those over 3 storeys high, dwellings often had thicker walls with the thickness reducing at each upper floor level. Lime cement mortars were commonly used.
In the 1930s, cavity walls became more common. These walls were typically 11 inches (280mm) thick with a 2 inch (50mm) cavity of air. The external face of the cavity was typically composed of facing bricks, while the internal face was composed of common brick with a layer of plaster on the inside. Cement mortar started replacing lime cement mortar. From 1945, cavity wall construction continued, although the inner leaf of the cavity began to be built from blockwork such as stone and industrial waste aggregates like clinker and breeze blocks. Many different types of system-built construction can be found in this period.
Increased attention to energy efficient dwellings after 1975 led to building regulations with insulation requirements. Cavity walls began to be constructed with lightweight block on the inner leaf as opposed to brick.
In 1980, the U-value requirement dropped to 1, meaning further insulating requirements. The most commonly found wall constructions during this period were cavity walls composed of brick – air cavity – thermal block (usually aerated concrete at 450kg/m^3), or brick – air cavity – 25mm expanded polystyrene – dense block. Plasterboard became more common than wet plaster.
In the 1990s the U-value dropped to 0.45. An increase of the cavity insulation to 50mm was observed, with fully filled cavity walls with lightweight inner blocks or wider cavity walls with partial fill insulation being common constructions. Mineral wool became increasingly common as a form of insulation. From 2002, insulation has increased to around 100mm.

The dimensions of the material components and layers of the building fabric were estimated based on standard material sizes, BREDEM [10], existing archetypes [8], and documented building trends [93, 277]. All wall types consisting of less than 5% of the total number of walls for each age/structure combination were ignored.

Data on internal walls and ground floors were not available in the EHS, and were therefore estimated from historical building trends and existing models. Internal walls were taken to be either solid single brick or solid Autoclaved Aerated Concrete (AAC), depending on the construction of the outer walls. Ground floors were taken to be either solid concrete slabs or suspended wooden floors. There is no published information available on the proportion of solid versus suspended ground floors in UK housing stock, so assumptions were made based the SAP U-Value calculation methodology which assumes that dwellings built after 1929 have solid floors. Above-ground timber floors and ceilings were based on the work of Allen and Pinney. An insulated roof was assumed for all dwellings.

Dwellings have a natural permeability which allows for air change within the building. The permeability of the walls was applied to the different archetypes based on the wall type (Concrete, Solid Brick, Cavity Brick), as per the Building Research Establishment (BRE) [257].

7.5.3 Materials Data

Current standardised material data (e.g. [37]) provides moisture content at 50% RH and 80% RH, which can be used to estimate the water absorption and desorption behaviour of materials [138]. However, an accurate moisture storage function at high water contents was considered to be critical for this study due to the need to model liquid transport. Therefore, hygrothermal material data was taken from the WUFI database [149] and were chosen to be as close as possible to the parameters provided by the standards referred to, and to those expected to be found in the London housing stock (e.g. London Stock Bricks). Generally, it is assumed in the materials databases that fibrous insulation exhibits non-hygroscopic behaviour, and little information is available with regard to liquid water transport at saturation. Since fibrous insulation has been observed to retain moisture when exposed to high moisture levels, hygrothermal material data for glass fibre with moisture transport information up to saturation was taken from Hokoi and Kumaran [136].

7.5.4 GIS

The research area for the present study was selected to be an area of London extending from Richmond in the West to Greenwich in the East – an area covered by approximately 250,000 homes, and at risk of flooding (Figure 7.4). The extent of the research area was determined by the available housing stock and surface height data, and computing power.

7.5.4.1 Dwellings

The main GIS database used was the OS Mastermap, a continuously updated cadastral map that has a Topographic Layer with individual building footprints and crude land use information. As it is the most recently updated topographic map available, the building footprints were used as a basis for the model. CR produces a landuse database with dwelling footprints classified as one of 15 dwelling types and 17 age categories, enabling the archetypes proposed above to be mapped to individual properties within the GIS system. Conversely, the CR geographic dataset is less frequently updated, less widely available, and a less clear provenance than that of the OS Mastermap. For this reason, the OS Mastermap was used as the basis for the cadastral map of the dwellings within the research area.

CR building classifications were joined to the OS data through a spatial join, so that the individual OS buildings would be matched with corresponding CR building information on the basis of the location. The resulting building stock database was filtered to show only dwellings by searching the

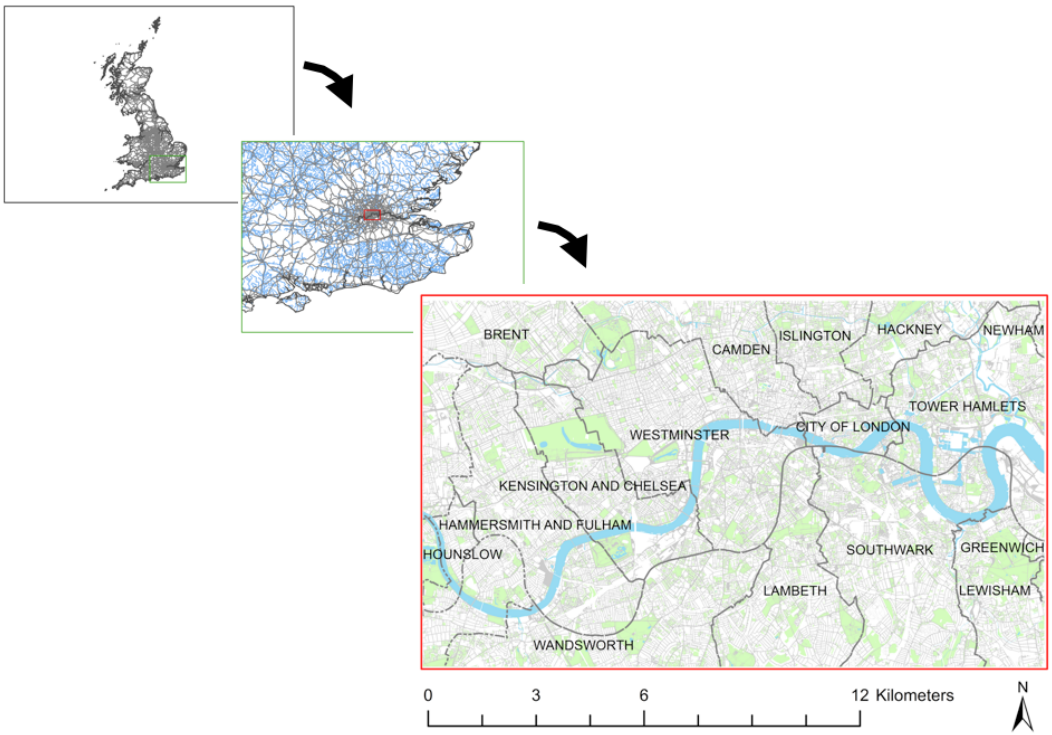

Figure 7.4: The extent of the research area in London.

CR landuse classifications of individual dwellings. In multiple occupancy buildings such as purpose-built flats, OS Address Point data was used to estimate the number of dwellings on the ground floors of buildings. The total domestic address points in a dwelling were counted, and building height information used to estimate the number of storeys in the building. Ground floor flats were then estimated assuming that each storey had the same number of flats.

7.5.4.2 Walls

While the EHS analysis describes the frequency of different wall types within dwelling archetypes, the frequency of cavity wall insulation in archetypes with cavity walls is expected to change, depending on the locations of the dwellings due to regional differences in income and local government programs. To account for regional variation in insulation rates, HEED data on insulation and wall type was used to supplement the CR landuse data by informing the proportion of the archetypes with cavity wall insulation within a COA. Data was downloaded from the online HEED database at the COA-level and joined to the GIS database. The relative frequency of cavity wall insulation for all dwellings with cavity walls within the COA was calculated, and this frequency assigned to the individual dwellings. By doing so, the most common (modal) wall types within the areas could be estimated. The frequency of cavity wall insulation in the research area is depicted in Figure 7.5.

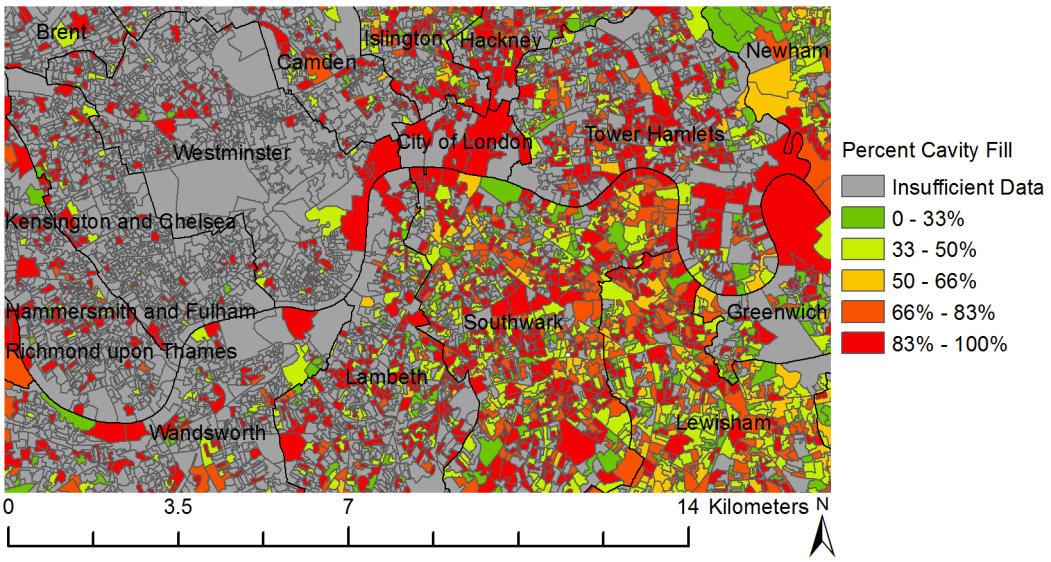

Figure 7.5: The frequency of insulation in cavity walls.

7.5.4.3 Terrain Height

A DTM was developed by filtering a LiDAR-generated DEM raster provided by CR to remove buildings and other non-terrain features. To filter buildings from the DEM, the building footprints from the original unfiltered OS Mastermap data were used as a mask; using external data as a mask is an established technique in DEM filtering. A 3m buffer was drawn around the outside of the individual building footprints in order to account for the 2m resolution of the LiDAR data and the area within the buffer clipped from the LiDAR dataset.

Other heights also needed to be filtered out of this raster, such as trees, bushes, and street furniture which can also cause errors in the terrain heights. To filter the DEM further, a slope-based technique was employed, as per the EA [230]. The raster was analysed for sudden changes in ground slope. The sudden slopes were removed using the extract attributes tool, which identifies sudden changes in gradient in the DEM above 66.6 Degrees. A 3m buffer was drawn around these high-gradient locations, which were then filtered from the DEM in the same manner as the buildings had been filtered. This removed the slopes but isolated high points surrounded by areas of no data remained. These remaining high points were removed using a low-pass filter which did not ignore the areas of no data, but assigned outlying area values more in keeping with their neighbours.

Eliminating sudden slopes and outliers did not remove all of the non-terrestrial features, as some objects such as bridges remained. However, since these would not have an impact on the calculation of flooded dwellings, these raster areas were not filtered out. Once the raster had been filtered, the gaps were filled by re-interpolating to a 2m resolution using an Inverse Distance Weighting (IDW) algorithm, leaving a DEM which represented the height of the ground without man-made or vegetation features.

Dwelling Code	Cavity Masonry	Concrete	Metal Frame	Solid Masonry	Timber Frame	Other
H01	16.3%	0%	0%	83.7%	0%	0%
H02	56%	1.7%	0.1%	42%	0.1%	0%
H03	67%	1.5%	0.2%	31.2%	0.2%	0%
H04	66%	27.6%	0.3%	5.5%	0.6%	0%
H05	16.3%	0%	0%	83.7%	0%	0%
H06	59%	25.8%	0%	15.2%	0%	0%
H07	89.1%	5.6%	0.8%	2.2%	2.4%	0%
H08	16.3%	0%	0%	83.7%	0%	0%
H09	62.1%	0.3%	0.3%	35.3%	2.0%	0%
H10	78.7%	8.8%	0.8%	6.8%	4.9%	0%
H11	66%	27.6%	0.3%	5.5%	0.6%	0%
H12	29.3%	3.4%	0%	67.2%	0%	0%
H14	82.2%	9.7%	0.3%	7.1%	0.7%	0%
H15	59%	25.8%	0%	15.2%	0%	0%

Table 7.3: External building fabric types for dwelling archetypes.

7.6 Results

7.6.1 Building Envelope

The analysis of the EHS data shows the change in the building methodologies as time changes, with cavity walls and insulation becoming more prevalent the newer the dwelling. The breakdown of the types of building fabric found in each of the dwelling archetypes in the SPSS analysis can be seen in Table 7.3.

Comparing the majority construction type of the front and backs of properties, it was found that 94.8% of structures had the same wall types at both front and back of the property. The finishing of the different property sides showed that 90.7% of dwellings had the same majority finishing on the back as on the front of the dwellings. The EHS also included information on any alterations or extensions to the properties, and the period in which these alterations were made. It was found that 16.7% of dwellings had been extended to add space for amenities, and 14% had been altered for additional living space.

The EHS showed that the surface finishing of the different properties showed more variation within individual properties, with only 65% of the fronts of properties having a single finishing type, and 75.5% of the backs of properties having a single finish. Most finishes were masonry and non-masonry pointing, with rendered surfaces also a common occurrence. Again for simplicity, it was decided to ignore exterior surface finishes and perform a test in the building simulation to determine the possible impacts of rendering.

To narrow down the number of simulations required, only walls with an occurrence of more than 5% were modelled. Rendered walls were found to be commonplace in the EHS, however since there was no way to determine the spatial distribution of rendered properties, these were ignored, and the impact of surface coatings is examined in Chapter 9.

<table>
<tr><td></td><td colspan="5">Dwelling Age</td></tr>
<tr><td>Building Fabric Construction</td><td>1902-1914</td><td>1915-1945</td><td>1946-1959</td><td>1960-1979</td><td>1980-2008</td></tr>
<tr><td>Solid Masonry</td><td>220mm Brick
10mm Plaster</td><td colspan="2">or
335mm Brick
10mm Plaster</td><td colspan="2"></td></tr>
<tr><td rowspan="2">Masonry Cavity</td><td rowspan="2">102mm Brick
50mm Air Gap
102mm Brick
10mm Plaster</td><td rowspan="2">or</td><td rowspan="2">102mm Brick
50mm Glass Fibre
102mm Brick
10mm Plaster</td><td>102mm Brick
50mm Glass Fibre
102mm AAC
10mm Plaster</td><td>102mm Brick
100mm Glass Fibre
102mm AAC
10mm Plaster</td></tr>
<tr><td colspan="2">102mm Brick
50mm Air Gap
102mm AAC
10mm Plaster</td></tr>
<tr><td>Solid Concrete</td><td colspan="5">70mm Concrete
60mm Concrete (No Diffusion)
70mm Concrete
10mm Plaster</td></tr>
<tr><td>Floor</td><td>70mm Concrete
100mm Air Gap
12mm Spruce</td><td colspan="4">70mm Concrete</td></tr>
<tr><td>Internal Walls</td><td colspan="3">10mm Plaster
102mm Brick
10mm Plaster</td><td colspan="2">10mm Plaster
102mm AAC
10mm Plaster</td></tr>
<tr><td>Internal Floors</td><td colspan="5">10mm Plaster
100mm Air Gap
12mm Spruce</td></tr>
</table>

Table 7.4: Proposed building fabric constructions.

Following the analysis of energy models, historical building trends, and standard material sizes, different fabrics were proposed for the different age classes (Table 7.4). These wall types were assigned to the dwelling archetypes according to dwelling age and distribution of different wall types determined in the EHS analysis above (Table 7.3).

7.6.2 Materials

The complete building material data chosen for the archetypes, including all moisture transport isotherms and thermal conductivities, can be seen in Appendix B. Material information selected for modelling the building fabrics and a comparison with the standard values used for building simulation can be seen in Table 7.5. It was not always possible to find a material which matched precisely with a standardised value. However, the majority of material properties used fell within the ranges of the standardised values for building simulation. The lack of appropriate materials data is problem in hygrothermal simulation, and the materials data chosen reflect the closest possible values to the standardised and London-specific materials, while providing additional liquid transport information that the standardised values lack.

7.6.3 GIS

The result of the geodatabase development was a map of the research area containing individual dwellings classified according to dwelling archetype and supplemented with local area data on the frequency of cavity wall insulation. The housing stock model for London showed a range of potential

	AAC		Air Gap		Brick		Concrete		Glass Fibre		Gypum		Plasterboard		Spruce	
	Model	ISO	Model	ISO	Model	ISO	Model	ISO	Model	ISO	Model	ISO	Model	ISO	Model	ISO
Conductivity {W/m-K}	0.12	-	0.02	0.03	0.60	-	1.60	1.2-2	0.07	-	0.20	0.18-0.56	0.20	0.18-0.56	0.23	0.12
Density {kg/m^3}	600.00	300-1000	1.20	1.23	1900.00	1000-2400	2300.00	1800-2400	60.00	10-200	850.00	600-1500	850.00	600-1500	455.00	450.00
Specific Heat {J/kg-K}	850.00	1000.00	1004.00	1008.00	850.00	-	850.00	1000.00	850.00	1030.00	850.00	1000.00	850.00	1000.00	1500.00	1600.00
Porosity	0.77	-	1.00	-	0.24	-	0.18	-	0.98	-	0.65	-	0.65	-	0.73	-
Moisture Content at 50% RH	2.88	15.60	0.01	-	4.84	13.30	48.00	46.00	1.80	0.00	3.60	-	3.60	-	45.00	-
Moisture Content at 80% RH	11.00	27.00	0.01	-	18.00	22.80	85.00	80.50	1.98	0.00	6.30	-	6.30	-	80.00	-
Water Vapour Resistance Factor Dry	16.00	10.00	0.00	1.00	10.00	16.00	180.00	50.00	1.30	1.00	8.30	10.00	8.30	10.00	130.00	50.00
Water Vapour Resistance Factor Wet	-	6.00	-	1.00	-	10.00	-	40.00	-	1.00	-	4.00	-	4.00	-	20.00

Table 7.5: The values selected for the model from the WUFI database [149] and the literature compared with the standardised (ISO) values [40].

built forms which could be analysed and visualised using GIS. Figure 7.6 shows an example subset of the research area with individual dwellings assigned dwelling archetypes.

Due to limitations in the coverage of the CR landuse data, gaps are present in the housing stock dataset (Figure 7.7). These gaps occur where dwellings lack landuse data that would allow their archetype to be classified. The incomplete coverage of the data means that some areas are not able to be mapped.

The DTM model developed eliminated surface features such as buildings and vegetation from the DEM, and provided a basis for the calculation of the flood depth for individual properties using flood risk maps. Small artefacts remained in the DTM, for example bridges, railway viaducts, ships on the Thames, and LiDAR data from buildings that did have footprint information, however, these were ignored as they were not considered to be important to remove.

7.7 Discussion

A number of different data sources have been combined in order to create an understanding of the London housing stock, from the individual building materials used in construction, to the geographical distribution of the housing stock. By combining existing archetypical built forms with the outcomes of the EHS survey data analysis on building fabric, assumptions used in other building simulation models, historical data, and materials information, it has been possible to develop dwelling models with sufficient information to perform whole-building hygrothermal simulations. Combining this information with geospatial databases with individual dwelling and terrain height information can allow for the calculation of the exposure of individual properties to flood risk and flood depth calculations. The proposed dwelling archetypes can be simulated using HAM models under different flooding conditions, including season and flood height, in order to predict drying times, while functions similar to depth-damage curves, can be created which can be used to predict the risk inside a flooded dwelling over time. The developed functions can be applied to flooding scenarios in areas of flood risk, by taking into account the location of individual dwellings, dwelling characteristics, and the likely depth to which they will be flooded.

A number of inaccuracies may exist in the datasets used. The OS and CR cadastral maps have been developed largely using aerial photography, and the boundary locations of the dwellings are subject to the resolution of the aerial photographs used in developing the maps. The OS Mastermap was used as the cadastral basis for the analysis, as their unique Topographic Identifiers (TOIDS) make the results more transferable to other researchers, and Mastermap is continually updated. The classifications of dwellings in the CR dataset is performed through a mixture of aerial and drive-by surveys, and will be subject to the judgement of the surveyor. Like with any subjective classification, there exists the potential for error. However, there is a lack of highly accurate dwelling information for London that is publicly available. The Valuation Office Agency (VOA) has the most

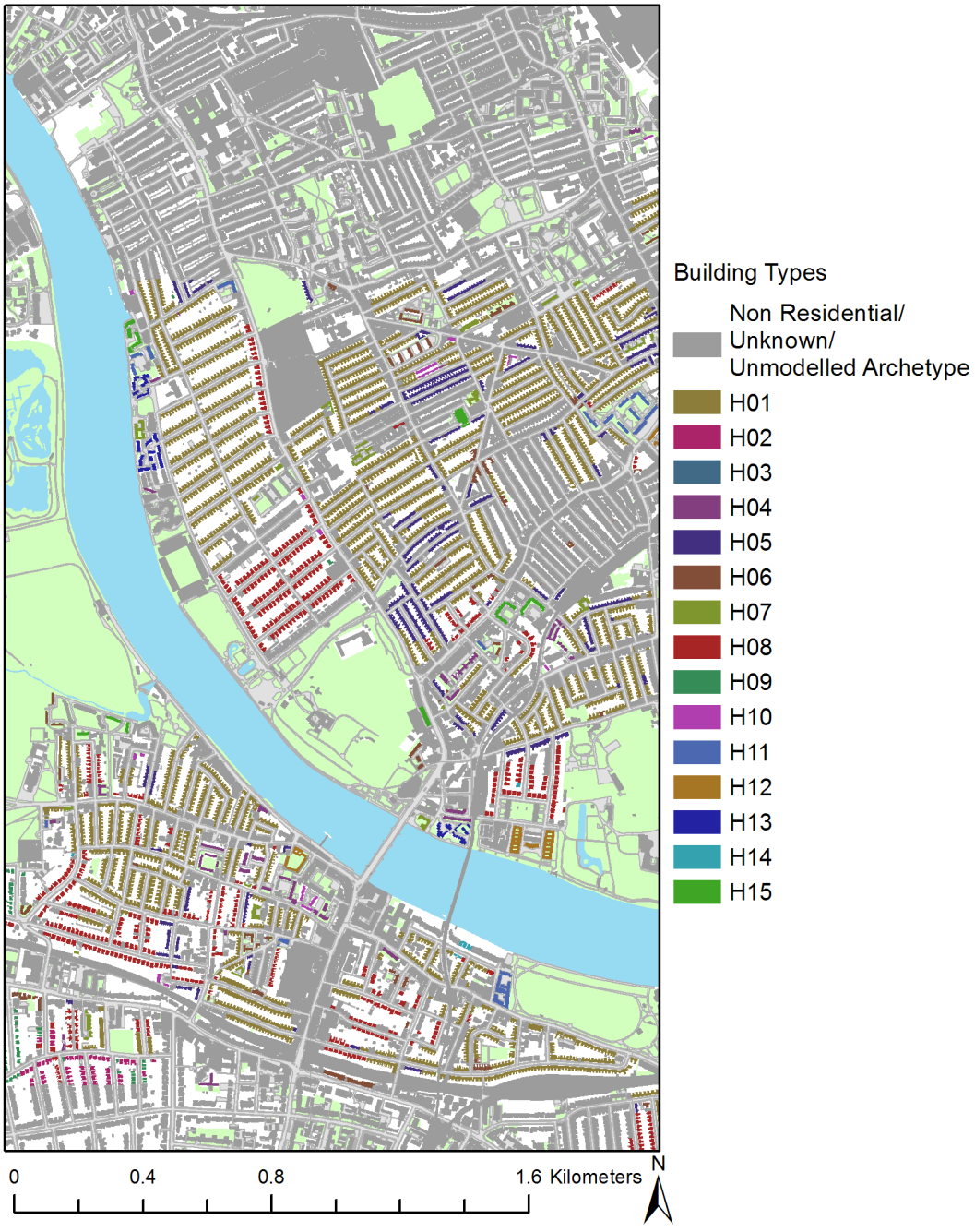

Figure 7.6: A subset of the research area showing the archetypical classification of individual dwellings.

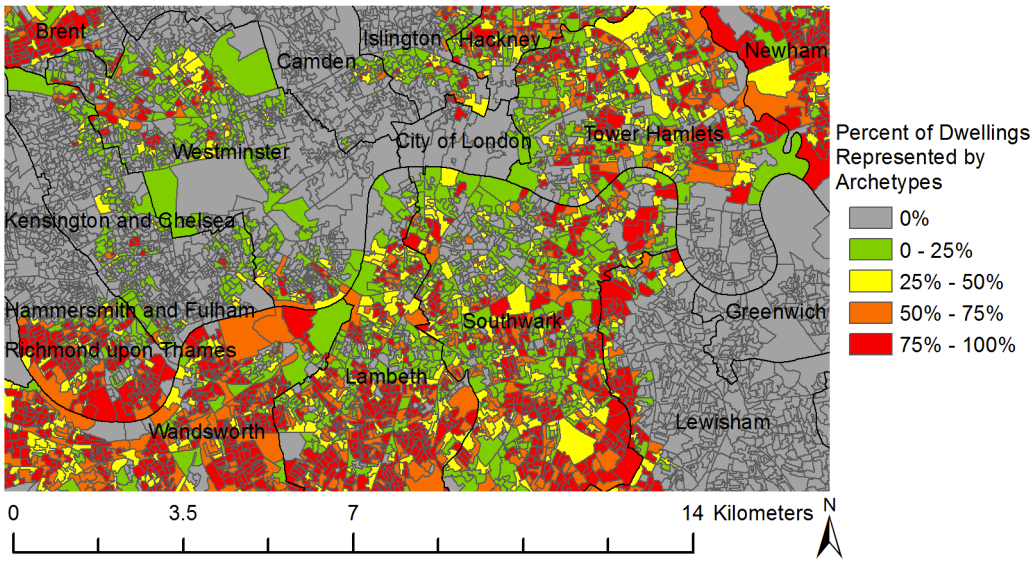

Figure 7.7: Coverage of CR dwelling data for the research area.

extensive property attribute data set, however the majority of this data is undigitised, [285] and not available without significant cost. The CR database is however continually improving, and offers the best solution for the immediate requirements of this study. Likewise, the HEED database is based on surveys and retrofits in existing properties, and may not offer good coverage within an area; moreover it was not made available to us on a specific-dwelling level. As such, it must be treated with the same caution as the other databases, and used primarily as a best-estimate of the local conditions within the area. While data is held in the geodatabase at the individual-dwelling level, it is unlikely that the model will accurately predict the result for individual properties. Inaccuracy in housing stock models occurs when aggregated housing stock characteristics are assigned to individual dwellings, while further limitations are inherent in the assumptions made with regard to construction and materials. However, when aggregated to a larger area, the inaccuracies decrease, implying that the model should be applicable over a larger area. While minority wall types have been ignored, the possibility exists that such wall types may be grouped in areas of flood risk, making them more significant than their numbers would suggest. Without knowing the building fabric at the individual-building level, it is not possible to account for such a phenomena.

The EHS was also developed through a survey of different dwellings in England, and will be subject to the opinions and decisions of the surveyors visiting the properties. There was some conflicting data found in the EHS datasets - for example, walls being reported as being both solid and cavity in the same surface of a property. The surveyors were required to make assumptions about the construction of the dwelling without performing destructive tests to determine the exact means of construction; therefore the exact type of construction may not be properly reported. In addition, the EHS survey examined properties throughout England and may not offer an ideal representation

of the local London housing stock. Detailed information on the material used was also not available in the EHS - for example, the EHS classifies masonry walls without specifying the type of masonry, meaning that assumptions had to be made regarding the type (brick or AAC) used. The lack of location-specific dwelling information and detailed data on building fabric is an issue which influences all housing stock studies.

The selection of the materials data was also limited by a lack of available hygrothermal material data, in addition to limited values provided by standards. The approximations required to select the hygrothermal material properties mean that the moisture behaviour of the materials will not exactly match those in the true dwellings. Again, this is likely to be an issue in all hygrothermal modelling studies, and a sensitivity analysis will need to be performed in order to better understand the uncertainties these approximations cause.

Despite limitations caused by a lack of data, and the necessary assumptions, a housing stock model for the HAM simulation of typical London dwellings and the mapping of the simulation results has been developed. By integrating data from a number of different dwelling information sources and mapping datasets (Figure 7.8), the model parameters for performing the simulations and developing the drying curves can be obtained.

7.8 Conclusions

The developed dwelling archetypes provide the required information for simulating the drying of dwellings, from the material to the whole-building level. The dwelling archetypes draw on information from a range of different sources, using techniques and methodologies established in energy modelling studies. By combining the different data sources, dwelling archetypes for hygrothermal flood simulation have been developed to represent a large proportion of the London housing stock; these can be used to perform whole-building HAM simulations of flooding and drying. Geospatial information will allow the results of the simulations to be mapped in order to predict localised areas of prolonged damp, and shed light on the potential for chronic health problems or displacement that may arise, and in doing so providing valuable information for disaster response planning.

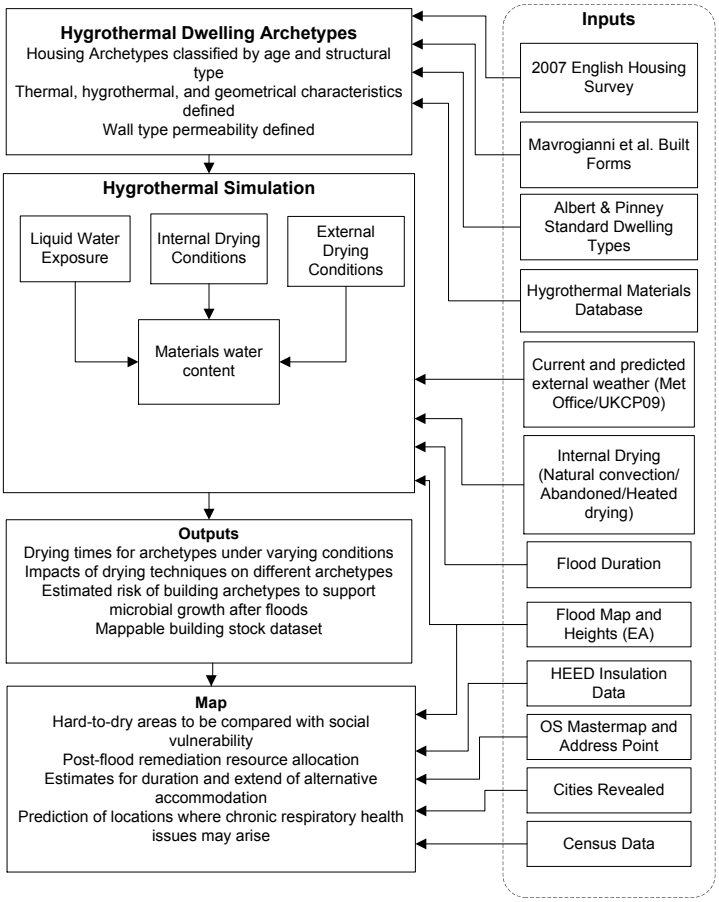

Figure 7.8: Data integration model

Chapter 8

Introduction to HAM Modelling

8.1 HAM Modelling

Water inside buildings can exist as a solid, a liquid, and a vapour. Potential sources of building moisture include indoor and outdoor air humidity, construction damp (for example, drying concrete), precipitation, water leakage, moisture in the ground, or, in the case of this thesis, a flooding event. In the case of a flood, liquid water in contact with building materials can move into the structure, while water vapour can circulate around the rest of the building not in direct contact with floodwater. As the floods recede, the drying of a structure is closely aligned to the material's ability to absorb and retain water, to dry, and the ventilation of the building.

The movement of heat, air, and moisture through a building is a complex phenomenon that requires an understanding of the different transport mechanisms and the interaction between them. Heat and moisture can move through porous building materials due to a number of different potentials (Table 8.1) which may be considered in HAM modelling. Understanding how water can enter the building fabric, and dry out is critical to predicting how different dwelling types can dry after a flood. Evaluating the performance of different wall systems and buildings can be done through physical experimentation, or through simulation using specialised modelling techniques.

8.2 Flooding and Drying of Physical Constructions

Research into the drying of wet building materials has been performed to observe their drying behaviour. A number of authors have studied the susceptibility of samples of porous building materials to liquid water absorption due to floodwater or rising damp problems [121, 126, 135]. Studies into the drying of saturated porous building materials indicate there are two stages of drying [128]. The first stage has a constant drying rate, dependent on the RH of the surrounding air, air velocity, and temperature. The second stage has a slower drying rate, which is dependent on the material properties. The moisture behaviour of a material will also depend on its neighbouring materials; Wilson and colleagues [294, 295] experiment with the absorption of water into constructions of two or

	Transport Mechanism	Potential
Heat	Conduction	Temperature differences
	Radiation	Temperatures at boundary surfaces and surroundings
	Air flow	Air pressure
	Enthalpy Flow	Vapour diffusion, phase change, and liquid transport in temperature field
Water Vapour	Gas diffusion	RH, Temperature, atmospheric pressure
	Effusion (Knudsen Effect) and Diffusion in heavy traffic	RH, Temperature
	Solution diffusion	Partial pressure gradients
	Convection of air	Pressure Gradients
Liquid Water	Capillary conduction	Suction stress
	Surface Diffusion	Relative humidity at RH$>$ 30%
	Hydraulic flow	Floodwater pressure, gravity
	Electrokinesis	Electrical fields (generally neglected)
	Osmosis	Ion concentration gradients (generally neglected)
Salts	Solution diffusion	Ion concentration gradients, solubility (generally neglected)

Table 8.1: Movement of heat and moisture in HAM models.

more material types, and conclude that the absorption rate decreased as water passed the join from the material of higher sorptivity to the material with the lower sorptivity. The drying behaviour of a material is highly complex, and depends on the hygrothermal material properties, surrounding climate conditions, and vapour and heat transfer conditions, including air velocity and surface roughness [242]. To quantify the ability of different materials to dry, a drying coefficient representing the amount of time required to dry out 1m of material, has been proposed for building materials [242].

Constructing a scale model of a wall or building for experimental flooding and drying tests has not been widely performed. Escarameia and colleagues [97] built a range of typical UK new-build wall and floor structures and exposed them to water in order to observe their water leakage and drying rates. By recording the moisture content at the bottom of the walls, they observed a wide range of drying times under the ambient experimental conditions (average 12.2^{o}C, 72% RH), ranging from around 90 hours (solid rendered AAC wall) to an estimated 5 months (glass fibre insulated brick/AAC cavity). The experiment was performed using stand-alone walls inside a warehouse rather than whole building systems, thus the effects of ventilation were not quantified.

In the U.S., the United States of America Army Corps of Engineers (USAACE) tested the resilience of brick and concrete block walls to hydrostatic pressures from a simulated flood [276]. Oak Ridge National Laboratory (ORNL) and Tuskegee University tested the physical resistance to wetting and drying of small prototype timber-framed buildings under a range of physical flood scenarios [5]. The buildings tested were allowed to dry using natural ventilation, and the behaviour of the materials was recorded. This study found that, while the timber-framed buildings could be considered flood resilient, fibreglass insulation can wick and retain water and delay drying. Since the structures were single-roomed, the results would have to be extrapolated to full-building scenarios.

The wetting and drying of replica historic brick and stone wall structures was carried out as part of the Engineering Historic Futures project. Walls were flooded and their drying under assisted and unassisted drying conditions monitored at various locations within the structure [14]. As part of the Cultural Heritage Protection Against Flood (CHEF) research programme, full-scale masonry models of buildings had the walls naturally contaminated by salts and then soaked for several days [23]. Following the simulated flooding, walls were allowed to dry naturally, and non-destructive testing of the water contents was employed to observe the drying.

Klintberg [4] tested the resistance of the Air Gap Method of construction of a building to dampness and mould by flooding a 24m^2 apartment with domestic wastewater. The Air Gap design is intended to allow buildings to dry quickly from water damage. The buildings were found to dry out rapidly, minimising the effects of water damage.

Some examples of the drying rate of different flooded buildings, as observed by researchers and remediation organisations (Rameses and Munters), can be found in the technical documentation

of the research project 'Improving the Flood Resilience of Buildings through Improved Materials, Methods, and Details' [264]. Indoor air RH and the WME (Wood Moisture Equivalent) water content of the walls was recorded as part of the drying process in buildings professionally restored by remediation companies. Higher drying rates were observed in warmer months, and for external walls, suggesting that temperature and external airflow are influential for rapidly drying buildings. Significant scatter in the moisture levels recorded on the surfaces of walls was noted, and was attributed to the difficulty in recording moisture levels on the walls, the redistribution of moisture within the building, and the accuracy of the WME sampling equipment.

The amount of physical experimentation into the drying of buildings following flooding is limited. Constructing physical structures is expensive, time consuming, and requires a great deal of space. The flooding and drying event is constrained to tests of one scenario at a time, and is limited by the accuracy of the moisture measuring equipment. Furthermore, in cases where only a single wall, floor type, or room is tested, the results must be extrapolated to the whole-building situation.

Building simulation offers the possibility to study the drying of flooded dwellings without the cost of physical construction or the time required to build, flood, and dry the building. Multiple built forms, envelope types, and drying scenarios can be tested over a short period of time. Building simulation is therefore an efficient complement to physical experimentation.

8.3 Introduction to HAM Modelling

Heat, Air, and Moisture (HAM) computer models simulate the transport of heat, air and moisture within building assemblies with the objective of evaluating temperature and moisture conditions in a building over time. Such models have been developed due to the importance of moisture to indoor air quality, energy consumption, and building material durability. HAM models vary markedly in their complexity, from simple steady-state models (that do not consider changing external and internal conditions), to complex whole-building simulation models (that calculate air and heat flow throughout the building and take transient heat, air, and moisture levels into account).

Steady-state models ignore the change of environmental conditions over time, and so are much simpler than transient models and require less computing. They tend to be easy to use but require little input data and produce crude predictions of moisture conditions. The steady-state model methods commonly used to assess the moisture balance of a building are the Dew–point and Glaser methods [196]. The models consider boundary conditions to be at a steady-state, and water vapour to be perpendicular and one-dimensional to the building envelope. They do not consider capillary moisture transport or the sorption capacity of the material. The inability of the steady-state methods to address issues of liquid transport in the building materials means that they are inappropriate for models examining precipitation, summer condensation, and rising damp, as well as being limited to

light-weight structures [168]. Significant differences can be found between the results of steady-state models and transient models [196].

The number of factors considered in a HAM simulation increases the level of complexity of the calculations. Detailed, transient models calculate HAM transfer in individual building components as internal and external boundary conditions change. These more complicated models are capable of taking into account the material properties of the elements in the building envelopes, the changing internal and external temperature and moisture levels, and moisture sourves such as driving rain. These models can be used to predict, for example, the humidity of indoor air and condensation risk within the building fabric.

The most advanced HAM models take into account a whole building. The location, orientation, and design of a building, HVAC, user behaviour, permeability, and external shading can all impact on the HAM behaviour. Current research is developing and improving whole-building simulation methods [298].

8.4 HAM Modelling Description

Transient HAM models require material information for the materials present, the physical geometry of the building fabric, and the interior and exterior conditions surrounding the fabric. HAM algorithms are then used to calculate heat, moisture, and air flow through the building fabric and structure. The number of factors that can affect the transport of heat and moisture in buildings accounted for in the HAM calculations varies with the complexity of the model. The range of factors governing the movement of heat, moisture, and air in a building are described in the following sections.

8.4.1 Heat

Energy in buildings can be considered in terms of the conservation of energy in a control volume, where the total energy stored in the volume is the sum of the energy that enters the volume, the energy that leaves the volume, and the energy that is generated inside the volume:

$$\frac{dE_{Stored}}{dt} = \dot{E}_{in} - \dot{E}_{out} + \dot{E}_{generated} \tag{8.1}$$

Where E_{Stored} is the amount of energy in the volume (J), and $\dot{E}_{in}$, $\dot{E}_{out}$ and $\dot{E}_{generated}$ are energies entering the volume, leaving the volume, and being produced inside the volume, respectively, and varying with time. In this case, thermal energy can enter and leave the dwelling through heat fluxes and energy fluxes due to mass flows, while energy generation is due to, for example, human activity, heating equipment, or electrical appliances. Energy in buildings is often discussed in terms of enthalpy, or total energy in the thermodynamic system that is the control volume. In flooded dwellings we can consider energy to enter and leave the building through, for example, air moving

through open windows, while energy may be generated via the drying equipment installed inside the building.

Enthalpy flow through a system can occur through the mass flow of energy in air, water vapour, or liquid water into and out of the system. The energy gain through enthalpy will be related to the enthalpies of air or vapour (h_{air} or $h_{watervapour}$, (J/kg)) and the mass flux into and out of the system ($\dot{m}$ (kg/s)):

$$\dot{E} = h \cdot \dot{m} \tag{8.2}$$

The specific enthalpies of the mass flow in the air are calculated separately for dry air and water vapour, and are dependent on the temperature (T), the specific heat of the air (c_{DryAir}) and water vapour ($c_{WaterVapour}$), and the latent heat of vapourisation of the water (L_v):

$$h_{DryAir} = c_{DryAir}T \tag{8.3}$$

$$h_{WaterVapour} = L_v + c_{WaterVapour}T \tag{8.4}$$

In addition to heat gain through mass transport, heat can move through a structure based on conduction, convection, and radiation. Convection is the movement of heat between the solid surface of the building fabric surface and the moving air surrounding it, and is primarily caused by advection, or the movement of heat due to the motion of the air surrounding the wall. Convection will depend on the amount of air flow and the temperature difference between the material and the surrounding air. The convective heat flow (q_c) can be calculated as:

$$q_c = h_c A \left(T_s - T_f\right) \tag{8.5}$$

where q_c is the thermal energy (W), h_c is the heat transfer coefficient for convection (W/(m^{2}K)), A is the surface area of the heat being transferred (m^2), T_s is the temperature of the surface (K), and T_f is the temperature of the moving air (K). The heat transfer due to convection is particularly important when considering the heat loss on external walls due to wind, or in buildings with open windows and airflow through a building structure.

More movement of the surrounding air increases heat transfer by altering the heat transfer coefficient. The rate of airflow in the external environment can usually be calculated in HAM models through information in the weather files, however in order to determine the internal heat transfer coefficient requires an understanding of the internal airflow. Often it is assumed that heat transfer on external surfaces is resultant from the movement of air, while transfer in internal surfaces is temperature dependent, thus ignoring the impact of airflow.

Radiative heat transfer is the result of the exchange of electromagnetic (EM) radiation. Radiation from a surface depends on its surface temperature and physical properties (specifically, its spectral distribution and orientation). Shortwave radiation is mostly in the visible spectra, and tends to come from the sun, whereas longwave radiation is mainly infrared and is emitted from surfaces at ambient temperatures. Radiation in building simulations is generally modelled by considering the shortwave radiation incident on building surfaces (on external surfaces exposed to sunlight, or on internal surfaces through windows), and longwave radiation considers the radiative exchange between both outdoor and indoor surfaces.

Building surfaces are often assumed to act as grey bodies in building physics, since surface properties tend to be independent of wavelength and have diffuse radiation. It also is possible to account for behaviour of building surfaces that do not respond as perfect grey bodies by differentiating between long wave and short wave radiation properties.

The total amount of heat transfer to a building surface through radiation will be the difference between the radiation that it receives from other sources, and that which it emits. The radiative exchange between surface for long wave radiation is often described in terms of:

$$q_r = h_r A \left(T_1 - T_2\right) \tag{8.6}$$

where q_r is radiated energy (W), h_r is radiative heat transfer coefficient (W/(m^{2}C)), A is area of the radiating surface (m^2), and $T_1 - T_2$ represents the temperature difference between the surface and its surroundings.

For short wave, radiative exchange depends on the amount of solar radiation incident on the surface. Here, the heat flow is related to the materials' short wave radiation absorptivity (a_s)(-) and the solar radiation vertical to the surface (l_v)(W/m^2):

$$q_r = a_s l_v \tag{8.7}$$

Conduction describes the movement of heat within a solid, and is due to energy transport from molecular activity. In homogenous, still media conduction heat transfer can be described by:

$$\frac{\partial T}{\partial t} = \frac{\lambda}{\rho c} \nabla T \tag{8.8}$$

where λ is thermal conductivity (W/mC), ρ is material density (kg/m^3), c is specific heat capacity of the dry material (J/kgC), and ∇T is the temperature gradient across the material. The rate at which a material transports heat is therefore dependent on its thermal conductivity and the temperature gradient.

Between different types of materials, heat transfer depends on the boundary material (whether it is another solid material or whether it is air). When two solid materials are in contact, the heat transfer between them tends to ignore any resistance between the two materials.

In cases where the boundary material is air, heat transfer will depend on the boundary conditions, which can be in a state of constant temperature, constant heat flux, or linear surface flux.

8.4.2 Moisture

Moisture within buildings is the sum of the water in the air, in the building materials, and that produced by moisture sources, including resident behaviour and external weather conditions. In the air inside cavity spaces and rooms, the dominant form of water is water vapour, while inside the pores of materials, water is usually found in absorbed or condensed form.

Water vapour is produced inside buildings through human activity, such as cooking, laundry drying, showering, and breathing. The mass of water contained in the air can be calculated using a number of moisture-related measurements, including partial vapour pressure, vapour concentration, or dew point temperature, since atmospheric air can be described as behaving like an ideal gas. The vapour concentration (v) can therefore be described as:

$$v = \frac{p_{WaterVapour}}{R_{H_2O}T} \tag{8.9}$$

where $p_{WaterVapour}$ is the partial pressure of water vapour (Pa), and R_{H_20} is the specific gas constant for water (461.5 J/kgK). The maximum amount of water vapour possible in air is strongly dependent on temperature, and water vapour levels are often described relative to the maximum amount possible under the same conditions. RH, defined as the ratio between actual amount of water vapour in a volume of air and maximum possible amount of water vapour within the volume at the same temperature, is used to describe the relative water vapour concentration. The transport of water vapour through the internal air is dependent on the movement of air through the building.

8.4.2.1 Moisture in Building Materials

Building fabrics can be constructed from a multitude of building materials. Macroscopically, these building materials are generally considered to be homogenous. Microscopically, however, hygroscopic building materials consist of pores and capillaries, into which water and air holding water vapour can move in and out. The moisture behaviour of a material will depend on the material characteristics which dictate the ability of moisture to absorb and desorb water.

The amount of water transport through a material is the sum of water vapour transport (g_{vapour}), liquid water transport mechanisms (g_{liquid}), and any moisture generated ($g_{generated}$):

$$g_{total} = g_{vapour} + g_{liquid} + g_{generated} \tag{8.10}$$

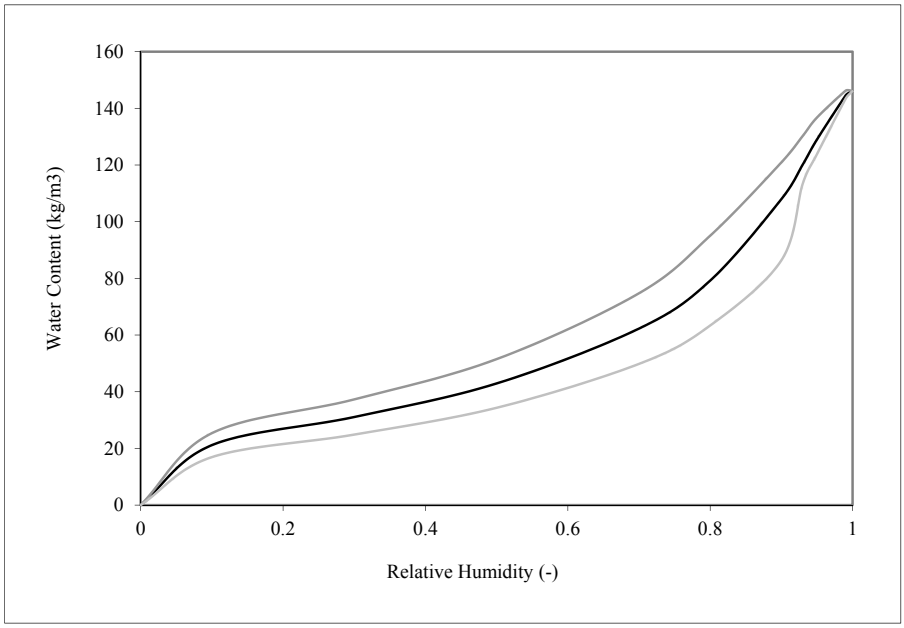

Figure 8.1: Sorption curve for a reference brick (EN15026).

A hygroscopic building material can absorb water into its structure. Porous materials can achieve varying degrees of saturation. The maximum achievable water content of a material – vacuum saturation - can be accomplished by removing the air from the pores of the material using a vacuum chamber before saturating. In normal situations, for example, if a material is immersed in water, air will remain trapped in the pores of the material, and the water content will reach capillary saturation, which is also known as free saturation.

Moisture moves into dry building materials through diffusion (water vapour), capillary suction, Darcy flow, and surface diffusion (liquid water), and through convective moisture flow of humid air moving through cracks and assembly joints. The movement of moisture within building materials can be calculated using different models, depending on the driving potential, which can be either partial vapour pressure, RH, or water content. The moisture behaviour of a material in terms of the transient water transport is often described using sorption curves (Figure 8.1) for models using RH gradient-driven models. These functions illustrate how the water content of a material increases as the RH increases.

The accumulation of moisture in building materials depends on moisture conditions and material properties. In dry porous material, moisture accumulates through molecular adsorption of water to the surface of the building material in the lower relative RH ranges (below 40%). At a higher RH, capillary condensation occurs in the pores when surface tension causes water to form a meniscus. Under equilibrium-state conditions, smaller pores are the first to become filled with water due to capillary condensation when exposed to increased levels of atmospheric RH. As the RH increases in the material, larger pores start to become filled with water. During sudden wetting of a building

material, for example, when exposed to a head of floodwater, non-equilibrium water distributions occur in the material. All pores, whether small or large, contribute to moisture uptake and transport. In this case, liquid water is drawn into the material primarily through capillary action.

Hysteresis, or a difference between the moisture retention functions for absorption and desorption, is often present in the moisture behaviour of building materials. Generally, this difference between absorption and desorption is ignored, and a single curve is approximated from the two. This assumption can lead to errors, as the differences between the moisture conductivities during wetting and drying may be significant. The limitations caused by this assumption, and modelling its effects needs to be acknowledged, particularly for flood modelling.

While water content in building materials is often described in terms of a sorption curve (Figure 8.1), the behaviour of liquid water in a material can also be described using a suction curve, which relates the suction pressure of the liquid in the pores of the material (P_{suc}) to the water content. Sorption curves can be converted to suction curves by using the Kelvin equation. The suction curve better illustrates the conditions in the high moisture region (RH > 98%), since the sorption curve is often very steep in this region. The Kelvin equation relates the RH of the pore air and the hydraulic pressure:

$$ln\left(\varphi\right) = ln\left(\frac{p}{p_s}\right) = \frac{P_h}{\rho_w . R_{H_2O} \cdot T} = -\frac{2\sigma\cos\left(\theta\right)}{\rho_w \cdot R_{H_2O} \cdot T \cdot r_k} \tag{8.11}$$

where φ is RH of the pore air, p is vapour pressure, p_s is saturation vapour pressure, P_h is hydraulic pressure of water inside the material pores (Pa), σ is surface tension of water (73×10^{-3}N/m at 20^{o}C), ρ_w is density of the water (kg/m^3), r_k is pore radius (m), and θ is the contact angle between the capillary absorbed water and the walls of the material pore. In order to take into account any resistance to liquid water transport in the building material, the liquid water permeability can be used to alter the suction curve using Darcy's Law.

$$g_{liquid} = -K\frac{\partial P_h}{\partial x} = K\frac{\partial P_{suc}}{\partial x} \tag{8.12}$$

where K is water permeability (kg/msPa), which describes the ability of liquid water to move through the material, and $P_{suc}$is suction pressure (Pa). The water permeability, and therefore the liquid moisture transport, will increase as moisture content increases, and is included in the materials data for water pressure-driven models (Figure 8.2).

When using sorption curves, moisture-varying liquid transport coefficients can be used to describe the movement of water in relation to the water contents in the material. The Liquid Transport Coefficient for suction (D_{ws}) refers to the movement of water into a water-soaked material face, while the Liquid Transport Coefficient for redistribution (D_{ww}) describes the movement, or redistribution of the liquid water throughout the material as it dries.

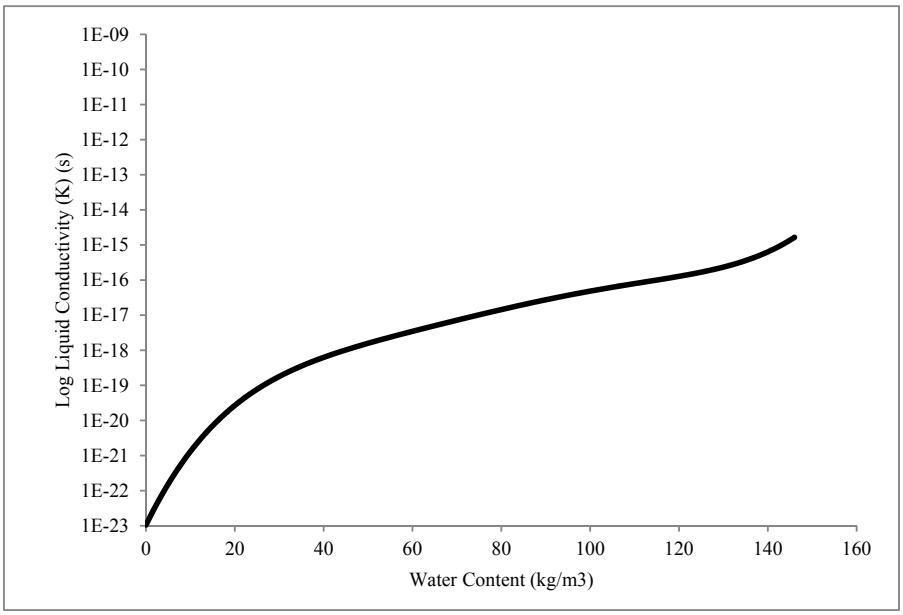

Figure 8.2: Liquid Conductivity for reference brick (EN15026).

The transport of water in the form of water vapour is performed with Fick's Law using partial pressure:

$$g_{vapour} = -\delta \frac{\partial v}{\partial x} \tag{8.13}$$

which describes the movement of water across a distance x, according to the water vapour diffusion coefficient in air (δ)(kg/msPa). Materials may have an inherent resistance to water vapour diffusion. The water vapour permeability itself is a function of the water content of the material, as wet materials tend to exhibit higher permeability than dry materials. The Diffusion Resistance Factor describes how the diffusion resistance of the material differs when compared to standing air, and can be dependent on the moisture conditions of the material. When related to the RH of the air, this is referred to as the Water Vapour Diffusion Resistance Factor (μ).

The movement of water from the materials into the boundary air layers due to convection can be described using the formula:

$$g_{convection} = \beta \cdot (v_{air} - v_{surface}) \tag{8.14}$$

where β is the moisture transfer coefficient (m/s), v_{air} is the water vapour content in the air, and $v_{surface}$ is the water vapour content at the surface of the material. The movement of moisture into the air at the boundary is also related to the heat transfer coefficient through the Lewis formula:

$$\beta = \frac{h}{\rho_{air} \cdot c_{air}} \tag{8.15}$$

where ρ_{air} is density of the air (kg/m^3), c_{air} is heat capacity of the air, and h is surface heat transfer coefficient (W/m^{2}K).

Moisture and heat transfer are closely linked processes. Moisture affects heat flow by altering the thermal conductivity, the latent heat transport, and the specific heat capacity in materials. Thermal conductivity increases due to the fact that additional pore space is taken up by water, which has a higher thermal conductivity than the standing air, and due to the heat-pipe effect caused by water evapourating and condensing inside the material. Latent heat transport occurs when moisture evapourates at the warm side of a wall and moves through the wall assembly as water vapour, condensing on the colder side. Specific heat capacity of materials increases due to the higher heat capacity of water.

Conversely, heat also impacts on moisture flow. Heat influences water vapour movement by altering the maximum water vapour content of the air, and therefore the RH. Heat also affects the movement of liquid water by causing a change in suction pressure due to the effect of heat on the surface tension of water. Thermal diffusion and effusion are capable of causing moisture transport due to a temperature gradient, but their effects are relatively small.

8.4.3 Air

Airflow through buildings is caused by pressure differences, and can be through doorways and windows, cracks, and the natural permeability of the walls in a structure. The nature of the airflow will depend on type of opening. For small openings, mass airflow ($\dot{m}_{air}$) is due to the pressure differences across the opening ($\triangle P_{air}$), density of the air (ρ_{air}), a flow coefficient (C_s) that depends on the size and type of opening, and an exponent (n) that describes the type of air flow.

$$\dot{m}_{air} = C_s \rho_{air} \left(\triangle P_{air}\right)^n \tag{8.16}$$

For large openings such as doors and windows, airflow can be in both directions simultaneously, due to varying pressure differences across the opening.

Airflow inside rooms will depend on the pressures from air entering the room, and the forces of natural convection. Temperature and RH of the air will dictate the air density, with differing densities leading to buoyancy forces and air movement. Warm air and wet air both have smaller densities than cold, dry air, and so will tend to rise inside a room. Like with heat and mass transport in the built form, the movement of air is strongly coupled to temperature and water content.

8.4.4 Boundary Conditions

Boundary conditions refer to the interior and exterior environmental conditions surrounding the simulated building fabric. Boundary conditions influence heat and moisture levels within a material due to surface transfer from the environment to the material surface. With exterior conditions,

weather files are generally used to describe conditions outside the building, and can include important information such as temperature, RH, long and shortwave radiation, wind speed and direction, and amount of rainfall. The building geometry can also be used to help describe the external boundary conditions by taking into account surfaces that may shade the external building fabric from sunlight and wind, and the orientation of the building relative to the position of the sun and instantaneous direction of the wind. High atmospheric RH, driving rain, rising damp, and floodwater are examples of boundary conditions which can introduce water into a material. Wind speed can affect the vapour and heat transfer coefficients, changing the hygrothermal interaction between the wall and surrounding air. Light can also have an impact, with long and short-wave radiation absorptivity of the material affecting its ability to absorb energy from the suns' radiation and warmth. Coatings on the material surfaces can effect the hygrothermal interactions between a surface and the environment by impeding water vapour diffusion.

In the internal environment, determining the boundary conditions can be more difficult since the conditions in the inside of the building depend on temperature, moisture, and air interactions of the fabric and built form of the building and the external environment due to, for example, ventilation, air movement, and heat and mass transfer between the internal and external environment.

8.4.5 Materials Information

Different building materials exhibit different behaviours in response to changes in temperature and moisture levels. Clarke and Yaneske classify materials into four different types according to their behaviour [57]:

- Impermeable: Materials which act as barriers to liquid and/or vaporous water, and do not change hygrothermal properties when wet.
- Non-Hygroscopic: Lightweight insulants such as mineral wool and foams that have a water vapour permeability, no hygroscopic water content, but a thermal conductivity.
- Inorganic-Porous: Masonry and related materials which have pores and can absorb significant amounts of water, thus altering their thermal and moisture behaviours.
- Organic-Porous: Products such as wood that are strongly hygroscopic and display a non-linear water vapour permeability.

Organic-porous materials are difficult to model because of their moisture characteristics. At high moisture content wood may undergo structural changes due to swelling, thereby causing pore sizes to increase and reducing hygroscopic effects [57]. The strong non-linear changes to the water vapour permeability of wood with water content is difficult to model due to a lack of available material information, and is likely to be underestimated in cases of high RH.

8.4.6 Spatial Discretisation

Solving complex HAM models requires dividing elements of the model into cells or zones that can calculate the transfer of heat or mass according to the required resolution of the outputs. The equations that can calculate flow can be either differential or partial differential equations. In HAM, these are typically solved using Finite Difference Methods (FDM), Finite Element Methods (FEM), or Response Factor Methods (RFM). FDM can be used for the calculation of differential equations (e.g. Vapour diffusion, heat conduction, liquid and airflow movement), while FEM can calculate partial differential equations for more complex geometries. RFM, used by the Effective Moisture Penetration Depth (EMPD) algorithm for moisture transport in EnergyPlus, uses the superposition principle and time series to calculate the heat transfer across a surface, but is not generally used for hygrothermal calculations. Grids produced in order to calculate HAM transfer using FDM or FEM can be coarse or fine, depending on the resolution required. Calculations can be done in 1D, 2D, or 3D.

The built form is typically divided into elements in whole-building simulation to account for air and water vapour movement. These can be highly granular grids, such as the FEM used for Computation Fluid Dynamics (CFD) models of air movement in indoor spaces, or a more general system of nodes, where each node represents a zone such as a room.

8.5 HAM Models

There is a wide range of HAM simulation software available which use different algorithms to calculate the conditions within a building fabric. For an in-depth review of the many models available, readers are referred to Woloszyn [298], who describe the 16 models used in the International Energy Agency (IEA) Annex 41 Common Exercises. This section will review the modelling principles employed by the HAM models in this research - Delphin, WUFI, and University College London Heat And Moisture Transport (UCL-HAMT).

8.5.1 Delphin

Delphin is a coupled HAM model developed at the Dresden University of Technology, that allows for the transient calculation of heat, air, moisture, and salt flows through building surfaces. Simulations can be run to solve 1D, 2D, and symmetrical 3D problems.

In Delphin 4, moisture transport is calculated based on the driving potentials of vapour pressure, and moisture content or water pressure, depending on the selected model for liquid water movement. The accompanying material database contains hygrothermal material information for a number of common building materials with either moisture-content driven sorption curves or water pressure-driven suction curve information. The software solves for a number of hygrothermal variables which

describe the behaviour of a building envelope under specific boundary conditions using differential equations describing heat, moisture, and air transport.

The water-pressure driven model allows for the inclusion of gravitational and hydrostatic effects in the model calculations, making it ideal for calculating floodwater movement into the building fabric. By using water and vapour pressure as the driving potential for moisture movement through building materials, Delphin is able to take into account the additional pressures forcing water movement in the material. Delphin describes the movement of moisture through moisture conductivities due to capillary pressure gradients, water vapour pressure gradients, and gas pressure gradient. The liquid water flux (g_{liquid}) in Delphin is calculated using liquid water conductivity (K_l, s) to describe movement due to pressure gradients:

$$g_{liquid} = -K_l \left[\frac{\partial P_h}{\partial x} + \rho_w g \right] \tag{8.17}$$

where P_l is liquid water pressure (Pa), ρ_w is density of the water, and g is gravitational constant (m/s^2). K_l is provided with the material data in the Delphin database and is used to calculate the capillary moisture conductivity or the hygroscopic moisture conductivity in order to describe the moisture transport at any particular material water content. The advantage of this calculation method over the water content gradient methods is that the pressures from heads of water or gravity can be applied directly to calculate moisture movement within materials. Like the other models discussed, Delphin takes into account the influence of moisture on thermal conductivity and vapour diffusivity of the building materials.

Weather data in the Delphin model is applied individually to the surfaces, reflecting both external and internal weather conditions. The Delphin model takes into account the effects of temperature, RH, long and shortwave radiation, driving rain, and heads of water to determine the movement of heat and moisture into and away from surfaces. Conditions inside the building have to be entered as separate weather files, with the exception of Delphin 4 which has a limited ability to calculate coupled air transport within the model.

In Delphin 4, the interaction between a hygrothermal surface in the model and indoor air can be calculated by specifying the surface area that the modelled surface accounts for, the total volume of the room, and the air change rate. This allows for the exchange of air in the room to be modelled, but cannot calculate the airflow through the property due to the physical structure and geometry of the building. Furthermore, the boundary conditions on the internal and external surfaces need to be input as separate conditions depending on their type (temperature, RH, long-wave radiation, etc.) and does not read full weather files. Internally, the boundary conditions also have to be entered individually, and there is no means for calculating the transient airflow, temperature, and RH values caused by a naturally ventilated or permeable property. Like WUFI and UCL-HAMT,

the moisture-related functions do not consider hysteresis when modelling moisture movement, and this ignores whether the material is wetting or drying.

Delphin 5 is also available, and contains an extended database of materials with water-pressure driven material information. The ability to model air change through ventilation has not yet been implemented in the Delphin 5 model (as of this writing). Further model capabilities, such as the implementation of a salt transport and crystallisation module, CFD computation in wall cavities, and material VOC transport and storage are in development. The program has been validated according to EN15026 [42], EN10211 [41], and Heat, Air and Moisture Standards Development (HAMSTAD) Benchmarks 1 and 5 [124]. Delphin comes with an extensive material database for use in simulations.

8.5.2 WUFI

WUFI is a hygrothermal model capable of calculating coupled heat and moisture transport based on vapour pressure and moisture content potentials. It calculates water vapour permeability, thermal conductivity, liquid transport coefficients, and heat capacity of materials within the building fabric based on the RH. It is available in three different forms: the normal 1D WUFI, WUFI 2D, and WUFI Pro.

WUFI is able to simulate the movement of liquid water into a building envelope through the water content gradient rather than the water pressure. By using the water content gradient to calculate the movement of moisture, WUFI is not capable of directly simulating the hydrostatic pressures that exist in floodwater. Liquid transport in WUFI is based on the equation

$$g_{liquid} = K_1 \frac{\partial P_h}{\partial x} \tag{8.18}$$

where K_1 is a Permeability coefficient (kg/msPa), and ∂x is the change in distance.

Whereas water transport in Delphin was calculated via the suction pressure, water transport in WUFI is based on the RH of the pore air. The Kelvin Equation (Equation 8.11) can be used to convert between the two driving potentials. As the permeability coefficient can vary according to capillary saturation, the Kelvin formula is substituted in WUFI in place of capillary suction stress. By substituting Kelvin's equation into the liquid flux density equation and assuming that w, R_D, and K_1 are constant and can be described as a new Capillary Conduction Coefficient (K_2), the liquid transport equation becomes:

$$g_{liquid} = K_2 \nabla T \ln \varphi \tag{8.19}$$

where φ is the RH. By introducing the idea of the Moisture Dependent Liquid Transport Coefficient (D_w) and eliminating negligible terms, the liquid conduction coefficient can be derived from the moisture storage function and the capillary transport coefficient, meaning liquid transport can be described using the equation.

$$g_{liquid} = -D_w \frac{\partial w}{\partial \varphi} \nabla \varphi \tag{8.20}$$

The Moisture Dependent Liquid Transport Coefficient can be in two different forms – one for suction (D_{ws}), and one for redistribution (D_{ww}). The suction coefficient is for situations where the material surface is wet due to rain or exposure to direct moisture. The redistribution coefficient is for circumstances where the surface is no longer wet and moisture is moving throughout the building material. Rain flags in the weather files cause the switch between the two types of coefficients used in the calculation.

The Moisture Dependent Liquid Transport Coefficient is not valid for water contents above free water saturation, since at this level there is no relationship between capillary transport and water content. The Moisture Dependent Liquid Transport Coefficient approximation is adequate for calculating the moisture behaviour of building components in contact with water for only short periods of time, such as heavy rain, but it is not necessarily suitable for sustained exposure to floodwater.

Water vapour diffusion in WUFI is modelled as being related to the partial pressure of water vapour, and the water vapour diffusion coefficient and resistance.

$$g_{vapour} = -\frac{\delta}{\mu} \nabla p_{WaterVapour} \tag{8.21}$$

where g_v is water vapour diffusion flux density (kg/m^{2}s), $p_{WaterVapour}$ is water vapour partial pressure (Pa), δ water vapour diffusion coefficient in air (kg/msPa), and μ is the moisture dependent water vapour diffusion resistance factor (-). Adding a water vapour resistance factor for each type of building material to the equation for water diffusion in air allows for Fick's diffusion.

It is possible to model liquid water absorption into a structure without including the hydrostatic pressures in WUFI. This can be achieved by producing a weather file with a density of rainfall set to 1000 kg/m^3 (density of normal water), and setting the rainfall absorption factor to 1. This mimics moisture movement into a wall resultant from immersion, but given the lack of consideration for the hydrostatic pressures caused by floods of different heights, the results may not be accurate for some materials with large pore radii (Section 9.2).

In WUFI, the heat and moisture transport are fully coupled. Heat storage capacity $\frac{\partial H}{\partial T}$ and the moisture content of the material are linked through the equation:

$$\frac{\partial H}{\partial T} = (c\rho + c_w w) \tag{8.22}$$

where c is the material specific heat capacity (J/kgC), ρ is the material density (kg/m^3), c_w is the specific heat capacity of water (J/KgC), and w is the moisture content (kg/m^3). The moisture dependent thermal conductivity is used to describe the relationship between the water content of the

material and the ability to conduct heat. The thermal conductivity at a specific moisture content is calculated by interpolating between data points entered in WUFI.

Weather data in the WUFI model can be entered as a proprietary WUFI weather file, selected from a map provided along with the software, or as EnergyPlus weather files. The external conditions are calculated based on the weather files specified, while the internal conditions require specifying the internal boundary conditions. The WUFI model is able to take into account the effects of temperature, RH, long and shortwave radiation, wind, and driving rain to determine the movement of heat and moisture into and away from surfaces.

Surface coefficients can be entered in WUFI to reflect the heat transfer coefficients, from which the vapour transport coefficients can be estimated. The heat transport coefficients can be set manually, or can be made wind-dependent to reflect the boundary conditions. Additional resistances to vapour transport, caused for example, by paint, can be set by adding a layer of air which will have a diffusion resistance equivalent to an additional layer. Surface absorptivity and emmissivity can be specified to model the impact of radiation on the heat transfer coefficient of surfaces.

WUFI+ is a whole-building version of WUFI, which can account for moisture sources and sinks inside a room and can be used to perform energy calculations. WUFI has been validated by laboratory measurements and complies with EN15026 [42]. Like Delphin, WUFI comes with a large material database.

8.5.3 EnergyPlus

EnergyPlus is a whole-building simulation program used to calculate heating, cooling, lighting, ventilation, energy flows, and water use in modelled buildings. EnergyPlus allows for the simultaneous calculation of coupled systems at defined time steps. It can model a number of different building behaviours that are likely to be important to the drying of flooded dwellings, including natural and mechanical ventilation, multizone airflow, advanced fenestration, heating and heat conduction, and building construction, geometry and orientation. It is capable of simulating detailed airflow through the building through the Airflow network, while heat and moisture transport through the building fabric can be simulated via moisture transport algorithms (UCL-HAMT).

8.5.3.1 Airflow Network

Airflow through a building can be modelled by explicitly inputting airflow rates for certain components into the model, or through the development of an airflow network. For complex, uncontrolled airflows, an airflow network can be developed which describes the movement of air between a series of nodes. EnergyPlus allows for the simulation of air movement through multiple zones in a building using either the direct input of airflow parameters or by using the AirflowNetwork model. The

AirflowNetwork treats the zones of buildings as a series of nodes that are connected through airflow components.

AirflowNetwork can simulate the movement of air at each timestep based on factors such as external wind direction and speed, permeability of surfaces, size and position of vertical openings, outdoor air temperature, and temperatures within zones. In the AirflowNetwork model, building zones and exteriors of buildings are described as nodes. Linkages within the model include exterior and interior walls, windows, and internal and external doors. Pressure calculations are first used to determine the pressure at each node within the model, while airflow calculations are used to calculate the movement of air from node to node. Each linkage requires two nodes – an inlet and an outlet node – and is described in terms of its relationship between pressure and airflow. Once the movement of air between nodes has been calculated, the temperature and RH at each node is then calculated based on air temperatures and humidity ratios.

AirflowNetwork takes into account the exterior wind pressure, speed, and direction to calculate the movement of air inside passively ventilated buildings. It is capable of modelling airflow through the cracks in exterior walls, making it ideal for modelling the permeability of building fabrics. AirflowNetwork can also simulate the effects of natural ventilation through open external windows and doors, taking into account building orientation. Movement within buildings can be modelled based on the permeability of internal surfaces, cracks, and open doors. In addition, buoyancy effects can account for the varying densities of air at different heights.

8.5.3.2 UCL-HAMT

UCL-HAMT is a one dimensional water content gradient driven hygrothermal model integrated into EnergyPlus Version 3.1.0 and capable of simulating the movement and storage of moisture within building surfaces from internal and external environments. The model applies a finite element grid to the building surface, allowing for the simulation of heat and moisture transfer across external and internal walls and ground floors. Since the algorithm is integrated into EnergyPlus, whole-building simulation can be used to simulate moist air movement through the property, while the hygrothermal model allows for simulation of moisture absorption of the non-flooded surfaces from the damp air. UCL-HAMT has undergone some initial testing and validation according to the Common Exercises of the IEA [298] with excellent agreements with the consensus solutions [236]. The required inputs for UCL-HAMT can be seen in Table 8.2.

The UCL-HAMT Heat Balance Algorithm describes the heat and moisture transfer algorithm used in the construction. The Combined Heat and Moisture Finite Element algorithm employs the UCL-HAMT algorithm to calculate the movement of heat and moisture within the building fabric. The UCL-HAMT model is completely coupled, meaning that moisture and heat calculations are

	Input
Exterior Conditions	Dry bulb temperature Wet bulb temperature RH Ground temperature Wind speed Wind direction Solar and Environmental radiation Cloud cover
Interior Conditions	Dry bulb temperature Wet bulb temperature Radiation Specified inputs House Schedule (e.g. windows opening, heating on) Occupant Schedule (e.g. cooking, showering)
Material Properties	Thickness Roughness Thermal conductivity Density Specific heat Thermal absorbance Solar absorbance Visible absorbance Porosity Initial moisture content Moisture storage function Liquid transport coefficient (suction) Liquid transport coefficient (redistribution) Water vapour diffusion resistance factor Moisture-related thermal conductivity
Assembly and Boundary Conditions	Latitude and longitude Shading Terrain Geometry of construction Interior walls, windows, doors, and floors, ceilings, and roofs Permeability of surfaces Orientation of surfaces

Table 8.2: Inputs for UCL-HAMT.

integrated in the mass transport calculations inside the material, and with mixing with the internal and external environments.

In the UCL-HAMT model, "surfaces" are considered to be constructions composed of any combination of "layers", or building materials. Surfaces are automatically split into cells throughout its depth, with the cell width being thinner near the material and surface boundaries, to account for the locations where temperature and moisture changes are expected to be greatest. The number of cells that materials are divided into is normally no more than 10, but the software can be customised to make the cell count greater or less, depending on the accuracy or speed of computation required. Virtual boundary cells with no cell thickness exist on either side of the surface that represents the surrounding conditions.

Heat and mass transport in the UCL-HAMT model is based on the equations of Künzel [167], described in the WUFI model outlined above. The driving potentials of moisture movement in the UCL-HAMT model are RH and vapour pressure. RH is used to calculate the moisture content of the material through the moisture storage function. The combined movement of liquid water and water vapour through the wall can be described in terms of:

$$\frac{\partial w}{\partial \varphi}\frac{\partial \varphi}{\partial t} = \frac{\partial}{\partial x}\left(D_w \frac{\partial w}{\partial \varphi}\frac{\partial \varphi}{\partial x}\right) + \frac{\partial}{\partial x}\left(\frac{\delta}{\mu}\frac{\partial T}{\partial x}\right) \tag{8.23}$$

The moisture storage function, Moisture Dependent Liquid Transport Coefficient for suction and redistribution, and the moisture dependent vapour resistance factor are all entered as a series of data points, between which the UCL-HAMT model interpolates the value for the instantaneous moisture content, up to the maximum moisture content, equivalent to the total porosity of the material.

The transfer of heat between the cells of the UCL-HAMT model is calculated considering heat storage, transport, and generation in the equation:

$$\frac{\partial H}{\partial T}\frac{\partial T}{\partial t} = \frac{\partial}{\partial x}\left(k^w \frac{\partial T}{\partial x}\right) + h_v \frac{\partial}{\partial x}\left(\frac{\delta}{\mu}\frac{\partial T}{\partial x}\right) \tag{8.24}$$

where $\frac{\partial H}{\partial T}$ is the moisture dependent heat storage capacity, ∂t is the timestep, K^w is the moisture dependent thermal conductivity, h_v is the evapouration enthalpy of water, δ is the vapour diffusion coefficient in air, and μ is the moisture dependent vapour diffusion resistance factor.

Weather data is entered into the UCL-HAMT model as EnergyPlus weather files, which calculate the external environment to which the building envelope is exposed. The boundary conditions that the internal surfaces are exposed to is calculated on the basis of the movement of air into and out of the building, the heat and mass transport with which this entails, and the production of heat and moisture inside the building. The UCL-HAMT model is able to incorporate the effects of temperature, RH, long and shortwave radiation, and wind to determine the movement of heat and moisture into and away from surfaces.

Surface convection algorithms are used in EnergyPlus to determine the movement of heat from building surfaces into external or internal air. The detailed algorithm takes into account the heat transfer according to temperature difference and orientation. Convective vapour transfer can be accounted for either by stipulating the transfer rate (SurfaceProperties:vapourCoefficients), or by allowing the values to be calculated dynamically using heat transfer coefficients. The UCL-HAMT surface convection algorithms take into account the heat gain through radiation, as defined by the absorbtivities and emissivities of the materials. The surface roughness of the materials and local surface wind speed are also considered when calculating the exterior heat transfer coefficient, as these affect the surface convection.

8.6 Summary

A summary of the different HAM models reviewed above can be seen in Table 8.3. Understanding the drying behaviour of flooded building materials and envelope assemblies is a complex process, which requires information on the hygrothermal material properties and surrounding environmental conditions. Experiments have been performed in the lab with material samples, with whole-wall or whole-building physical experiments in controlled settings, and in field studies of buildings following flood events in order to better understand the drying behaviour of buildings. However, physical experiments can be costly, time-consuming, and difficult to conduct for a wide range of building fabrics, built forms, and drying conditions. HAM models capable of simulating the movement of moisture and heat through structures, from simple 1D building envelope assemblies to whole buildings, offer a good alternative to physical studies. A range of HAM models that can potentially be used to model the drying behaviour of a structure are available. Using HAM for flooding requires a special set of considerations; these will be discussed in the next chapter.

		Model Name			
		Delphin	WUFI	WUFI+	UCL-HAMT
Envelope		1/2D HAM	1/2D HAM	1 Zone	Multizone
Whole Building		No	No	Yes	Yes
Airflow		Well mixed volume	Well mixed volume	1 well mixed zone	Interzonal flows
Liquid Diffusion	Vapour	Yes	Yes	Yes	Yes
	Liquid	Yes	Yes	Yes	Yes
	Moist Air	Yes	No	No	No
Hysteresis		No	No	No	No
Driving Potential		Vapour pressure for vapour diffusion & Moisture Content or Water Pressure for liquid water	Vapour Pressure and Moisture Content	Vapour Pressure and Moisture Content	Vapour Pressure and Moisture Content
Validation		[145]	[167, 180]	[139]	[236], Chapter 9

Table 8.3: Summary of features of reviewed HAM models.

Chapter 9

HAM in Flooding: Considerations and Validation

9.1 Introduction

HAM models are widely used to assess the hygrothermal performance of buildings, but they have not been used extensively for simulating the drying of flooded buildings. The modelling of the drying of a wooden church after a flood [25], and the simulations of the forced drying of historic wall constructions [26] have been done using EnergyPlus and WUFI, respectively. Delphin was used to simulate walls of buildings in Dresden following the flooding of the River Elbe in 2002 [118, 119]. HAM simulations offer a quicker and cheaper method of examining the absorption and drying of flooded buildings as compared to the alternative of physically constructing walls and buildings, flooding them, and then measuring the rate of drying.

However, a number of important considerations need to be made when modelling a flooded building using a HAM model. These issues are discussed in this chapter, and the limitations of HAM models in flood modelling are identified. The suitability of UCL-HAMT for modelling the drying of flooded buildings is assessed through a validation exercise and by comparing the simulation results to data from physical studies.

9.2 Flood Modelling Considerations

Liquid water movement into porous building materials is driven by capillary conduction, surface diffusion, hydraulic flow, electrokinesis, and osmosis. Hydraulic flow includes movement due to gravitational forces and pressure from heads of liquid water, which are often ignored in HAM modelling, but can have an important role in the modelling of floods. The dominant force drawing water into material during flooding will be capillary suction pressure on water. The radius of material pores (r) is critical to the capillary pressures, which can be calculated using a variation of the Kelvin Equation.

$$P_h = \frac{2\sigma}{r}\cos(\theta) \tag{9.1}$$

where P_h is capillary pressure (Pa), σ is surface tension (N/m), and θ is the contact angle of the water with the pore walls.

9.2.1 Gravity

The gravitational forces on liquid water inside small-pored building materials are significantly less than the capillary forces [258]. This is due to the inverse relationship between capillary pressure and the radius of the capillaries within materials. As pore sizes increase, capillary pressures reduce and the relative effects of gravity become more apparent (Table 9.1). The gravitational pressure on water inside any material will be determined by height of the water level above the ground. Gravitational pressures can be calculated using the equation:

$$P_h = \rho g h_f \tag{9.2}$$

where ρ is density of water (kg/m^3), g is gravitational constant (9.8m/s^2), and h_f is height of the flooded section of wall above ground level (m).

Gravity-driven liquid flow can be important for the modelling of the movement of water in large pored materials or non-capillary active materials, where capillary pressures are not dominant or do not exist. One such material is glass fibre insulation. Fibrous insulation is non-capillary active due to the fibrous nature of the material, and the effects of gravity can be seen following immersion in water [263]. Flooded fibrous insulation has been observed to drain through gravity within a few hours, leaving a top layer of material with a moisture content of 3-5% by volume, and a lower 10 to 20cm layer of saturated material [241]. This lower section dries over a period of months through the vapourisation of water.

However, in the majority of hygroscopic building materials, gravity makes little difference to the drying behaviour. This can be demonstrated by simulating the drying of saturated brick, gypsum, AAC, and concrete samples at 20^{o}C and 50%RH using Delphin, which can model liquid water flow due to gravitational forces. The surface RH of the materials at a height of 0m and 1m as the material dries is shown in Figure 9.1, and illustrate that, for the materials used in this research, there is little difference in drying rate at different heights due to gravity.

Gravitational drainage of water away from the building fabric requires assumptions regarding the drainage ability of the bottom boundary conditions. If the boundary is modelled with a damp-proof layer, then water will not be able to drain from the base of the structure. In this case, the gravitational pressure will lead to a higher water content at the bottom of the materials as the gravitational pressures force water towards the bottom of the material, where it is unable to drain

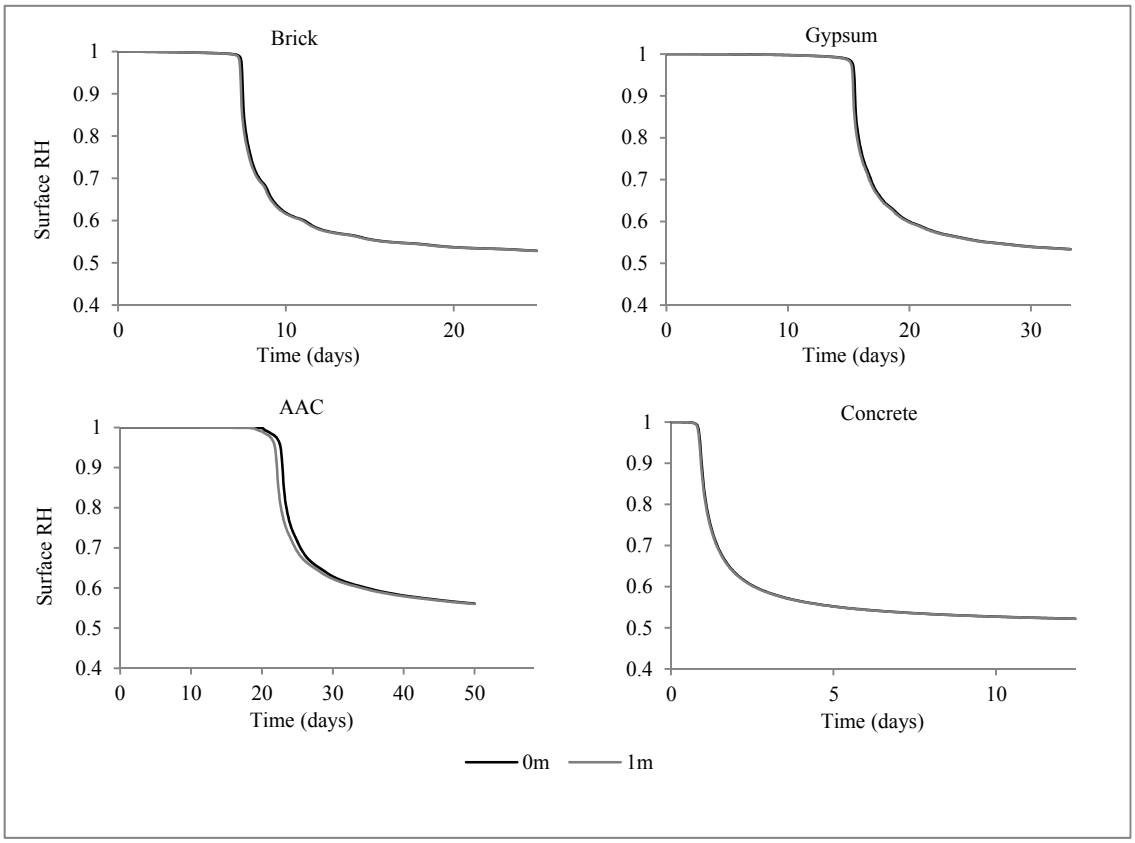

Figure 9.1: The effects of gravity on the surface RH of drying hygroscopic materials at different heights.

out through the bottom, and must instead move towards the surface of the wall and leave through vapourisation.

Capillary forces on the water inside building materials can lead to capillary rise. Capillary forces pull liquid water into a material in all directions equally, provided the material is homogenous. Capillary rise occurs when the capillary forces draw water up from wet material – for example, wet soil or a flooded section of the wall - to a height where the capillary forces drawing the water upwards are equal to the gravitational forces pulling the water downwards.

9.2.2 Head Pressure

Like with gravity, the impact of liquid pressure on a building material relative to capillary pressures will depend on the material characteristics. Capillary pressures in small pored material tend to be much higher than the pressures found under a head of water at depths one would expect from a flood (e.g. under 2m). This impact of water pressure has been described previously [127], where the water sorptivity of a clay brick increases by less than 50% under 100m head of water. As with gravity, the influence of pressure heads relative to capillary pressure will depend on the pore diameter. The hydrostatic pressure due to different flood heights can be calculated using Equation 9.2.

	Mean Pore Diameter (μm)(Blondeau et al, 2003 [27])	Capillary Pressure (Pa)	Hydrostatic Pressure (0.5m Head)(Pa)	Gravitational Pressure (0.5m Height)(Pa)
Brick	1.98	$1.47x10^5$	$4.90x10^3$	$4.90x10^3$
Concrete	0.96	$3.04x10^5$		
Mortar	0.07	$4.17x10^6$		
Gypsum Board	1.41	$2.07x10^5$		
Aerated Concrete	66.03	$4.42x10^3$		
Particle Board	70.25	$4.16x10^3$		

Table 9.1: Comparison of hydrodynamic pressures in flooded materials.

The effects of hydrostatic and gravitational pressure on water relative to the capillary forces in the materials will depend on the pore sizes. For most materials, the pressures due to floodwater and gravity will be much smaller than capillary pressures, and so can be ignored. For other large-pored materials, such as particle board, the impact will be important and should be considered.

9.2.3 Salt and Sediments

Floodwaters can often contain appreciable levels of salts, particularly tidal floods. Salts in building materials can be found dissolved in water or precipitated. Dissolved salts affect the liquid moisture behaviour, including liquid density and viscosity, and hygroscopic sorption and water retention behaviour by altering the surface tension and contact angle [171]. The evaporation rate of the water from the structure into the surrounding air can also be reduced due to the vapour pressure of the salt. Precipitated salts alter the pore structure of the material, blocking pores and restricting water movement. Sediment within the floodwater may also change pore structure, making surfaces harder to dry. Hygrothermal models with salts have been developed [117], but have not yet been included in the HAM models available to this study, and the effects are not considered in this research.

9.2.4 Dimensionality

Flood-related moisture movement in buildings is inherently a 3D problem, with gravity and capillary rise affecting vertical movement and flood pressure impacting horizontal movement. The geometry of the building fabric will also affect the moisture behaviour with corners, for example, able to absorb more water while experiencing reduced airflow, and potentially acting as thermal bridges. However, 3D hygrothermal models are computationally expensive, particularly for whole-buildings simulations.

Internal corners are likely to dry more slowly than the majority sections of the wall. The main driver of the prolonged drying period in the simulations is likely to be the difference in the amount of water within the sections of the wall geometry. To demonstrate this, the 24 hour flooding and subsequent drying of the corner of a solid brick wall was performed in WUFI 2D under typical UK external climate conditions, and 20^{o}C and 50% RH internal conditions. The RH across the wall

profile at the beginning of a flood and after 3 hours of flooding can be seen in Figure 9.2, showing how moisture moves into the wall at a rate dictated by the liquid water permeability of the materials. In corners, the centre remains drier than the centre of the main sections of wall, because the centre is farther from the liquid water-exposed internal and external surfaces. If a flood lasts long enough, the centre of the corner section will become fully wet, and will hold a greater amount of water than the main sections of wall. Having a greater amount of water within the corner appears to prolong drying time after longer floods, as the results of the drying phase of the simulation reveal (Figure 9.3).

Dimensionality and geometry may also affect the drying rate of certain locations within the building through thermal bridges. Thermal bridges, for example in building corners, affect the heat and mass transport in the building envelope. The temperature of the wall will impact on the moisture transport, and thus the drying rate of the wall.

Corners may also dry more slowly following flooding due to the lack of convective airflow in the corners, which removes damp air from the internal surface, allowing for drying to take place. Some HAM models are coupled with a CFD model for indoor airflow, which would be able to take into account the vapour removal from the damp surface. However, a whole-building CFD model coupled to a HAM model is computationally expensive.

The computational complexity of considering a 3D whole-building hygrothermal model with CFD airflow, and analysing the subsequent data, means that certain simplifications are necessary. For this research, moisture transport will be considered as a 1D problem, while noting that the drying behaviour of certain envelope geometries may differ from the main sections of the wall.

9.2.5 Surface Materials

Buildings often may have the same building fabric type, but surface coatings may differ. Different surface coatings may impact the behaviour of buildings during flooding due to their resistance to liquid water conduction as water moves into the structures, and the vapour diffusion resistance which may prevent moisture from leaving. There is a wide range of different surface coatings found on the external surfaces of UK dwellings (Section 7.6.1), such as renderings, stucco, and timber panelling. Internal finishings, such as tiling, carpet, wallpapers, and paint are also frequently found on internal surfaces, but there is little to no data on their relative frequency within the London housing stock.

The effect of internal coatings such as paint and wallpaper on the hygrothermal performance of building envelopes is usually accounted for by adding an additional water vapour transfer resistance to the envelope, which limits the ability of water vapour to move from the boundary into the internal facing layer. Liquid transport and thermal conductivity information for internal coatings are not easily available, and so using vapour diffusion resistance allows for the moisture resistance of the coating to be accounted for under normal operating conditions. In WUFI and UCL-HAMT, this

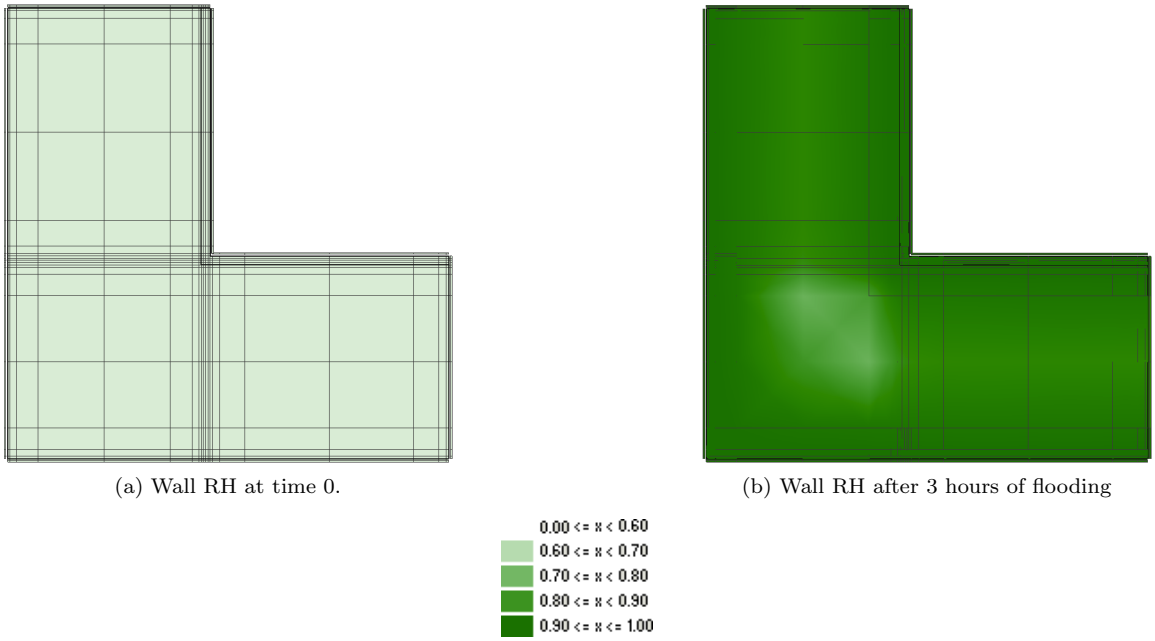

(a) Wall RH at time 0.

(b) Wall RH after 3 hours of flooding

Figure 9.2: Movement of water into a corner section of wall from WUFI 2D Motion, showing the main sections of the wall at time 0 (9.2a) and after 3 hours (9.2b) as it becomes wet during flooding.

vapour diffusion resistance is in the form of a diffusion thickness which corresponds to the thickness of a layer of air with the equivalent resistance to the coating. With flooding scenarios, this resistance cannot be applied, since liquid water movement dominates the moisture flow into the material, and is also important in redistribution of the water inside the wall. Therefore, internal surface coatings must be ignored unless they have liquid transport information available.

External coatings may also impact a building's resilience to flooding. Finishes such as renders, timber or stone cladding, tiles, and paint are commonly found in the UK housing stock, and information on their frequency of occurrence is more readily available through, for example, the EHS. External surface coatings may influence a building's resilience to flooding by preventing moisture ingress into the building surface. This may be caused by the surface coating having moisture transport characteristics that prevent water ingress into the structure, or it may act to seal imperfections in the construction through which water may seep into the building. Some materials, such as timber and renders, will have hygrothermal materials data with liquid transport information, while others such as paints need to be approximated as a layer of air with a vapour diffusion resistance, as per the internal finishings. External surface coatings may also alter the overall air permeability of the building, affecting the natural air change rate of a sealed building, and indirectly impact the drying rate of different wall types in whole-building simulations.

Taking external finishes into account in modelling the flooding and drying of dwelling archetypes would require a significant number of additional simulations, and there is little data on the spatial

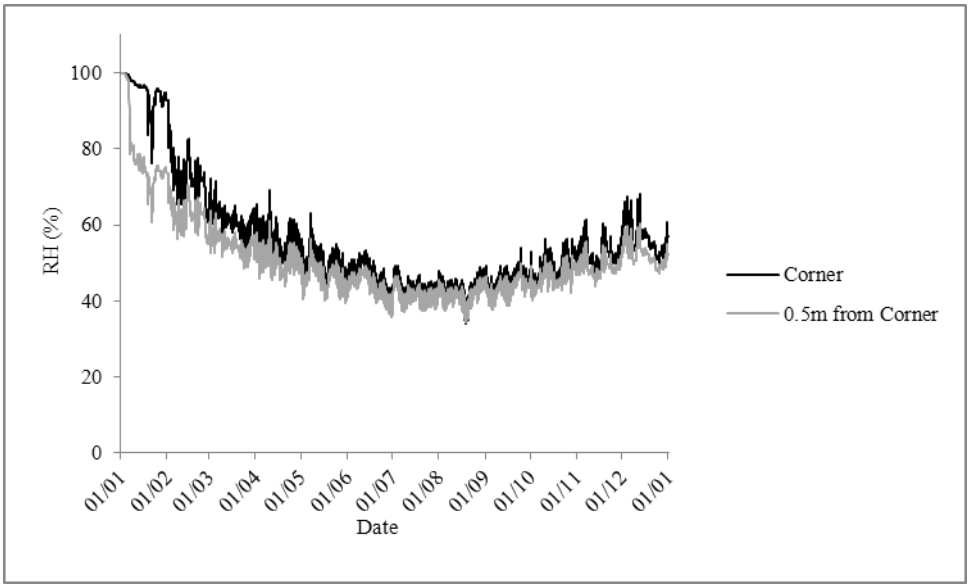

(a) Winter flood drying.

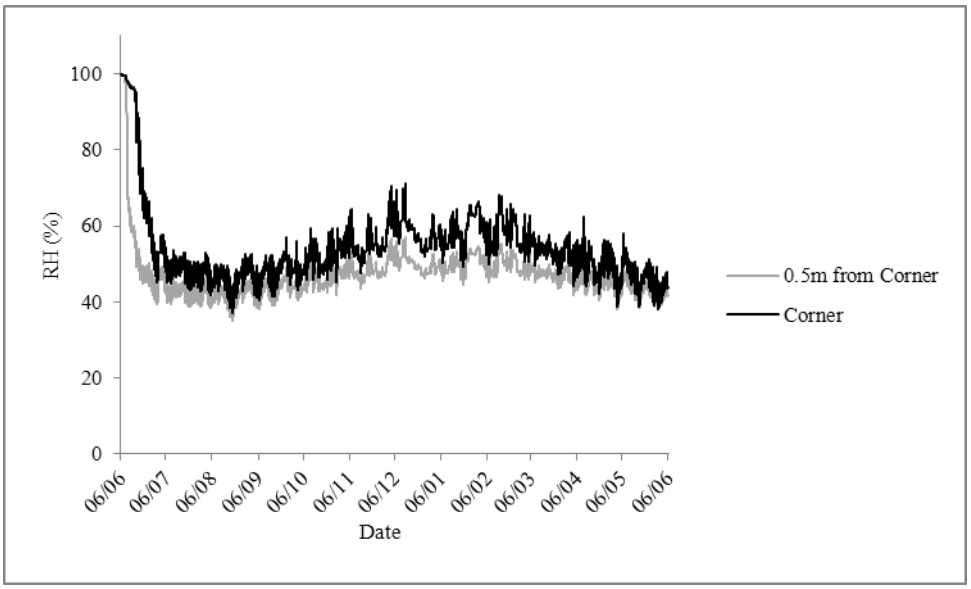

(b) Summer flood drying.

Figure 9.3: Comparison of the RH decline in a drying solid brick wall following winter and summer floods in a corner of the wall versus 0.5m from the corner.

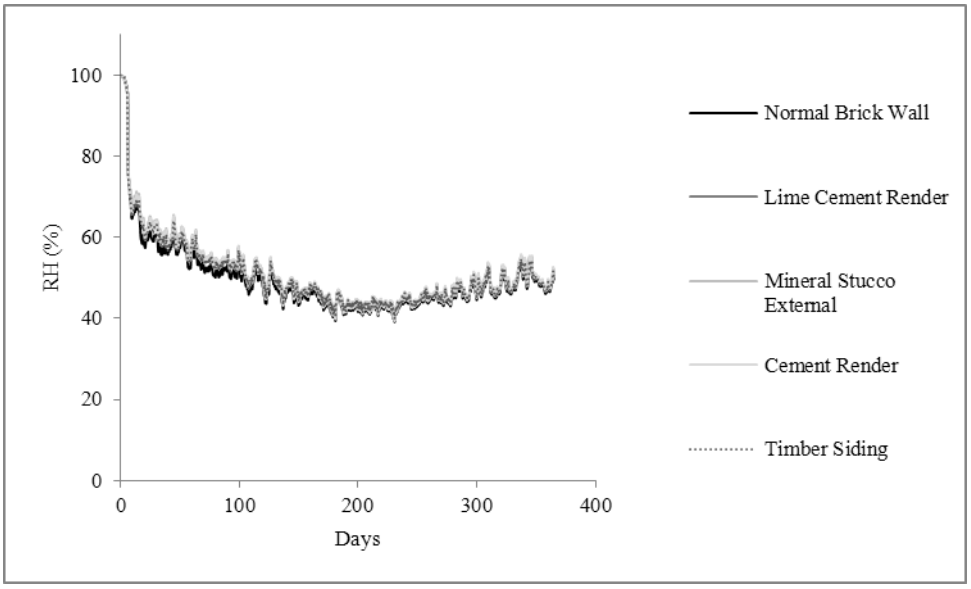

Figure 9.4: Comparison of the drying rate of walls with different external finishes.

variation of the different wall finishes across the research area, meaning the drying behaviour of dwelling archetypes with different surface finishes could not be mapped spatially. In addition, since there is limited information on the air change rates of walls with different surface finishes, it is not possible to account for these permeability differences in this study. A preliminary examination using the 2D WUFI model was performed to examine the influence of external finishes on the drying rate of solid 9" brick walls under typical London external climate conditions, and 50% RH and 20^{o}C internal conditions. The water absorption and drying rate of walls with different external surface coatings under the same climate conditions suggests that the different surface finishes do not make a major difference to the drying behaviour of the internal surface of the walls (Figure 9.4). Therefore, surface finishes are ignored in this study.

In addition to internal and external surface finishes, some walls may have a moisture barrier designed to prevent moisture movement into the building under normal operating conditions. These barriers are more likely to be found in modern cavity walls, and typically act to prevent water vapour from moving into the structure. As such, they are unlikely to be effective in preventing liquid water ingress under flood conditions, but their restriction of air and water vapour movement may impact the drying ability of a dwelling under sealed conditions. There is currently little data on the frequency and type of moisture barriers used in UK constructions, although these are likely to become more frequent in the future; nonetheless these are ignored in the simulations. This is unlikely to affect the results, as vapour transport in air through the building surface is not considered in either the UCL-HAMT or WUFI models.

9.2.6 System Complexity

The physical and simulation-based studies of post-flood drying have focused on varying levels of complexity, from examining the drying of a material coupon (for example, in Chapter 5), to typical wall assemblies (for example, Escarameia and colleagues [97]), to whole-building assemblies. When comparing the results of different studies, it is important to take into account the physical differences that may impact the drying behaviour of the materials.

Due to restricted laboratory space, material coupons are likely to be smaller in size than those used in constructing dwellings. The size of a material plays an important role in the drying behaviour [242] as the surface to volume ratio differs from larger materials, giving the material a greater relative surface area with which to exchange water vapour with the drying surrounding air. In addition, moisture in the centre of the material will have less distance to move to the drying surface. In constructions of whole surfaces, such as walls, the surface area to volume ratio will be significantly reduced. In the centre of the surface, four of the potential six drying surfaces are often considered to be adiabatic due to the lack of moisture movement from the surfaces not exposed to boundary conditions or different materials. In addition, the hygrothermal properties of neighbouring materials may cause materials in whole constructions to exhibit a different drying behaviour. As such, materials in whole constructions are likely to dry much slower than material coupons - a fact which needs to be taken into account when comparing the drying behaviour of different sized materials.

The drying behaviour of materials is likely to change even more when extrapolated to whole-building scenarios. Walls constructed for the purpose of quantifying the drying ability of walls following flooding will be exposed to the same temperature and RH boundary conditions on both the internal and external faces of the wall. The boundary conditions will impact on the ability of the surfaces to dry, particularly in regards to the ability of the surrounding air to remove water vapour from the wall surface. In whole buildings, internal and external conditions will differ, and the water vapour removal rate of the indoor air will depend on the building air change rate. In addition, the exposure of the internal and external surfaces may differ in terms of their exposure to radiation sources which may impact the drying rate. Therefore, physical or simulation studies of the drying rate of wall types can identify the relative drying abilities of different walls, but do not necessarily describe how they will perform in a whole-building environment.

As an example of how the level of complexity of a study impacts on material drying, a plaster coupon the same size as the ones used in Chapter 5 and one of the most common wall types in the UK, a solid 9" brick wall with 10mm plaster coating, were simulated in Delphin 4 drying without consideration for the air change rate of the surrounding air (i.e. unlimited ventilation of damp air). To demonstrate the impact of wall types and ventilation, the same solid brick wall and a wall that has been observed to take longer to dry, a brick cavity wall with glass fibre insulation, were simulated drying at 20^{o}C and 50%RH in a model 8m^3 room, where all the walls were flooded to a nominal

height of 2m. An air change rate of 4 air changes per hour (ach), approximately equal to that of a single storey building with open windows and cross ventilation [34] was provided. Materials properties for brick, gypsum plaster, and glass fibre were taken from the IEA Annex 24 [176]. The RH of the plaster 0.5 mm inside the interior surfaces was output hourly. The drying coupons and walls show a wide range of different results for the RH of the plaster surfaces, depending on the construction of the wall and the inclusion of internal ventilation rates in the simulation (Figure 9.5). This indicates the importance of understanding the building as a whole when determining the drying rate of material surfaces following flooding.

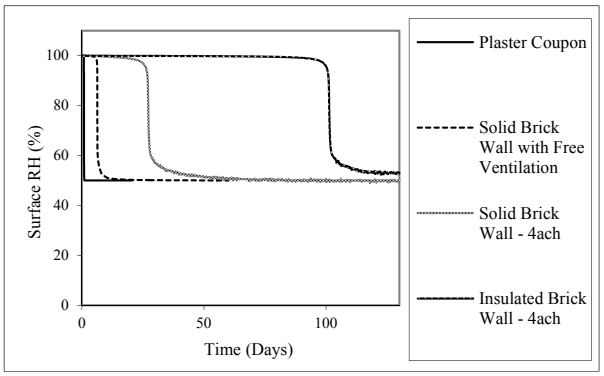

Figure 9.5: Drying ability of material according to size/model complexity.

9.3 Model Selection: Delphin and UCL-HAMT

As discussed in Chapter 8, modelling flooding using hygrothermal simulations requires the ability to model moisture movement into the flooded building surfaces during the flood event, and the drying out of the building under a range of conditions following the flood. In addition, as discussed above, the level of complexity is also important for modelling the drying ability of walls in different buildings. Therefore, for modelling the drying of the flooded dwelling archetypes, the following characteristics of a HAM model would be desired:

- Liquid Transport
  - The ability to model floodwater moving into the dwelling structure taking into account hydrostatic pressures from the flood heights at different levels.
  - The gravitational effects on water within the wall as it dries.
  - The capillary action on water in the wall, drawing the water up into the non-flooded section of the wall.
  - The impact of salts, sediments and gravity on the drying rate would allow for the understanding of how these phenomena affect drying times.

- Dwelling Geometry
  - The location and size of windows, doors, and air permeable surfaces, dictating the potential airflow through the dwelling under different weather conditions.
  - The orientation of the dwelling and shading surfaces, determining the amount of windflow and solar radiation incident on the drying surface.
  - The ability to model the whole dwelling in order to understand the movement of the wet air to non-flooded sections of the property, and the impacts of different drying methodologies on the overall dampness of the property.
- Ventilation
  - Air movement into and out of the dwelling due to permeability of the building envelope and open doors and windows.
  - Ventilation inside wall cavities and subfloors.
- Weather
  - The ability to calculate the effects on heat, moisture, and air movement within the model based on the weather data critical for the drying of flooded dwellings, including temperature, RH, wind speed and direction, radiation, and rainfall.
- Equipment
  - The means of simulating the use of different flood remediation equipment, such as forced air driers and dehumidifiers, and the impacts of different drying strategies.

In addition, the model should be fully validated for modelling moisture transport in both the liquid and vapour phases. There is, unfortunately, no HAM model that allows for the modelling of the wide range of effects which are likely to be important for flood modelling. Delphin is capable of simulating the movement of water into the different building fabrics of the various dwellings according to the flood heights, the effects of gravity and capillary rise, and can simulate the effects of salt content in the wall, but the commercially available product is currently limited to simulating individual surfaces and cannot simulate the effects of the full house in the ability of the dwelling to dry.

WUFI and WUFI+ can model the movement of water into the structure due to capillary forces, but does not include hygrostatic forces. While more advanced versions of WUFI can simulate whole buildings, it does not offer the wide range of modelling capabilities as do other whole-building systems such as EnergyPlus.

UCL-HAMT does not have the ability to model the movement of liquid moisture into the structure of the walls from an external head of floodwater, nor can it account for salt, sediment, or gravitational

effects on moisture movement. In addition, while an initial validation has been performed on the model for vapour transport, validation has not yet been performed for liquid transport. However, UCL-HAMT is very strong at computing whole-building effects, including air movement within the dwelling, local shading effects, and the heat and moisture generation by occupants and equipment in the dwelling. EnergyPlus also has the advantage of being customizable, meaning that algorithms for gravitational flow and salts can be implemented into the model at a future date.

The processing of the many factors which will impact the drying of flooded properties will also be computationally expensive, particularly if the gravitational effects are to be considered in the flooded walls. Including gravitational effects will require 2D simulation models, which increases the number of cells and calculations required for the finite element model. To perform this for all walls in a flooded building would be computationally expensive, particularly for a highly granular discretisation. The number of output values for the water content in the walls would also increase significantly, depending on the number of vertical cells.

As there is no ideal model to simulate the flooding and drying of a dwelling that includes all of the potentially important factors, a compromise was proposed. Delphin 5 was used to model the flooding of materials using the hydrostatic floodwater pressures, and the 1D moisture content across the profile recorded. This moisture content was used to create profiles of flooded surfaces in UCL-HAMT, and then simulated using UCL-HAMT in order to examine the drying time under different whole-building drying scenarios to include the impacts of the built form on drying ability of dwelling archetypes. The effects of gravity on different surfaces was approximated by dividing the flooded sections of the horizontal walls into two sections to reflect the higher water contents exhibited by some materials prone to gravitational water movement.

9.3.1 Validation of UCL-HAMT

IEA Annex 24 identified three methods for validating hygrothermal models: intermodel comparison, analytical verification, and empirical validation [132]. There are a number of published validation methodologies for HAM models, which examine the performance of the models in response to a defined set of conditions. Some validation methodologies examine simple steady state 1D heat and moisture [42] or thermal bridge [41] problems in building envelopes, and transient 1D heat and moisture problems [124]. The validation of more complex whole-building models has been outlined in the IEA Annex 41, where the Common Exercises describe a methodology for validating models based on the calculated boundary conditions [299]. Other validation methods have been employed by researchers to compare the behaviour of the models with data from physical experiments.

The HAM models discussed above have been tested and validated to different standards. Both WUFI and Delphin have been validated in terms of their liquid transport under steady state conditions [42], while transient validation for liquid transport has been performed with physical exper-

imentation for WUFI (e.g. [167], among others) and transient standards for Delphin (e.g. [124]). Whole-building simulations for WUFI+, Delphin, and UCL-HAMT have been performed according to the IEA Common Exercises under 'normal' operating conditions [236, 299].

While both WUFI and Delphin have been validated for liquid transport, UCL-HAMT has not. As an initial validation of the liquid transport performance of UCL-HAMT, an inter-model comparison between UCL-HAMT and WUFI was performed. In addition, the validation replicated the constructions and boundary conditions described in physical experiments in order to demonstrate that HAM models can be used to obtain a useful estimate of the drying behaviour of different building types.

9.3.1.1 Validation Methodology

In order to validate the UCL-HAMT model, simulations were run to compare the results of UCL-HAMT and WUFI. WUFI was chosen for this inter-model comparison exercise because it has undergone extensive validation (discussed above), and uses the same algorithms as UCL-HAMT to calculate heat and mass transport. The simulations were run for three types of walls for which physical data was available [97], under the same static experimental conditions in order to also provide comparison between model predictions and measured data.

An uninsulated brick/AAC cavity wall, a brick/AAC cavity wall with 100mm of fibrous insulation, and a solid AAC wall with lime cement render on the internal face were considered. In order to provide suitable initial moisture contents, the walls were first modelled with the tool 'Delphin'. Water absorption into the structures was modelled by Delphin for three days (outside surface) and one day (internal surface and cavity) in order to approximate the water content following a flood. The walls were then modelled in WUFI and UCL-HAMT, segmented in order to reflect the varying moisture contents in the AAC, but without internal plaster finishing on the cavity walls, which was removed for drying during the experiment.

The walls were allowed to dry under the average climate conditions reported for the experiment (12°C and 72%RH) for one year. For the purpose of this validation exercise, heat transfer coefficients (8W/m^{2}K) and vapour transfer coefficients (2E-8 kg/Pa.s.m^2) were simply kept constant for both faces to reflect the fact that both sides of the experimental wall were exposed to the same internal laboratory conditions. Water content directly below the surface (1.3mm) and the RH throughout the profile were output hourly. The modelled relative water contents at the surfaces of the walls were compared with each other and also to the drying times reported by Escarameia and colleagues (2007).

9.3.1.2 Validation Results

The results of the validation can be seen in Figures 9.6 and 9.7. UCL-HAMT demonstrated a good agreement with the moisture contents calculated by WUFI at different depths within the wall

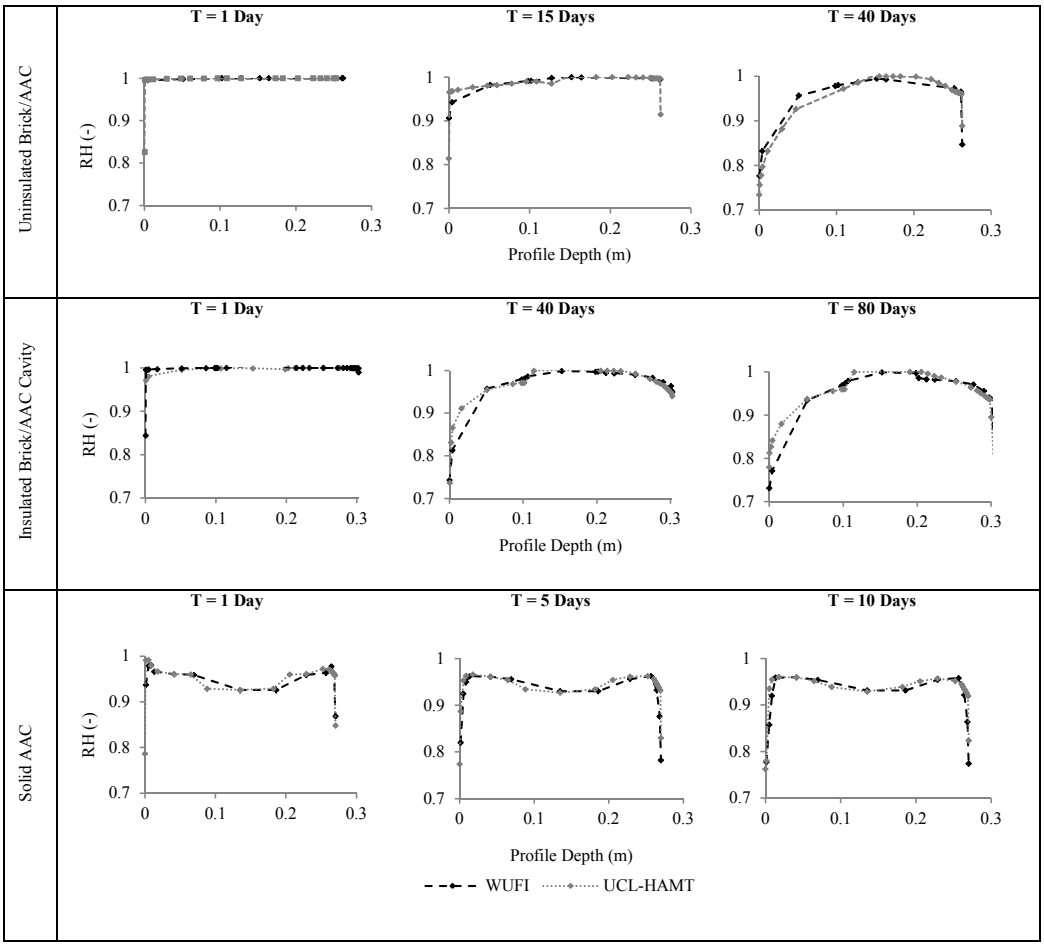

Figure 9.6: Comparison of wall profiles for drying walls modelled in WUFI and UCL-HAMT at different times.

profiles. The agreement between WUFI and UCL-HAMT indicate that UCL-HAMT is providing a valid calculation result. The experimental results from Escarameia and colleagues showed the times required for the internal surfaces of the walls to dry were 4 days (solid AAC wall), around 35.5 days (uninsulated brick/AAC cavity), and over 5 months (insulated brick/AAC cavity). The surface results of the simulations in UCL-HAMT and WUFI reflect this relative difference in drying ability, with the moisture content on the surface stabilising in solid walls after 3 days, uninsulated cavity after 40 days, and insulated cavity after 60 days.

Comparing the building fabric calculation in WUFI with the whole-building simulation model of UCL-HAMT required adapting UCL-HAMT for constant internal and external conditions, eliminating the whole-building nature of the model. Comparing a single-surface model with a whole-building model presents challenges but UCL-HAMT and WUFI nevertheless showed a good agreement in their calculation results.

The hygrothermal models provided a reasonable estimate of the drying behaviour of the unin-

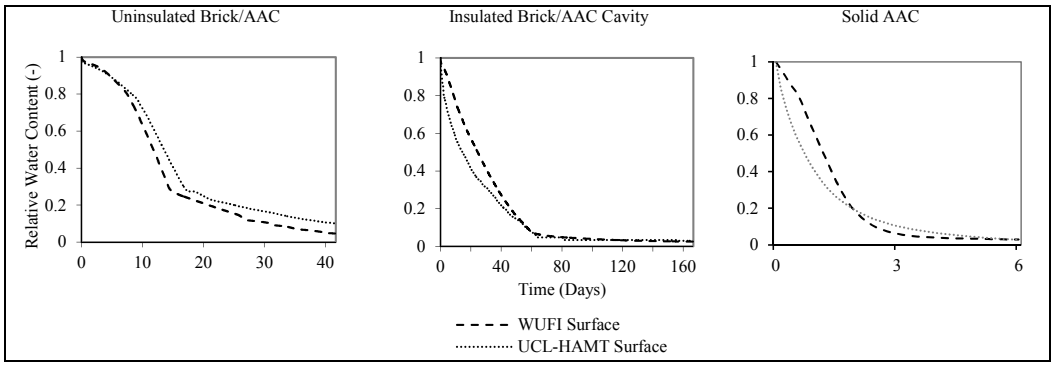

Figure 9.7: Surface drying comparison of walls between WUFI and UCL-HAMT.

sulated walls. There are a number of limitations when comparing the simulation results to physical data. Neither the specific hygrothermal parameters for the materials, nor the transient boundary conditions used in the physical experimentation are available, and the surface moisture measurements in the physical experiment were measured using a protimeter with the associated uncertainties. Nonetheless, UCL-HAMT provides a useful estimate of the drying rate of different building fabric types for the uninsulated walls. The simulation results of the brick/AAC wall with fibrous cavity insulation showed a longer drying time than the uninsulated equivalent, however it was less than the extrapolated drying time determined in the experimental study. This may be due to differences in the hygrothermal data for the fibrous insulation and the insulation in the physical study, as well as the extrapolated drying time of the physical study overestimating the actual drying time. A lack of available moisture transport data for fibrous insulation under high moisture contents meant that this study was limited to using the data taken from Hokoi and Kumaran [136] which had hygrothermal material characteristics different from those reported for the insulation used in the experiment. However, the uncertainty in the drying times for fibrous insulated cavity walls associated with the lack of sufficient material data must be acknowledged.

9.4 Conclusions

There are a number of specific requirements of HAM models when they are to be used for simulating the flooding and drying of buildings, in terms of the calculation of liquid water transport, and the ability to model whole building geometry, ventilation, and air movement. Other factors such as salts and sediment, gravity, hydrostatic pressure, and the physical geometry of the building envelope may also play important roles in the flooding and drying behaviour of a building. The influence of external and internal finishes of buildings are difficult to take into account without data on their liquid transport properties, but an initial examination suggests that they have little influence on the drying of the wall in 1D simulations.

As there is no ideal HAM model for flood simulation, UCL-HAMT will be used to perform the drying simulations based on estimates of surface water content from 1D Delphin simulations. An initial inter-model validation of UCL-HAMT for liquid transport shows that the model is calculating the drying of the walls correctly, and that the results provide a useful estimate of the drying behaviour of walls from physical experimentation. Simulations of typical London dwelling archetypes drying under different conditions following a flood will be performed using UCL-HAMT in the following chapter.

Chapter 10

Whole-Building Simulation of Flooded Dwellings

10.1 Introduction

This chapter introduces a modelling technique for the simulation of whole-building drying of flooded London dwelling archetypes. The objectives are to:

- Examine the differences in drying rate of different London archetypes, taking into account their built forms, types of walls found in the properties, and ventilating ability of the archetypes.
- Understand the impact of external weather conditions and flood height on the drying rate of dwellings.
- Compare the impacts of different drying regimes on the drying of the archetypes, taking into consideration internal and external conditions of the dwelling.
- Model the microbial risks to occupants from mould and bacteria inside the drying archetypical dwellings.
- Assess the uncertainty of the UCL-HAMT model to variations in material and geometrical parameters through a differential sensitivity analysis.

Dwelling archetypes adapted for hygrothermal simulations in Section 7.4 were used for the simulations in order to examine the drying behaviour of different dwelling archetypes under different drying scenarios. A winter flood with a nominal height of 0.5m, based on the modelled maximum height of a 1-in-100 year fluvial flood risk for Hackney, East London [246] was used as a basis for comparing the drying rates of different property types under different scenarios. Simulations were performed with the common wall types found in the properties, as determined in the EHS analysis in Section 7.4. Five different drying scenarios were modelled using Delphin 5 and UCL-HAMT, including:

	Drying Scenarios				
	Windows Open	*Windows Open & Central Heating*	*Abandoned*	*Temporary Heater*	*Climate Change*
All Built Forms	✓	✓	✓	✓	
Modal Wall	✓	✓	✓	✓	✓
Range of Walls	✓	✓	✓		
Seasons			✓		
Flood Heights			✓		
Mould Models	✓	✓	✓	✓	✓
Bacteria Models	✓	✓	✓		

Table 10.1: Summary of simulations performed.

- Natural ventilated drying, where the windows and internal doors were left open and the dwellings allowed to dry through airflow through the property after a 0.5m flood event occurring in the winter (January 1st).
- The above natural ventilation flood scenario, with the addition of indoor central heating operating in each room.
- The natural ventilation flood scenario, with the addition of a high-powered temporary heater in the living room of the property.
- Abandoned properties, with their windows and external doors shut, drying at a range of flood heights during both winter and summer (July 1st) flood events.
- Investigating the potential impacts of climate change on the drying ability of a specific property using natural ventilation and under abandoned scenarios following a 0.5m flood.

The first two drying scenarios are representative of interventions available to all residents (without the additional heaters, dehumidifiers, and fans that professional restoration services may use), while the use of a powerful temporary heater is representative of a typical professional intervention, and the abandoned scenario is representative of no remediation action being taken. The mould model of Clarke [58] was used to predict the internal surface area at risk of mould growth within the dwelling at each time interval for *A. versicolor* and *S. chartarum*, while the bacterial models developed in the previous chapters were used to calculate the risk of bacteria persistence (above 1% of the initial population size) on the surfaces. The types of simulations performed are summarised in Table 10.1. This tool can be used in future studies to examine the potential health impacts of different flood events and drying practices, as well as to optimise remediation techniques.

10.2 Methodology

As discussed in Section 9.3, no simulation package is available that will allow both the simulation of water movement into a structure using a pressure head of water, and the whole-building simulation

of the internal and external drying of the dwelling. Therefore, two separate HAM models are used to simulate the flooding and drying of the dwellings. Delphin 5.6 is used to model the flooding of the wall and floor assemblies, while UCL-HAMT is used to simulate the whole-building drying of flooded dwellings.

10.2.1 Hygrothermal Flooding Simulations

Delphin was used to simulate a 24 hour flood in the external and internal walls and floor assemblies using materials selected from the Delphin material database that were similar to those taken from the WUFI database for the housing stock model. It was assumed that water penetrated the building surfaces from both the interior and exterior sides. Water was assumed to fill the cavity instantly due to the presence of airbricks and cracks in the exterior and interior sheaths of the wall, and the observation that water is able to penetrate a wall soon after flooding commences [263]. The flooding simulations account for the potential impact of the head of pressure (0.5m), while a moisture source was used to simulate the presence of water inside wall cavities, implying that water absorption was considered from external, internal, and internal cavity surfaces.

10.2.2 Hygrothermal Drying Simulations

10.2.2.1 Building Surfaces

The simulations in Delphin provided an estimate of the amount of water penetration into building surfaces. The Combined Heat and Moisture finite element algorithm in EnergyPlus UCL-HAMT was used to model drying. Building surfaces were divided into vertical 'flooded' and 'non-flooded' sections in UCL-HAMT, and the results of the Delphin simulations of water movement into the wall and floor fabrics were then used to approximate the water content levels for the 0.5m high flooded sections. In cases where the Delphin simulation predicted different water contents within a single material layer of a wall (for example in AAC, where the core remained drier than the surface), walls were divided into horizontal sections with different initial water contents. Dry sections of the dwellings were prepared with an initial RH of 80%, chosen as the yearly average for the external weather file. UCL-HAMT automatically divided the walls into a coarse grid with 12 (solid 9" wall) to 22 (insulated AAC cavity wall) cells across the wall profile. The depth of the surface cells in a HAM grid will affect the moisture outputs because in drying walls, the core of the wall dries more slowly than the surface, so a deeper surface cell will appear to dry slower than a shallow surface cell. In addition, larger cells will be less able to report the high localised changes in moisture content that may occur during drying due to interactions with the boundary conditions, and may even result in inaccurate moisture transport calculations. To ensure that the internal face of all surfaces shared the same cell depth, all surfaces were modelled with a 1cm layer facing the internal space. In doing this, it forced the surface cells in all of the layers to be the same depth in the automatic discretisation

and made sure that the surface cell was small enough to reflect the transient changes in the internal environment. The construction of the dry walls and floors with their materials and dimensions can be seen in Figure 10.1, while the dimensions and different starting RH values for flooded walls can be seen in Figure 10.2.

To account for gravity, flooded sections of walls were divided into a further two sections. Walls that would be impacted by gravity (i.e. glass fibre-insulated walls) were modelled with an insulation moisture content at effective saturation ($0.98 m^3/m^3$ water) on the bottom 20cm of the wall, while the rest of the flooded section was modelled with an RH of 100%, according to the observations made by Sandberg [241]. Gravitational influences on other materials were ignored. Concrete walls can exhibit signs of self-sealing which causes liquid water to stop absorption at a certain distance into the material [166]. Because of this, concrete materials were divided into two different types – outer layers with liquid conductivity 70mm thick, and a central core with liquid conductivity turned off and only vapour diffusion permitted.

The materials data used to model the surfaces of the dwellings were determined in Section 7.6.2, and the complete material information can be seen in Appendix B. Materials were assigned a surface roughness of 'Rough' for the EnergyPlus Detailed Surface Convection Algorithm, which was used to calculate the heat transfer coefficients of the surfaces. A thermal absorptance (0.9), solar absorptance (0.7), and visible absorptance (0.7) were set for all materials in order to calculate the radiative exchange, based on values from the WUFI database and DesignBuilder material database [76].

The size and location of the windows in the models was defined by the dwelling archetypes. Windows were modelled as single paned in all dwellings except for modern dwellings (those with insulated AAC cavity walls), which were given doubled paned windows. Doors were also included in the model, and in all cases were assumed to be wooden (spruce) and 4cm thick.

10.2.2.2 Geometry and Zones

Flooded and non-flooded sections of the same rooms were joined into a single zone so that there would be free air transfer between the flooded and unflooded sections. The lowest section was given wall profiles corresponding to a wet wall or cavity insulated wall with supersaturated glass fibre insulation inside the cavity. The second level represented the flooded section of the wall without saturated insulation. The dry section of the wall comprised the uppermost, unflooded level of the zone. Window size in the dwellings were calculated based on the ratio of the wall surface area that was glazed, according to the archetype description. As a single window could not span both flooded and dry surfaces on a wall, the glazing ratio was applied by the software to the flooded and dry surfaces of a wall seperately, with the total glazed surface area summing to the area dictated by the dwelling archetype.

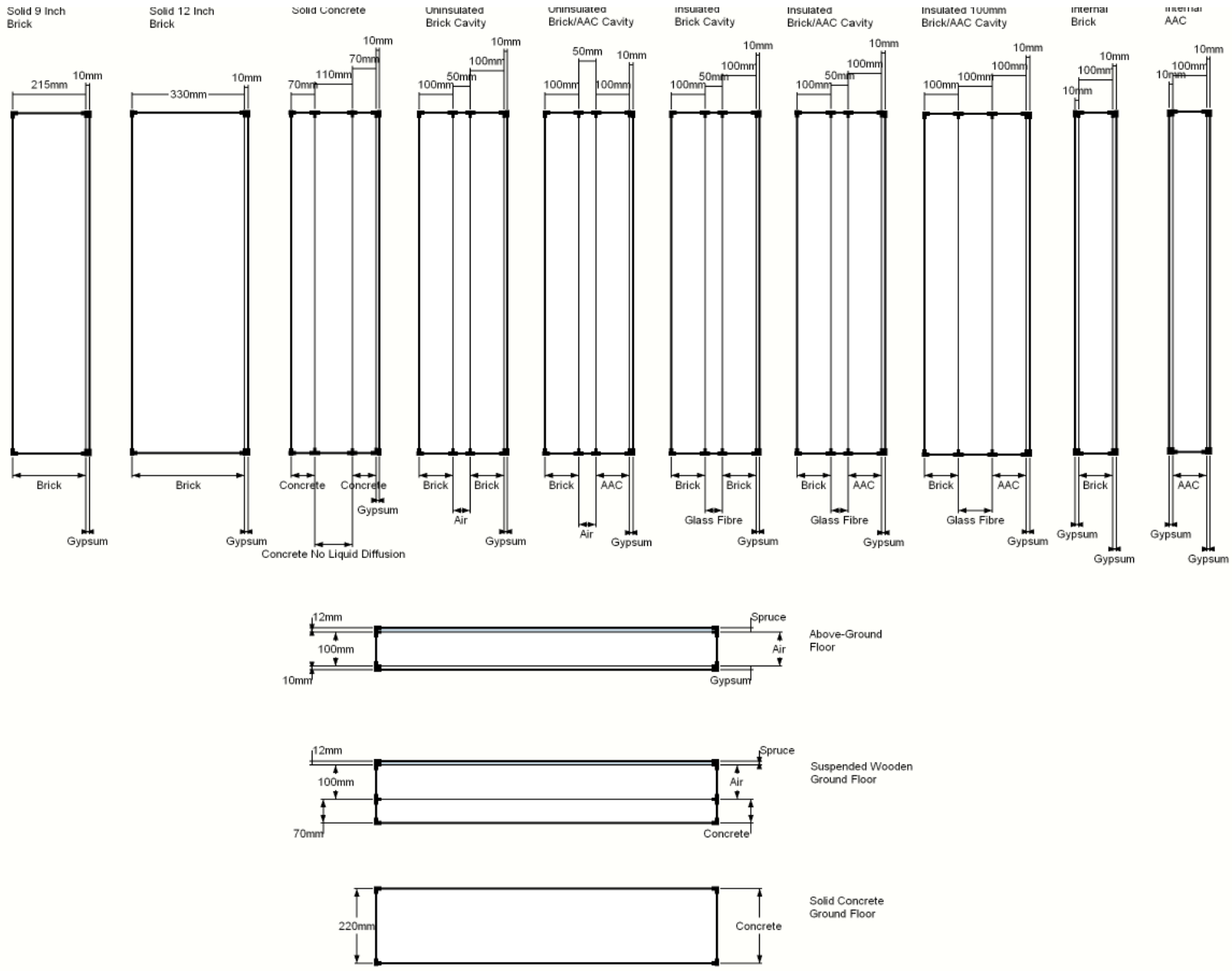

Figure 10.1: The wall types as modelled in UCL-HAMT, with materials and dimensions.

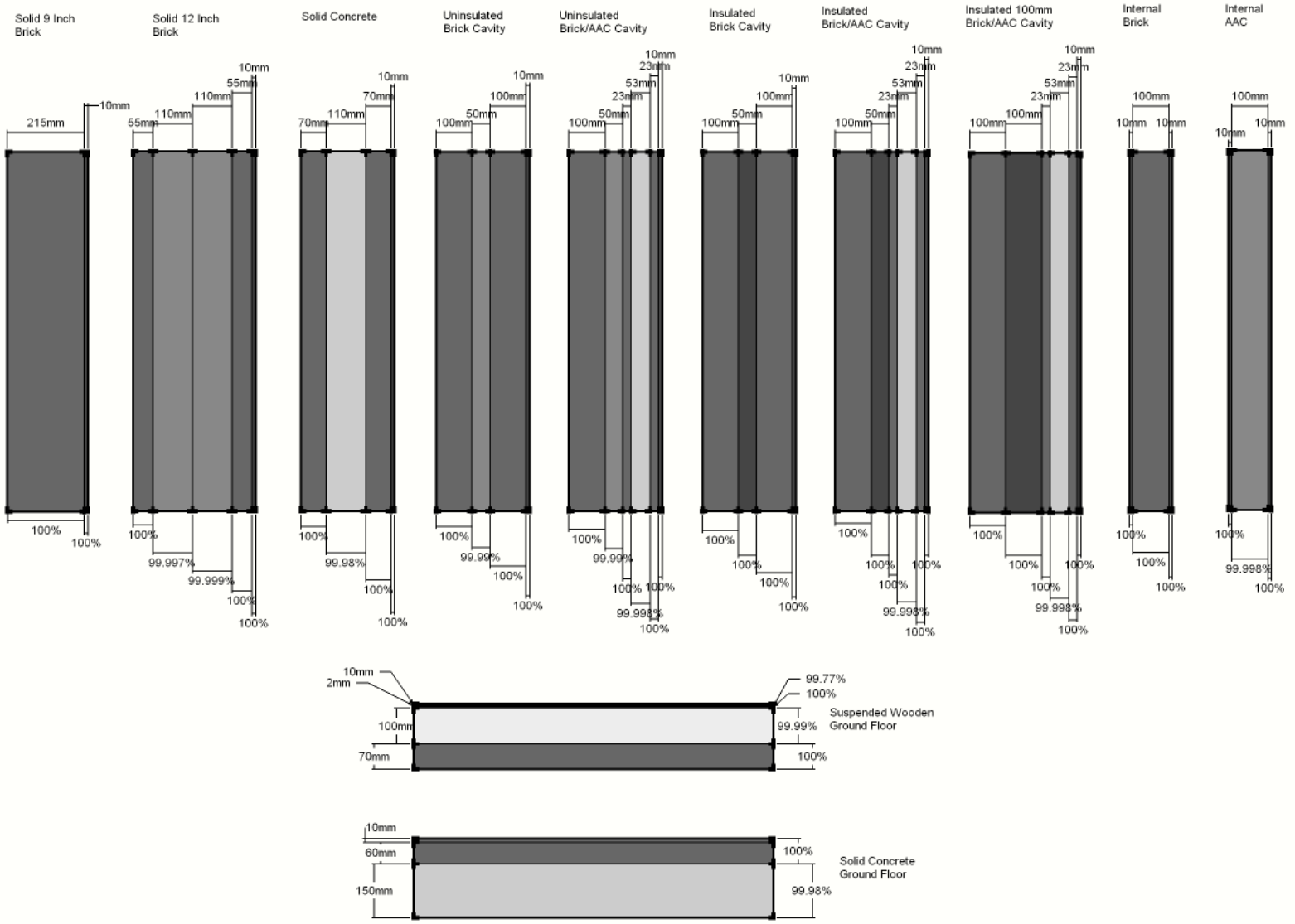

Figure 10.2: The wall types as modelled in UCL-HAMT, with dimensions and initial RH values for flooded sections.

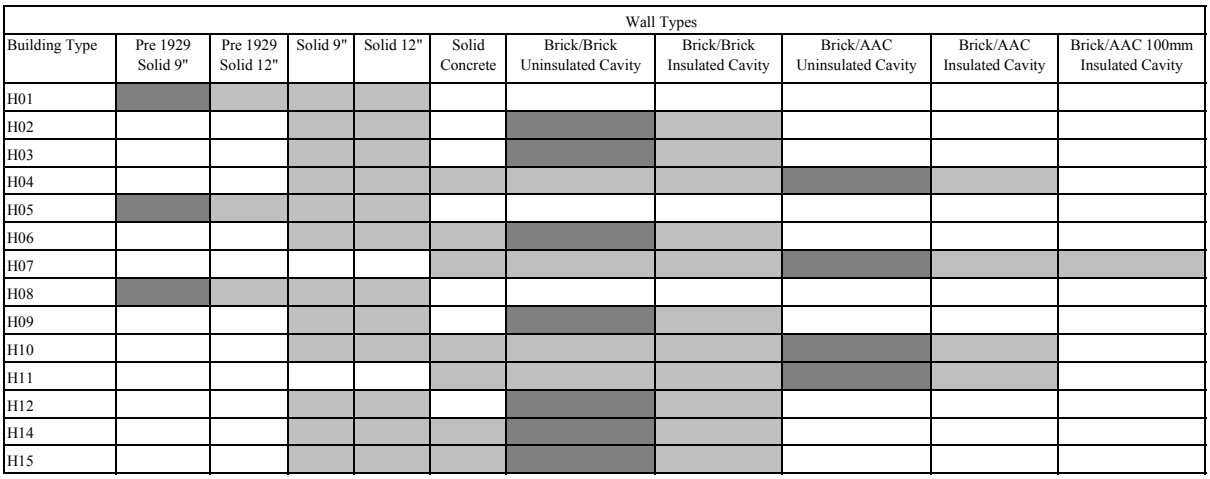

Figure 10.3: Built forms and the different wall types simulated, including their most common (mode) and less common (range) wall types, as determined in Section 7.6.1.

Different flood heights were modelled for each dwelling and wall type in order to gauge the impact of the heights of floods on the drying behaviour in abandoned dwellings. The flood heights modelled were 0.1m, 0.5m, 1.0m, and 2m. The software requirement for internal doors to be 2m tall and located on a single surface meant that some purpose-built flat archetypes with low ceilings could not be modelled at a 1.0m flood height, and so were modelled at 0.7m or 0.8m flood height instead.

External walls were exposed to outdoor weather conditions, while internal walls and party walls were shaded from solar radiation and wind. Ventilation inside cavities and subfloors was not modelled due to a lack of information on the use of air brick frequency in the London housing stock and the difficulty in modelling ventilated cavities within a building surface in UCL-HAMT. Cavities in the external wall and subfloor were modelled in certain assembly types by including a material layer of air or insulation in the UCL-HAMT assembly. Ventilation within these spaces was not modelled, an assumption which may impact drying behaviour, but is representative of a worst-case scenario where air bricks are blocked or not present.

The dwellings were assumed to be in an urban environment. By assigning the terrain to be 'Urban' in EnergyPlus, the local wind speed is determined from the global wind speed values in the weather file using specific terrain-dependent coefficients, as determined from the American Society of Heating, Refrigerating and Air Conditioning Engineers (ASHRAE).

10.2.2.3 Airflow

Air mixing within the zones was modelled using EnergyPlus Well Stirred model for room air. Airflow from zone to zone was modelled using the EnergyPlus Airflow network (Multizone without distribution), which simulated the movement of air from zone to zone throughout the dwellings based on the air entering the property through open windows, or the natural permeability of the building

Wall Type	Permeability (m/h @ 50Pa)
Solid Brick Wall	10.08
Cavity Brick Wall	12.98
Concrete Wall	10.8

Table 10.2: Permeability of external walls.

envelope. Air movement into the dwelling was determined by the permeability and orientation of the walls, height of the wall section, and the wind pressure (as calculated using a wind pressure coefficient array), and the location and opening schedule of the windows. Cracks were placed on all external and internal surfaces, to define their airflow at reference conditions in order to account for dwelling permeability. These cracks were placed at the top and the bottom of each surface to show the spread of permeability across the wall, and to account for the changing atmospheric and wind conditions across the height of the dwellings.

The reference conditions for the airflow through the cracks were taken from the permeability measurements for different wall types, as per Stephen [257] (Table 10.2). The reference permeability in m/h at 50Pa was scaled in terms of the size of the wall surface and converted to kg/s for the EnergyPlus simulation. The airflow network model required permeability values for the internal walls to complete the network. Since no data was available on the permeability of internal walls, arbitrary values were used of 20m/h at 50Pa. The permeability of internal walls accounted for all shared surfaces, including those with only partial overlaps. The influence of these was assumed to be small in the results, as all simulations were performed with the internal doors open, and airflow through the doors would be much more significant than the airflow due to the permeability of the internal walls. The roof, windows, and the internal floors were not given a permeability, while windows and doors within the dwelling were specified as a detailed opening.

The movement of heat and moisture from the walls into the internal and external environments was characterised by the convection coefficients. The indoor and outdoor heat transfer coefficients and vapour transfer coefficients were calculated by UCL-HAMT, based on airflow through the internal zones and the outdoor environment using the Detailed Surface Convection algorithm.

10.2.3 Scenario Modelling

10.2.3.1 Internal Conditions

The four different drying scenarios were modelled to predict the risk to occupants or remediators entering properties following a flood. Three of those scenarios - abandoned, natural ventilation, and natural ventilation with central heating, were representative of measures that could be taken by homeowners without employing professional remediation equipment. An abandoned house was modelled with external windows and doors closed, heating turned off, and air change exclusively due to permeability dependent on the wall type (Solid, Filled and Unfilled Cavity, Concrete) and

permeable surface area. In the natural ventilation scenarios, all external windows and internal doors were modelled as being constantly open, and air was considered to move in and out of the dwellings due to open windows and permeability. For the natural ventilation/heating scenario, the simulation was the same as with natural ventilation, except with electric baseboard heating on at a setpoint of 21°C in all major rooms (living room, kitchen, hallways, bedrooms, bathrooms, and bedrooms). Simulations were run for flood heights of 0.5m for all wall types that were determined to occur in a dwelling archetype in order to compare the drying times based on wall type, built form, and drying scenario.

A forced drying scenario was used to represent the drying of a property using professional intervention, and was used to contrast the effectiveness of a high-impact professional intervention with the other interventions that do not use external equipment. High-powered heaters are considered to be one of the best methods for rapid drying of flooded dwellings by remediation professionals [231]. A 56kW oil-fired heater, such as those used by Polygon Ltd. to perform flood remediation in domestic properties [59], was modelled in the living room of all dwelling archetypes with all external windows and internal doors open.

In addition, to examine the impact of different building surfaces and heating duration when using a high-powered heater, simulations were run for all surface types in a purpose built flat (H11) using a 56kW heater. In these simulations, the first week following flooding was modelled as per the 'abandoned' scenario, with windows closed, and ventilation only through the permeability of the building surfaces. Following this abandoned initial period, the heater was activated and windows and internal doors were opened. Heating periods were modelled lasting for 2 days, 1 week, and 3 months, following which windows were closed and the abandoned scenario resumed. Simulations were run for a year in total.

10.2.3.2 External Conditions

Dwellings simulated under current weather conditions were run with a Chartered Institution of Building Services Engineers (CIBSE) Test Reference Year (TRY) climate file for London Heathrow (Figure 10.4). To reduce the number of simulations, the dwellings were all considered to be oriented south.

Simulations were run for a year-long cycle, with winter floods occurring on January 1st, and summer floods on July 1st. All scenarios were simulated under winter conditions, while the 'Abandoned' scenario was performed for both summer and winter floods. Ground surface temperatures for the simulation, taken from the heat island models of Mavrogianni et al. [190], can be seen in Figure 10.5.

In addition, the effect of future climates on the drying the purpose built flat (H11) under abandoned and naturally ventilated conditions after a 0.5m flood was simulated for both summer and win-

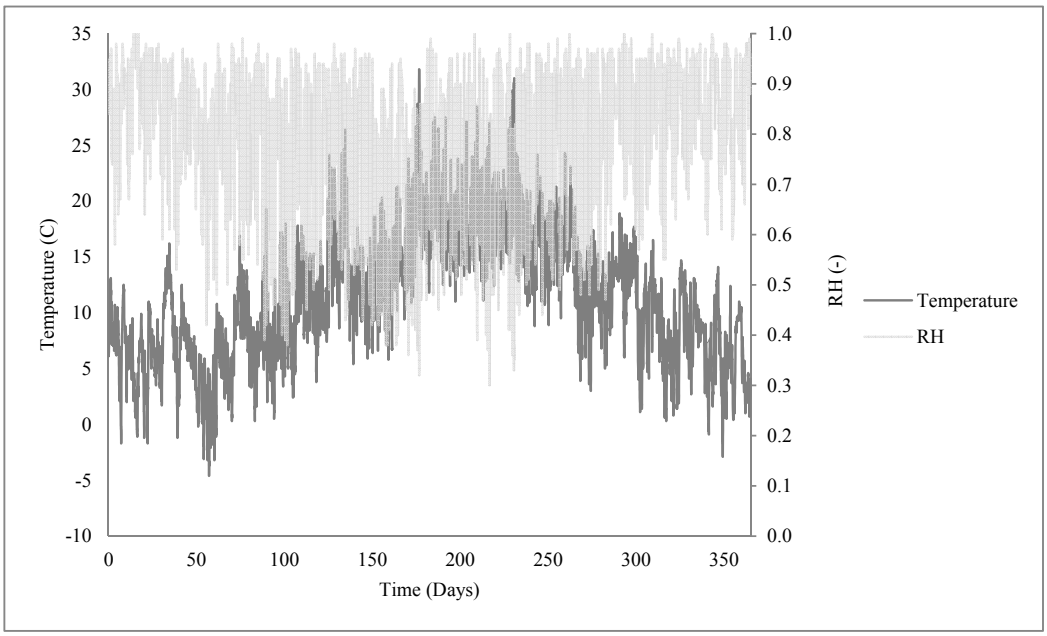

Figure 10.4: External temperature and RH data from the simulation weather file.

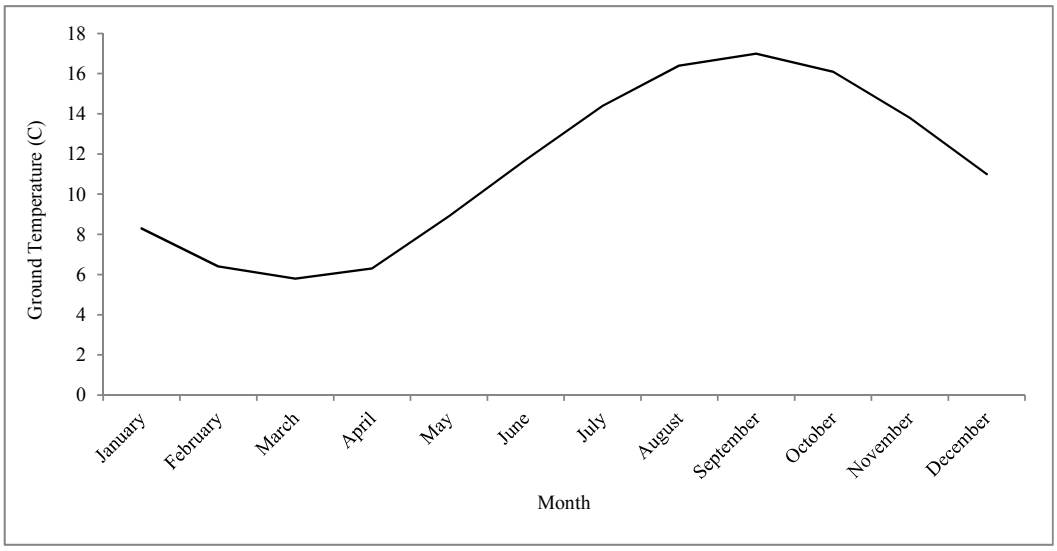

Figure 10.5: Ground temperatures for UCL-HAMT simulation.

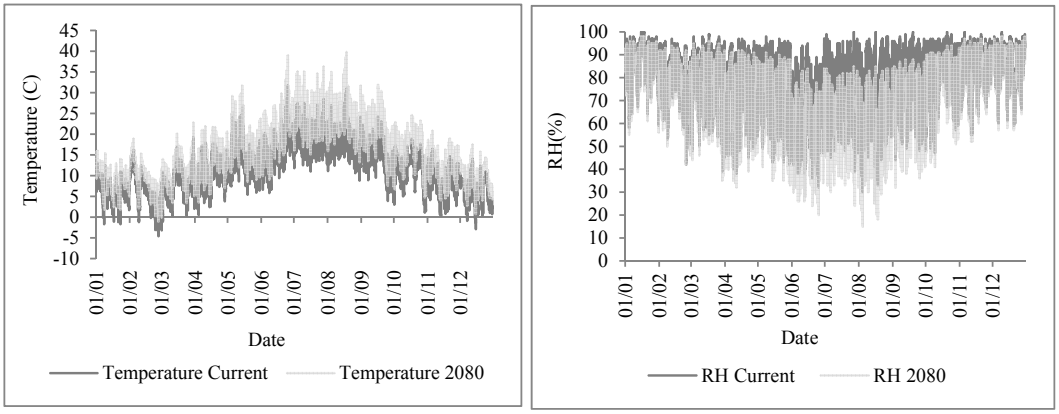

(a) Temperature.

(b) RH.

Figure 10.6: Temperature and RH in the current London Heathrow weather file, and in the generated 2080 high emission scenario weather file.

ter floods. Climate data for 2080 under high emission scenarios was downloaded from the UKCP09 website [273], and the application CCWeatherGen [262] used to 'morph' the Heathrow weather file for London to create new EnergyPlus TRY files. These weather files reflect the potential weather conditions for London under the high emission scenario in 2080, which would represent the most significant change in climate from the current conditions.

10.2.4 Simulation

Simulating the movement of moisture in a HAM models requires short timesteps. In this case, the model was calculated every minute and the temperature and RH value output hourly for the internal cell of the walls. Simulation duration took from 4-12 hours to simulate a single dwelling on a 2.83GHz Intel processor, depending on dwelling structure and complexity of building fabric. In order to increase the speed of simulation, naïve parallelisation was used to run multiple simulations on a single quad-core computer. Additionally, multiple instances were run on the Amazon Elastic Compute Cloud (EC2), as per Hopkins [140].

10.2.5 Outputs and Means of Comparison

There is no suitable, agreed level of what constitutes a 'dry' property. The water content of the interior surfaces and within building cavities depends on the weather, operating conditions within the dwelling, and the construction of the building fabric. Under typical conditions, different fabrics will contain different water contents. Because of this, the use of a mould model was considered. Mould models are typically employed by using the boundary temperature and RH conditions of the surface to calculate the risk of mould growth. In EnergyPlus, information on the temperature and moisture conditions on the internal surface of the walls can be output as the conditions of the

UCL-HAMT cell of the boundary layer (i.e. the last cell in the UCL-HAMT grid, which represents the boundary air layer), or as the UCL-HAMT interior 'surface' conditions. These outputs provide the same value – essentially, the conditions in the boundary air layer of the model, which is a virtual cell without any thickness.

In this study the main source of moisture on the internal face of the surfaces is from the damp wall rather than moisture produced in the indoor environment. The difference between RH of the boundary air layer and the RH of the surface cell, as calculated at the node of the first material cell 1.3mm from the surface, can be seen in Figure 10.7. The first 'true' cell in the UCL-HAMT surface closely follows the boundary layer RH, with none of the large fluctuations caused by changes in the internal air RH that can occur when the dwelling is naturally ventilated and outdoor air moves through the structure. In addition, contaminating microorganisms are likely to be able to utilise the water available within the material to a certain depth, through hyphal growth for mycelial species, or through transport of the microorganism into the material itself with the water. This means that the conditions slightly inside the surface may be a safer and more stable indication of the water available to microbial contaminants than the water levels at the boundary layer in cases where walls are the primary source of moisture in a building. Finally, the cell depth of 1.3mm showed the closest agreement with the decline in moisture content measured on the surface of walls when compared to physical studies (Section 9.3.1.2). For this reason, the conditions of the first internal cell, 1.3mm from the surface, were used to calculate the risk of microbial growth.

The daily average of the RH and temperature for the first cell were used to calculate the risk of mould growth using the model developed by Clarke [58] for *A. versicolor* and *S. chartarum* over time. The microbial models for *E. coli*, *Salmonella*, and *Listeria* developed in Chapter 6 were also used to calculate the risk of bacterial contamination of the internal surfaces using the output temperature and RH values. A Microsoft Excel macro was used to automate the import of the EnergyPlus output files and the total surface area of the dwelling susceptible to mould growth, and bacteria persistence was calculated using the models. The resulting surface areas for the dwelling archetypes were compared in terms of their drying rates by examining the declination of surface area microbial risk over time.

In addition, cumulative energy use data was output from simulations where heating was used to accelerate drying, while the air change rate was output for dwellings drying under natural ventilation and abandoned scenarios. Finally, in the forced drying simulations of different building surface types within archetype H11, the RH of cells in the central 'core' of the walls was output in order to demonstrate how the increased temperature can impact RH through the entire wall.

Results were analysed using Microsoft Excel. The differences between the drying ability of different types of walls, different built forms, and different drying regimes were compared in order to assess the impacts of the different factors on a dwelling's ability to dry following a flood.

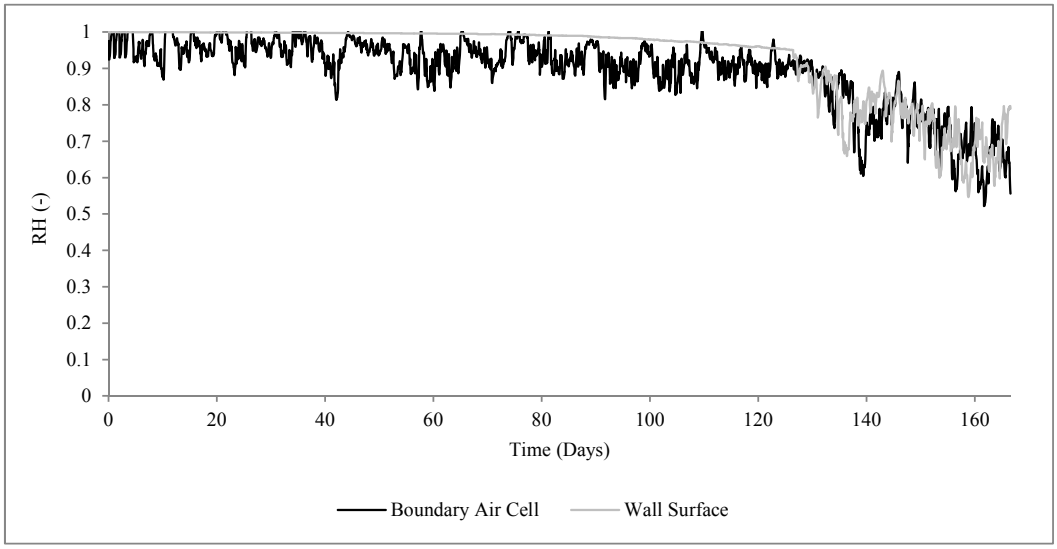

Figure 10.7: Comparing the RH of the boundary layer cell and the first cell (1.3mm deep) in the surface construction.

10.3 Sensitivity Analysis

The variability of different data input parameters in the UCL-HAMT model will have an impact on the simulated drying of the structures. In order to quantify this variability, a Differential Sensitivity Analysis (DSA) of UCL-HAMT was performed to determine the uncertainty of the simulation results based on deviations in the hygrothermal material input parameters within the building fabrics, as well as geometrical inputs including dwelling volume, window size, orientation, and permeability. The objective of the sensitivity analysis was to examine the individual sensitivities of the input parameters, and to gain an understanding of the uncertainty of the model outputs based on uncertainties in inputs. A separate sensitivity test was performed for each building fabric modelled in this research.

As the whole-building simulation of built forms with internal walls took a long time to simulate, a simplified building was used – in this case, a built form based on the Building Energy Simulation Test (BESTEST) building [160]. The result of the BESTEST simplification means that the drying rates are not comparable with those of the individual built forms, however it does allow for a better understanding of the impacts of specific parameters on drying. Surface constructions were given a saturated initial water content across the entire profile, a simplification which meant that surfaces took longer to dry than those modelled with different water contents across the profile. The simulations were performed under constant conditions at 15°C at 50%RH and with 60 time steps per hour. To calculate the sensitivity of the results to variations in the material parameters, the RH in the surface cell of wall opposite the window was recorded.

The estimated standard deviation of the building material parameters are shown in Table 10.3 and

Parameter	Brick	Gypsum	AAC	Concrete	Spruce	Glass Fibre
Thermal Conductivity	10%	10%	10%	5%	5%	10%
Density	15%	15%	15%	15%	15%	15%
Specific Heat Capacity	5%	5%	5%	5%	5%	5%
Thermal Absorbance	10%	10%	10%	10%	10%	10%
Solar Absorbance	10%	10%	10%	10%	10%	10%
Visible Absorbance	10%	10%	10%	10%	10%	10%
Porosity	10%	10%	5%	10%	10%	3%
Moisture dependent moisture storage capacity @ 100%RH	15%	15%	15%	15%	15%	15%
Moisture dependent moisture storage capacity @ 80%RH	15%	15%	15%	15%	15%	15%
Liquid Transport Coefficient Suction	15%	15%	15%	15%	15%	15%
Liquid Transport Coefficient Redistribution	15%	15%	15%	15%	15%	15%
Moisture dependent vapour diffusion resistance factor @ 100%RH	20%	20%	20%	20%	20%	10%
Moisture dependent thermal conductivity @ 100%	15%	15%	15%	15%	15%	15%
Thickness	10%	10%	10%	10%	10%	10%

Table 10.3: Standard deviations for material parameters for sensitivity analysis.

the geometrical parameters in Table 10.4. Readers are referred to the UCL-HAMT documentation [94] and Chapter 8 for parameter definitions and model description. The standard deviations for the materials used in the sensitivity analysis are meant to represent the standard deviation of the materials found in the UK housing stock. However, since little data exists that quantifies the variability of building materials, deviations had to be estimated from a range of sources. The presented deviations are best estimates based on deviations from materials within the WUFI material database, British Standard (BS) 10456 [40], the IEA Annex 24 Final Report [176], and previous sensitivity analyses [110, 138].

The standard deviations were used to perform a DSA [184] running simulations with material parameters varied plus or minus two standard deviations (95% certainty) on each of the different wall types studied. The differences between the base case and deviated case were calculated and the

Geometrical Parameter	Standard deviations
Building Volume	10%
Window Size	10%
Building Orientation	45º
Permeability	10%

Table 10.4: Standard deviations for geometrical parameters for sensitivity analysis.

negative and positive deviations added separately in quadrature. The uncertainties of the drying surfaces were graphed using Microsoft Excel.

10.4 Results

The full results of the drying behaviour of the different dwelling archetypes and their typical walls under different drying conditions, and with different microbial contaminants can be found in Appendices D, E, and F. The results and their differences observed will be discussed below.

10.4.1 Building Fabrics

The different types of building fabrics simulated showed a wide range of drying times when dried under the same climate conditions. Figure 10.8 shows the decline in the moisture content of the different external wall types as they dry under naturally ventilated conditions. All walls showed a distinctive loss in the total moisture content by mass over time. Thicker brick walls were found to dry slower than thinner walls, while the presence of a fibrous mineral insulation or AAC greatly increased the drying times of the walls. Solid concrete walls did not exhibit a large decline due to the low potential water content of concrete.

Figure 10.9 shows the internal surface cells of the different external wall types under the same conditions (i.e. the same wall in the living room of the built form H11 under the naturally ventilated conditions following a 0.5m flood). Under naturally ventilated conditions, the RH of the surface cells of the walls were much more prone to fluctuations in RH of the air used to ventilate the properties, and began to follow the trend exhibited in the weather file (Figure 10.4). As a result, the RH of the surface cells began to increase once again after having dried, as the open windows allowed the winter air to enter the property. For simplification, the fluctuations caused by the external weather file in preceding graphs of naturally ventilated scenarios have been smoothed by calculating a one week rolling average.

The internal surface of solid concrete floors was found to be worse than suspended wooden floors in their ability to dry, however, data was not output for the subfloor space which may remain damp. Internal walls also showed varying rates of drying ability, with AAC wall drying slower than brick walls. While the internal surfaces of solid brick and concrete walls could be expected to dry out

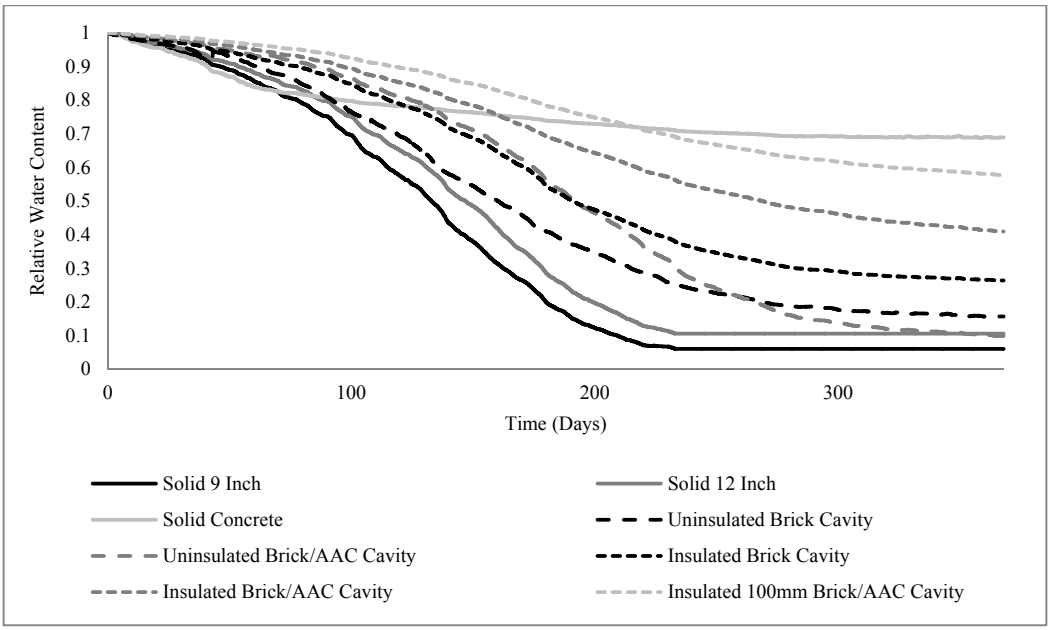

Figure 10.8: The moisture content of whole walls (kg/kg) decreases as they dry through natural ventilation.

under naturally ventilated conditions within 1 – 3 months, glass fibre and AAC walls were observed to take as long as half a year to dry on the surface.

An examination of the results indicated the RH and water contents of the surfaces of the walls did not necessarily reflect the water content throughout the wall as the cores of the walls remained wet longer than the surfaces. An example simulation of the RH across the profile of a solid 9" brick wall and a mineral fibre insulated brick cavity wall drying using natural ventilation indicates that the mineral fibre retains moisture from floodwater throughout the year-long simulation time (Figure 10.10) This trend was seen in all walls with a cavity, including those without insulation, whereas solid walls show more complete drying. The profiles of all the different wall types as they dry through natural ventilation are shown in Appendix C.

10.4.2 Built Form

The RH of all indoor surfaces was high immediately following the flood, including on surfaces untouched by floodwater. The surface RH in first and second level rooms was as high as 99%, indicating that a flood can impact the moisture levels on all surfaces throughout an affected dwelling. The decline of the RH of the internal surfaces were found to vary between dwellings and, indeed, between rooms of dwellings. Figure 10.11 demonstrates the difference in drying rate of floors in the rooms of a bungalow, which indicates that smaller rooms dry slower than those in larger rooms with access to ventilation.

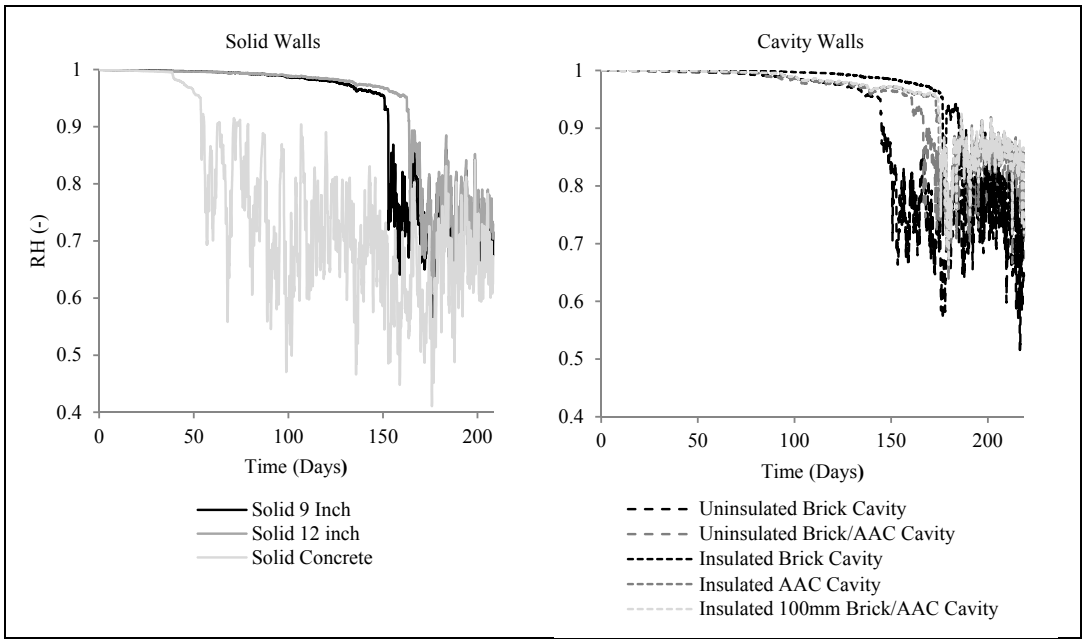

Figure 10.9: The decrease in surface RH of walls as they dry through natural ventilation.

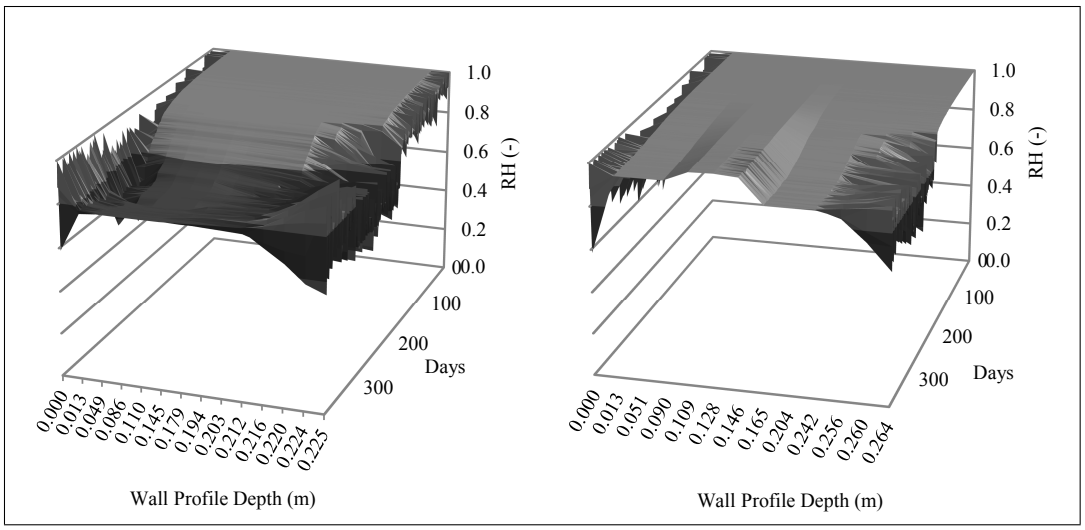

Figure 10.10: The cross section of a solid 9" brick wall (left) and an insulated brick cavity wall (right) drying under natural ventilation over time. The exterior of the walls are on the left and the interior on the right.

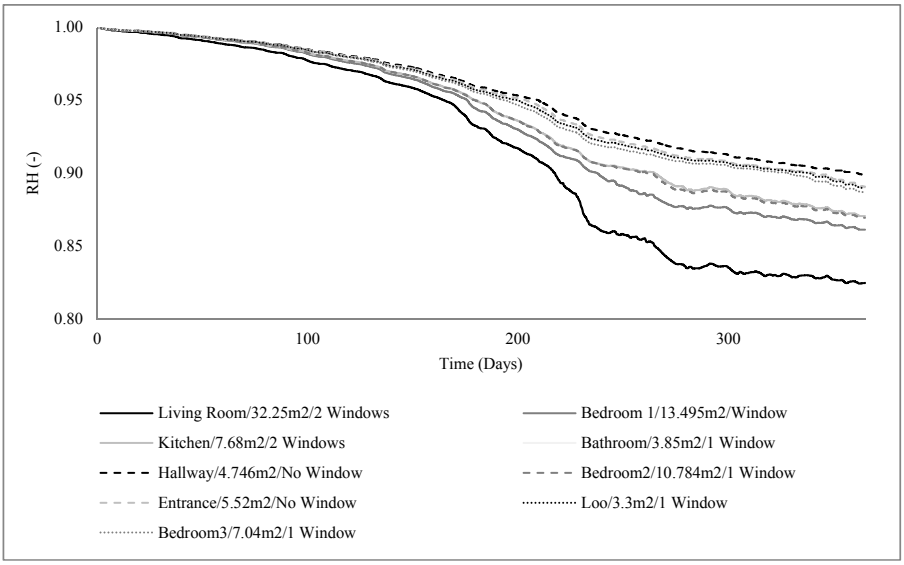

Figure 10.11: The drying of the surface of the floors in a bungalow using natural drying, for different rooms/ room footprint areas / and access to natural ventilation.

In addition, different built forms dried at different rates. Figure 10.12 shows the decrease in the surface area suitable for the growth of *A. versicolor* over time for different built forms with the same external wall type and floor (9" solid brick/solid concrete floor) under naturally ventilated and abandoned scenarios. Multi-storey dwellings had a high initial surface area prone to mould growth as damp air moved around the dwellings. The surface area prone to mould growth in these dwellings declined relatively quickly when windows were open, compared to single-level dwellings flooded to the same height. In cases of abandoned dwellings, purpose-built flats also performed poorly, while larger detached and semi-detached properties performed the best.

Particular archetypes were found to be prone to long-term damp following flooding due to their unique combination of built form and typical building fabrics (Figure 10.13). Archetypes H04, H07, H10, and H11 were found to be at risk to *A. versicolor* growth following flooding for a year following the flood event when abandoned. In the cases of dwellings H04 and H07, the most common wall type (mode) was found to be particularly hard to dry, thereby increasing the risks inside these properties. The length of time needed for the contamination risk of flood-borne microorganisms in naturally ventilated dwelling archetypes to decrease to zero can be seen in Appendix H.

10.4.3 Drying Scenarios

The drying scenario simulated had a clear impact on the rate of drying of the different dwellings. Dwellings that were naturally ventilated dried much faster than the sealed dwellings, whose air change rate was determined only by the permeability of the building envelope and could often remain at risk for mould growth throughout the dwelling for the entire year-long simulation. Table

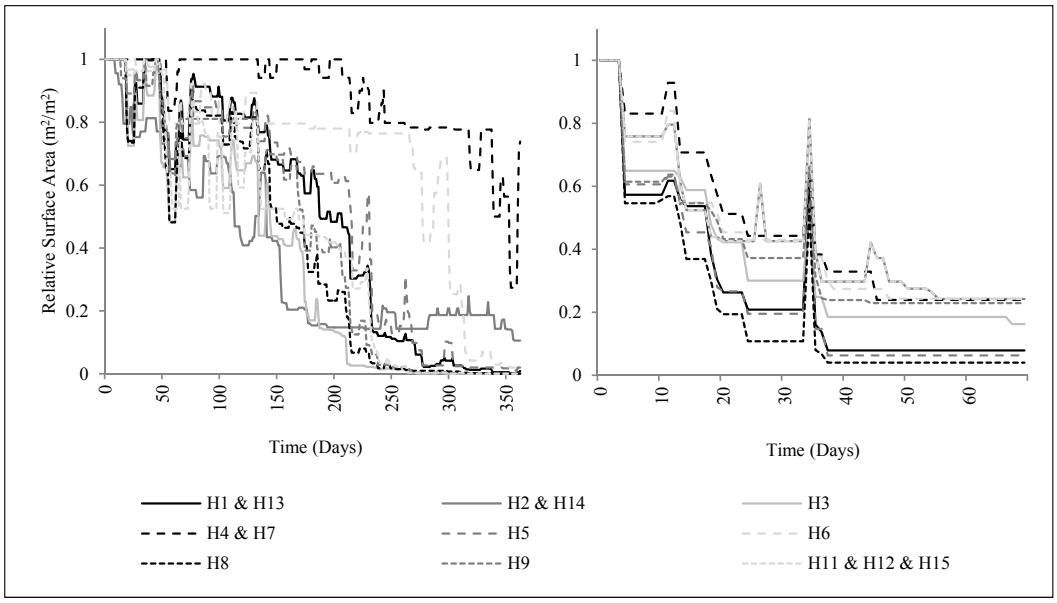

Figure 10.12: Decrease in relative surface area suitable for mould growth inside dwelling archetypes with a 9" brick wall under abandoned (left) and natural ventilation (right) scenarios.

10.5 shows the yearly average air changes rates in the different dwelling archetypes for naturally ventilated and abandoned dwellings with modal wall types. In cases when the external air had a high RH, such as during the winter, the higher air change rate of the naturally ventilated dwellings meant that there were periods when a mould growth risk was present in dwellings, despite their having previously dried to the point where no mould risk growth was present.

Multi-storey dwellings and those with the ability to have cross-ventilation showed a greater air change rate when windows were open, while archetypes such as purpose-built flats had a lower air change rate. When windows were closed under the abandoned scenario, those with a small external surface area to internal volume ratio showed a smaller air change rate due to the lack of permeable surface area. The archetype with the highest air change rate under both scenarios was the bungalow, while the dwelling with the lowest air change rate were modern purpose-built flats.

Figure 10.14 shows an example of the reduction in the internal surface area suitable for *A. versicolor* growth in a bungalow with the three different drying scenarios. The modes represent the most common building fabric type – in this case uninsulated brick cavities, while the range represents the different types of building fabrics generally found in each archetype according to the EHS analysis (Table 7.3). The fluctuations in surface area at risk of mould growth caused by humid external air entering the property during natural ventilation scenarios can be clearly seen after 250 days in Figure 10.14.

Heating the dwelling using the central heating caused the fastest drying rate of the occupant-led scenarios modelled, with a rapid decrease in the conditions suitable for mould growth. With natural

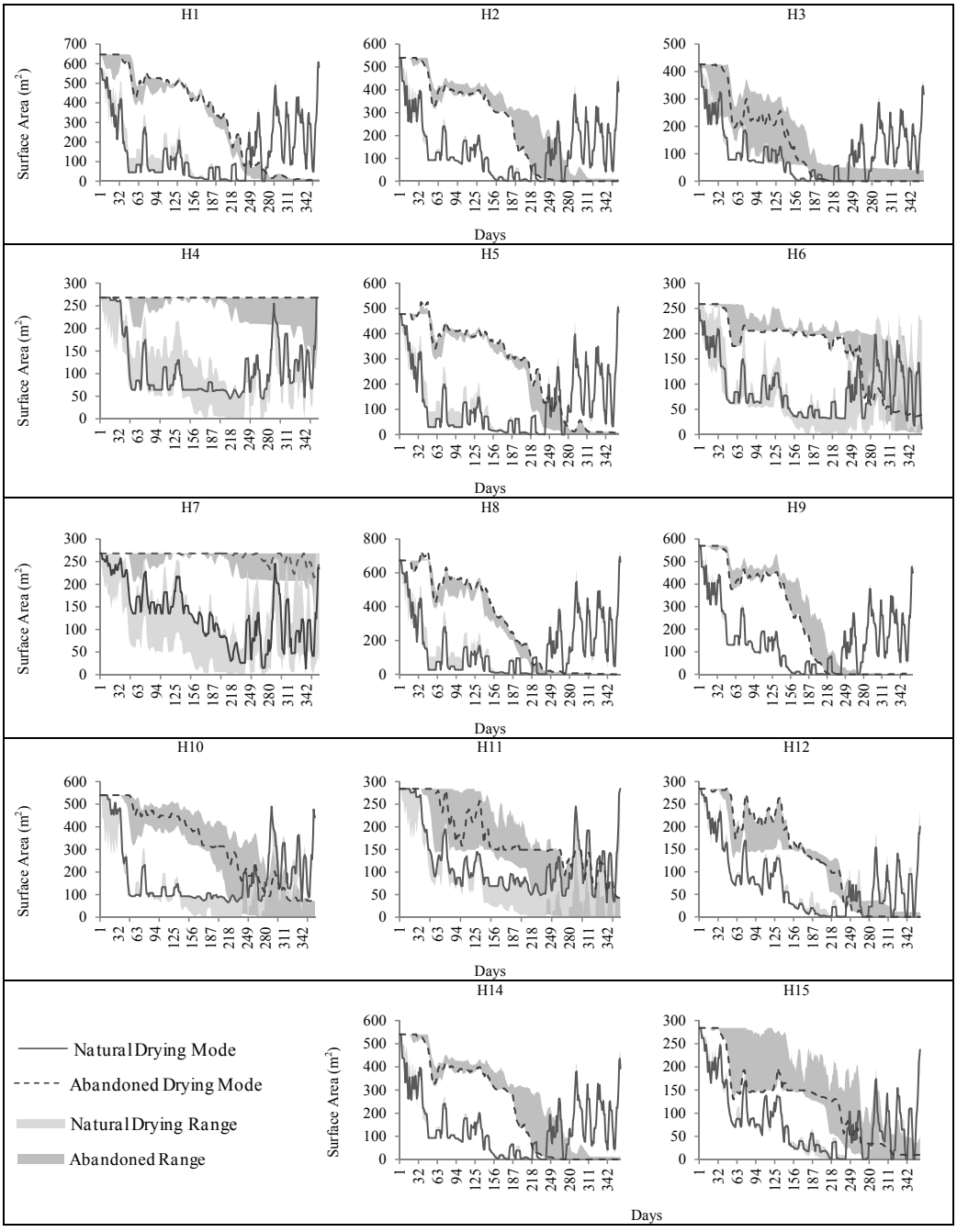

Figure 10.13: Decline in internal surface area suitable for mould growth over time for different built forms. The most frequent wall type for each dwelling type is shown as the mode.

Archetype	Ventilation	
	Window Open (ach)	Abandoned (ach)
H01	30.4	0.08
H02	30.9	0.11
H03	51.0	0.21
H04	15.3	0.12
H05	28.3	0.08
H06	16.3	0.21
H07	15.3	0.12
H08	34.4	0.10
H09	63.6	0.22
H10	29.8	0.11
H11	16.3	0.13
H12	16.6	0.10
H14	30.9	0.11
H15	16.5	0.14

Table 10.5: Yearly average air changes per hour (ach) in naturally ventilated and abandoned archetypes with modal wall types.

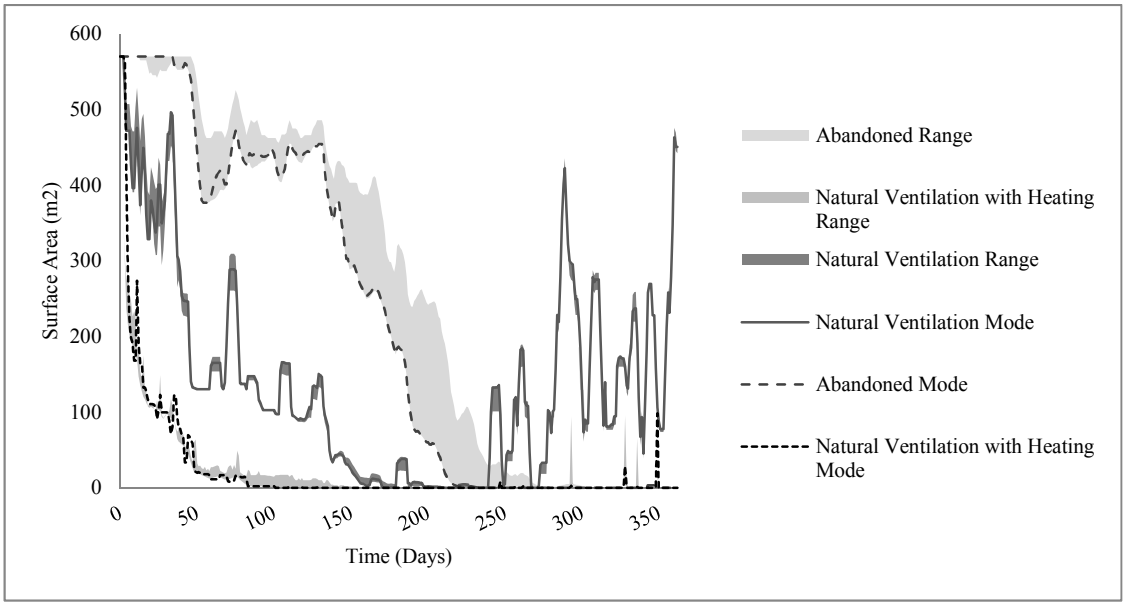

Figure 10.14: Difference in internal surface area at risk of mould growth for a bungalow with 9" solid brick walls according to treatment type.

airflow, differences in drying rates between wall types was minimised due to the convective airflow removing moisture from the internal surface of the walls, and differences in drying rate observed in Figure 10.9 were minimised due to the small relative flood height. In all drying methods the decrease of the damp surface area was limited by the concrete floor, which took a long time to dry.

The time and energy costs associated with drying the different dwelling archetypes using natural ventilation with no heating, central heating with the windows open, or a high-powered heater to the point where *A. versicolor* no longer presented a growth risk can be seen in Table 10.6. Heating was found to accelerate the drying of all dwelling archetypes in both central heating and high-powered heating scenarios. In smaller dwellings, those with a single high-powered heater were found to dry faster than those using central heating, as hot air was better able to move through the property. In larger dwellings, such as those with multiple storeys, a high-powered heater did not provide a significant difference to the drying performance of the dwelling, and using central heating from electric baseboards in each room often made the dwellings dry faster, and with lower energy costs. The most noticeable improvement in drying time when using heat was observed in properties that were found to dry the slowest using natural ventilation or when abandoned. These archetypes, such as purpose-built flats, were often found to dry faster with heat than the dwelling archetypes which had performed better under natural ventilation only.

While the energy required to run the 56kW heater remained the same regardless of the size of the property, the energy use for drying using central heating depended on size of the property and number of rooms where electric baseboard heaters were installed. In larger dwellings, using central heating was energy intensive, and may not offer enough cost-benefit over drying using natural ventilation if all heaters are to be used. Archetypes with insulated walls took longer to dry than those without insulation under heated conditions, and had a higher energy cost, although the energy use was lower due to the higher thermal properties of the walls.

The 56kW heater showed the ability to raise temperatures inside the room significantly, with temperatures reaching up to 50^{o}C. The surface of the walls dried using the high-powered heater were found to dry much faster than the cores, particularly in walls with moisture-retaining insulation. The results of using the high-powered heater for differing lengths of time on the surface and the cores of the different walls can be seen in Appendix G. When the heater was used for an insufficient length of time – for example, under 2 weeks – then the wall would remain wet in the core of the wall once the heater was stopped. The result was that when windows were closed and heating stopped, the surface of the walls would again become damp as water from the core migrated to the internal surface. The external sides of the walls were observed to dry the slowest, as they were not directly exposed to the warm indoor air. As with all wall types, the surface of the walls dried the fastest, while the core of the wall remained wet longer.

Archetype	Modal Wall Type	Natural Ventilation		Central Heating		Temporary High-Powered Heater	
		Time (days)	Energy	Time (days)	Total Energy (kWh)	Time (days)	Total Energy (kWh)
H01	Pre 1929 Solid 9" Brick	201	-	139	1.65E+05	175	2.35E+05
H02	Uninsulated Brick Cavity	180	-	88	1.01E+05	96	1.29E+05
	Insulated Brick Cavity	234	-	134	1.44E+05	139	1.87E+05
H03	Uninsulated Brick Cavity	162	-	103	1.18E+05	107	1.44E+05
	Insulated Brick Cavity	219	-	152	1.60E+05	109	1.47E+05
H04	Uninsulated Brick/AAC Cavity	>365	-	35	1.88E+04	119	1.60E+05
	Insulated Brick/AAC Cavity	>365	-	53	2.72E+04	130	1.75E+05
H05	Pre 1929 Solid 9" Brick	234	-	104	1.15E+05	123	1.65E+05
H06	Uninsulated Brick Cavity	191	-	54	3.00E+04	105	1.41E+05
	Insulated Brick Cavity	261	-	92	5.18E+04	140	1.88E+05
H07	Uninsulated Brick/AAC Cavity	>365	-	35	1.88E+04	119	1.60E+05
	Insulated Brick/AAC Cavity	>365	-	53	2.72E+04	130	1.75E+05
H08	Pre 1929 Solid 9" Brick	237	-	139	1.78E+05	117	1.57E+05
H09	Uninsulated Brick Cavity	172	-	97	1.46+05	139	1.87E+05
	Insulated Brick Cavity	218	-	140	1.92E+05	179	2.41E+05
H10	Uninsulated Brick/AAC Cavity	>365	-	142	1.47E+05	140	1.88E+05
	Insulated Brick/AAC Cavity	>365	-	189	1.73E+05	172	2.31E+05
H11	Uninsulated Brick/AAC Cavity	>365	-	54	3.21E+04	29	3.91E+04
	Insulated Brick/AAC Cavity	>365	-	61	3.74E+04	38	5.12E+04
H12	Solid 9" Brick	233	-	44	2.60E+04	38	5.12E+04
H14	Uninsulated Brick Cavity	180	-	88	1.01E+05	96	1.29E+05
	Insulated Brick Cavity	234	-	134	1.44E+05	139	1.87E+05
H15	Uninsulated Brick Cavity	218	-	35	2.12E+04	20	2.70E+04
	Insulated Brick Cavity	272	-	51	2.98E+04	36	4.85E+04

Table 10.6: Energy costs required to dry dwelling archetypes using heating interventions.

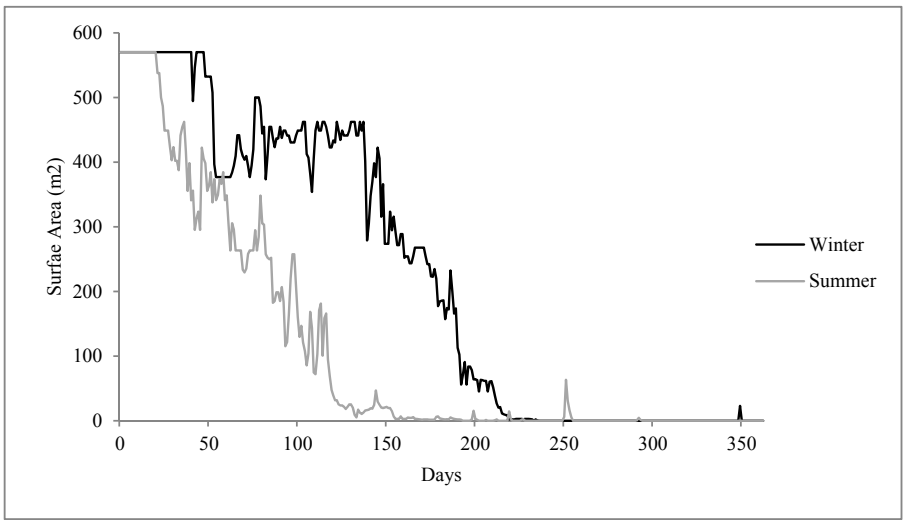

Figure 10.15: Differences in the reduction of surface area at risk of *A. versicolor* growth following a winter and summer flood for an abandoned bungalow with solid 9" walls.

10.4.3.1 Seasonal Differences

Figure 10.15 presents the differences in the drying rate for abandoned dwellings following a winter and summer flood. Winter floods were generally found to dry slower than summer floods due to the colder, more humid weather. Exceptions were observed for dwellings with a wall type or built form that was particularly slow to dry, where the drying period ran into the winter, extending the amount of time required for the structure to dry.

10.4.3.2 Climate Change

The UK climate is predicted to become more humid, and prone to more extreme rainfall events in the future. The simulation results for archetype H11 under current climate conditions and the 2080 high emission scenario suggest that climate change will have an impact on the drying rate of dwellings (Figure 10.16). In both winter and summer scenarios, the dwellings were found to exhibit a faster decline in the internal surface area suitable for mould growth under the 2080 high emissions scenario weather conditions due to the higher temperature.

10.4.3.3 Flood Height

An example of the impact of the flood height on drying rate in abandoned dwellings can be seen in Figure 10.17. As expected, dwellings that were flooded to a greater depth took longer to dry than the more shallow flood events. The drying rates for flooded dwellings characterised by modal wall types with different flood heights can be seen in Appendix I. Following deep floods (for example 1-2m), many dwellings showed a risk for microbial growth for the entire year-long simulation period.

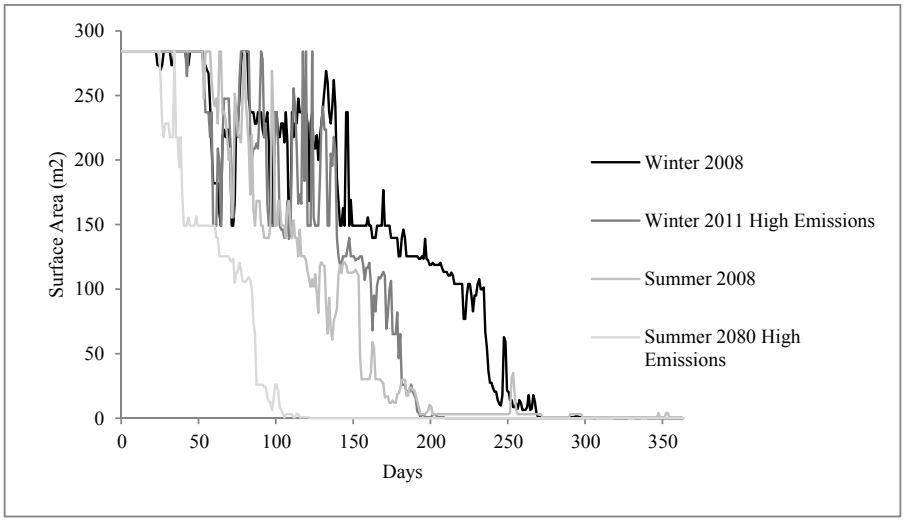

Figure 10.16: Impact of climate change on the reduction of surface area at risk of *A. versicolor* growth inside archetype H11 following a 0.5m flood.

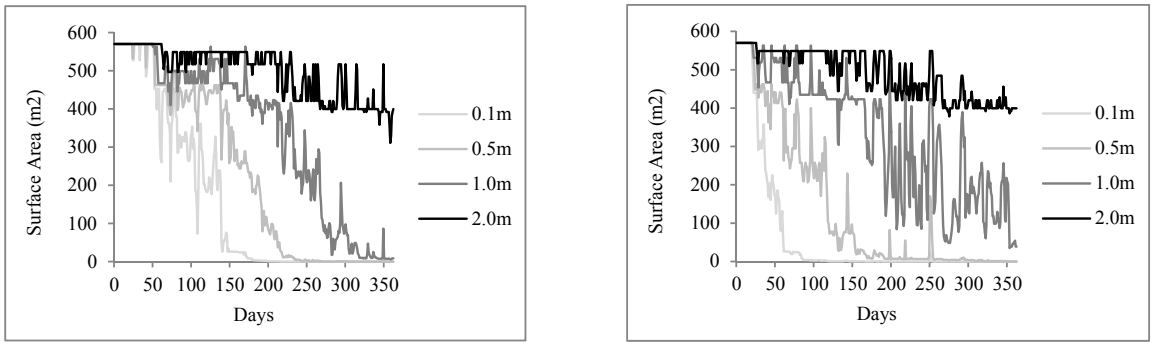

(a) Winter flood.

(b) Summer flood.

Figure 10.17: Impact of flood height on drying time of a flooded dwelling in terms of surface area suitable for *A. versicolor* growth.

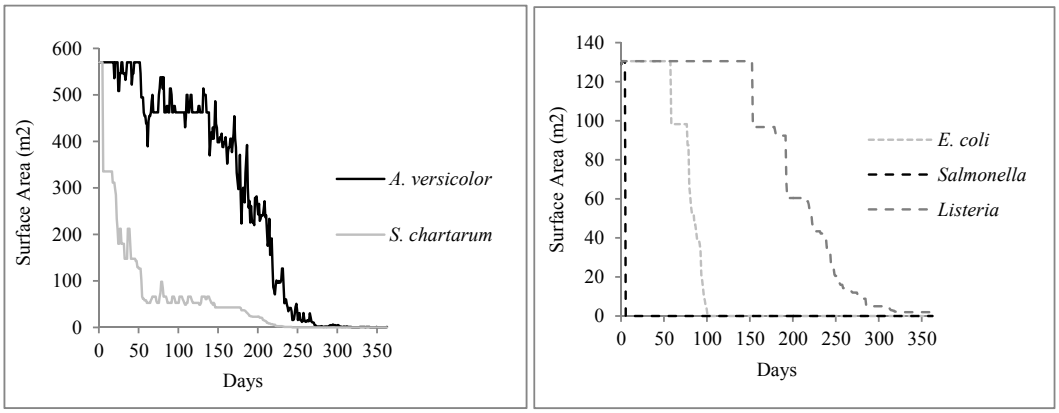

(a) Mould Species. (b) Bacterial Species.

Figure 10.18: Decline in surface area at risk of microbial contamination inside an abandoned dwelling (H09) with 9" solid brick walls flooded to 0.5m in the winter.

10.4.4 Microbial Persistence

The different modelled microbial contaminants within the dwellings displayed a variety of durations of risk on the surfaces inside the flooded dwellings. *A. versicolor* was seen to persist longer that *S. chartarum* inside flooded properties due to the lower moisture requirements dictated by the model. Of the bacterial species modelled, *Listeria* was found to last the longest, with some cases showing contamination risk for the entire simulation period. *E. coli* showed a shorter duration, lasting from 50-100 days, and *Salmonella* lasted the shortest period of time, around 5-10 days. For *E. coli* and *Salmonella*, the height of the flood did not make a significant difference to the amount of time required for surfaces inside the dwelling to become 'safe'. The seasonality of the flood was also important for *E. coli* and *Salmonella* survival, as cold winter floods demonstrated a higher persistence of the bacteria. The thermal dependence of *Salmonella* was also demonstrated in the relatively prolonged duration of risk inside properties with poor insulation, such as those with solid brick walls and suspended wooden floors.

The mould models and bacterial models are not directly comparable due to the fact that the bacteria model accounted for population decline under transient conditions, while the mould model was a simple growth/no growth model; however the results give an indication of the amount of time required before a property becomes safe. An example of the decline in internal surface area prone to contamination of the various species can be seen in Figure 10.18.

10.4.5 Sensitivity Analysis

The sensitivity analysis indicated that the material parameters with the greatest influence on the drying behaviour of the structures were the moisture storage functions, the liquid transport curves, and the vapour diffusion resistance. Other hygrothermal parameters, such as the material porosity,

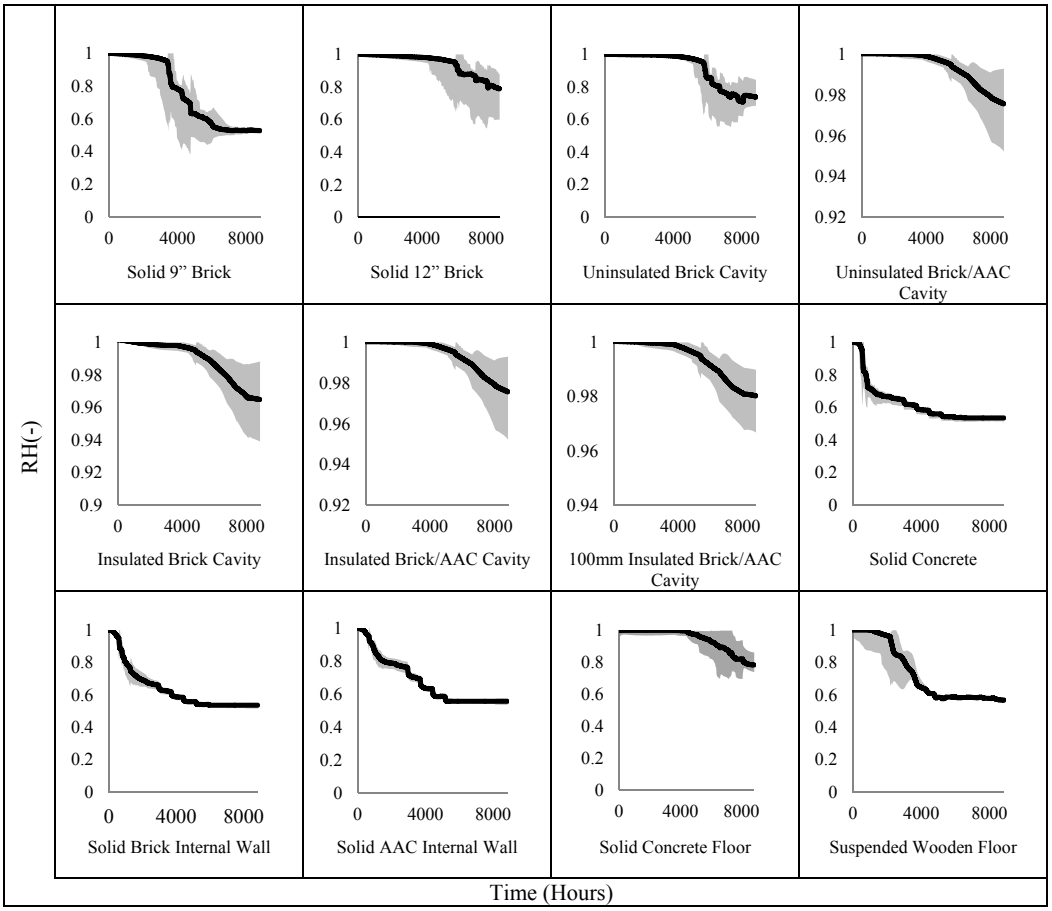

Figure 10.19: Sensitivity analysis showing uncertainty in the drying rate of different wall types.

density, thermal conductivity, and solar absorbance were found to have a minimal effect on the drying behaviour. In terms of the dwelling structure and ventilation properties, the air change rate had the greatest effect on the drying rate. The results of the sensitivity test (Figure 10.19) suggest that material properties have a significant influence on the UCL-HAMT model, and that modelling studies should aim to use the most accurate and appropriate material data possible.

As discussed in Section 8.4.5, the type of material is known to exhibit different moisture behaviour based on its hygrothermal classification. This model includes three of the four proposed material classes: Non-hygroscopic (glass fibre insulation), Inorganic-porous (brick and AAC), and Organic-porous (Spruce wood). Wood in particular has unique material properties which make prediction of drying behaviour difficult due to structural changes and non-linear water vapour permeability. However, the model is also limited by the lack of available data, and so this sensitivity analysis helps to illustrate what these uncertainties may be. Despite the wide variation due to uncertainty in the sensitivity analysis results, there were significant differences in the drying ability of different fully-saturated wall types drying under these conditions.

10.5 Discussion

This chapter presents the results of using a hygrothermal modelling approach to simulate the drying of different types of properties found in the London housing stock. These results may be used to estimate the health risk inside untreated and treated properties, as well as form the basis for future research into the best practices for drying affected dwellings. While there are a number of variables not addressed in this study, such as the quality of the water and the presence of internal furnishings, these results provide insight into the drying of different built forms in the UK.

The relative drying times of walls were similar to those expected, based on physical measurements from researchers and flood remediation organisations [263], although it is likely that the drying times of insulated walls was underestimated. Walls with fibrous insulation took significantly longer to dry than solid walls. This thesis is in agreement with the recommendations from the Department of Communities and Local Government (DCLG) that new constructions in flood-prone locations should avoid glass fibre insulation [68]. Those entering flooded properties need to have a good understanding of the wall types within the property and their ability to retain damp.

There was a major difference between drying rates of dwellings depending on which drying scenario was modelled. Natural drying with central heating turned on provided the fastest drying rate for internal surfaces of all interventions available without using professional remediation equipment, while abandoned dwellings showed a very poor drying ability. Where natural drying was employed, peaks of internal mould growth following surface drying were noted, and were caused by the weather conditions of the external air used to ventilate the interior. In many cases, such as those with fibre-glass insulated walls, the internal surfaces of abandoned properties could remain at risk for mould growth for the entire year-long simulation period. As a result, it is advisable that flooded homes be provided with as much ventilation as possible before remediation workers enter to restore the property. While it is unreasonable because of security reasons to suggest that windows be left open indefinitely in order to dry a dwelling, ventilation is critical for drying a building, and should be maximised. Moreover, understanding the treatment history of the building can help clarify the risks present to those entering the property.

In addition to wall type, naturally ventilated dwellings showed differences in drying based on the potential airflow through the interior of the building. Smaller rooms without or with limited direct external ventilation, such as hallways, bathrooms, and entrances of the bungalow, were found to dry slower than those with windows. Of the types of dwellings studied here, purpose-built flats were found to dry slower than other structures using natural ventilation, which is likely due to the flood height representing a larger proportion of the total dwelling surface area, the lack of exposure of the flooded building fabric to solar radiation and wind on the shared walls, and limited window space and airflow potential.

For sealed dwellings, drying depended on the proportion of the flooded surface areas relative to the total surface area, wall type, permeabilities of the different wall types, and surface area of the dwelling exposed to external conditions and capable of permeable air exchange with dry outdoor air. The worst performing dwellings for drying under abandoned conditions were flats, particularly post-war and recent flats, and terraces, due to their limited permeable external surface area and dominant walls types. Particular archetypes found to be prone to mould growth for extended periods following a flood due to their combination of built form and dominant wall type, were 1960-1979 Purpose-Built Flats (H04 and H11), Post 1980 Purpose-Built Flats (H07), and 1960-1979 Terraced dwellings (H10). Purpose-built flats are also the types of accommodation most common among low-income residents, suggesting that long-term damp may affect those least likely to be insured or who may be unable to temporarily re-locate. Low income is also a significant factor in the susceptibility of a population to post-flood health effects [268]. With the move towards energy-efficient building methods, dwellings are becoming more airtight and natural permeability is being reduced. This suggests that modern properties may be prone to serious mould issues if left sealed.

Some interesting results of the simulations are worth noting. RH in unflooded locations, such as ceilings and above ground storeys, was found to be high enough to support mould growth following a flood event. This was due to the movement of damp air throughout the building zones via the airflow network. This is noteworthy, because the surface moisture content of walls in unflooded sections of a dwelling are often used as a reference for what 'dry' moisture levels should be during building remediation [38]. The simulations carried out in this thesis suggest that this may be inappropriate. As the dwellings dried, the amount of surface area that would be suitable for mould growth rapidly declined for the species *S. chartarum*, which has higher moisture requirements due to the non-flooded sections and storeys losing high surface RH caused by damp air relatively quickly, while *A. versicolor* lingered in many of the dwellings for a longer period for all drying scenarios.

Heating the properties using a high-powered heater or the dwelling's central heating system helped dry the internal surfaces when used alongside natural ventilation. For smaller dwellings, heat from a single 56kW heater was better able to move through the property, rapidly drying out all internal surfaces and preventing mould growth, however, in larger dwellings a single high-powered heater was insufficient. In larger dwellings, using central heating with the electric baseboards on in each room performed better than the professional high-powered heater method. The setpoint of 21^{o}C reflects the assumption that dwellings are heated to this temperature according to the methods described in the SAP documentation. This temperature was selected as one which may be attainable by a typical domestic central heating system, but may not reflect the reality of the prebound effect where inadequately insulated properties are not able to be heated to such a temperature during cold weather. To provide sufficient ventilation, scenarios were modelled with windows and internal doors open, meaning that there would be significant heat loss through the air changes. As a result, both

methods of drying while using heat had a significant energy cost. Their use in this manner provides a drying benefit, but the energy cost may make this use prohibitive. Further studies are necessary to understand the impact of fans and dehumidifiers on the drying rate of dwellings in order to establish the most cost efficient method for remediating different property types.

When modelling a single room, the 56kW heater dried the properties out the fastest of all remediation techniques tested, which was expected, since this is considered to be one of the optimal treatments available [231]. The high temperatures were able to remove moisture effectively from the building surfaces, while the open windows provided sufficient air changes to remove the moist air from the dwellings. There is a clear risk that if the wall is not completely dry to its core, then damp could re-occur on the surface when drying equipment is halted and windows are again closed. This is evident by the dips in RH shown in the graphs in Appendix G, where the use of the 56kW heater over short periods of time only temporarily reduced the internal surface RH. It is therefore crucial that the core of the wall be tested for moisture content in order to ensure that drying is complete. In addition, the elevated temperatures provided by the high-powered heater can raise the temperature to around 50^{o}C. Human pathogenic microorganisms can grow at higher temperatures, therefore it is critical that the moisture content of the wall be reduced as quickly as possible if heaters are to be used, or if the weather is expected to be hot. The heat may enter the cavities of walls and subfloors, where limited ventilation means that moisture cannot escape. If not properly employed, heating may increase the microbial risk inside properties, and remediators should be wary of the risks when, for example, removing fibrous insulation from inside flooded wall cavities.

The suggestion of lingering damp within the wall and floor cavities inside drying dwellings indicates that damp may remain in dwellings that are superficially dry. Water content levels on interior surfaces were found to be non-representative of the levels throughout the wall, as conditions within the wall and on the surfaces of cavities could remain damp for extended periods. This is a concern, as it has been shown than mould spores can move from underfloor spaces and wall cavities into the internal air [7, 183, 261]. While the surfaces may appear to be dry, moisture will migrate to the surfaces of the wall over time, potentially leading to further mould growth once treatment has stopped. In cavity walls and subfloors, vapour removal by air change was not considered, thus the potential for mould growth inside cavities could not be estimated. Ignoring cavity ventilation is likely to have led to an over-estimation of surface drying times of cavity walls, however the simulations are intended to represent a worst-case scenario, for example, situations where air bricks or ventilators are blocked or absent.

The contaminating species modelled has shown varying degrees of persistence on the building surfaces, with the rate of decline related to the drying out ability of different dwellings, and the moisture and temperature requirements of species. Of the contaminating mould species, *S. chartarum* has higher moisture requirements and was seen to decline quicker than *A. versicolor* inside

the drying dwellings. Bacterial contaminants also showed differing rates of decline, with *Salmonella* decreasing quickly regardless of drying scenario, *E. coli* taking 50-100 days, and *Listeria* often persisting for the extent of the simulation period. Mould growth is a major problem following flooding, and dwellings that showed a slow removal of moisture from the walls were more prone to mould growth based on the model predictions. While isopleth-based models such as the Clarke model provide a useful indication of the lowest temperature and RH levels available for growth, an established mould colony can generate its own water sources by hydrolysing the material upon which it is grows. Mould spores can resist desiccation, which means that drying to temporarily low conditions may not kill mould, and growth may recommence in the future. Therefore, further research into the limits for mould spore survival is necessary in order to determine a 'safe' dry point for flooded dwellings. Mould growth in subfloors or within wall cavities was not considered, but may be likely to occur, given the high RH levels observed throughout these surfaces.

The external climate was observed to impact on the drying rate of flooded properties for both abandoned and open window scenarios. Summer flood events in dwellings were observed to dry out faster than winter floods if the drying was completed before winter weather set in. In cases where the archetype was particularly prone to prolonged damp following a flood, summer floods could take longer to dry than winter floods, as the drying period would be extended by the colder, more humid winter weather. The example simulation of high emissions climate change scenarios for London indicated that drying for both winter and summer floods would be faster. However, climate change is predicted to bring more frequent periods of intense rainfall. The modelling methodology does not factor in the impacts of driving rain on moisture movement into the structure, so the possibility that this may prolong drying time has not been considered.

The results of the sensitivity analysis indicate distinct differences between the drying rates of certain wall types, even when the uncertainty in material parameters is taken into account. In addition, the air change rate of the dwellings is an important factor dictating the ability of a dwelling to dry out, as determined by window size and wall permeability. DSA is dependent on the assumption that the parameters are distributed normally around the base-case, and that the sensitivity of individual inputs are independent of the value of other inputs. This is not strictly true in complex hygrothermal systems, but is reasonable with small changes in the input parameters, and DSA has been used to assess other water content-driven hygrothermal models [138].

In flood-prone areas, properties are often made 'flood-proof' by making them resistant to water penetration ('dry' flood proofing), or by minimising the potential damage floodwater can cause ('wet' flood proofing). Perfect 'dry' flood proofing of a building is very difficult to achieve [296] and if it has not been performed seamlessly with all potential water access points sealed, then the property may take longer to dry out than it would do otherwise because of the moisture barrier preventing water from exiting the structure. Additionally, flooded properties with glass fibre insulation may

experience a permanent reduction in the thermal performance of their building following drying, due to the structural changes in the fibrous insulation following saturation [247], while wall ties may corrode due to the damp. It is recommended that fibrous insulation be removed if damaged by water, as they can take a long time to dry and the retained moisture may hold contaminants and cause corrosion damage. Fibrous insulation can be removed from a damp cavity by creating holes at the base of the wall and blowing or vacuuming the insulation out.

10.5.1 Limitations

The sensitivity test performed considered the variances of different building fabrics, basic building geometry, and simple ventilation when simulating the drying of the walls. While this would account for the variances in the construction dimensions and hygrothermal material parameters of the walls for the simplified BESTEST construction, it does not account for any uncertainty in the more complex built forms of the dwelling archetypes. Changes in the built form that could impact on the airflow or air change rate in rooms will affect the drying rate, but modelling the wide range of variances possible in specific dwelling archetypes would be extremely difficult, and for this study such a task has been ignored.

The presence of vapour barriers, internal and external finishings such as paint and rendering, and any flood-proofing has not been considered in these simulations. As indicated by the simulations of building fabrics in Chapter 9, surface coatings are not expected to have a significant impact on the moisture absorption and drying of building fabrics, particularly with regard to the internal surfaces. Additionally, UCL-HAMT is currently unable to model the absorption of water due to wind-driven rain. Heavy rainfall may influence the drying of the structures by penetrating the exterior surface of the walls. The vapour transfer coefficient of the surfaces describes how water vapour can move from building surfaces into the surrounding air. This coefficient was calculated based on the airflow inside and outside the dwelling, as determined by the airflow network and outdoor wind speed. The model does not account for the restriction in air change caused by indoor furnishings.

There are a number of limitations to modelling flooding using UCL-HAMT. These include:

- The inability of the model to simulate the absorption of a head of water into the material, and the reliance on an alternative model to simulate this stage.
- Ignoring gravitational forces on the movement of water within small-pored materials.
- Ignoring the presence of salts or sediment in water and in building materials, which can impact the moisture transport behaviour of a material [171], causing drying to take longer. These are particularly relevant for tidal or sewage floods.
- Ignoring the potential for capillary rise of the water within the building materials.

- Using a 1D hygrothermal model to simulate flooding requires estimates about the gravitational influence on water and ignores the 2 and 3D geometry of the building fabric, which is likely to impact on the drying rate in corners and at thermal bridges.
- HAM models assume a uniformity of hygrothermal properties throughout the materials, perfect contact between material layers, and excludes consideration of cracks and poor workmanship, meaning that the simulation results reflect ideal constructions that will not exist in reality.
- Material parameters to describe liquid moisture behaviour for non-hygroscopic, non-capillary active materials like fibrous insulation is not widely available.
- Approximating air and fibrous insulation as porous materials, and ignoring the effects of hysteresis on desorption for many of the materials were necessary to run the UCL-HAMT model.

Despite the limitations of the model and the assumptions necessary to simulate something as complex as a whole building, UCL-HAMT was quickly able to simulate a wide range of built forms, constructions, and drying scenarios that would not have been possible to test using physical constructions.

10.6 Conclusions

This chapter has demonstrated the potential for HAM models to simulate the flooding and drying of dwelling archetypes. Dwellings were found to dry at different rates, depending on the treatment, wall type, built form, external climate conditions, and flood height. The fastest drying walls were solid 9" brick walls and brick cavity walls, while glass fibre insulated cavities and cavities with an AAC inner leaf were found to be the worst performing, thus agreeing with physical studies. The drying methodologies had a significant impact, with natural ventilation with central heating drying the internal surfaces faster than those without heating. Abandoned dwellings were found to remain damp internally for longer than the year-long simulation time for certain dwelling types, suggesting that those who enter flooded properties need to be aware of the building type and treatment history in order to assess the microbial risk inside a flooded dwelling. Using a temporary high-powered heater to dry the property proved to quickly dry the internal surfaces, but the risk for the surface RH to increase following treatment due to the core of the wall remaining wet was identified as a potential issue. Built form was found to impact on drying, with smaller rooms without direct outside air drying slower, and purpose-built flats drying slower than other dwellings. The ability of moist air to move around flooded properties meant that even following a 0.5m flood, all surfaces within each dwelling type were damp and therefore capable of supporting mould growth.

Understanding the drying rates of specific properties under different scenarios can help inform flooding remediation companies of the most efficient and cost-effective means to dry flooded

dwellings. By using the risk of mould and bacterial presence as an indicator of the risk to occupants living inside flooded dwellings or workers entering an abandoned flooded dwelling, we can predict the potential microbiological hazards to which people will be exposed. Using established dwelling archetypes to simulate the drying behaviour of dwellings means that the results can be mapped to identify locations where properties will be relatively difficult to dry following a major flood event. By performing the simulation of abandoned dwellings drying at different flood heights under winter and summer conditions, curves can be generated to describe the drying behaviour of dwellings. These curves can then be applied to specific flooding scenarios in order to identify areas where the combination of built form, modal wall type, and flood depth will result in microbial risk inside the properties.

Part IV

Flood Mapping

Chapter 11

Mapping the Results

11.1 Introduction

The results of the building simulations indicate differences in drying rates of different dwelling types following a flood due to the built form and building fabric construction, drying type, season, and flood height. The London housing stock model developed in Chapter 7 showed that the types of dwellings and the cavity wall insulation rates vary spatially throughout London, meaning that the drying results from the previous chapter can be analysed to determine the drying performances of different locations within the research area. Furthermore, the depth of floodwater during flood events will also vary spatially; the implication here is that the results of simulations that account for flood height may be applied to models of specific flood events in order to predict areas of vulnerability within London. In addition, dwellings may also be at an increased risk of contamination from certain microbes based on their proximity to point sources of microbial pollution. Finally, the city population will vary in terms of its sociodemographic and population distribution, in that the population exposed to a flood and its consequent vulnerability to health problems will differ spatially for a flood event.

Using GIS software, this chapter will explore the spatial variation of the different dwelling types in London in terms of their vulnerability to prolonged contamination risk following a flood, both in relation to comparative drying ability and the drying performance following a specific flood event. The location of potential point sources for contamination within the research area are identified, and the household density and social vulnerability of different areas of London to flooding is calculated. Finally, areas which may be at high risk due to a combination of flooding risk location, proximity to contamination point sources, social vulnerability, and poor dwelling drying behaviour are identified. The results of this analysis can be used to identify areas where London may be particularly vulnerable to the effects of flooding based on dwellings, location, and population vulnerability.

11.2 Methodology

11.2.1 Flood Maps

A raster representing the projected flood heights above Mean Sea Level of a 1-in-200 year tidal flood event was obtained from the EA. In order to determine the flood heights above ground level, the DTM obtained in Section 7.5.4 was subtracted from the flood height raster using raster math, resulting in a new raster. To determine the flood height for individual properties, the ArcGIS Zonal Statistics tool was used. A buffer was drawn 1m inside the OS Mastermap building shapefiles and the ArcGIS Spatial Analyst Zonal Statistics tool used to determine the mean floodwater height within the buffered area, and the results were joined to the housing stock dataset. Dwellings that had a flood height below the simulated range of 0.1m to 2.0m were approximated to be 0.1m, while those above 2.0m were assumed to have suffered structural damage, and were not considered in this analysis. The total surface area covered by the floodwater within the research area was summarised for each Local Authority using the ArcGIS Spatial Overlay tool.

11.2.2 Mapping Dwelling Types

As discussed in Section 7.4, the CR landuse database contains information on the built form and age of different properties in London. The built form/age combinations corresponding to the simulated dwelling archetypes were selected from the CR housing stock data, and were assigned a modal wall type based on the most frequently observed type of wall for the archetype in the EHS analysis for the built form/age combination. It was assumed that the EHS building fabric data was representative of the dwellings in the London housing stock.

The HEED database was used to gather additional information about the building fabrics of dwellings in the CR database. COA-level data on the percentage of properties with cavity wall insulation was used to determine the probability of a dwelling with cavity walls having insulation in these areas using the ArcGIS spatial overlay tool. The calculated frequency of insulation within a COA was used to adjust the modal wall type of individual dwellings within the areas to reflect the local insulation rates.

Two different applications of the building simulation results were used to determine the drying behaviour of the city: drying times of different properties after a 0.5m flood under natural ventilation conditions (comparative drying behaviour), and drying times of abandoned dwellings following a specific flood event, based on the flood height data and curves fit to the building simulation results (absolute drying behaviour).

11.2.2.1 Comparative Drying Behaviour

The comparative drying behaviour described the amount of time different dwelling archetypes took to dry to the point where no microbiological risk was present inside the dwellings, under the same

drying conditions, and without considering the height of the flood. By mapping the results, the vulnerability of different areas of London to prolonged damp following flooding based on the duration of microbial risk can be identified.

Drying times were calculated as being the amount of time taken for the microbial risk inside dwellings drying in winter under natural ventilation conditions to decrease to zero on all internal surface areas. The drying time for each dwelling archetype with their modal wall type was calculated for each microbial species modelled (Appendix H). The drying time values for the built form/wall type combinations were joined to the geodatabase of individual dwellings with CR built form and HEED cavity wall insulation data. The areal mode drying time was then calculated for each COA in the research area using the ArcGIS Overlay-Spatial join tool, resulting in a map with the drying times of the most common dwelling archetypes in the COAs. Maps were created for the comparative drying times of the different contaminating species modelled and used to identify locations where the dwelling types would be vulnerable to long-term damp following flooding. In cases where the built form/wall type combinations did not dry using natural ventilation within the year-long simulation period, the individual dwellings were classified as being > 1 year.

11.2.2.2 Absolute Depth-drying Curves and Specific Flood Events

As demonstrated in Chapter 10, flood height has a significant impact on the drying behaviour of a dwelling. To describe how flood height can impact the drying behaviour of dwellings, depth-drying curves were developed based on the depth-damage curves introduced in Section 7.2.2 and widely used to calculate the relationship between financial damages and flood height. These curves were used to calculate the absolute height-dependent drying times of individual dwellings following specific flood events, and the mapped results used to identify vulnerable locations following specific flood scenarios.

Depth-drying curves were developed from the simulated data for dwellings under abandoned scenarios, as it was assumed that following a major flood event dwellings would be left abandoned and sealed in order to prevent intruders into the property. The height-dependent drying data for abandoned dwellings can be seen in Appendix I. Due to a lack of variation in the drying time for *E. coli* and *Salmonella* at different flood heights, curves were not produced for these contaminating species, while curves for *Listeria* were not calculated due to there being few archetypes which showed a complete elimination of risk within the year-long simulation period.

In order to describe both the instantaneous risk within a property and the amount of time required for the risk to decrease to zero for *A. versicolor* and *S. chartarum*, a 3D function was fit to the simulation results for the data in the simulated ranges of 0.1m to 2.0m for different dwelling types and seasons. A 3D logistic decline model describes a curve showing the reduction in surface area at risk to mould growth, as observed in the simulation results:

$$SA = \frac{a}{1 + \exp\left(-\left(b + c \cdot t + d \cdot h + f \cdot t \cdot h\right)\right)} + g \tag{11.1}$$

where SA is internal surface area at risk of mould growth (m^2), h is flood height (m), t is time (days), and a, b, c, d, f, and g are model parameters that describe the behaviour of the curve. The logistic equation could be re-arranged to resolve the amount of time required for the internal surface areas inside the dwellings to reduce to a set value for floods as a function of flood height:

$$t = -\frac{\ln\left(\frac{a}{-g} - 1\right) + b + d \cdot h}{c + f \cdot h} \tag{11.2}$$

This logistic model displays an asymptote which approaches zero over time. In order to force the model to go through SA = 0, the models were fit using a fixed offset (g) set to a nominal value below zero (-10). A major strength of the 3D logistic model is the ability to alter the shape of the decline (concave vs. convex decline) by eliminating a model parameter, and making the model applicable to the declines exhibited by both mould species as the dwellings dried over time.

The data was fit to the curve using the online tool ZunZun [307], fitting to the lowest sum of squared (SSQ) absolute error. A step-wise procedure was followed to eliminate parameters with a large confidence interval. The results were checked against the original data to ensure that the estimate for the drying time (zero-intercept) provided a good estimate of the model results. An example surface plot of the 3D logistic model fit to the simulated drying results for an abandoned dwelling can be seen in Figure 11.1.

The parameters for the depth-drying curves were calculated for each built form/wall type combination, including both uninsulated and insulated cavity walls in some dwelling types. The parameters were imported into ArcGIS and joined to the individual dwelling geodatabase, as per Section 11.2.2.1. In abandoned properties there was little difference in drying rates between insulated and uninsulated dwellings, so local insulation rates for dwellings were based on the modal wall types determined from the HEED database.

The duration of contaminant risk for *A. versicolor* and *S. chartarum* for both summer and winter floods was calculated for each individual property within the research area according to the flood depth calculated for individual properties in the EA 1-in-200 year tidal flood map, and the archetype-specific depth-drying curve. The areal mean for the COAs was calculated using the ArcGIS Overlay-Spatial join tool, and the results mapped.

11.2.3 Mapping Population Demographics and Vulnerability

Mapping has also been used to show the vulnerability of resident populations to floods based on socioeconomic data and using research into past flooding events. The SFVI [268] assesses the vulnerability of populations to adverse health effects based on three social characteristics and four

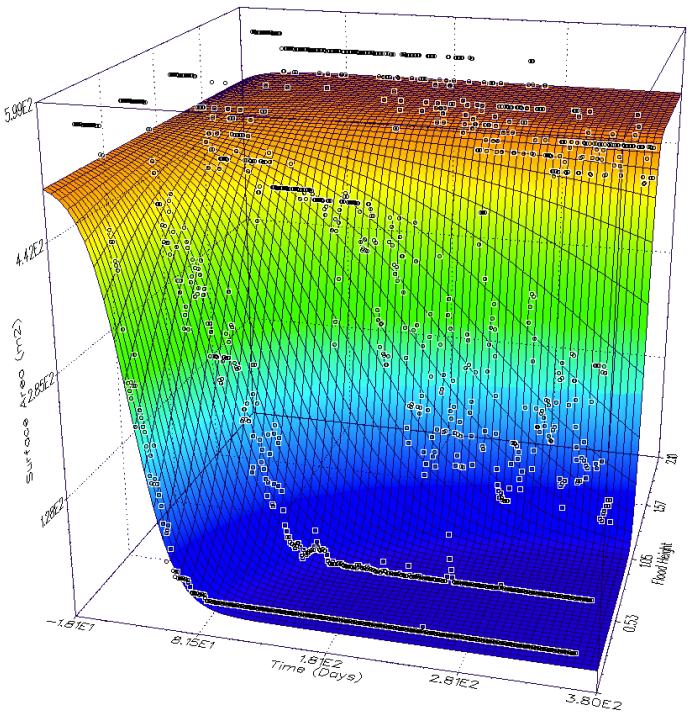

Figure 11.1: Modelled fit of the logistic model to the simulation data for the *A. versicolor* surface area inside an uninsulated bungalow drying during the winter.

financial-deprivation indicators. To know which populations are at risk from floods for socioeconomic reasons informs the development of processes to predict regions vulnerable to flooding in London. The UK Census [212] provides aggregate statistics on the demographics and socioeconomics of the UK within specific geographic areas. This data is used extensively to determine population characteristics within a region, and can be used to describe a flood-affected population.

To map the vulnerability of Londoners to a flood event, the methodology proposed by Tapsell and colleagues to calculate the SFVI was followed [268]. 2001 Census data was acquired from the Census Dissemination Unit for the four financial indicators (Unemployment, Overcrowding, Non-car ownership, and Non-home ownership) and three social indicators (Long-term sick, Single parents, and the Elderly (over 75)) over a COA. Data was transformed in order to normalise the skewness and kurtosis of the distribution using the transformation methods shown in Table 11.1, and data for each indicator standardised as Z-scores. The four financial indicators (Townsend indicators) were summed separately and multiplied by 0.25 before summing with the social characteristics data in order to remove any financial bias, as per Tapsell and colleagues [268]. The resultant SFVI was mapped using ArcGIS to the COA level.

In addition to the SFVI, Census data was obtained for the number of individuals living in households and the number of households within the COAs. This data was used to calculate the

Indicator	Transformation
Lone Parents	Square Root
Elderly	Square Root
Long-Term Sick	Square Root
Non-Homeowners	Natural Log
Unemployed	Natural Log
Non-Car Owners	Square Root
Overcrowding	Square Root

Table 11.1: Transformation method used in the compilation of the SFVI for London.

number of individuals and households affected by the EA 1-in-200 year tidal flood event within the research area for each Local Authority using the Spatial Overlay tool.

Finally, the average number of individuals per household was calculated for each COA using census data. The average absolute drying time predicted for each COA for *A. versicolor* and *S. chartarum* for the EA 1-in-200 year tidal flood event was multiplied by average number of individuals per dwelling within the COA and total number of flooded dwellings in order to estimate the number of person-years residents would be exposed to damp indoor spaces (should they choose to stay), or displaced (should they leave their damp homes). The results were mapped according to COA, and summarised according to Local Authority, using the Spatial Overlay tool, as above.

11.2.4 Mapping potential contaminant point sources

There is scant publicly available data on the locations of potential contaminant sources in London, such as sewage outlets and drains. However, as a case study to demonstrate the potential for contaminant point sources to spread in floodwater to nearby dwellings, available data on the locations of agricultural and landfill spaces in London were obtained from EA and the CR landuse database. Analysis of EA-provided data on landfills indicated that there are no current landfills within the research area, so the analysis focused on agricultural point sources. Floods over agricultural land may transport a number of potential bacterial contaminants in the floodwater through rural diffuse floods. All landuse types were selected that would be related to agriculture, including agricultural buildings, pasture land, fallow land, field crops, plowed fields, and allotments. A 500m buffer was drawn around the agricultural point source locations, and used as a rough estimate of the location of dwellings which may have an elevated risk of bacterial contamination.

In addition, the outline for a 1-in-100 fluvial flood event was obtained from the EA, and used as an indicator for areas at risk of bacterial contamination from fluvial sources, which can include *E. coli O157*, *Listeria*, and *Salmonella,* among others).

11.2.5 Locations of Concern

ArcGIS was used to identify vulnerable locations due to a combination of slow-drying housing stock, sociodemographic characteristics, flood depths of specific events, and proximity to contaminant source. COAs were selected based on the following combinations:

- COAs where housing stock will exhibit a prolonged comparative contamination risk ($>$ 1 year risk of *A. versicolor* growth for a naturally ventilated dwelling following a 0.5m winter flood) that lie in areas at risk of flooding (1-in-200 year tidal flood event outline).
- COAs where housing stock will exhibit the above prolonged comparative contamination risk and where the population will be most vulnerable (SFVI $>$ 1, 'High' or 'Very High').
- COAs where dwellings will exhibit the above prolonged comparative contamination risk and where the flood may be particularly deep (greater than 1.1m, or the deepest 5% of flood depth for the 1-in-200 tidal flood scenario).
- COAs where housing stock will exhibit a prolonged comparative potential for contamination from bacteria (*E. coli* longer than 115 days, *Salmonella* longer than 6 days, or *Listeria* longer than 290 days) and that lie within 500m of a potential agricultural contaminant point-source, or in an area at risk of a 1-in-100 year fluvial flood.

A COA was considered to be at risk of flooding in the EA 1-in-200 year tidal event if the outline of the flood contained any part of the COA. Electoral wards containing a number of vulnerable COAs were identified and named as areas that should be prioritised following a flood event.

11.3 Results

The results of combining the building simulations and microbial models identified areas in London likely to be vulnerable to flooding, based on types of dwellings present, resident population, and proximity to flood risk and contaminant sources.

11.3.1 Sociodemographics of Research Area

The numbers of people affected by a flood event will depend on the population distribution across the research area. The number of individuals per household in the research area can be seen in Figure 11.2. Areas in the North East of the research area had the highest number of individuals per household, meaning that a greater proportion of people will be exposed to poor indoor environments and contamination following a flood event in these areas than in other locations in the city.

The social vulnerability to flooding analysis identified the more vulnerable populations that live within London based on socioeconomic data. The results of the SFVI analysis can be seen in Figure

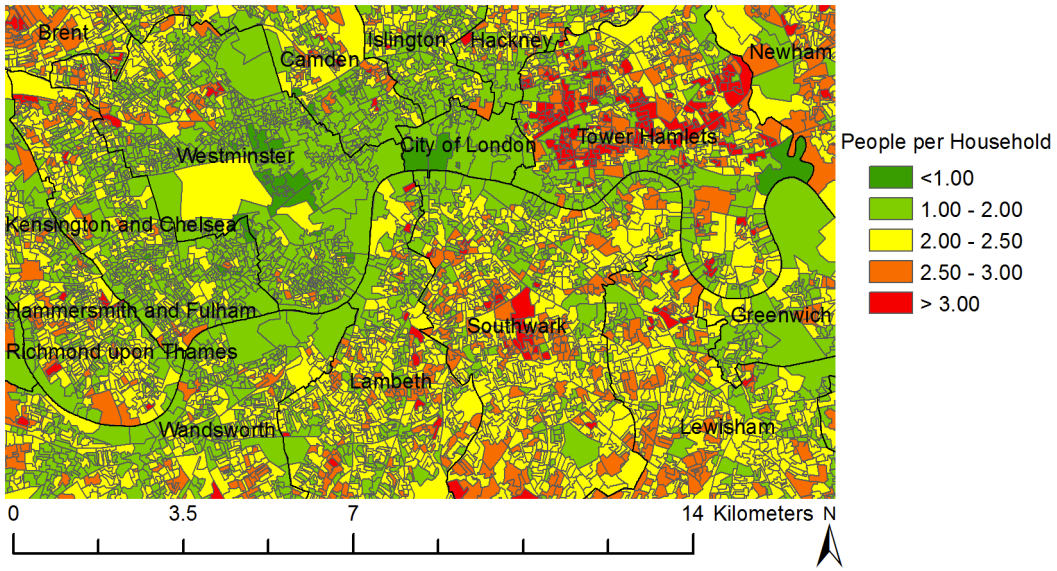

Figure 11.2: The number of people per household across the research area.

11.3. As with the number of individuals per household, the areas most vulnerable to flooding were observed in the North East, and was particularly high in the London boroughs of Newham, and close to the river in Southwark. The two analyses suggest that not only are the individuals in East London more vulnerable to flooding due to socioeconomic factors, the higher household populations suggest a greater absolute number of residents may be affected as well.

11.3.2 Comparative Drying Behaviour

The comparative drying performance of the different areas based on the types of dwelling present was determined by calculating the mode drying time of dwellings flooded and dried under the same conditions within the COAs. An example of the drying times of dwellings of individual dwellings, as represented by the amount of time required to reduce the internal surface area prone to *A. versicolor* growth inside dwellings following a 0.5m winter flood with open windows, can be seen in Figure 11.10a.

The areal mode of the comparative drying times of the dwelling archetypes within London for the different contaminants modelled can be seen in Figures 11.4, 11.5, 11.6, 11.7, and 11.8. These maps suggest a higher proportion of slow-to-dry properties in the East of the study area. Southwark and Tower Hamlets appear to be particularly vulnerable because of their large number of slow drying properties. There was insufficient data to calculate many of the areas in the study, due to a lack of coverage of the CR housing stock data. However, the results give an indication of the drying rates across many areas of the city.

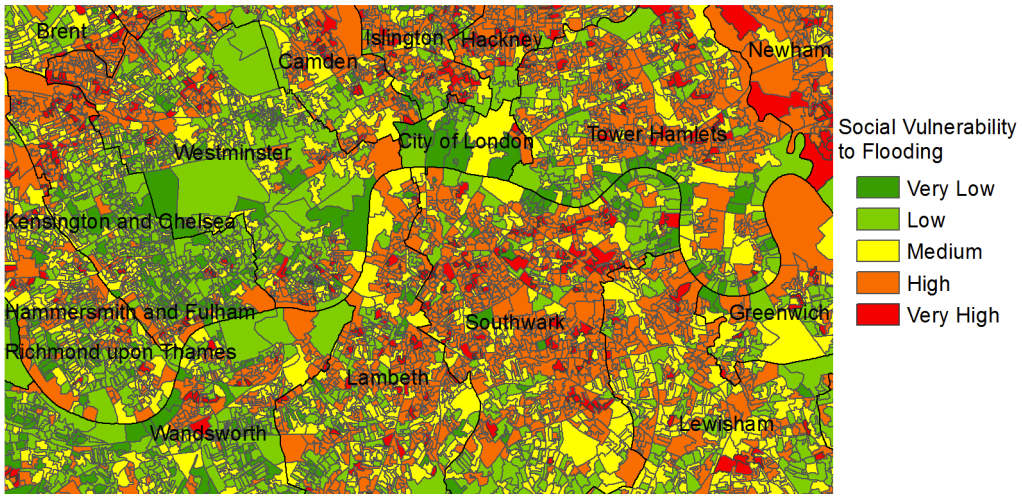

Figure 11.3: Social vulnerability of populations in London to flooding based on the SFVI.

11.3.3 Absolute Drying Behaviour

11.3.3.1 Depth-Drying Curves

The parameters and model fits or the depth-drying curves for each dwelling, majority wall type found in the dwelling, season, and contaminant can be seen in Appendix J. The fit of the model is indicated by the R^2 and RMSE of the model fit, and the confidence intervals of the parameter estimates. The models were found to offer a strong estimate of the variation of the drying rates of dwellings flooded to different heights.

11.3.3.2 Specific Flood Scenarios

The raster indicating the calculated depth of the flood event based on the differences between the predicted flood heights provided by the EA and the calculated DTM can be seen in Figure 11.9. The average depth was found to be 0.8m, with parts of Southwark close to the Thames particularly vulnerable to deep flooding based on this scenario.

The depth-drying curves calculated the impact of flooding on individual properties within the study area based on the dwelling parameters and the projected flood height at the location of the dwelling. An example of the applied depth-drying curves to abandoned individual properties for the EA 1-in-200 year tidal flood risk scenario can be seen in Figure 11.10b.

Calculating the mean drying times of all known dwellings within the COAs in London allowed for the estimation of how the variation in flood heights may impact on the drying rates of properties based on their location. The application of the depth-drying curves to the tidal flood risk scenario for the mould contaminants following winter and summer floods can be seen in Figures 11.11, 11.12, 11.13, and 11.14. As with the comparative drying results, Southwark was found to be particularly vulnerable to long-term damp, and by taking into account flood depth, the problem was emphasised.

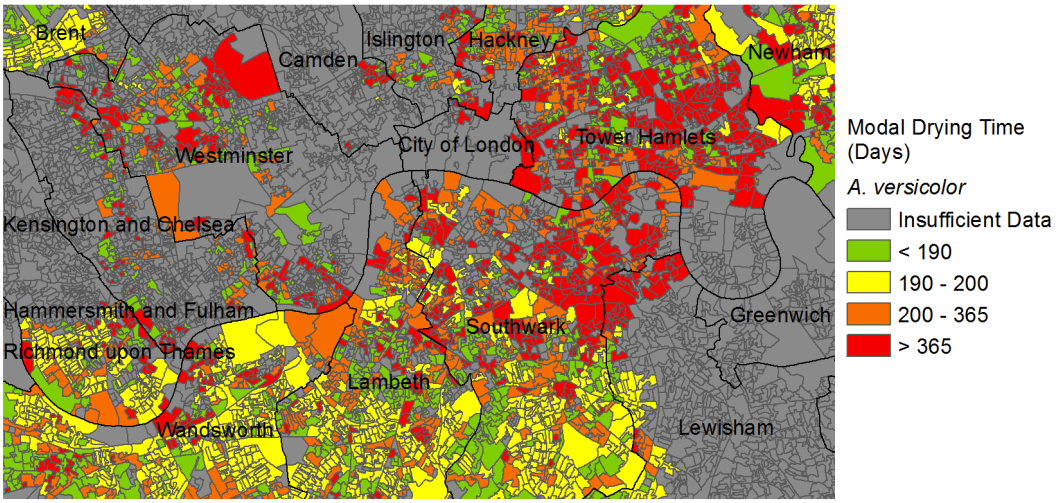

Figure 11.4: Comparative vulnerability of the London housing stock to prolonged *A. versicolor* risk following flooding.

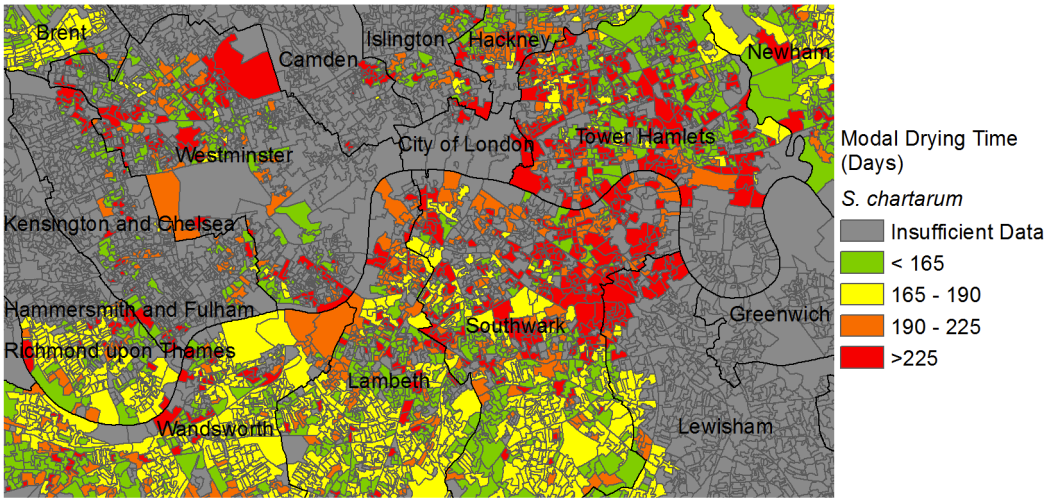

Figure 11.5: Comparative vulnerability of the London housing stock to prolonged *S. chartarum* risk following flooding.

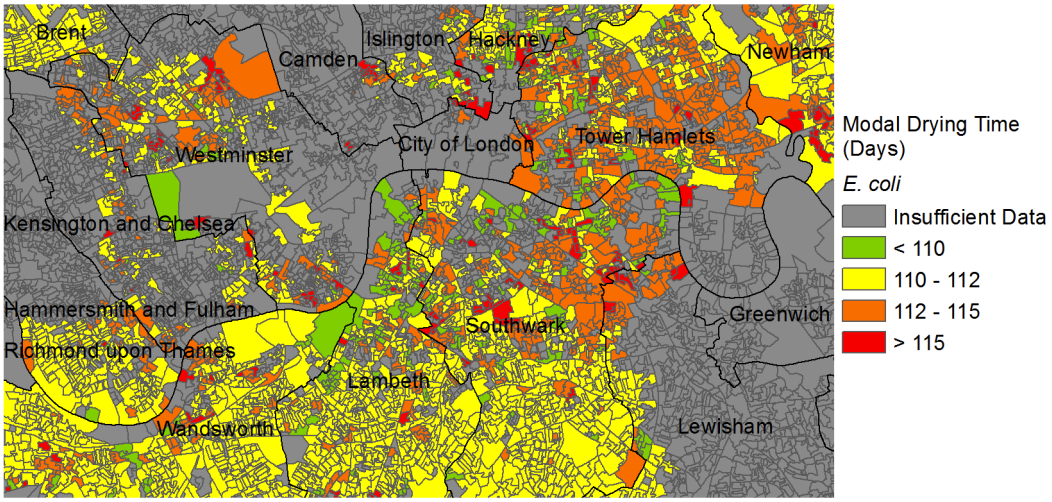

Figure 11.6: Comparative vulnerability of the London housing stock to prolonged *E. coli* risk following flooding.

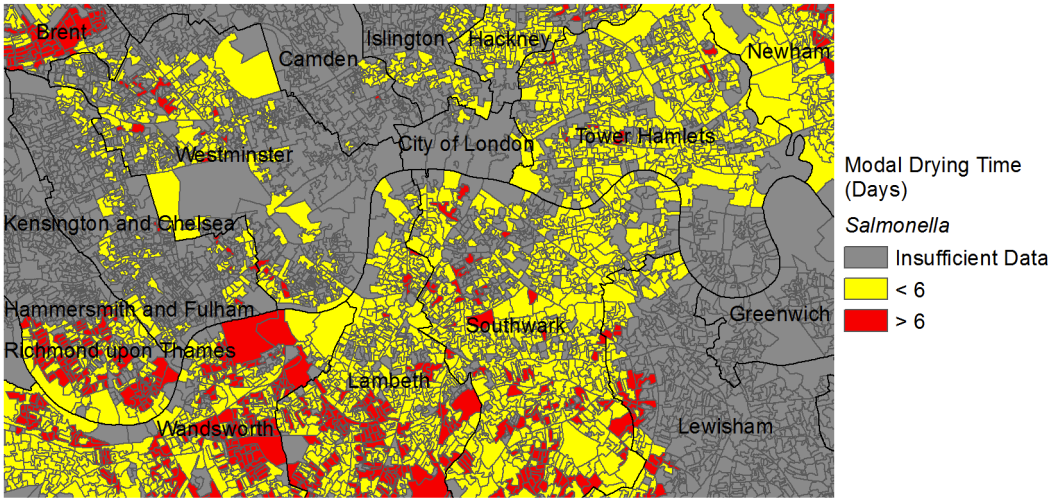

Figure 11.7: Comparative vulnerability of the London housing stock to prolonged *Salmonella* risk following flooding.

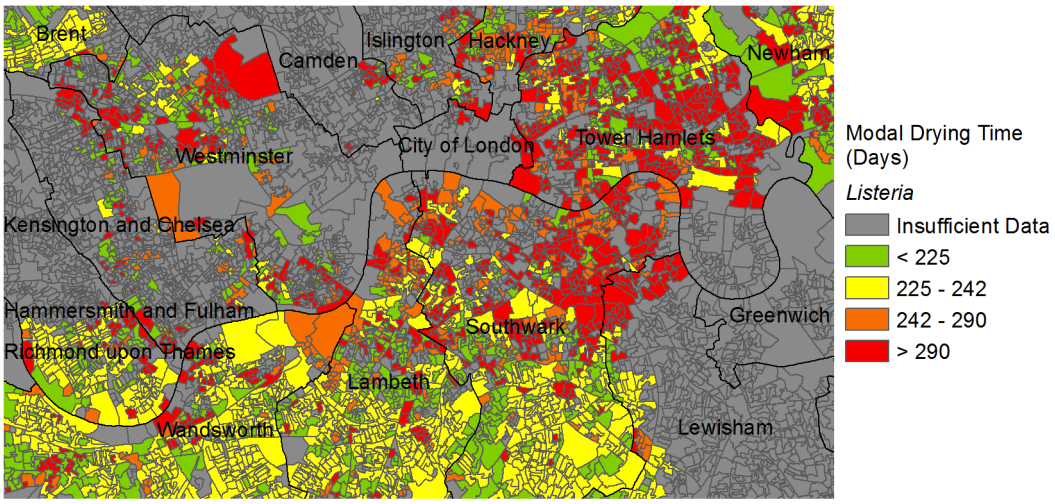

Figure 11.8: Comparative vulnerability of the London housing stock to prolonged *Listeria* risk following flooding.

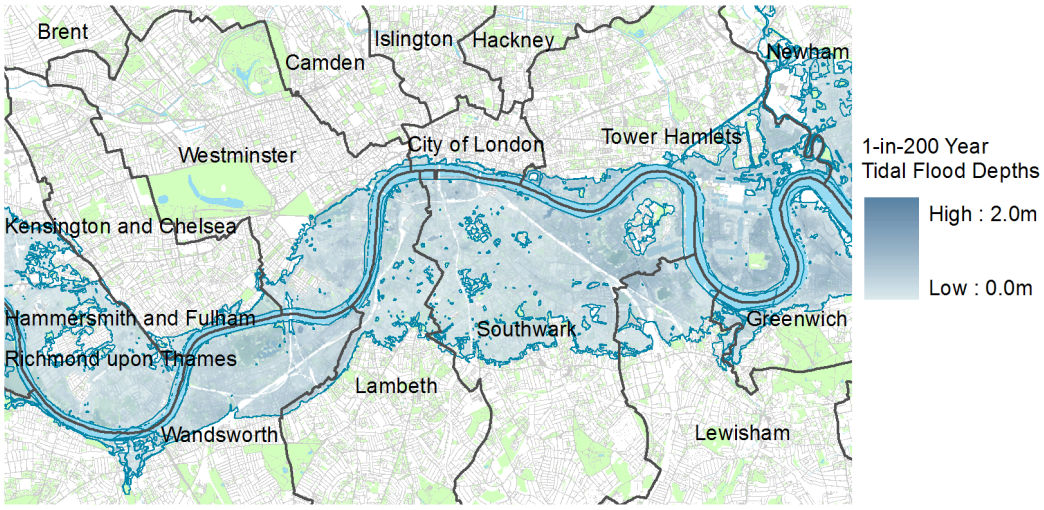

Figure 11.9: The depths of a 1-in-200 year tidal flood event in London.

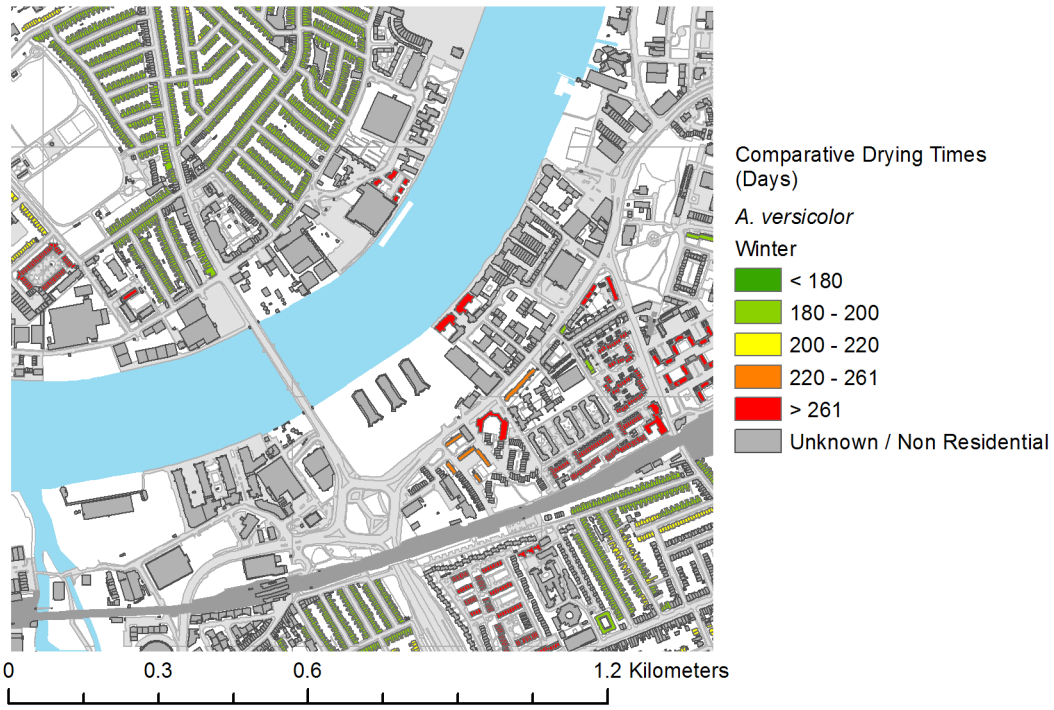

(a) Comparative drying times for *A. versicolor* contamination following winter floods.

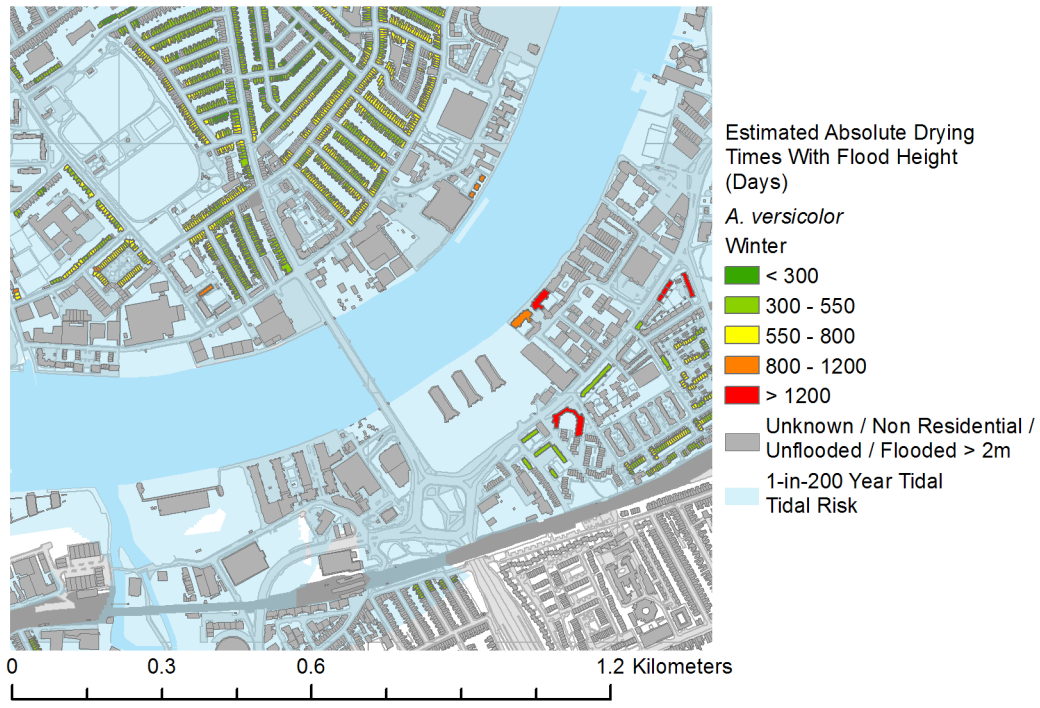

(b) Absolute drying times based on depth-drying curves and flood height for *A. versicolor* contamination following winter floods.

Figure 11.10: Close-up examples of (a) comparative and (b) absolute drying times (days) applied to individual dwellings in the research area.

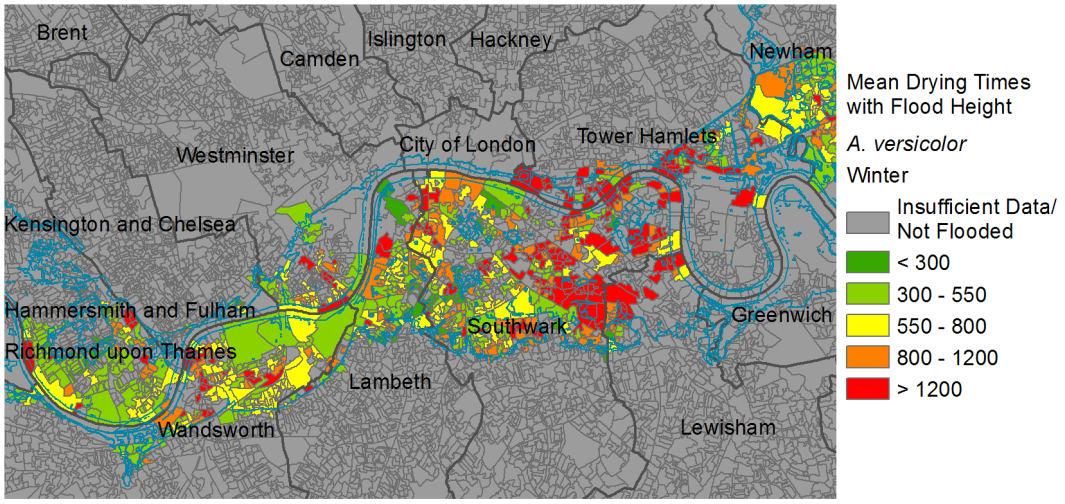

Figure 11.11: Duration of risk of contamination for *A. versicolor* following a winter flood.

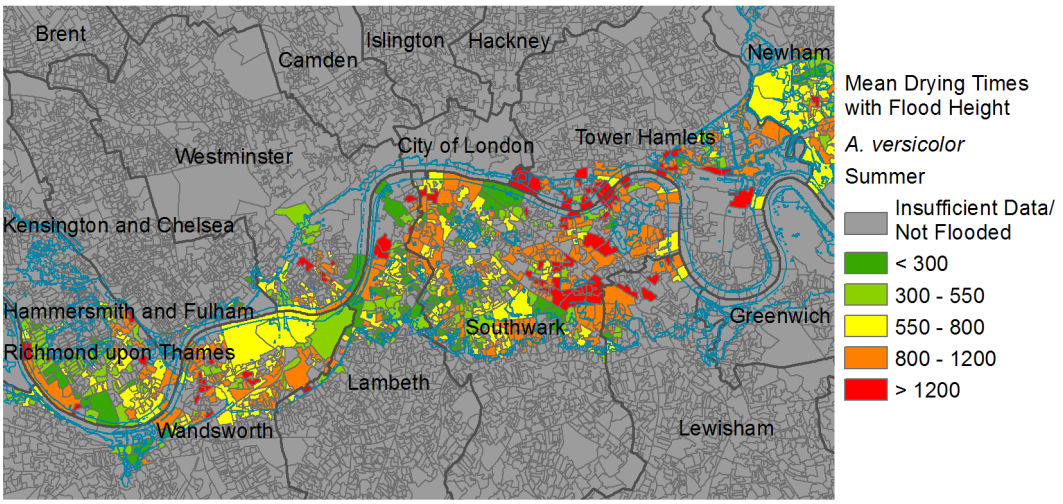

Figure 11.12: Duration of risk of contamination for *A. versicolor* following a summer flood.

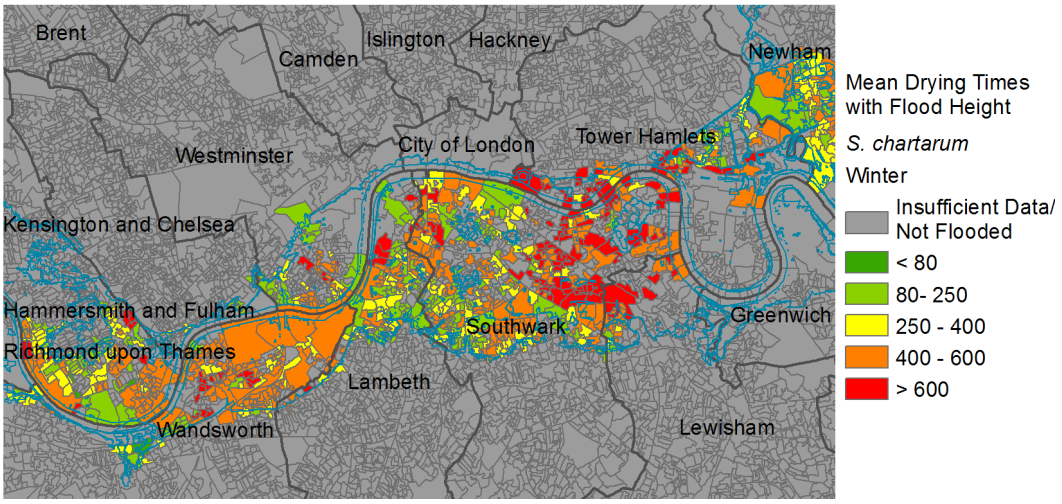

Figure 11.13: Duration of risk of contamination for *S. chartarum* following a winter flood.

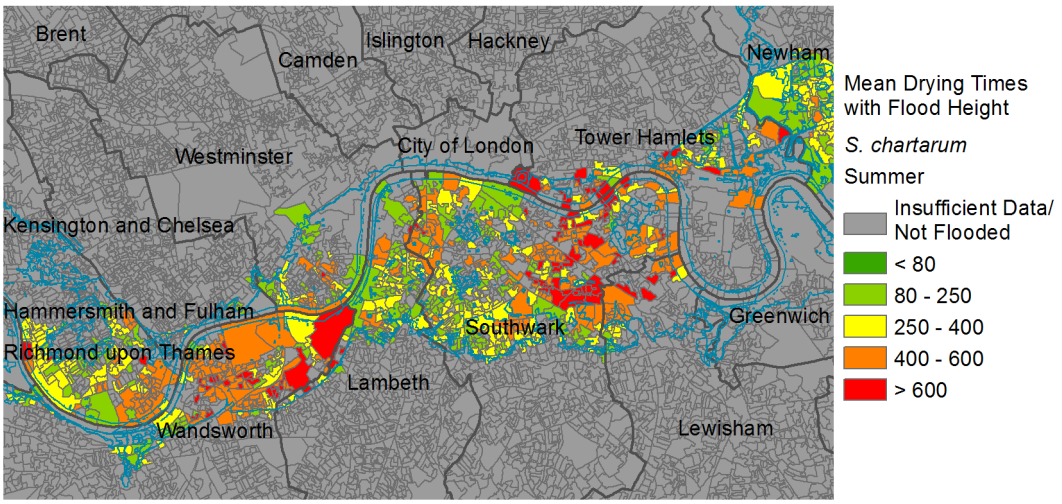

Figure 11.14: Duration of risk of contamination for *S. chartarum* following a summer flood.

Summer floods showed an exaggeration of the drying time differences predicted by the winter floods because dwelling archetypes that would dry quickly during a winter flood would dry even faster during a summer flood due to the warmer temperatures and lower RH. Slow-drying archetypes in winter floods would dry even slower following summer floods, as the drying time extended into the following winter when conditions would become less conducive to drying.

11.3.3.3 Human Impact

Combining GIS Census data and flood maps indicated that a large of population of Londoners would be affected by the 1-in-200 year tidal flood scenario. The area submerged by the floodwater, the number of dwellings flooded, the estimated population affected, and the number of person-years that the population would be impacted due to the drying behaviours of the dwellings for each Local Authority can be seen in Table 11.2. Southwark and Hammersmith and Fulham are likely to experience the highest coverage of floodwater for the 1-in-200 year tidal flood, the greatest number of flooded dwellings, and total flooded population. The largest impact in terms of person-years was observed in the Borough of Southwark. The calculated person-years affected by the flood event are mapped in Figures 11.15, 11.16, 11.17, and 11.18.

11.3.4 Contaminant Point Sources

The contaminant point sources for agriculture and their surrounding area, as well as the outline for fluvial 1-in-100 year flood events can be seen in Figure 11.19. The most commonly found source of potential contaminants were garden allotments. Dwellings within the fluvial flood risk area, or close in proximity to an agricultural point source, may be at greater risk of becoming flooded with water contaminated with bacteria, and the drying behaviour of these dwellings will influence the rate of microbial death and the potential for infection of dwelling occupants.

11.3.5 Locations of Concern

The locations of concern identified areas where the vulnerability of the housing stock to prolonged damp following a flood event occurred in the same location as flood-vulnerable areas, vulnerable populations, and in locations close to potential pathogen point-sources. There were a number of locations within the EA 1-in-200 year tidal risk area that had a majority build type which was slow to dry ($>$ 1 year drying time for a naturally ventilated dwelling following a 0.5m winter flood, for *A. versicolor*) (Figure 11.20).

COAs where the predicted depth of the 1-in-200 year tidal flood event is deep, and that contain properties slow to dry based on comparative drying scenarios, can be seen in Figure 11.21. There are relatively few areas vulnerable to this combination due to the large depth of the flood.

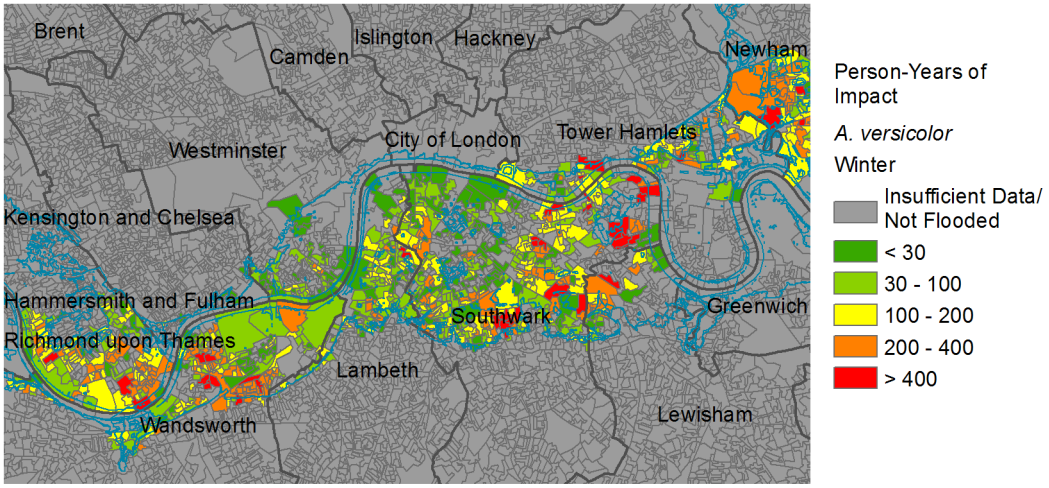

Figure 11.15: Impact of the tidal 1-in-200 year flood event in terms of the potential displacement or exposure to poor indoor conditions in person-years for *A. versicolor* following a winter flood.

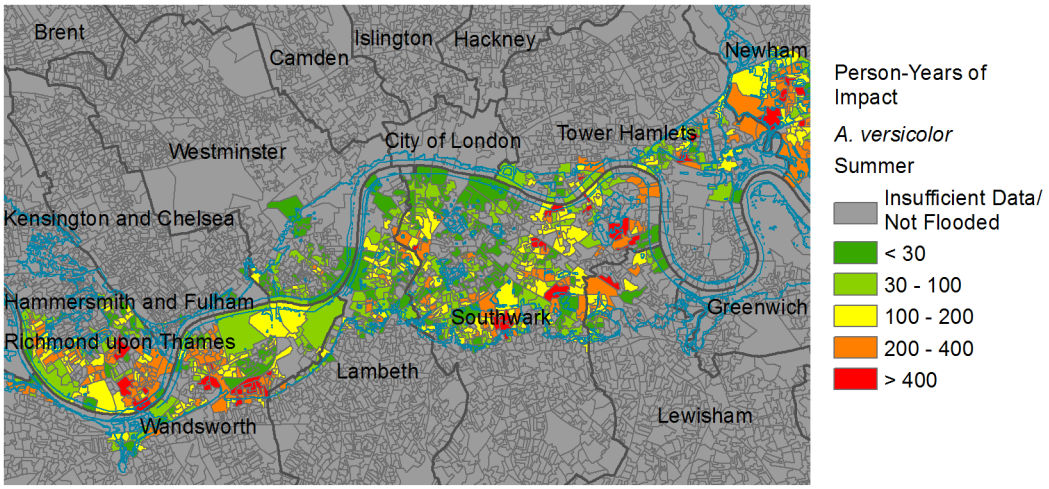

Figure 11.16: Impact of the tidal 1-in-200 year flood event in terms of the potential displacement or exposure to poor indoor conditions in person-years for *A. versicolor* following a summer flood.

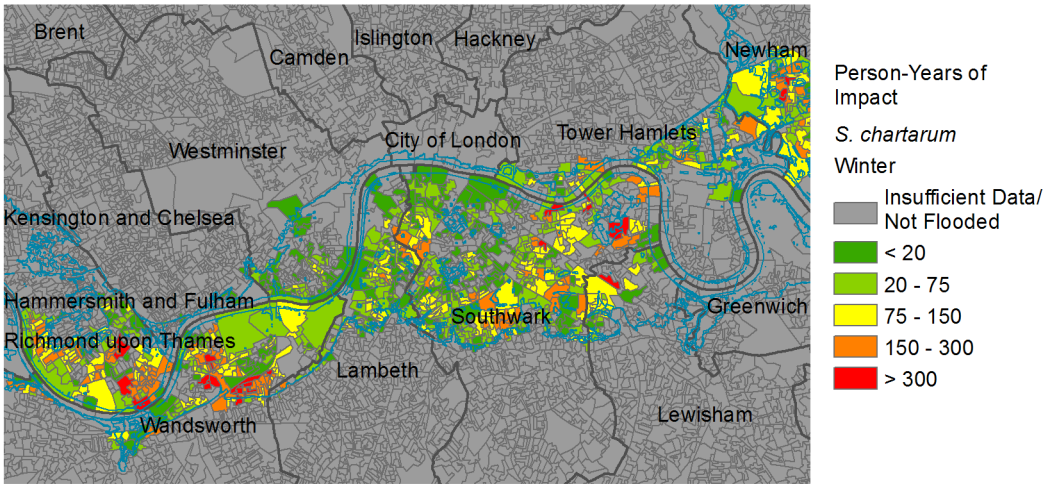

Figure 11.17: Impact of the tidal 1-in-200 year flood event in terms of the potential displacement or exposure to poor indoor conditions in person-years for *S. chartarum* following a winter flood.

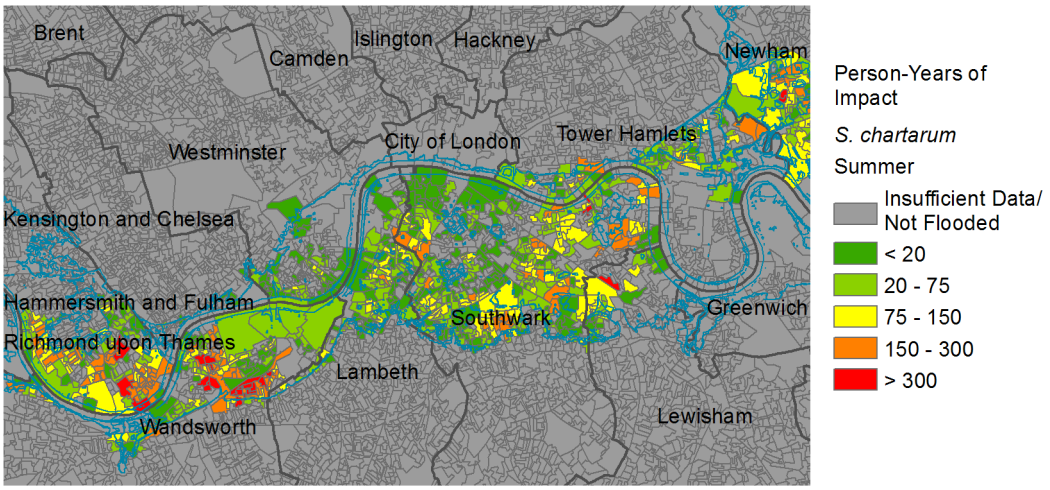

Figure 11.18: Impact of the tidal 1-in-200 year flood event in terms of the potential displacement or exposure to poor indoor conditions in person-years for *S. chartarum* following a summer flood.

Local Authority	Surface Area (km^2)			Population	Dwellings Flooded		Total Person-Years			
	Total	Flooded	% Flooded	Estimated Flooded	Total	Of which are known and modelled	*A. versicolor* Winter Flood	*A. versicolor* Summer Flood	*S. chartarum* Winter Flood	*S. chartarum* Summer Flood
City of London	3.2	0.308	9.77%	18	17	0	-	-	-	-
Greenwich	50.4	1.110	2.20%	6,949	3,418	0	-	-	-	-
Hammersmith and Fulham	17.2	7.383	43.02%	44,226	21,060	7,876	55,239	66,454	45,913	45,090
Kensington and Chelsea	12.4	0.545	4.40%	2,052	1,115	134	2,940	3,166	1,175	969
Lambeth	27.3	2.664	9.77%	9,979	4,752	2,058	20,072	18,959	10,621	9,300
Lewisham	35.3	2.185	6.18%	9,674	4,152	664	26,936	23,839	14,590	12,086
Newham	38.7	2.251	5.82%	8,909	3,759	3,965	14,901	16,248	8,080	6,881
Richmond upon Thames	58.8	0.361	0.61%	196	98	0	-	-	-	-
Southwark	29.9	12.462	41.68%	46,513	20,952	7,077	115,582	10,6478	59,551	50,387
Tower Hamlets	21.6	6.253	28.99%	13,440	6,046	1,361	39,025	36,555	17,019	14,988
Wandsworth	35.2	3.975	11.29%	18,626	9,299	5,570	32,146	37,461	23,215	24,403
Westminster	22.0	3.281	14.89%	6,336	3,627	675	13,342	12,922	5,916	5,345
Total	351.8	42.8	1.8%	166,919	78,295	29,380	320,183	322,081	186,079	169,449

Table 11.2: The impact of the EA 1-in-200 year tidal flood event on Local Authorities within the research area. Person-years describes the estimated total flooded population, multiplied by number of flooded dwellings and average drying time of dwellings.

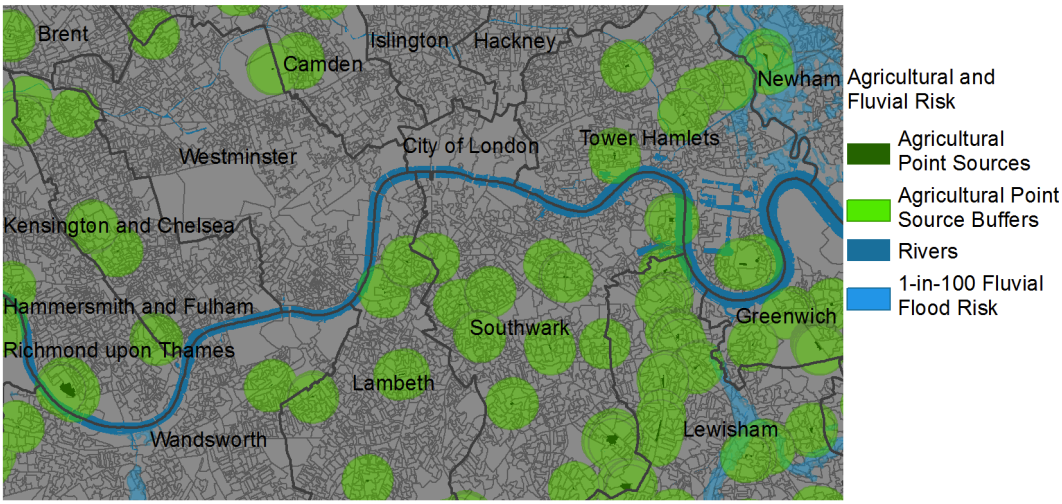

Figure 11.19: Landfill and agricultural sites within London according to the CR landuse database.

The effects of flooding on vulnerable populations may be accentuated by living in a particularly vulnerable dwelling type. The areas considered to be at risk due to a combination of social vulnerability (SFVI $>$ 1, 'High' or 'Very High') and prolonged risk of *A. versicolor* growth are shown in Figure 11.22.

COAs that lay within 500m of an agricultural point source, or within the 1-in-100 fluvial flood zone that contained a large number of dwellings vulnerable to prolonged contamination of *E. coli*, *Salmonella*, and *Listeria,* can be seen in Figure 11.23. Wards that were found to contain a number of vulnerable COAs were identified and are listed in Table 11.3. Due to the combination of the various factors examined, these areas may require special attention following flooding in order to minimise chronic public health problems after a flood event. A large map detailing these areas is represented in Appendix K, which identifies vulnerable areas resultant from multiple factors.

11.4 Discussion

The building simulation research in the previous chapter has demonstrated how different dwelling archetypes will exhibit a range of drying behaviours following a flood, based on type of dwelling, height of flood, drying conditions, and contaminating microorganism of concern. The dwelling archetypes were compared in terms of their drying behaviour under the same flood and drying conditions, as well as the impact of flood height. By applying the building simulation and microbial modelling results to the geospatial database developed in Chapter 7, areas of London which are particularly vulnerable to flooding due to their combination of dwelling archetypes, flood risk, proximity to contaminant sources, and sociodemographic data have been identified.

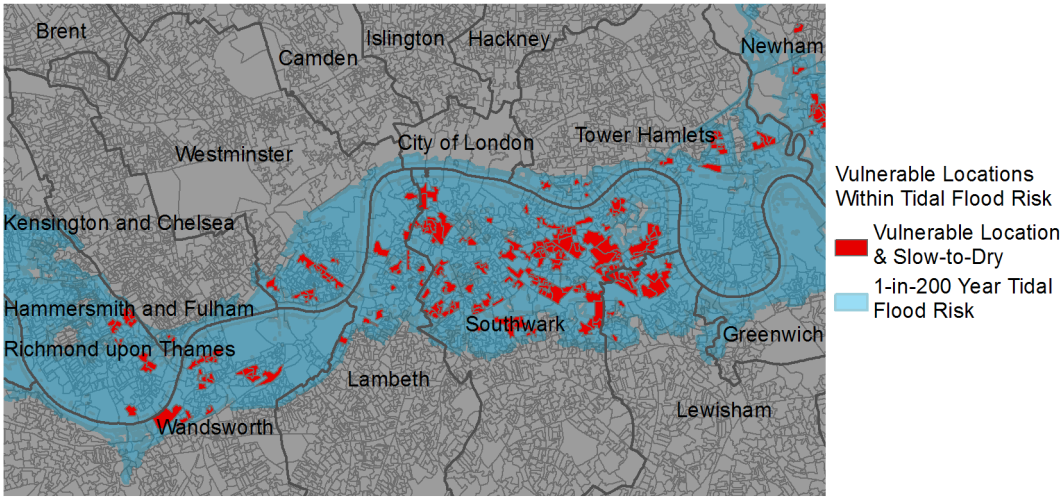

Figure 11.20: The areas within the 1-in-200 year flood risk area with vulnerable dwellings.

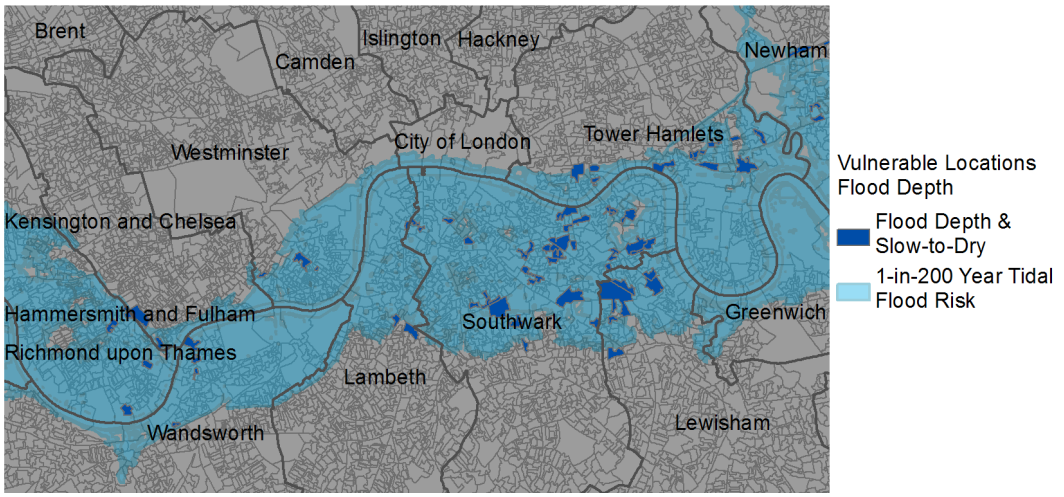

Figure 11.21: The 1-in-200 year tidal flood depth and dwelling vulnerability.

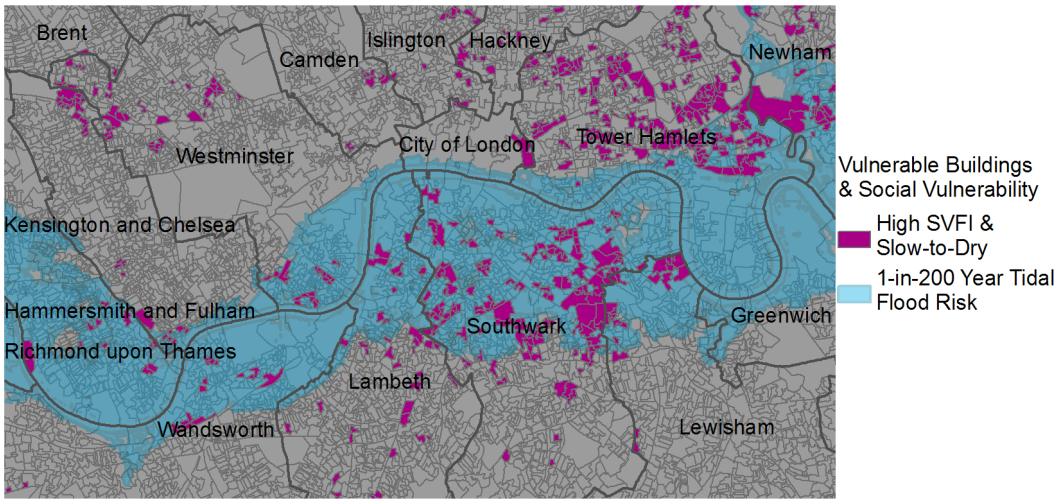

Figure 11.22: Locations with a vulnerable population and with archetypes showing an increased risk of prolonged *A. versicolor* contamination.

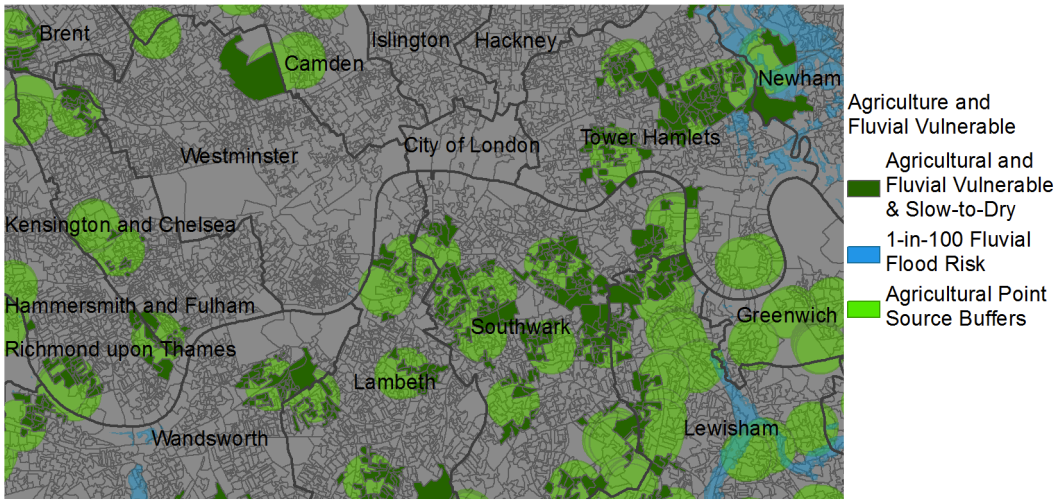

Figure 11.23: COAs with dwellings with a prolonged bacterial risk that lie within 500m of an agricultural source or within a 1-in-100 fluvial risk area.

Locations of vulnerable dwellings in area at risk of flooding	Locations of vulnerable dwellings in area at risk of deep flooding	Locations of vulnerable dwellings and population	Locations of vulnerable dwellings close to agricultural point-sources or at risk of fluvial flooding	Locations of high person-years of post-flood damp or displacement
Evelyn Cathedrals Fulham Broadway Grange New Cross Newington Riverside Rotherhithe South Bermondsey St. Mary's Park Surrey Docks	Faraday Limehouse New Cross Rotherhithe South Bermondsey	Bromley-by-Bow Church Street East India and Lansbury Faraday Golborne Limehouse Livesey Mile End and Globe Town Newington Queen's Park Palace Riverside Peckham Portoken Rotherhithe Vassall Westbourne	Brixton Hill Bromley-by-Bow Canning Town North East India and Lansbury Evelyn Faraday Herne Hill Kensal Green Livesey Mile End and Globe Town Mile End East Munster Newington Nunhead Palace Riverside Peckham Queenstown Regent's Park South Bermondsey Telegraph Hill Tulse Hill	Livesey Rotherhithe St. Katherine's and Wapping Surrey Docks

Table 11.3: Areas of heightened vulnerability.

11.4.1 Spatial Distribution of Comparative Dwelling Drying Behaviour

By comparing the drying time of dwellings flooded to the same height and drying under the same conditions, it was possible to demonstrate the vulnerability of local areas to prolonged damp following flooding based on the most commonly occurring dwelling types.

The mould species analysed showed a greater potential for long-term contamination in flooded dwellings in the East of the research area, alongside the Thames. The London Borough of Southwark was found to be particularly vulnerable to long-term mould growth following flooding. As had been observed in Chapter 10, *A. versicolor* remained a risk across the research area for longer than *S. chartarum*.

The bacterial species modelled were found to pose a prolonged risk to areas in the East as well, with the exception of *Salmonella*, which has a more strongly temperature-dependent decay rate than *Listeria* and *E. coli*. In this case, the opposite was true and properties in the West were found to be more vulnerable to prolonged *Salmonella* contamination. For *E. coli* and *Salmonella*, there was little difference in the drying rates according to the dwelling archetype, meaning that bacterial models did not show the variation in drying times exhibited by the mould models, and the areas mapped to be at-risk did not have a major difference in drying times. In addition, the small difference in drying times between dwelling types, and the small difference between drying times of flood heights, meant that depth-drying curves were not developed to describe the drying behaviour of different dwelling archetypes for bacterial contaminants.

This information can help identify locations vulnerable to a flood event, without modelling a specific flooding scenario, and is relevant to insurance organisations, remediation organisations, and

government officials responsible for disaster response. While the maps are for specific microbial species following a flood, the comparative drying behaviour mapped can be generalised to inform the potential for contamination of a range of moisture-dependent flood-borne contaminants.

11.4.2 Dwelling Drying Behaviour for Specific Flood Events

The predictions of vulnerable locations within the research area using depth-drying curves and the 1-in-200 year tidal flooding scenario provided predictions consistent with the comparative drying rate observations, with the East of the research area around the Thames identified as being particularly vulnerable to mould contamination. The developed curves can be applied to other flood depth models in the future for other specific flooding scenarios, provided there is sufficient coverage of housing stock data with known archetypes.

The depth-drying curves developed from the simulation data are best-estimates based on the simulation results, and are not definitive values. These curves can be applied to estimate the drying duration for periods up to one year, and in some cases can be used to extrapolate the drying time for longer periods when simulation results show some degree of decline in contamination levels within the simulation period. In the case of modern purpose-built flats with brick/AAC walls flooded to 2.0m, there was minimal decline in the contamination levels over the period of 1 year. The extrapolated results for the 2.0m flood were sense-checked in order to determine that a reasonable value was predicted relative to the drying performance of other archetypes, but the results for this archetype may not be as accurate as for the others.

The curves are only valid for heights above 0.1m and below 2.0m. Attempts to fit curves through 0.0m for unflooded properties produced unstable models, and were therefore not incorporated. For all properties flooded above 0.0m but below 0.1m, the assumption is that the floor would be made wet, meaning that the total surface area of the flooded dwelling at risk of mould growth would not differ significantly from the 0.1m flood height (excluding only the surface area of the walls); the implication here is that this is likely to offer a good estimate of the drying times of smaller floods.

The depth-damage curves modelled based on the simulation data are applicable to the scenarios used in the building simulation - namely, a 24 hour flood with freshwater. In mapping the response of the housing stock to a specific flood event, a large-scale tidal flood has been used to determine the water depth. The 1-in-200 year tidal flood was used rather than any of the freshwater flooding scenarios, as it allowed for the demonstration of the drying ability across a wide range of the London housing stock due to its widespread effects. Since tidal floods will contain salts, it is likely that drying will take longer than the simulation results suggest. Nonetheless, the maps produced provide an indication of the relative drying abilities of the different COAs following a flood. For floods over 24 hours in length, more water may be absorbed into the building fabric. For many of the modelled cases (Solid 9" Brick Walls, Brick Cavity Walls, Concrete), the walls reach capillary saturation within

24 hours and no further water is absorbed, meaning the additional duration of the flood will not impact on the drying time. For walls containing AAC, the longer duration will allow more water to move into the material. This will result in the already slow-drying AAC and insulated AAC walls taking even longer to dry, since there is a greater amount of water to remove from the fabric. Consequently, a longer flood duration will result in the already at-risk areas becoming more at-risk while the low-risk areas will remain the same.

The depth-drying curves also assume that the ground floor is at the same height as the surrounding terrain, meaning that basements and subfloors are not considered. It is difficult to estimate the ground floor level of dwellings relative to surrounding terrain without conducting individual surveys of dwellings within the research area, however, an EHCS analysis included in the EA Contaminated Land Exposure Assessment (CLEA) model suggests that the rate of basements within properties modelled in this study is low (0 - 7.8% depending on archetype) [83]. As housing stock models improve, it may be possible to refine the model further to account for basements.

The likelihood of a flood event occurring which matches the extent and depth predicted by the risk models is unlikely, as flood models predict areas at risk, but that may not necessarily experience flooding. However, as flood risk models can identify vulnerable properties within a location, depth-drying curves can be used to identify vulnerable properties similar to how depth-damage curves can be used to predict the cost of damage to a specific property, given a flood event. The curves may also be applied retrospectively to predict the instantaneous risk inside properties which have been abandoned following a flood event, to provide information to occupants and remediation staff entering these properties for the first time after a flood.

11.4.3 Social Vulnerability and Dwelling Drying Behaviour

The results of the SFVI indicate that the most vulnerable populations live in Southwark, Newham, and in the North West of the research area in Brent and Westminster. The SFVI has been developed to determine the relative vulnerability of populations to health problems following a flood event. As has been noted in Chapter 4, there are a number of different potential health consequences following flooding, including exposure to microorganisms and mental health issues caused by the trauma of a flood event and potential displacement from homes. By identifying areas where both populations are vulnerable to flooding and dwellings are susceptible to long-term damp and microbial contamination, it is possible to predict locations that may have an increased health risk to the resident population. This is particularly relevant when considering health issues caused by long-term exposure to contaminants in the indoor environment, or the length of time that an inhabitant is displaced from their property, which will both be related to the drying behaviour of their dwelling.

As mentioned in the discussion of Chapter 10, the slow-drying dwelling archetypes were post-war and modern purpose-built flats, which may be the types of properties occupied by more socially

vulnerable individuals. There was no correlation observed between COAs with high SFVI values and those with a large number of comparatively difficult to dry dwellings. Nonetheless, the type of property an individual occupies may be a factor in their vulnerability to long-term health problems following a flood event, and deserves further research.

The SFVI applied was developed following research into different flood events across the UK, and so is likely to offer reasonable insights into the behaviour of the London population. However, the London population may differ from the research population for many of the metrics used to calculate the SFVI index - for example, non-car owners will be more prevalent in London than in other areas of the UK. The differences in the population statistics and behaviour may mean that the models estimate a higher vulnerability across the research area than may actually exist.

11.4.4 Contaminant Sources and Dwelling Drying Behaviour

The proximity to contaminant sources offers a rough estimate of the areas that may be at risk from contamination from agricultural or fluvial sources. The fluvial risk map used provides an estimate of the area at risk for flooding under a 1-in-100 year scenario, and so is a realistic representation of at-risk areas. The estimate of the areas at risk from agricultural contaminants used a nominal radius from the centre of the contaminant source, and so acts as a very rough guide of vulnerable locations. This can be improved upon in future analyses by including hydrological models in the GIS analysis to better estimate the flow direction and sink accumulation of floodwater around potential agricultural contaminant point sources.

There is little large-scale agriculture within the research area, but there are many small local areas of privately-held land dedicated to growing plants or raising animals. One of the most common land uses identified in the research area that could pose a risk of contamination were allotments, which may have elevated bacterial levels due to the use of manure-based fertiliser. Other point sources of contamination, such as sewage outflows into the river Thames would have been useful to model, but such data was not made available for this project.

There are a number of microbial contaminants which may be present in fluvial or agricultural floods, of which *E. coli*, *Salmonella*, and *Listeria* represent only a small sample. While these bacteria were selected due to their relevance to urban flood events and their differing decay behaviour under drying scenarios, they do not represent the full picture of all possible contaminants which may be present, nor the potential for prolonged contamination in dwellings due to communalistic microbial behaviour, such as the formation of biofilms on indoor surfaces. However, these maps are useful indicators of areas that exhibit a comparatively prolonged contamination risk for typical flood-borne bacteria from fluvial and agricultural sources, and their risk of flooding from such sources.

11.4.5 Highly Vulnerable Areas

Areas where the absolute drying time and the exposed population were high resulted in high person-years of exposure to damp dwellings or long-term displacement. The hardest affected borough is Southwark, with Hammersmith and Fulham and Lambeth both showing high numbers of person-years of impact following the 1-in-200 year flood event. Person-years provides a simple indication of the level of exposure to either displacement or damp indoor conditions, and further analysis by epidemiologists may shed light on the health consequences across the research area. The person-years calculated may also help plan the disaster response by providing an indication of the numbers and duration of alternative accommodation necessary to prevent inhabitants remaining in unfit homes.

There were a number of locations where the vulnerability of the local housing stock coincided with locations that were at flood risk, where the population was vulnerable, and had a proximity to a potential contaminant source. Wards such as Livesey, Rotherhithe, and South Bermondsey were vulnerable for multiple reasons, and so should be given priority during long-term flood response planning. This may include taking additional measures to ensure that the local population is provided with alternative accommodation rapidly, and that mental health services are made available to those affected by a flood event. Special measures should also be taken to remediate the properties, ensuring that surfaces are cleaned with an appropriate disinfectant, and that dwellings are monitored so that building surfaces, including the core of the walls, return to an adequately dry level to prevent microbial growth from recurring.

Highly vulnerable properties include those built and administered by Local Authorities as low-income housing. The information produced by this research will enable Local Authorities to better plan the recovery and remediation of council-owned flats in order to prevent major health problems among residents.

11.4.6 Limitations

As discussed in Chapter 7, there were limits to the amount of housing stock data available across the research area. Areal information on drying times was estimated only from the numbers of known dwelling types within the areal units, and unmodelled archetypes were ignored in the spatial mapping of the vulnerability of areas of London. By using the modal wall built forms and wall types within the COAs to estimate the comparative drying time, the results provide an indication of the majority built form, age, and wall type combination within the area. This ignores the variation of the housing stock within the areal units, which is unlikely to be consistently of the same type, but is not vulnerable to skewing from properties that take an extended period to dry. The average dwelling time was calculated when mapping the absolute drying time using the depth-damage curves. The number of known and modelled properties within a COA will influence the uncertainty of the estimate of the drying times for both modal and average calculations, and can be improved as

housing stock information becomes more complete. The depth-drying curves of different dwellings can also be improved on by developing models for different dwelling archetypes, archetypes with minority wall types, and those drying under different scenarios. When mapping, all dwellings with cavity wall insulation were assumed to have glass fibre insulation, representing a worst-case scenario [97]. Information on the type of insulation in individual properties is held by HEED, but it was not made available for this research; therefore, by using the results for glass fibre rather than solid insulation, the model is able to account for one of the worst performing insulation types possible in flooded dwellings.

The ecological fallacy is a misinterpretation of statistical data arising from the assumption that individual members of a population have the average characteristics of the population as a whole. The values presented in the areal units represent the drying time and vulnerability levels to flooding of all the dwellings within this area, and it would be unreasonable to conclude that these values apply to any individual unit within the area. The drying behaviour of any individual property would be better estimated using the drying curves derived from the simulations, keeping in mind that the simulations represent a best-estimate of what has occurred inside the dwelling.

Both the comparative and absolute drying predictions make assumptions about the built form and wall type within the properties, which may not provide a precise estimate of the contaminant load and drying time within specific properties in relation to variations in dwelling geometry and fabric.

In mapping, the Modifiable Areal Unit Problem (MAUP) occurs when point-based phenomena is aggregated into areas. The areal values are heavily influenced by the 'modifiable' boundaries of the areas which can, in the UK for example, be reported in terms of COAs, Postcode Areas, Medium Level Census Output Areas, Local Authorities, Boroughs, and so on. By adjusting the boundaries, the areal value can change, and the interpretation of the map can change. By calculating areal statistics based on individual properties within areal units, the MAUP needs to be recognised. COAs were used as boundaries since they are the smallest units available with census and HEED data, and because of the very local variations in housing stock and flood risk and depth. Using larger areal units may change the conclusions of the study, as the differences between areas may average out.

Despite the assumptions and limitations of the research, the results present a useful prediction of the vulnerability of the London domestic housing stock to flooding, and when combined with other flood-risk factors, a useful picture of the potential chronic problems following a flood event can be obtained.

11.5 Conclusions

Application of the simulation results to the GIS-based housing stock data has revealed areas of London where the housing stock will be particularly prone to long-term contamination risk following flooding. Many of these areas at risk of prolonged contamination also lie in areas at risk of flooding, where the population may be more numerous or vulnerable, or where there may be the potential for elevated contamination in the water. In particular, due to the combination of dwelling types, flood risk and depth, social vulnerability, and population density, the London Borough of Southwark is predicted to be at particular risk following a large flood event. Understanding these vulnerable locations can help to plan the response of the health authorities, emergency services, remediation organisations, and local authorities to a flood event. While the immediate response to flooding will depend on those hit hardest at the time of the flood, the long-term response should consider the vulnerability of the population and the dwellings they inhabit in order to best manage the allocation of health resources, the remediation of properties, and the provision of temporary accommodation for victims.

Part V

Conclusions

Chapter 12

Conclusions and Future Work

The basis of this research is that the growth or survival of microorganisms on building surfaces will be dependent on how long the environmental conditions on the surfaces remain hospitable, and that the drying rate and environmental conditions on building surfaces are likely to vary due to the building envelope and built form characteristics. As the distribution of dwellings and population profiles varies geographically across London, it is also assumed that different areas would be at greater risk of long-term damp or displacement following a flood event.

In order to examine this further a number of research objectives were set:

- To review the historical, present, and future flood risks to London, and to describe the current opinions in flood prevention, response, and remediation.
- To review the existing knowledge of the health risks to dwelling occupants associated with microbial contamination in flooded and damp indoor environments.
- To describe the survival of contaminating microbial species on flooded indoor environments by using microbiological laboratory techniques to ascertain how drying conditions, water quality, and material drying characteristics impact on the decay rate of contaminating bacteria.
- To create a model describing how transient temperature and water conditions can affect the survival of contaminating species.
- To create a housing stock model which describes London dwelling archetypes with the information necessary to simulate the heat and moisture performance of the archetypes following flooding, to calculate flood depths at the individual dwelling level, and to map the results.
- To assess the suitability of different building simulation models for flood modelling, and validate a model for this purpose.
- To simulate the drying of typical London dwelling archetypes using building simulation models to examine the drying behaviour of these dwellings under different flooding and drying scenarios.

- To use simulation results alongside existing and novel microbial models in order to describe the duration of microbial risk inside dwelling archetypes.
- To use maps to visualise the geospatial variation of dwelling archetypes throughout the London research area in terms of their drying characteristics, and to use this data to predict the areas most at risk from long-term health issues, displacement, or social vulnerability following a flood event.

By combining microbiological laboratory work, microbial modelling techniques, housing stock development, building simulation, and GIS, these research objectives have been met. The results of this research is manifest in a series of models which can be applied to predict the microbial decay on flooded building surfaces, the drying behaviour of flooded dwellings, and the regions at increased risk due to the poor drying behaviour of the dwellings. Individually, the microbial model can be used to predict the duration of risk on building surfaces as they dry following a flood, while the building simulation model can simulate the effects of different drying measures to determine how different structures dry. Collectively, this tool can help health authorities and remediation organisations plan for post-flood recovery and displacement of a population.

There are a number of useful research outcomes and novel contributions stemming from this work, which can be used to develop recommendations for flood restoration and emergency planners in London. This research also provides a platform for future studies into flood resiliency and recovery.

12.1 Summary of Research Outcomes

The research outcomes of this work can be used to inform and predict the consequences of flooding from microbial to whole-city scale. The research outcomes include:

1. Microbiological outcomes

   (a) The survival of bacterial species on building surfaces following a flood is dependent on surrounding environmental conditions, including temperature, RH, and nutrient content of floodwater. The speed of drying is critical to human and opportunistic pathogen survival, as a faster reduction of RH makes the conditions less hospitable. The type of floodwater also plays an important role in the survival of bacteria, with the decay rate of species on sewage-flooded materials slower than in those flooded with distilled water. At high temperatures and with the rate of material surface drying restricted due to a lack of ventilation, growth of the human pathogenic bacteria can be observed. This outcome has implications for professional remediation services, where industrial heaters can be used to raise the internal temperature to accelerate drying.

(b) The temperature and RH-dependent decay rate of bacteria on building surfaces means that tertiary microbiological models are ideal for describing the decline of risk inside properties. A novel predictive microbiological model has been developed to describe the decay of bacteria on drying surfaces.

2. Built Environment Outcomes

(a) Different building fabrics and built forms found in typical UK dwellings exhibit a wide range of drying times once they are flooded. Certain combinations of built form and fabric can remain at risk of mould growth for long periods of time once flooded, particularly purpose built flats with cavity walls containing glass fibre insulation and AAC inner leafs. Solid concrete floors were found to dry more slowly than suspended wooden floors, while internal AAC walls dried slower than internal brick walls.

(b) The built form of typical UK properties can affect the drying speed by limiting the ventilation of the dwelling, thus preventing an exchange of damp internal air with dry external air. Built form impacts on the ability of dwellings to dry with natural ventilation by restricting window size and cross ventilation potential, as well as the surfaces of the walls exposed to dry outside air. For sealed and abandoned properties, walls with reduced permeability, and dwellings with a smaller externally-exposed surface area will dry more slowly due to less ventilation potential, which means that the risk of microbial contamination will persist longer. For all properties, rooms dry out at a rate dependent on the availability of fresh outdoor air and heat, implying that rooms without direct access to dry outdoor air (for example, through windows) or heat sources (for example, central heating) dry at a slower rate.

(c) The drying scenario has a significant impact on the drying rate. In the event that professional restoration is not immediately available, opening windows and turning on the central heating provides the best option for reducing contamination risk. Leaving a property abandoned with all windows and doors sealed is the worst possible option for repairing the house and making it habitable once again. Those who choose to remain inside their flooded dwellings should make every effort to ventilate the property as much as possible to allow for drying.

(d) Properties dry fastest with high levels of ventilation and heating. Using high-powered heaters quickly dries the internal surfaces of the rooms where the heater is located compared to natural ventilation with or without central heating, however, a single 56kW heater used with open windows may not dry a larger property effectively due to hot air not moving to other flooded rooms within the dwelling. Using central heating with open windows can also speed up the drying process, and may provide a better drying option

than an indirect heater, particularly in larger dwellings. Both heating options are likely to consume substantial amounts of energy if used over the long-term.

(e) Surface RH is not necessarily indicative of whether a wall is 'dry', and employing measures to dry the property without ensuring the core of the wall is dry can lead to the return of damp conditions. If the wall is not dry throughout its profile, moisture inside the core of the wall can migrate towards the internal surface over time, leading to the return of damp. This is particularly evident in cases where walls have been dried rapidly, such as when powerful heaters are used over a short period of time. Remediators should drill into the core of the wall to test for damp before declaring a property fully dry.

(f) Moist air can move around a flooded property, and may also migrate to unflooded levels above the ground floor. This moist air can make the surfaces of non-flooded rooms damp and prone to mould growth. Remediators often use surface moisture levels of non-flooded rooms as a reference for the level of moisture typically found within properties, and as a target for the moisture levels of the flooded sections of a dwelling. This may be inappropriate.

(g) The hard-to-dry properties identified by the building simulation suggest that purpose-built flats with insulated or uninsulated brick/AAC walls are hardest to dry. These properties are also among those most likely to be occupied by low income residents who may be unable to leave their properties or properly restore them after a flood event. Easy-to-dry properties include those with solid 9" brick walls and uninsulated brick/brick cavity walls. Dwelling archetypes that are easy to dry include simple terraces (1914-1959), large semi-detached properties (1914-1945), and bungalows (1914-1945).

3. GIS Mapping Outcomes

(a) The most at-risk borough within the research area was Southwark, which may experience flooding of up to 41% of its surface area under the 1-in-200 year tidal flood scenario, thereby affecting 38,100 dwellings and 134,000 residents within the borough.

(b) Analysis of the spatial distribution of comparatively hard-to-dry properties in London suggests that there are an above-average number such properties in the East and South East of the Central London area, including Southwark and Newham.

(c) When mapped against the extent of specific flood scenarios, the wards of Evelyn, Cathedrals, Fulham Broadway, Grange, New Cross, Newington, Riverside, Rotherhithe, South Bermondsey, St. Mary's Park, and Surrey Docks are all areas containing a high number of vulnerable property types. Taking the potential depth of the flood into account, Faraday, Limehouse, New Cross, Rotherhithe, and South Bermondsey may all be particularly vulnerable during a 1-in-200 year tidal flood event.

(d) Wards where both social vulnerability and dwelling vulnerability are high include Bromley-by-Bow, Church Street, East India and Lansbury, Faraday, Golborne, Limehouse, Livesey, Mile End and Globe Town, Newington, Queen's Park, Palace Riverside, Peckham, Portoken, Rotherhithe, Vassall, and Westbourne.

(e) Areas that lie close to agricultural point sources and fluvial flood risk zones that may have a high number of dwellings vulnerable to long-term contamination from *E. coli*, *Salmonella*, or *Listeria* include Brixton Hill, Bromley-by-Bow, Canning Town North, East India and Lansbury, Evelyn, Faraday, Herne Hill, Kensal Green, Livesey, Mile End and Globe Town, Mile End East, Munster, Newington, Nunhead, Palace Riverside, Peckham, Queenstown, Regent's Park, South Bermondsey, Telegraph Hill, and Tulse Hill.

(f) The number of person-years impacted will be worst in the Borough of Southwark. Livesey, Rotherhithe, St. Katherine's and Wapping, and Surrey Docks are particularly vulnerable wards.

(g) Areas that are vulnerable due to all of the factors (social vulnerability, proximity to fluvial or agricultural areas, tidal flood region and depth, and dwelling vulnerability) are Newington, Rotherhithe, and South Bermondsey.

12.2 Recommendations

Based on the research conducted in this thesis, a number of recommendations can be put forward:

1. The decay of bacteria inside a flooded property will depend on the water quality and the drying conditions, meaning that those entering a property should be aware of the source of the floodwater and the conditions that have been present inside the dwelling. Restoring the property using heat should only be done if there is sufficient ventilation in the dwelling, as growth of human pathogenic bacteria may occur.

2. Surfaces may remain contaminated with flood-borne bacteria for an extended period of time, depending on the quality of the floodwater and the drying conditions inside the dwelling. Gloves should be worn when touching contaminated surfaces or objects, and ATP swabs should not be relied upon as indicators of contamination, as they depend on swabbing on a contaminated surface; a positive result does not necessarily indicate contamination with a harmful microorganism, and some microorganisms do not produce ATP. The length of time after which a dwelling is safe will depend on a number of variables; defining a single duration of risk for all dwellings, as has been done in the past, is not appropriate.

3. Studies into the persistence of microorganisms on drying damp surfaces should consider the impact of the hygrothermal material properties, size, and boundary environmental conditions

of the experiments, as these have significant impacts when interpreting the results, and when extrapolating the results to full building constructions.

4. Walls such as glass fibre insulated brick/AAC constructions can offer a high level of thermal insulation, but do not perform well in floods. Modern properties constructed in areas of flood risk should avoid using glass fibre insulations and unsealed AAC in order to meet thermal insulation standards, and should instead use materials more suitable to flood resilience. Care should be taken when examining cavities with fibrous insulation, as these spaces may not have been adequately ventilated, and there may be a greater risk of microbial contamination.

5. High moisture levels in the core of a wall can be present despite the wall surface being dry. Moisture can migrate from the core to the internal surface over time, causing damp to reappear if the core is not sufficiently dry. To ensure the building is dry and will remain dry, the moisture content in the core of walls should be measured and compared against an unflooded surface. As an indication of the normal unflooded moisture content in the walls, the core of a wall in an unflooded level of the property (and above any capillary rise line) should be used rather than on the surface of unflooded location in the building, due to the movement of moist air throughout the building.

6. Built form can have an important impact on drying rate. Physical experiments on the drying ability of building envelope constructions can provide useful information on the comparative drying performance of building surfaces, but such experiments can not account for built-form specific ventilation and airflow patterns that can be determined from whole-building studies.

7. If residents choose to stay in their properties, they should keep all windows open as much as possible in order to ventilate the property, and if possible keep the central heating on. Closing internal doors and external windows and leaving the property may lead to a major microbial infestation inside the dwelling, making the property a health hazard.

8. High-powered heaters may not work well if the hot air they produce is not able to move through the property, and in certain circumstances using the central heating system may offer a faster and cheaper option for drying the property. Heating without appropriate levels of ventilation, however, may increase the microbial risk in properties.

9. Certain locations will be more vulnerable to a flood event, depending on their location, the construction of the dwellings, and the vulnerability of the resident population. Insurance agencies, remediators, and emergency workers should prioritise properties in areas where the population is most vulnerable, and where the properties are slowest to dry (Table 11.3).

10. Councils should plan to respond rapidly with remediation and alternative accommodation in order to prevent residents of vulnerable dwellings from remaining in their homes following a flood. Such dwellings may include post-war and modern purpose-built flats, which take longer to dry out. Person-years analysis of flood events can help to quantify the potential duration of impact arising from a major flood event in terms of exposure to damp indoor environments or displacement.

12.3 Novel Contributions of the Research

The research detailed in this thesis provides new knowledge that can be used to help further our understanding of recovering dwellings and built environments from a major flood event. Novel contributions and work achieved by this research include:

1. A literature review of the potential microbiological contaminants within a flooded property, and the pathways in which they can impact on occupants' health.

   As described in Chapters 2, 3 and 4, and 'Flood Management: Prediction of microbial contamination in large-scale floods in urban environments' published in Environment International.

2. Laboratory results indicating that the growth and survival of human pathogens on flooded surfaces is dependent on the speed with which the materials dry and the type of water involved in the flood event.

   As described in Chapter 5 *and 'The persistence of flood-borne pathogens on building surfaces under drying conditions' published in International Journal of Hygiene and Environmental Health.*

3. A novel microbiological model capable of estimating the microbial load on a building surface, based on outputs from building simulations that provide insights into the risk factors for those living inside or entering the property.

   As described in Chapter 6.

4. A housing stock model that supplements existing dwelling archetypes used in energy modelling with hygrothermal material data in order to calculate the moisture transport within the building fabrics, and which contains information on the types of individual properties within London, the probability of the dwellings having cavity wall insulation, and the height of the property above sea level in a GIS database.

   As described in Chapter 7 *and 'The Simulation of the Post Flood Drying of Dwellings in London' in the Proceedings of the International Conference on Sustainable Built Environments*

5. An EnergyPlus-based model that can be used to simulate the drying of these dwelling archetypes under a range of different drying scenarios, including but not limited to the scenarios modelled in this research.

   As described in Chapter 10 and 'Using building simulation to model the drying of flooded building archetypes' published in the Journal of Building Performance Simulation.

6. A description of the drying behaviour of different dwelling archetypes found in London under different drying scenarios in terms of their microbial risk levels.

   As described in Chapter 10 and 'Using building simulation to model the drying of flooded building archetypes' published in the Journal of Building Performance Simulation.

7. Depth-drying curves which provide an estimate of the surface area within flooded properties that will be prone to mould growth following floods of different heights in abandoned properties.

   As described in Chapter 11 and 'Predicting the duration of microbial risks in flooded urban dwellings using GIS, building simulation, and microbial models' published in Environment International.

8. A GIS-based map showing the location of areas containing a high number of comparatively difficult to dry properties for different contaminants, as well as maps that predict drying times for specific flood events based on the depths of the flood.

   As described in Chapter 11 and 'Predicting the duration of microbial risks in flooded urban dwellings using GIS, building simulation, and microbial models' published in Environment International.

9. Combining predictions on population levels and social vulnerability of inhabitants in areas of London, the proximity of locations to contaminant sources, and the flood risk, and relating this data to the vulnerability of the dwellings in these areas to long-term drying problems.

   As described in Chapter 11 and 'Predicting the duration of microbial risks in flooded urban dwellings using GIS, building simulation, and microbial models' published in Environment International.

The outcomes of this research can be used to help London deal with the chronic health impacts of a major flood event, and plan for an efficient response based on the location, types of properties, and demographics of those affected. By prioritising areas vulnerable to long-term damp following flooding emergency planners, health authorities, remediation organisations, and local councils can better manage the long-term health consequences of a flood event, and plan for alternative accommodation for those most vulnerable.

12.4 Limitations of Research

The limitations in this work have been described in the separate chapters as part of the discussion into the results, however it is worth addressing these limitations as they relate to the final conclusions of the thesis. The Clarke model used to determine the risk of mould growth is limited in that it is derived from experimental data on mould growth on an ideal substrate, and as such will not be representative of the building materials found in typical UK properties, but may provide a realistic estimate of growth on highly-contaminated surfaces. While the model can provide an indication of when conditions reach a point where there is a risk of growth, there is no consideration of the length of time that these conditions need to be present before growth risk occurs, and it does not take into account mould decline and the potential for survival under growth-limiting conditions. Like the Clarke model, the bacterial model has been developed using data obtained from experiments on ideal substrate. Without knowledge of the amount of bacteria deposited on a surface following a flood, nor information on the lowest concentration of bacteria which can pose a risk to humans, a nominal value of 1% of the initial contamination had to be assumed. Despite this, these models provide a useful indicator of the extent and duration of contamination risk within a flooded dwelling.

A lack of housing stock data and the need to make assumptions about the built form, fabrics, and materials is one of the major limitations of this research, as it is for many studies looking at the performance of the domestic building stock. Each of the data sources used to develop the housing stock model has its own set of limitations. The Cities Revealed dataset has been generated through a combination of aerial imagery and drive-by surveys, and classification may be dependent on the opinion of the surveyor. Assumptions about building fabric only considered majority wall types, and materials for the simulations had to be selected from generic materials databases that were not specific to the London housing stock. The impact of this uncertainty in the building fabric and built form on the building simulation results was addressed in the sensitivity analysis of UCL-HAMT. The modelling process was unable to account for salts and sediments, building geometry such as corners, and ventilation in cavity spaces. However, as demonstrated by the comparison between simulation results and physical experiments, simulations for cleanwater floods provided realistic drying results, and future model developments should allow more variables to be considered.

The mapped results contained the uncertainties in the mould models, housing stock model, building simulations as well as the uncertainty in the flood risk map. As models and data availability improve, the extent of this uncertainty can be established further and the maps can be improved to cover areas where there is little housing stock data. Despite these uncertainties, the mapped results are able to provide a useful indication of vulnerability across the research area.

12.5 Future Work

This thesis provides a platform for further research into the drying of flooded properties. Of the potential drying actions taken, this work has only simulated those which the homeowner can easily perform by him or herself (natural ventilation with and without heating), and the extreme remediation responses (abandoned and high-powered heating). There are a number of different techniques that can also be performed by professionals or homeowners with access to this type of equipment, including different types of dehumidification and the introduction of fans. Further work needs to be carried out in order to better understand which are the optimal drying techniques for different types of properties.

Research into the survival of different microorganisms on flooded surfaces would also be beneficial. The mould model employed in this study, for example, has identified the lower boundary of temperature and RH above which there is a risk of mould growth. Once mould growth has established, it is capable of hydrolysing its own moisture sources and surviving in lower humidity conditions. In addition, mould growth can stop but start again rapidly when or if conditions once again become suitable for growth. While the mould model offers a projection of the conditions above which mould growth is possible, it was designed as a tool for mould growth prevention inside dry houses, not as a drying target for flooded properties.

Limited data coverage of the types of properties in London mean that there were significant areas where there was insufficient data coverage to predict the types of properties present. There are a number of more detailed databases of built form – such as the VOC and HEED databases of individual dwellings, but these were not made available for this study. A better understanding of hygrothermal material data for London and UK-specific dwellings would indeed be beneficial.

Finally, this work predicts property types and areas that will suffer from long-term damp due to their construction type, and assumes that dwellings that will take longer to dry pose a greater health risk to occupants through either exposure to damp dwellings, or due to long-term displacement from their property as the dwelling is restored. Comparison of this model with epidemiological data from previous flood events may help validate the assumptions made by this model for major past events, and help to create better projections for future flooding scenarios.

The outcomes of this research have implications for the insurance industry. Flood insurance premiums and terms and conditions reflect the likely flood incidence and severity, as well as the cost of reinstatement. Slow or difficult to dry dwellings in flood-vulnerable areas may face higher insurance premiums, reflecting the extra cost to insurers of remediation. Such dwellings are likely to already have high insurance costs due to flood risk, and the suggestion that these dwellings are more likely to be occupied by low-income residents means that flood insurance or professional restoration becomes unaffordable for some. Future work should enable those in vulnerable existing dwellings

to make their properties more resilient to floodwater at the dwelling and community scale, thereby reducing the insurance costs.

The outcomes from this research can also be used to inform government policy and regulations. Dwellings constructed in flood-vulnerable locations should be built using fast-drying building envelope systems, and have the capability to increase the natural ventilation should a flood occur and active ventilation systems become disabled. Future work specifying requirements for properties in flood-prone areas should be incorporated into building regulations.

Bibliography

[1] F.X. Abad, R. M. Pinto, and A. Bosch. Survival of enteric viruses on environmental fomites. *Applied Environmental Microbiology*, 60(10):3704–3710, 1994.

[2] O.C.G. Adan. *On the fungal defacement of interior finishes*. PhD thesis, Eindhoven University of Technology, Eindhoven, 1994.

[3] A. Adhikari, J. Jung, T. Reponen, J. S. Lewis, E. C. DeGrasse, L. F. Grimsley, G. L. Chew, and S. A. Grinshpun. Aerosolization of fungi, (1->3)-[beta]-d glucan, and endotoxin from flood-affected materials collected in New Orleans homes. *Environmental Research*, 109(3): 215–224, 2009.

[4] T. af Klintberg, G. Johannesson, and F. Bjork. Air gaps in building construction avoiding dampness and mould. *Structural Survey*, 26:242, 2008.

[5] H. Aglan. Field testing of energy-efficient flood-damage-resistant residential envelope systems summary report. Technical Report ORNL/TM-2005/34; TRN: US200617, Oak Ridge National Laboratory (ORNL), 2005.

[6] M. Ahern, R. S. Kovats, P. Wilkinson, R. Few, and F. Matthies. Global health impacts of floods: Epidemiologic evidence. 27(1):36–46, 2005.

[7] M. Airaksinen, J. Kurnitski, P. Pasanen, and O Seppänen. Fungal spore transport through a building structure. *Indoor Air*, 14(2):92, 2004.

[8] E.J. Allen and A. A. Pinney. A set of standard dwellings - details of dimensions, construction, and occupancy schedules. Technical report, Building Research Establishment, 1989.

[9] American Red Cross. Repairing your flooded home. Technical report, American Red Cross, Jessup, MD, 2007.

[10] B. Anderson, A. J. Clark, R. Baldwin, and N. O. Milbank. *BREDEM - BRE Domestic Energy Model: Background, Philosophy and Description*. IHS BRE Press, Watford, UK, 1985.

[11] M. A. Andersson, M. Nikulin, U. Koljalg, M. C. Andersson, F. Rainey, K. Reijula, E. L. Hintikka, and M. Salkinoja-Salonen. Bacteria, molds, and toxins in water-damaged building materials. *Applied Environmental Microbiology*, 63(2):387–393, February 1, 1997.

[12] B. Austin, P. Cheeseman, and C. Maggs. United Kingdom Floods. Technical report, Guy Carpenter, London, UK, 2000.

[13] L. Bachelor. Flood victims face a new problem: their insurers. *The Guardian*, Sunday 9 December 2007.

[14] P.H. Baker, C. Sanders, G.H. Galbraith, and R.C. McLean. *Engineering Historic Futures: Stakeholders Dissemination and Scientific Research Report*, chapter Investigation of wetting and drying behaviour of replica historic wall constructions, pages 73–95. Centre for Sustainable Heritage, University College London, 2007.

[15] J. Baranyi and M.L. Tamplin. Combase: a common database on microbial responses to food environments. *Journal of Food Protection*, 9:1967–1971, 2004.

[16] D.N. Barbeau, L. F. Grimsley, L. E. White, J. M. El-Dahr, and M. Lichtveld. Mold exposure and health effects following Hurricanes Katrina and Rita. *Annual Review of Public Health*, 31 (1):165–178, 2010.

[17] BDMA. Guidelines and standards: Flood recovery guidelines. Webpage, 2007. URL http://www.bdma.org.uk/Technical/Guidelines. Accessed July 5th, 2010.

[18] BDMA. Self help for victims of flooding: what can you do? Technical report, Building Damage Management Association, Mitcham, Surrey, 2007. URL http://www.bdma.org.uk/sites/default/files/fileuploads/admins/BDMA%20SELF%20HELP%20SHEETvbb%2007.pdf. Accessed July 5th, 2010.

[19] BDMA. Understanding basic flood recovery procedures. Technical report, Building Damage Management Association, Mitcham, Surrey, 2007. URL http://www.bdma.org.uk/sites/default/files/fileuploads/admins/BDMA%20Flood%20Recovery%20Inf%201w.pdf. Accessed July 5th, 2010.

[20] B. Bean, B.M. Moore, B. Sterner, L.R. Peterson, D.N. Gerding, and H.H. Balfour. Survival of influenza viruses on environmental surfaces. *The Journal of Infectious Diseases*, 146(1):47–51, 1982.

[21] G. Bennet. Bristol floods 1968: controlled survey of effects on health of local community disaster. *British Medical Journal*, 3(5720):454–458, 1970.

[22] S.G. Berk, R. S. Ting, G. W. Turner, and R. J. Ashburn. Production of respirable vesicles containing live Legionella pneumophila cells by two Acanthamoeba spp. *Applied Environmental Microbiology*, 64(1):279–286, 1998.

[23] L. Binda, G. Cardani, and L. Zanzi. Nondestructive testing evaluation of drying process in flooded full-scale masonry walls. *Journal of Performance of Constructed Facilities*, 24:473–483, 2010.

[24] A.R. Black and S. A. Evans. Flood damage in the UK: New insights for the insurance industry. Technical report, University of Dundee for AON Group Limited and CGU Insurance Plc, Dundee, UK, 1999.

[25] N. Blades, P. Biddulph, M. Cassar, and L. Tuffnell. Modelling of climate change effects on historic buildings. Technical report, UCL Centre for Sustainable Heritage, London, 2004.

[26] N. Blades, I. Ridley, T. Chen, and T. Oreszczyn. Development and use of computer modelling of historic wall constructions. Technical report, UCL Centre for Sustainable Heritage, London, 2007.

[27] P. Blondeau, A. L. Tiffonnet, A. Damian, O. Amiri, and J. L. Molina. Assessment of contaminant diffusivities in building materials from porosimetry tests. *Indoor Air*, 13:310–318, 2003.

[28] R. Blong. A new damage index. *Natural Hazards*, 30:1–23, 2003.

[29] M. Brandt, C. Brown, J. Burkhart, N. Burton, J. Cox-Ganser, S. Damon, H. Falk, S. Fridkin, P. Garbe, M. McGeehin, J. Morgan, E. Page, C. Rao, S. Redd, T. Sinks, D. Trout, K. Wallingford, D. Warnock, and D. Weissman. Mold prevention strategies and possible health effects in the aftermath of hurricanes and major floods. *Morbidity and Mortality Weekly Report*, 55(RR08):1–27, June 2006. URL http://www.cdc.gov/mmwr/preview/mmwrhtml/rr5508a1.htm. Accessed July 10th, 2010.

[30] BRE. Drying out buildings. Technical report, Building Research Establishment, Watford, UK, 1974.

[31] BRE. Repairing flood damage: foundations and walls. Technical report, Building Research Establishment, Watford, UK, 1997.

[32] BRE. Repairing flood damage: ground floors and basements. Technical report, Building Research Establishment, Watford, UK, 1997.

[33] BRE. Repairing flood damage: Immediate action. Technical report, Building Research Establishment, Watford, UK, 1997.

[34] BRE. The government's standard assessment procedure for energy rating of dwellings. Technical report, Building Research Establishment, Watford, UK, 2005.

[35] A.D. Brown. Microbial water stress. *Bacteriology Reviews*, 40:803–846, 1976.

[36] H. Bruckmann and D. Lewis. *New Housing in Great Britain.* Alec Tiranti Ltd., 1960.

[37] BSI. BS EN12524: Building materials and products - Hygrothermal properties - Tabulated design values, 2000.

[38] BSI. PAS 64:2005 - Professional water damage mitigation and initial restoration of domestic dwellings, 2005.

[39] BSI. BS EN ISO 8192:2007 - Water quality - Test for inhibition of oxygen consumption by activated sludge for carbonaceous and ammonium oxidation, 2007.

[40] BSI. BS EN ISO 10456: 2007 - Building materials and products - Hygrothermal properties - Tabulated design values and procedures for determining declared and design values, 2007.

[41] BSI. BS EN ISO 10211:2007 - Thermal bridges in building construction – Heat flows and surface temperatures – Detailed calculations, 2007.

[42] BSI. BS EN15026:2007- Hygrothermal Performance Of Building Components And Building Elements - Assessment Of Moisture Transfer By Numerical Simulation, 2007.

[43] R.K. Bush and J.J. Prochnau. Alternaria-induced asthma. *Journal of Allergy and Clinical Immunology*, 113(2):227–234, 2004.

[44] D.E. Caldwell, D.K. Brannan, M.E. Morris, and M.R. Betlach. Quantitation of microbial growth on surfaces. *Microbial Ecology*, 7(1):1–11, 1981.

[45] C.G. Carll and T.L. Highley. Decay of wood and wood-based products above ground in buildings, mechanism of brown-rot decay: Paradigm or paradox. *Journal of Testing and Evaluation*, 27(2):150–158, 1999.

[46] A. Caro, P. Got, J. Lesne, S. Binard, and B. Baleux. Viability and virulence of experimentally stressed nonculturable Salmonella typhimurium. *Applied and Environmental Microbiology*, 65 (7):3329–3232, 1999.

[47] CDC. Clean up safely after a natural disaster. Webpage, August 31, 2005. URL http://emergency.cdc.gov/disasters/cleanup/facts.asp. Accessed July 6th, 2010.

[48] CDC. Protect yourself from mold. Webpage, 2007. URL http://www.bt.cdc.gov/disasters/mold/protect.asp. Accessed July 4th, 2010.

[49] CDC. Get rid of mold. Webpage, 2010. URL http://emergency.cdc.gov/disasters/pdf/flyer-get-rid-of-mold.pdf. Accessed July 4th, 2010.

[50] CDC. NIOSH recommendations for the cleaning and remediation of flood-contaminated HVAC systems: A guide for building owners and managers. Webpage, January 2010. URL http://www.cdc.gov/niosh/topics/emres/Cleaning-Flood-HVAC.html. Accessed December 15th 2010.

[51] P.K. Chan, R. Y. Sung, K. S. Fung, M. Hui, K. W. Chik, F. A. Adeyemi-Doro, and A. F. Cheng. Epidemiology of respiratory syncytial virus infection among paediatric patients in Hong Kong: A seasonality and disease impact. *Epidemiology and Infection*, 123(2):257, 1999.

[52] P. Chapman. A geometrical model of dwellings for use in simple energy calculations. *Energy and Buildings*, 21:83–92, 1994.

[53] G.L. Chew, J. Wilson, F.A. Rabito, F. Grimsley, S. Iqbal, T. Reponen, M.L. Muilenberg, P.S. Thorne, D.G. Dearborn, and R.L. Morley. Mold and endotoxin levels in the aftermath of Hurricane Katrina: A pilot project of homes in New Orleans undergoing renovation. *Environmental Health Perspectives*, 114(12):1883, 2006.

[54] I. Chown. *Metric Handbook : Planning and Design Data*. Elsevier, Oxford, 1970.

[55] CIRIA. Repair and restoration of buildings following floods. Technical report, Construction Industry Research and Information Association, London, 2002.

[56] CIRIA. Guidance and standards for drying flood damaged buildings. Signposting current guidance: BD 2760. Technical report, Construction Industry Research and Information Association, London, 2010.

[57] J.A. Clarke and P.P. Yaneske. A rational approach to harmonisation of the thermal properties of building materials. *Building and Environment*, 44:2046–2055, 2009.

[58] J.A. Clarke, C.M. Johnstone, N.J. Kelly, R.C. McLean, J.A. Anderson, N.J. Rowan, and J.E. Smith. A technique for the prediction of the conditions leading to mould growth in buildings. *Building and Environment*, 34(1999):515–521, 1998.

[59] D. Clifton. Personal communication: Polygon group. Email, January 2011.

[60] E.C. Cole. *Workshop on Biological Pollutants in the Home*, chapter Remedial measures for biological pollutants in the home. American Lung Association, 1989.

[61] ComBase. Combase modelling toolbox. Webpage, March 2011. URL http://ifrsvwwwdev.ifrn.bbsrc.ac.uk/CombasePMP/GP/. Accessed January 5th, 2011.

[62] Committee on Damp Indoor Spaces and Health. *Damp Indoor Spaces and Health*. The National Academies Press, Washington, D.C., 2004. ISBN 9780309091930. URL http://www.nap.edu/openbook.php?record_id=11011. Accessed April 5th 2011.

[63] D. Crichton. A Scottish lead in managing flood risk. *Town & Country Planning*, 6:188–189, 2001.

[64] K.J. Cummings, J. Cox-Ganser, M.A. Riggs, N. Edwards, G.R. Hobbs, and K. Kreiss. Health effects of exposure to water-damaged New Orleans homes six months after Hurricanes Katrina and Rita. *American Journal of Public Health*, 98(5):869–875, 2008.

[65] L. Curtis, M. Ross, V. Persky, P. Scheff, R. Wadden, V. Ramakrisnan, and D. Hryhorczuk. Bioaerosol concentrations in the Quad Cities 1 year after the 1993 Mississippi River floods. *Indoor and Built Environment*, 9(1):35–43, 2000.

[66] R.E. Dales, H. Zwanenburg, R. Burnett, and C.A. Franklin. Respiratory health effects of home dampness and molds among Canadian children. *American Journal of Epidemiology*, 134(2): 196–203, 1991.

[67] DCLG. Planning Policy Statement 3 (PP3): Housing. Technical report, Department for Communities and Local Government, London, November 2006.

[68] DCLG. Improving the flood performance of new buildings. Technical report, Department for Communities and Local Government, London, May 2007.

[69] DCLG. English Housing Survey 2008: Annual Report. Technical report, Department for Communities and Local Government, London, June 2008.

[70] DCLG. English Housing Survey 2008. Database, June 2008. URL http://www.communities.gov.uk/housing/housingresearch/housingsurveys/englishhousingsurvey/. Accessed October 2nd 2010.

[71] DEFRA. Making space for water: taking forward a new government strategy for flood and coastal erosion risk management in England. Technical report, Department for Environment, Food, and Rural Affairs, London, October 20th, 2004.

[72] DEFRA. Making space for water: Government's first response. Technical report, Department for Environment, Food, and Rural Affairs, London, March 2005.

[73] DEFRA. The government's response to Sir Michael Pitt's Review of the Summer 2007 floods, 2009.

[74] DEFRA. Flooding and coastal change. Report, Department for the Environment, Food, and Rural Affairs, London, UK, 2010.

[75] DEFRA. UK Climate Change Risk Assessment (CCRA). Technical report, Department of Environment, Food, and Rural Affairs, London, February 2012.

[76] DesignBuilder. DesignBuilder Building Simulation Software. Software, 2011.

[77] A.M. Dixon, D. Butler, and A. Fewkes. Guidelines for greywater re-use: Health issues. *Water and Environment Journal*, 13(5):322–326, 1999. ISSN 1747-6593.

[78] G.H. dos Santos, N. Mendes, and P.C. Philippi. A building corner model for hygrothermal performance and mould growth risk analyses. *International Journal of Heat and Mass Transfer*, 52:4862–4872, 2009.

[79] J. Douwes. (1->3)-[beta]-d glucan and respiratory health: a review of the scientific evidence. *Indoor Air*, 15:160–169, 2005.

[80] J. Douwes, R. Siebers, I. Wouters, G. Doekes, P. Fitzharris, and J. Crane. Endotoxin (1->3)-[beta]-d glucans and fungal extra-cellular polysaccharides in New Zealand homes: a pilot study. *Annals of Agricultural and Environmental Medicine*, 13(2):361–365, 2006.

[81] A. Dubosc and G. Escadeillas. Development d'algues microscopiques sur les parements en beton: techniques d'etudes en laboratoire. In *Microbial Impacts on Building Materials*, Sao Paulo, July 2000.

[82] H. Dumon, A. Palot, C. Charpin-Kadouch, J. Quéralt, K. Lehtihet, M. Garans, and D. Charpin. Mold species identified in flooded dwellings. *Aerobiologia*, 25(4):341–344, 2009.

[83] EA. Review of building parameters for development of a soil vapour intrusion model. Technical report, Environment Agency, Bristol, 2005.

[84] EA. After a flood: Practical advise on recovering from a flood. Technical report, Environment Agency, London, 2007.

[85] EA. Thames catchment flood management plan. Technical report, Environment Agency, London, UK, 2009.

[86] EA. What to do before, during and after a flood: Practical advice on what to do to protect yourself and your property. Technical report, Environment Agency, London, November 2010.

[87] EA. 2007 summer floods - Environment Agency - a table showing the approximate number of properties and businesses flooded by Government Office Region. Technical report, Environment Agency, London, 2011.

[88] EA. A history of flooding on the tidal Thames. Webpage, January 2012. URL http://www.environment-agency.gov.uk/homeandleisure/floods/117047.aspx. Accessed November 5th 2011.

[89] ECI. 40 percent house. Technical report, Environmental Change Institute, Oxford, 2005.

[90] J.H. Edwards, A.J. Griffiths, and J. Mullins. Protozoa as sources of antigen in humidifier fever. *Nature*, 264(5585):438–439, 1976.

[91] K. Elke, J. Bergerow, H. Operman, U. Krämer, E. Jermann, and L. Dunemann. Determination of selected microbial volatile organic compounds by diffusive sampling and dual-column capillary GC-FID-a new feasible approach for the detection of an exposure to indoor mould fungi. *Journal of Environmental Monitoring*, 1(5):445, 1999.

[92] J.B. Ellis and W. Yu. Bacteriology of urban runoff: the combined sewer as a bacterial reactor and generator. *Water Science Technology*, 31(7):303–310, 1995.

[93] S. Emmitt. *Barry's Introduction to Construction of Buildings*. Wiley-Blackwell, London, 2010.

[94] EnergyPlus. Getting started with EnergyPlus. Technical report, US Department of Energy, Berkeley, CA, April 20th, 2008.

[95] EPA. Improved enumeration methods for the recreational water quality indicators: Enterococci and Escherichia coli. Technical report, U.S. Environmental Protection Agency, Washington, DC, 2000.

[96] EPA. Flood cleanup and the air in your home. Technical report, Environment Protection Agency, Washington, DC, 2007.

[97] M. Escarameia, A. Karanxha, and A. Tagg. Quantifying the flood resilience properties of walls in typical UK dwellings. *Building Services Engineering Research and Technology*, 28(3): 249–263, August 1, 2007.

[98] M.P. Fabian, S.L. Miller, T. Reponen, and M.T. Hernandez. Ambient bioaerosol indices for indoor air quality assessments of flood reclamation. *Aerosol Science*, 36(2005):763–783, 2005.

[99] M. Fedeski and J. Gwilliam. Urban sustainability in the presence of flood and geological hazards: The development of a GIS-based vulnerability and risk assessment methodology. *Landscape and Urban Planning*, 83(1):50–61, 2007.

[100] FEMA. Initial restoration for flooded buildings. Technical report, Federal Emergency Management Agency, Washington, DC, November 2006.

[101] F. Kovats S. Few, R. Ahern. M. Matthies. Floods, health, and climate change: a strategic review. Technical report, Tyndall Centre for Climate Change, 2004.

[102] L. Fewtrell and D. Kay. An attempt to quantify the health impacts of flooding in the UK using an urban case study. *Public Health*, 122(5):446 – 451, 2008. ISSN 0033-3506.

[103] L.K. Fewtrell, K. Smith, and D. Kay. *Flood Risk Science and Management*, chapter Assessment of Infection Risks Due to Urban Flooding, pages 429–441. Wiley-Blackwell, London, UK, 2010.

[104] J. Fidler, C. Wood, and B. Ridout. Flooding and historic buildings. Technical report, English Heritage, London, UK, 2004.

[105] J.N. Fink. *Allergy Principles and Practice*, chapter Hypersensitivity Pneumonitis. C.V. Mosby, St Louis, 1992.

[106] Flood Repairs Forum. Repairing flooded buildings: An insurance industry guide to investigation and repair. Technical report, Flood Repairs Forum, Watford, 2006.

[107] S. Garvin, J. Reid, and M. Scott. Standards for the repair of buildings following flooding. Technical report, CIRIA, London, 2005.

[108] C.C. Gaylarde and P.M. Gaylarde. Biodeterioration of historic buildings in Latin America. In *9th International Conference on Durability of Materials and Components*, Rotterdam, Netherlands, 2002.

[109] C.C. Gaylarde and L.H.G. Morton. Deteriogenic biofilms on buildings and their control: A review. *Biofouling*, 14(1):59–74, 1999.

[110] S. Geving. A systematic method for hygrothermal analysis of building constructions using computer models. In *6th IBPSA Conference*, pages 355–361, Prague, Czech Republic, 1997. International Building Performance Simulation Association.

[111] S. Gill, S. Pauleit, A.R. Ennos, S.J. Lindley, J.F. Handley, J. Gwilliam, and A. Ueberjahn-Tritta. Literature review: Impacts of climate change on urban environments. Technical report, Centre for Urban and Regional Ecology, The University of Manchester, Manchester, 2004.

[112] GLA. Climate Change Adaptaion Strategy. Report, Greater London Authority, London, UK, 2009.

[113] R.L. Gorny, T. Reponen, S.A. Grinshpun, and K. Willeke. Source strength of fungal spore aerosolization from moldy building material. *Atmospheric Environment*, 35(28):4853–4862, 2001.

[114] C. Grant, C.A. Hunter, B. Flannigan, and A.F. Bravery. The moisture requirements of moulds isolated from domestic dwellings. *International Biodeterioration and Biodegradation*, 25(4): 259–284, 1989.

[115] S. Gravesen, P.A. Nielsen, R. Iversen, and K.F. Nielsen. Microfungal contamination of damp buildings: Examples of risk constructions and risk materials. *Environmental Health Perspectives*, 107(3):505–508, 1999.

[116] L. Greenspan. Humidity fixed points of binary saturated aqueous solutions. *Journal of Research of the National Bureau of Standards - A. Physics and Chemistry*, 81A:89–96, 1976.

[117] J. Grunewald. Numerical simulation program DIM3.1 for coupled heat, air, salt, and moisture transport. In *10th International Symposium for Building Physics*, pages 181–191, Dresden, Germany, 1999.

[118] J. Grunewald and R. Plagge. Rechnerische bewertung von trocknungsverfahren für hochwassergeschädigtes mauerwerk. *Bauphysik*, 28 (2):88–95, 2006.

[119] R. Grunewald, J. Plagge. Optimal drying of flooded brickwork masonry. In *7th symposium on Building Physics in the Nordic Countries*, Reykjavík, Iceland, June 13-15th 2005.

[120] O. Guillitte. Bioreceptivity: a new concept for building ecology studies. *Science of The Total Environment*, 167:215–220, 1995.

[121] R.J. Gummerson, C. Hall, and W.D. Hoff. Capillary water transport in masonry structures: Building construction applications of Darcy's Law. *Construction Papers*, pt1:17–27, 1980.

[122] B. Gutarowska and M. Piotrowska. Methods of mycological analysis in buildings. *Building and Environment*, 42(4):1843–1850, 2007.

[123] F. Gyntelberg, P. Suadicani, J.W. Nielsen, P. Skov, O. Valbjørn, P.A. Nielsen, T. Schneider, O. Jørgensen, P. Wolkoff, C.K. Wilkins, S. Gravesen, and S. Norn. Dust and the sick building syndrome. *Indoor Air*, 4(4):223–238, 1994.

[124] C-E. Hagentoft, A.S. Kalagasidis, B. Adl-Zarrabi, S. Roels, J. Carmeliet, H. Hens, J. Grunewald, M. Funk, R. Becker, D. Shamr, O. Adan, H. Brocken, K. Kumaran, and R. Djebbar. Assessment method of numerical prediction models for combined heat, air and moisture transfer in building components: Benchmarks for one-dimensional cases. Technical report, HAMSTAD Project, 2002.

[125] Halcrow. Hungary flood control development and rehabilitation project final report. Technical report, Middlesex University Flood Hazard Research Centre, Swindon 1999.

[126] C. Hall. Barrier performance of concrete: A review of fluid transport theory. *Materials and Structures*, 27 (5):291–306, 1994.

[127] C. Hall and W.D. Hoff. *Water Transport in Brick, Stone, and Concrete.* Taylor & Francis, London, 2002.

[128] C. Hall, W.D. Hoff, and M.R. Nixon. Water movement in porous building materials vi. evaporation and drying in brick and block materials. *Building and Environment*, 19:13–20, 1984.

[129] B.D. Hardin, B.J. Kelman, and A. Saxon. Adverse human health effects associated with molds in the indoor environment. *Journal of Occupational Environmental Medicine*, 45(5):470–478, 2003.

[130] HEED. Homes Energy Efficiency Database. Database, 2009. URL http://www.energysavingtrust.org.uk/Professional-resources/Existing-Housing/Homes-Energy-Efficiency-Database. Accessed November 15th 2009.

[131] M. Heikkinen, M. Hjelmroos-Koski, M. Haggblom, and J. Macher. *Aerosols Handbook*, chapter Bioaerosols. CRC Press, 2005.

[132] H. Hens. Final Report Task 1: Modelling Common Exercises. Summary Reports Annex 24, Heat Air and Moisture Transfer in Insulated Envelope Parts. Technical report, International Energy Agency, 1996.

[133] L.G. Hersoug. Viruses as the causative agent related to dampness and the missing link between allergen exposure and onset of allergic disease. *Indoor Air*, 15(5):363, 2005.

[134] M-R. Hirvonen, A. Nevalainen, N. Makkonen, J. Mönkkönen, and K. Savolainen. Streptomyces spores from mouldy houses induce nitric oxide, TNF[alpha] and il-6 secretion from RAW264.7 macrophage cell line without causing subsequent cell death. *Environmental Toxicology and Pharmacology*, 3(1):57–63, 1997.

[135] D.W.S. Ho and G.J. Chirgwin. A performance specification for durable concrete. *Construction and Building Materials*, 10(5):375–379, 1996.

[136] S. Hokoi and M.K. Kumaran. Experimental and analytical investigations of simultaneous heat and moisture transport through glass fibre insulation. *Journal of Thermal Insulation and Building Envelopes*, 16:263–292, 1993.

[137] P.A. Holden, L.J. Halverson, and M.K. Firestone. Water stress effects on toluene biodegradation by Pseudomonas putida. *Biodegradation*, 8(3):143–151, 1997.

[138] A. Holm. Drying of an AAC flat roof in different climates. computational sensitivity analysis versus material property measurements. In *CIB W40*, Wellington, NZ, April 2001.

[139] K. Holm, A. Lengsfeld. Moisture-buffering effect - experimental investigations and validation. In *Buildings X Conference, Thermal Performance of the Exterior Envelopes of Whole Buildings*, Clearwater Beach, FL, USA, 2007.

[140] A. Hopkins, A. Lekov, J. Lutz, G. Rosenquist, and L. Gu. Simulating a nationally representative housing sample using EnergyPlus. Technical report, Ernest Orlando Lawrence Berkeley National Laboratory, 2011.

[141] M. Hoppert, A. Kemmling, and M. Kämper. Microbial biofilms on building stone. In *EGS - AGU - EUG Joint Assembly*, Nice, 2003.

[142] HPA. Flooding. Webpage, 2008. URL http://www.hpa.org.uk/flooding. Accessed July 5th, 2010.

[143] HPA. Health advice - how to clean up safely following floods. Webpage, 2009. URL http://www.hpa.org.uk/webc/HPAwebFile/HPAweb_C/1194947420817. Accessed July 5th, 2010.

[144] Hull City Council. Two years on - 2009. Technical report, Hull City Council, 2009.

[145] P. Häupl, H. Fechner, and H. Petzold. Interior retrofit of a masonry wall to reduce energy and eliminate moisture damages: Comparison of modeling and field performance. In *Proceedings Buildings IX Conference*, Clearwater Beach, Florida, 2004. ASHRAE Publisher.

[146] K. Huttunen, A. Hyvärinen, A. Nevalainen, H. Komulainen, and M.-R. Hirvonen. Production of proinflammatory mediators by indoor air bacteria and fungal spores in mouse and human cell lines. *Environmental Health Perspectives*, 111(1):85, 2003.

[147] K. Huttunen, J. Pelkonen, K. F. Nielsen, U. Nuutinen, J. Jussila, and M.-R. Hirvonen. Synergistic interaction in simultaneous exposure to Streptomyces californicus and Stachybotrys chartarum. *Environmental Health Perspectives*, 112(6):659–665, 2004.

[148] A. Hyvärinen, T. Meklin, A. Vepsäläinen, and A. Nevalainen. Fungi and actinobacteria in moisture-damaged building materials - concentrations and diversity. *International Biodeterioration and Biodegradation*, 49:27–37, 2002.

[149] IBP. WUFI-2D, PC-Program for calculating the coupled heat and moisture transfer in building components. Software, 2007. URL http://www.wufi.de/index_e.html.

[150] ICE. Learning to live with rivers. Final report of the Institution of Civil Engineers' presidential commission to review the technical aspects of flood risk management in England and Wales. Technical report, Institute of Civil Engineers, London, 2001.

[151] IFH. Coping with floods, cleaning up afterwards – and staying healthy. Technical report, International Scientific Forum on Home Hygiene, London, UK, 2007.

[152] IFRC. World Disasters Report 2010: Focus on Urban Risk. Technical report, International Federation of Red Cross and Red Crescent Societies, Geneva, Switzerland, 2010.

[153] IKSR. Übersichtskarten der überschwemmungsgefährdung und der möglichen vermögensschäden am rhein. Technical report, Kommission zum Schutz des Rheines (IKSR), 2001.

[154] Institute of Inspection Cleaning and Restoration Certification. S520 standard and reference guide for professional mold remediation, 2003.

[155] Institute of Inspection Cleaning and Restoration Certification. S500 standard and reference guide for professional water damage restoration, 2006.

[156] IPCC. Impacts, Adaptation, and Vulnerability - Contribution of Working Group II to the Fourth Assessment Report of the Intergovernmental Panel on Climate Change. Technical report, Intergovernmental Panel on Climate Change, Cambridge, 2007.

[157] B.B. Jarvis and J.D Miller. Mycotoxins as harmful indoor air contaminants. *Applied Microbiology and Biotechnology*, 66(4):367–372, 2005.

[158] F. Jensen. *The English Semi-detached House*. Ovolo Publishing, Cambridge, 2007.

[159] P. Jones, J. Patterson, and S. Lannon. Modelling the built environment at an urban scale – Energy and health impacts in relation to housing. *Landscape and Urban Planning*, 83(1): 39–49, 2007.

[160] R. Judkoff and J. Neymark. Building energy simulation test (BESTEST) and diagnostic method. Technical Report NREL/TP-472-6231, National Renewable Energy Laboratory, Golden, CO., 1995.

[161] M.A. Kavgic, A. Mavrogianni, D. Mumovic, A. Summerfield, Z. Stevanovic, and M. Djurovic-Petrovic. A review of bottom-up building stock models for energy consumption in the residential sector. *Building and Environment*, 45(7):1683–1697, 2010.

[162] I. Kelman. *Physical Flood Vulnerability of Residential Properties in Coastal, Eastern England*. PhD thesis, University of Cambridge, September 2002.

[163] B. Kidd, A. Tagg, M. Escarameia, B. von Christierson, J. Lamond, and D. Proverbs. Project: Guidance and standards for drying flood damaged buildings. Technical report, Communities and Local Government, London, 2010.

[164] D. King. Climate change science: Adapt, mitigate, or ignore? *Science*, 303:176–177, 2004.

[165] J. Klaus and R. F. Schmidtke. Bewertungsgutachten fur deichbauvorhaben an der festlandskuste - modellgebiet wesermarsch. Technical report, Untersuchungsbericht an den Bundesminister fur Ernahrung, Landwirtschaft und Forsten, 1990.

[166] H. Künzel, A. Holm, and M. Krus. Hygrothermal properties and behaviour of concrete. *WTA Almanach 2008*, pages 161–181, 2008.

[167] H.M Künzel. *Simultaneous Heat and Moisture Transport in Building Components.* PhD thesis, Fraunhofer Institute for Building Physics, Holzkirchen, 1995.

[168] H.M. Künzel. Moisture risk assessment of roof constructions by computer simulation in comparison to the standard glaser method, September 18-21, 2000.

[169] M. Kok, H.J. Huizinga, A.C.W.M. Vrouwenfelder, and A. Barendregt. Standard method 2004. damage and casualties caused by flooding. Technical report, Highway and Hydraulic Engineering Department, Netherlands, 2004.

[170] J. Komulainen, X. Lu, A. Hakkarainen, A. Weckstrom, M. Viljanen, and S. Liukkonen. Diffusion of some MVOCs through moisture barriers. In *2nd International Conference on Building Physics*, Leuven, 2003. Taylor & Francis.

[171] M. Koniorczyk and D. Gawin. Heat and moisture transport in porous building materials containing salt. *Journal of Building Physics*, 31(4):279–300, 2008.

[172] A. Korpi, J. Pasanen, and A. L. Pasanen. *Sensory Irritation of microbially produced volatile organic compounds in mice during repeated exposures.* Boyd Printing, Albany, New York, 2001.

[173] A. Korpi, J. Jarnberg, and A.-L. Pasanen. Microbial volatile organic compounds. *Critical Reviews in Toxicology*, 39(2):139–193, 2009.

[174] A. Kramer, I. Schwebke, and G. Kampf. How long do nosocomial pathogens persist on inanimate surfaces? a systematic review. *BMC Infectious Diseases*, 6(1):130, 2006.

[175] J.-U. Kreft, G. Booth, and J.W.T. Wimpenny. BacSim, a simulator for individual-based modelling of bacterial colony growth. *Microbiology*, 144:3275–3287, 1998.

[176] M.K. Kumaran. *Material Properties*, volume 3. Acco Leuven, 1996.

[177] D. Laußmann, D. Eis, and H. Schleibinger. Vergleich mykologischer und chemisch-analytischer labormethoden zum nachweis von schimmelpilzbefällen in innenräumen. *Bundesgesundheitsblatt - Gesundheitsforschung - Gesundheitsschutz,*, 47(11):1078–1094, 2004.

[178] LCCP. London's warming: The impacts of climate change on London. Technical report, London Climate Change Partnership, London, November 2002. URL http://www.london.gov.uk/lccp/publications/docs/londons_warming02.pdf. Accessed August 1st 2010.

[179] I. Lebert, C. Nicolas, S. Portanguen, and A. Lebert. Combined water transfer and bacterial models to predict Listeria innocua growth on the surface of gelatine gel during the drying process. *Journal of Food Engineering*, 78(4):1371–1381, 2007.

[180] K. Lengsfeld. Results of the complete Common Exercise 3. Presentation, IEA (International Energy Agency), Kyoto, 2006.

[181] U. Lignell. *Characterization of Microorganisms in Indoor Environments*. PhD thesis, University of Kuopio, 2008.

[182] A.H. Liu. Something old, something new: Indoor endotoxin, allergens and asthma. *Paediatric Respiratory Reviews*, 5(Supplement 1):65–71, 2004.

[183] D.L. Liu and W.W. Nazaroff. Modeling pollutant penetration across building envelopes. *Atmospheric Environment*, 35(2001):4451–4462, 2001.

[184] K.J. Lomas and E. Eppel. Sensitivity analysis techniques for building thermal simulation programs. *Energy and Buildings*, 19:21–44, 1992.

[185] T. Long and D. Or. Dynamics of microbial growth and coexistence on variably saturated rough surfaces. *Microbial Ecology*, 58(2):262–275, 2009.

[186] W. Lorenz, G. Sigrist, M. Shakibaei, A. Mobasheri, and C. Trautmann. A hypothesis for the origin and pathogenesis of rheumatoid diseases. *Rheumatology International*, 26(7):641–654, 2006.

[187] N.S.R. Lorraine. Canvey Island flood disaster, February, 1953. *British Medical Journal*, 91: 59–62, 1954.

[188] M.C. Mahl and C. Sadler. Virus survival on inanimate surfaces. *Canadian Journal of Microbiology*, 21(6):819–823, 1975.

[189] R.M. Maier, I. L. Pepper, and C. P. Gerba. *Environmental Microbiology*. Elsevier, 2009.

[190] A. Mavrogianni, P. Wilkinson, M. Davies, P. Biddulph, and E. Oikonomou. Building characteristics as determinants of propensity to high indoor summer temperatures in London dwellings. *Building and Environment*, 55:117–130, 2012.

[191] M.Y. Menetrez and K.K. Foarde. Microbial volatile organic compound emission rates and exposure model. *Indoor and Built Environment*, 11(4):208–213, 2002.

[192] M. Molmeret, M. Horn, M. Wagner, M. Santic, and Y. Abu Kwaik. Amoebae as training grounds for intracellular bacterial pathogens. *Applied Environmental Microbiology*, 71(1):20–28, 2005.

[193] H.J. Moon. *Assessing Mold Risks in Buildings under Uncertainty*. PhD thesis, Georgia Intitute of Technology, 2005.

[194] D.J. Moschandreas, K.R. Pagilla, and L.V. Storino. Time and space uniformity of indoor bacteria concentrations in Chicago area residences. *Aerosol Science and Technology*, 37(11): 899–906, 2003.

[195] D. Mudarri and W. J. Fisk. Public health and economic impact of dampness and mold. *Indoor Air*, 17(3):226–235, 2007. ISSN 1600-0668.

[196] D. Mumovic, I. Ridley, T. Oreszczyn, and M. Davies. Condensation risk: steady-state and transient hygrothermal modelling methods. *Building Services Engineering Research and Technology*, 27(3):219–235, 2006.

[197] MURL. Hochwasserschadenspotentiale am rhein in nordrhein-westfalen. Technical report, Ministerium fur Umwelt, Raumordnung und Landwirtschaft des Landes Nordrhein-Westfalen, 2000.

[198] M.M. Murphy and T.R. Ginn. Modeling microbial processes in porous media. *Hydrogeology Journal*, 8:142–158, 2000.

[199] S. Muthesius. *The English Terraced House*. Yale University Press, London, 1982.

[200] National Centre for Healthy Housing. Creating a healthy home: A field guide for cleanup of flooded homes. Technical report, National Centre for Healthy Housing, Columbia, MD, June 2008.

[201] A. Nevalainen, A.L. Pasanen, M. Niininen, T. Reponen, P. Kalliokoski, and M.J. Jantunen. The indoor air quality in Finnish homes with mold problems. *Environment International*, 17 (4):299–302, 1991.

[202] NHS Direct. Flood Health Advice from NHS Direct. Press Release, June 28, 2007.

[203] J. Nicholas, D. Proverbs, and G. Holt. An investigation into factors influencing the assessment of UK flood damaged domestic properties. Technical report, Royal Institution of Chartered Surveyors, London, UK, 2001.

[204] K.F. Nielsen, G.Holm, L.P. Uttrup, and P.A. Nielsen. Mould growth on building materials under low water activities: Influence of humidity and temperature on fungal growth and secondary metabolism. *International Biodeterioration and Biodegradation*, 54(4):325–336, 2004.

[205] A. Nilsson, E. Kihlström, V. Lagesson, B. Wessén, B. Szponar, L. Larsson, and C. Tagesson. Microorganisms and volatile organic compounds in airborne dust from damp residences. *Indoor Air*, 14(2):74–82, 2004.

[206] M. Nofal and K. Kumaran. Biological damage function models for durability assessments of wood and wood-based products in building envelopes. *European Journal of Wood and Wood Products*, 69(4):619–631, 2011.

[207] F.H. Norris. Range, magnitude, and duration of the effects of disasters on mental health: Review update 2005. Technical report, Dartmouth Medical School and National Centre for Post Traumatic Stress Disorder, Dartmouth, 2005.

[208] ODPM. Preparing for floods. Technical report, Office of the Deputy Prime Minister, London, UK, 2003. URL http://www.communities.gov.uk/documents/planningandbuilding/pdf/2187544.pdf. Accessed June 25th, 2010.

[209] ODPM. Consultation on planning policy statement 25: development and flood risk. Technical report, Office of the Deputy Prime Minister, London, December 2005.

[210] T. Ojanen, H. Viitanen, R. Peuhkari, K. Lähdesmäki, J. Vinha, and K. Salminen. Mold growth modeling of building structures using sensitivity classes of materials. In *Thermal Performance of the Exterior Envelopes of Whole Buildings XI*, Clearwater Beach, FL, USA, 2010.

[211] OML. London regional flood risk appraisal. Technical report, Office of the Mayor of London, London, UK, 2009. URL http://static.london.gov.uk/mayor/strategies/sds/docs/regional-flood-risk09.pdf. Accessed August 25th, 2010.

[212] ONS. 2001 Census: Census Output Area Statistics (England and Wales) [computer file]. Database, 2001.

[213] OPSI. Flood and water management act 2010. Report, Office of Public Sector Information, London, UK, 2010.

[214] OS. OS MasterMap Topography Layer. Geodatabase, 2011. Downloaded January 10th 2010.

[215] J.H. Park, D.L. Spiegelman, H.A. Burge, D.R. Gold, G.L. Chew, and D.K. Milton. Longitudinal study of dust and airborne endotoxin in the home. *Environmental Health Perspectives*, 108(11):1023–1028, November 2000.

[216] A.L. Pasanen, A. Korpi, J.P. Kasanen, and P. Pasanen. Critical aspects on the significance of microbial volatile metabolites as indoor air pollutants. *Environment International*, 24:703–712, 1998.

[217] S. Paul. *Apartments, Their Design and Development*. Reinhold Publishing Corporation, New York, 1967.

[218] R. Pauwels, G. Verschraegen, and M. Van Der Straeten. Ige antibodies to bacteria in patients with bronchial asthma. *Allergy*, 35(8):665–669, 1980. ISSN 1398-9995.

[219] J. Peltola, M.A. Andersson, T. Haahtela, H. Mussalo-Rauhamaa, F.A. Rainey, R.M. Kroppenstedt, R.A. Samson, and M.S. Salkinoja-Salonen. Toxic-metabolite-producing bacteria and fungus in an indoor environment. *Applied and Environmental Microbiology*, 67(7):3269–3274, July 2001.

[220] E. Penning-Rowsell and J.B. Chatterton. *The benefits of flood alleviation : A manual of assessment techniques*. Saxon House, Westmead, 1977.

[221] E. Penning-Rowsell and T. Wilson. Gauging the impact of natural hazards: the pattern and cost of emergency response during flood events. *Transactions of the Institute of British Geographers*, 31:99–115, 2006.

[222] E. Penning-Rowsell, C. Johnson, S. Tunstall, S. Tapsell, J. Morris, J. Chatterton, and C. Green. *The benefits of flood and coastal risk management: a manual of assessment techniques*. Middlesex University Press, London, 2005.

[223] P. Penttinen, J. Pelkonen, K. Huttunen, M. Toivola, and M.-R. Hirvonen. Interactions between Streptomyces californicus and Stachybotrys chartarum can induce apoptosis and cell cycle arrest in mouse RAW264.7 macrophages. *Toxicology and Applied Pharmacology*, 202(3):278–288, 2005.

[224] P. Penttinen, J. Pelkonen, K. Huttunen, and M.-R. Hirvonen. Co-cultivation of Streptomyces californicus and Stachybotrys chartarum stimulates the production of cytostatic compound(s) with immunotoxic properties. *Toxicology and Applied Pharmacology*, 217(3):342–351, 2006.

[225] S.R. Petterson and N.J. Ashbolt. WHO guidelines for the safe use of wastewater and excreta in agriculture: microbial risk assessment section. Technical report, World Health Organization, Geneva, 2003. (unpublished document, available on request from WHO/PHE, Geneva).

[226] C.G. Pilling and J.A.A. Jones. The impact of future climate change on seasonal discharge, hydrological processes and extreme flows in the Upper Wye experimental catchment, Mid-Wales. *Hydrological Processes*, 16(6):1201–1213, 2002. ISSN 1099-1085.

[227] I. Pirhonen, A. Nevalainen, T. Husman, and J. Pekkanen. Home dampness, moulds, and their influence on respiratory infections and symptoms in adults in Finland. *European Respiratory Journal*, 9(12):2618–2622, 1996.

[228] M. Pitt. Lessons learned from the 2007 floods. Technical report, The Cabinet Office, London, 2007.

[229] Polygon UK. Polygon homepage, 2011. URL http://www.polygongroup.uk.com.

[230] G. Priestnall, J. Jaafar, and A. Duncan. Extracting urban features from LiDAR digital surface models. *Computers*, 24:65–78, 2000.

[231] D.G. Proverbs and R. Soetanto. *Flood Damaged Property: A Guide to Repair*. Blackwell, Oxford, 2004.

[232] C.Y. Rao, M.A. Riggs, G.L. Chew, M.L. Muilenberg, P.S. Thorne, D. Van Sickle, K.H. Dunn, and C. Brown. Characterization of airborne molds, endotoxins, and glucans in homes in New Orleans after Hurricanes Katrina and Rita. *Applied Environmental Microbiology*, 73(5):1630–1634, March 2007.

[233] S. Rautiala, E. Torvinen, P. Torkko, S. Suomalainen, A. Nevalainen, P. Kalliokoski, and M-L. Katila. Potentially pathogenic, slow-growing mycobacteria released into workplace air during the remediation of buildings. *Journal of Occupational and Environmental Hygiene*, 1:1–6, 2004.

[234] M. Reacher, K. McKenzie, C. Lane, T. Nichols, I. Kedge, A. Iversen, P. Hepple, T. Walter, C. Laxton, and J. Simpson. Health impacts of flooding in Lewes: A comparison of reported gastrointestinal and other illness and mental health in flooded and non-flooded households. *Communicable Disease and Public Health*, 7(1):39–46, 2004.

[235] S. Reese. *Die Vulnerabilitat des schleswig-holsteinischen Kustenraumes durch Sturmfluten. Fallstudien von der Nord-und Ostseekuste*. PhD thesis, Universitat zu Kiel, 2003.

[236] I. Ridley, J. Freeman, P. Biddulph, and M. Davies. Testing and validation of UCL-HAMT module for EnergyPlus. Technical report, UCL, London, 2008.

[237] Margaret A. Riggs, Carol Y. Rao, Clive M. Brown, David Van Sickle, Kristin J. Cummings, Kevin H. Dunn, James A. Deddens, Jill Ferdinands, David Callahan, Ronald L. Moolenaar, and Lynne E. Pinkerton. Resident cleanup activities, characteristics of flood-damaged homes and airborne microbial concentrations in New Orleans, Louisiana, October 2005. *Environmental Research*, 106(3):401–409, 2008.

[238] M.A. Ross, L. Curtis, P.A. Scheff, D.O. Hryhorczuk, V. Ramakrishnan, R.A. Wadden, and V.W. Persky. Association of asthma symptoms and severity with indoor bioaerosols. *Allergy*, 55(8):705–711, 2000. ISSN 1398-9995.

[239] R. Rylander. Indoor air-related effects and airborne (1->3)-[beta]-d glucans. *Environmental Health Perspectives*, 107:501–503, 1999.

[240] J.-L. Sagripanti and A. Bonifacino. Resistance of Pseudomonas aeruginosa to liquid disinfectants on contaminated surfaces before formation of biofilms. *Journal of AOAC International*, 83(6):1415–1422, 2000.

[241] P.I. Sandberg. Thermal resistance of a wet mineral fiber insulation. In F.J. Powell and S.L. Matthews, editors, *Thermal Insulation: Materials and Systems*, pages 394–404. American Society for Testing and Materials, Philadelphia, 1987.

[242] R. Scheffler, G.A. Plagge. Introduction of a drying coefficient for building materials. In *Thermal Performance of the Exterior Envelopes of Whole Buildings XI*, Clearwater Beach, Florida, 2010.

[243] H. Schleibinger, C. Brattig, M. Mangler, D. Laußmann, D. Eis, P. Braun, D. Marchl, A. Nickelmann, and H. Rueden. Are microbial volatile organic compounds (MVOC) useful predictors for a hidden mould damage? In *Healthy Buildings 2003*, Singapore, December 2003.

[244] C.E.G. Scholler, H. Gurtler, R. Pedersen, S. Molin, and K. Wilkins. Volatile metabolites from actinomycetes. *Journal of Agricultural and Food Chemistry*, 50(9):2615–2621, 2002.

[245] K.J. Schwab, K.E. Gibson, D.L. Williams, K.M. Kulbicki, C.P. Lo, J.N. Mihalic, P.N. Breysse, F.C. Curriero, and A.S. Geyh. Microbial and chemical assessment of regions within New Orleans, LA impacted by Hurricane Katrina. *Environmental Science and Technology*, 41(7): 2401–2406, 2007.

[246] Scott Wilson. London Borough of Hackney Level 2 Strategic Flood Risk Assessment. Technical report, Scott Wilson, London, 2010.

[247] Scottish Executive. Planning advice note pan 69 - planning and building standards advice on flooding. Technical report, Scottish Executive, London, 2004.

[248] SDC. Sustainable buildings - the challenge of the existing stock. Technical working paper, Sustainable Development Commission, London, 2005.

[249] K. Sedlbauer. *Prediction of mould fungus on the surface and inside building components.* PhD thesis, Fraunhofer Institute for Building Physics, 2001.

[250] K. Sedlbauer. Prediction of mould growth by hygrothermal calculation. *Journal of Thermal Envelope and Building Science*, 25(4):321–336, 2002.

[251] L.M. Sehulster and R.Y.W. Chinn. Guidelines for Environmental Infection Control in Health-Care Facilities. Technical report, Centers for Disease Control, June 2003. URL http://cdc.gov/MMWR/preview/mmwrhtml/rr5210a1.htm. Accessed August 21st, 2010.

[252] L.M. Sehulster, R.Y.W. Chinn, M.J. Arduino, J. Carpenter, R. Donland, D. Ashford, R. Besser, B. Fields, M.M. McNeil, C. Whitney, S. Wong, D. Juranek, and J. Cleveland. Guidelines for environmental infection control in health-care facilities. recommendations from CDC and the healthcare infection control practices advisory committee (HICPAC). Technical report, Centres for Disease Control, Chicago, 2004. URL http://www.cdc.gov/ncidod/dhqp/pdf/guidelines/Enviro_guide_03.pdf. Accessed August 21st, 2010.

[253] R.C. Shoemaker and D.E. House. A time-series study of sick building syndrome: chronic, biotoxin-associated illness from exposure to water-damaged buildings. *Neurotoxicology and Teratology*, 27(1):29–46, 2004.

[254] J. Singh. *Building Mycology: Management of Decay and Health in Buildings*. Taylor & Francis, London, 1994.

[255] G.M. Solomon, M. Hjelmroos-Koski, M. Rotkin-Ellman, and S.K. Hammond. Airborne mold and endotoxin concentrations in New Orleans, Louisiana, after flooding, October through November 2005. *Environmental Health Perspectives*, 114(9):1381–1386, 2006.

[256] W.R. Solomon and T.A.E. Platts-Mills. Aerobiology and inhalant allergens. In E. Middleton, editor, *Allergy: Principles and Practice*, pages 367–403. Mosby Co., St Louis, 1998.

[257] R. Stephen. Airtightness in UK dwellings. Technical report, Building Research Establishment, Watford, January 2000.

[258] J.F. Straube. Moisture in buildings. *ASHRAE Journal*, 44(1):15–19, January 2002.

[259] M.S. Suleman, A. N'Jai, C.H. Green, and E.C. Penning-Rowsell. Potential flood damage data: A major update. Technical report, Middlesex Polytechnic Flood Hazard Research Centre, 1988.

[260] D. Summers. *The East Coast Floods*. David & Charles, London, UK, 1978.

[261] J. Suonketo and A. Pessi. The airflows and microbial contamination to indoor air from sandwich facade: case study. In *Healthy Buildings 2000*, volume 3, page 147, Espoo, Finland, 2000.

[262] Sustainable Energy Research Group. *CCWeatherGen*. Southampton, 2008. URL http://www.serg.soton.ac.uk/ccweathergen/. Accessed December 5th 2010.

[263] A. Tagg, M. Escarameia, and J. Molinero Ortiz. Improving the flood resilience of buildings through improved materials, methods, and details. Technical report, CIRIA, February 2007.

[264] A. Tagg, M. Escarameia, and J. Molinero Ortiz. Improving the flood resilience of buildings through improved materials, methods, and details: WP6 collation and analysis of post-flood observational data. Technical report, CIRIA, February 2007.

[265] J.W. Tang. The effect of environmental parameters on the survival of airborne infectious agents. *Journal of the Royal Society*, 6(Suppl 6):S737–S746, December 2009.

[266] S.M. Tapsell. Follow-up study of the health effects of the 1998 Easter flooding in Banbury and Kidlington. report to the Environment Agency, Thames Region. Technical report, Flood Hazard Research Centre, Middlesex University, Enfield, 2000.

[267] S.M. Tapsell and S.M. Tunstall. *The Health Effects of Floods*. Routledge, 2000.

[268] S.M. Tapsell, E. Penning-Rowsell, S. Tunstall, and T. Wilson. Vulnerability to flooding: Health and social dimensions. *Philosophical Transactions of the Royal Society*, 360:1511–1525, 2002.

[269] J.A.E. ten Veldhuis, F.H.L.R. Clemens, G. Sterk, and B.R. Berends. Microbial risks associated with exposure to pathogens in contaminated urban flood water. *Water Research*, 44(9):2910–2918, 2010.

[270] The Geoinformation Group. Cities Revealed: Leaders in aerial photos and GIS data. Geodatabase, 2010. URL http://www.citiesrevealed.com/.

[271] J. Thorn, J. Brisman, and K. Torén. Adult-onset asthma is associated with self-reported mold or environmental tobacco smoke exposures in the home. *Allergy*, 56(4):287–292, 2001.

[272] E. Torvinen, T. Meklin, P. Torkko, S. Suomalainen, M. Reiman, M.-L. Katila, L. Paulin, and A. Nevalainen. Mycobacteria and fungi in moisture-damaged building materials. *Applied and Environmental Microbiology*, 72(10):6822–6824, 2006.

[273] UKCP09. UK Climate Projections, 2009. URL http://ukclimateprojections.defra.gov.uk/. Accessed April 18th, 2010.

[274] UN/ISDR. Living with risk: A global review of disaster reduction initiatives. Technical report, United Nations and International Strategy for Disaster Reduction, Geneva, 2004. URL http://www.adrc.asia/publications/LWR/LWR_pdf/index.pdf. Accessed June 30th 2010.

[275] US-DOE. *EnergyPlus Energy Simulation software*, 2004. URL http://www.eere.energy.gov/buildings/energyplus.

[276] USACE. Flood proofing tests - tests of materials and systems for flood proofing structures. Technical report, US Army Corps of Engineers, Washington, DC, August 1988.

[277] UWE. Construction web site. Webpage, 2009. URL http://environment.uwe.ac.uk/video/cd_new_demo/Conweb/. Accessed February 11th, 2011.

[278] V.P. Valdramidis, A.H. Geeraerd, J.E. Gaze, A. Kondjoyan, A.R. Boyd, H.L. Shaw, and J.F. Van Impe. Quantitative description of listeria monocytogenes inactivation kinetics with temperature and water activity as the influencing factors; model prediction and methodological validation on dynamic data. *Journal of Food Engineering*, 76(1):79–88, 2006.

[279] M. C. M. van Loosdrecht, J. J. Heijnen, H. Eberl, J. Kreft, and C. Picioreanu. Mathematical modelling of biofilm structures. *Antonie van Leeuwenhoek*, 81(1):245–256, 2002. URL http://dx.doi.org/10.1023/A:1020527020464. 0003-6072.

[280] J.K. Varma, K.D. Greene, M.E. Reller, S. M. DeLong, J. Trottier, S.F. Nowicki, M. DiOrio, E.M. Koch, T.L. Bannerman, S.T. York, M.-A. Lambert-Fair, J.G. Wells, and P.S. Mead. An outbreak of Escherichia coli O157 infection following exposure to a contaminated building. *Journal of the American Medical Association*, 290(20):2709–2712, November 2003.

[281] H. Viitanen. Modelling the time factor in the development of mould fungi - the effect of critical humidity and temperature conditions on pine and spruce sapwood. *Holzforschung*, 51(1):6–14, 1997.

[282] H.A. Viitanen. Improved model to predict mold growth in building materials. In ORNL ASHRAE, DOE, editor, *Thermal Performance of the Exterior Envelopes of Whole Buildings*, Clearwater Beach, USA, December 2007.

[283] H.A. Viitanen and A-C. Ritschkoff. Mould growth in pine and spruce sapwood in relation for air humidity and temperature. Technical report, Swedish University of Agricultural Sciences, Department of Forest Products, Uppsala, 1991.

[284] J. Vinha. *Hygrothermal Performance of Timber-framed External Walls in Finnish Climatic Conditions: A Method for Determining the Sufficient Water Vapour Resistance of the Interior Lining of a Wall Assembly.* PhD thesis, Tampereen Teknillinen Yliopisto, Tampere, 2007.

[285] VOA. CTR(E) IA 111202 - Data Quantity / Quality Audit - Property Attributes Data, 2002. URL http://www.voa.gov.uk/publications/CouncilTaxIas/021211-ctre-ia.htm.

[286] Water Technology. Thames Tideway Project, London, United Kingdom, 2011. URL http://www.water-technology.net/projects/thameswater/. Accessed October 2011.

[287] D.N. Weissman and M.R. Schuyler. Biological agents and allergic diseases. In J.M. Samet and J.D Spengler, editors, *Indoor Air Pollution: A Health Perspective*, pages 285–305. Johns Hopkins University Press, Baltimore, 1991.

[288] H. W. Wellman and A. T. Wilson. Salt weathering, a neglected geological erosive agent in coastal and arid environments. *Nature*, 205(4976):1097–1098, 1965.

[289] V. Whitford, A.R. Ennos, and J.F. Handley. City form and natural process–indicators for the ecological performance of urban areas and their application to Merseyside, UK. *Landscape and Urban Planning*, 57(2):91–103, 2001.

[290] WHO. The World Health Report 2001 - Mental Health: New Understanding, New Hope. Technical report, World Health Organisation, Geneva, 2001.

[291] WHO. Floods: Climate Change and Adaptation Strategies for Human Health. Technical report, World Health Organisation, Geneva, 2002.

[292] WHO. WHO Guidelines for Indoor Air Quality: Dampness and Mould. Technical report, World Health Organisation, Copenhagen, 2009.

[293] H. Williams. Signs of E.coli after Cumbria floods. Online News Article, 04/12/2009 2009. URL http://news.sky.com/skynews/Home/UK-News/Cumbria-Flooding-Mud-From-House-Contains-DNA-Signature-Of-EColi-0157/Article/200912115490582?lid=ARTICLE_15490582_CumbriaFlooding:MudFromHouseContainsDNASignatureOfE.Coli0157&lpos=searchresults. Accessed January 5th 2011.

[294] M.A. Wilson, W.D. Hoff, and C. Hall. Water movement in porous building materials:xiv. absorption into a two-layer composite. *Building and Environment*, 30(2):221–227, 1995. ISSN 0360-1323.

[295] M.A. Wilson, W.D. Hoff, and C. Hall. Water movement in porous building materials: Xiii. absorption into a two-layer composite. *Building and Environment*, 30:209–219, 1995.

[296] J. Wingfield, M. Bell, and P. Bowker. Improving the flood resilience of buildings through improved materials, methods, and details: Review of existing information and experience. Technical report, CIRIA, Leeds, June 2005.

[297] A. Wolf-Rainer and F.W. Dirk. Fate of facultative pathogenic microorganisms during and after the flood of the Elbe and Mulde Rivers in August 2002. *Acta hydrochimica et hydrobiologica*, 33(5):449–454, 2005. ISSN 1521-401X.

[298] M. Woloszyn and C. Rode. Tools for performance simulation of heat, air and moisture conditions of whole buildings. *Building Simulation*, 1(1):5–24, 2008.

[299] M. Woloszyn and C. Rode. IEA Annex 41: Whole Building Heat, Air and Moisture Response - MOIST-ENG: Volume 1: Modeling Principles and Common Exercises. Technical report, International Energy Agency, 2008.

[300] E. Woodman and E. Greeves. *Home/Away: Five British Architects Build Housing in Europe: The Development of Housing in Britain 1870-2008*. British Council, London, 2008.

[301] WRc. Pollution prevention and control in sewer systems - microbiological decay rates. Technical report, Water Research Centre, Swindon, September 2000.

[302] WRc. *The Predictive Management Tool*. Water Research Centre, Swindon, 2010. URL http://www.wrcplc.co.uk/default.aspx?item=686.

[303] T. Yli-Pirilä, J. Kusnetsov, M.-R. Hirvonen, M. Seuri, and A. Nevalainen. Effects of amoebae on the growth of microbes isolated from moisture-damaged buildings. *Canadian Journal of Microbiology*, 52:383–390, 2006.

[304] T. Yli-Pirilä, J. Kusnetsov, M. R. Hirvonen, M. Seuri, and A. Nevalainen. Survival of amoebae on building materials. *Indoor Air*, 19(2):113–121, 2009. ISSN 1600-0668.

[305] R.A. Zabel and J.J. Morrell. *Wood microbiology: decay and its prevention*. Academic Press, San Diego, 1992.

[306] K. Zitek and C. Benes. Longitudinal epidemiology of leptospirosis in the Czech Republic (1963-2003). *Epidemiologie, mikrobiologie, imunologie*, 54(1):21–26, 2005.

[307] ZunZun.com. Online data modelling. Webpage, October 2011. URL http://www.zunzun.com. Accessed December 1st, 2011.

Appendices

Appendix A

Built Forms

H01

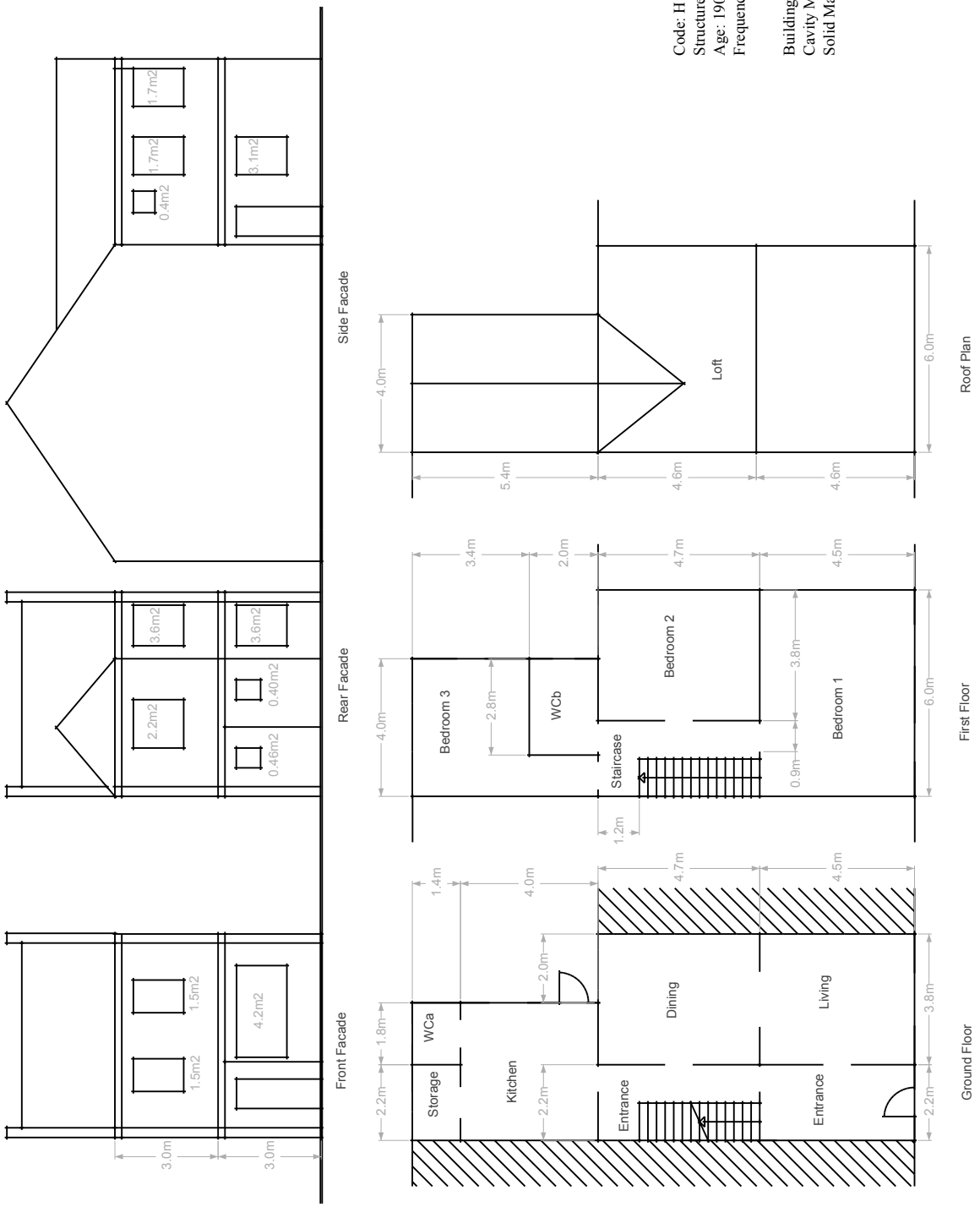
Code: H1
Structure: Terrace with large T
Age: 1902 - 1913
Frequency: 15.4%
Building Fabrics:
Cavity Masonry 16% (16%)
Solid Masonry 84% (2%)
Side Facade
Rear Facade
Front Facade
Roof Plan
First Floor
Ground Floor
Loft
Bedroom 3
WCb
Bedroom 2
Staircase
Bedroom 1
Storage
WCa
Kitchen
Dining
Living
Entrance
Entrance

H02

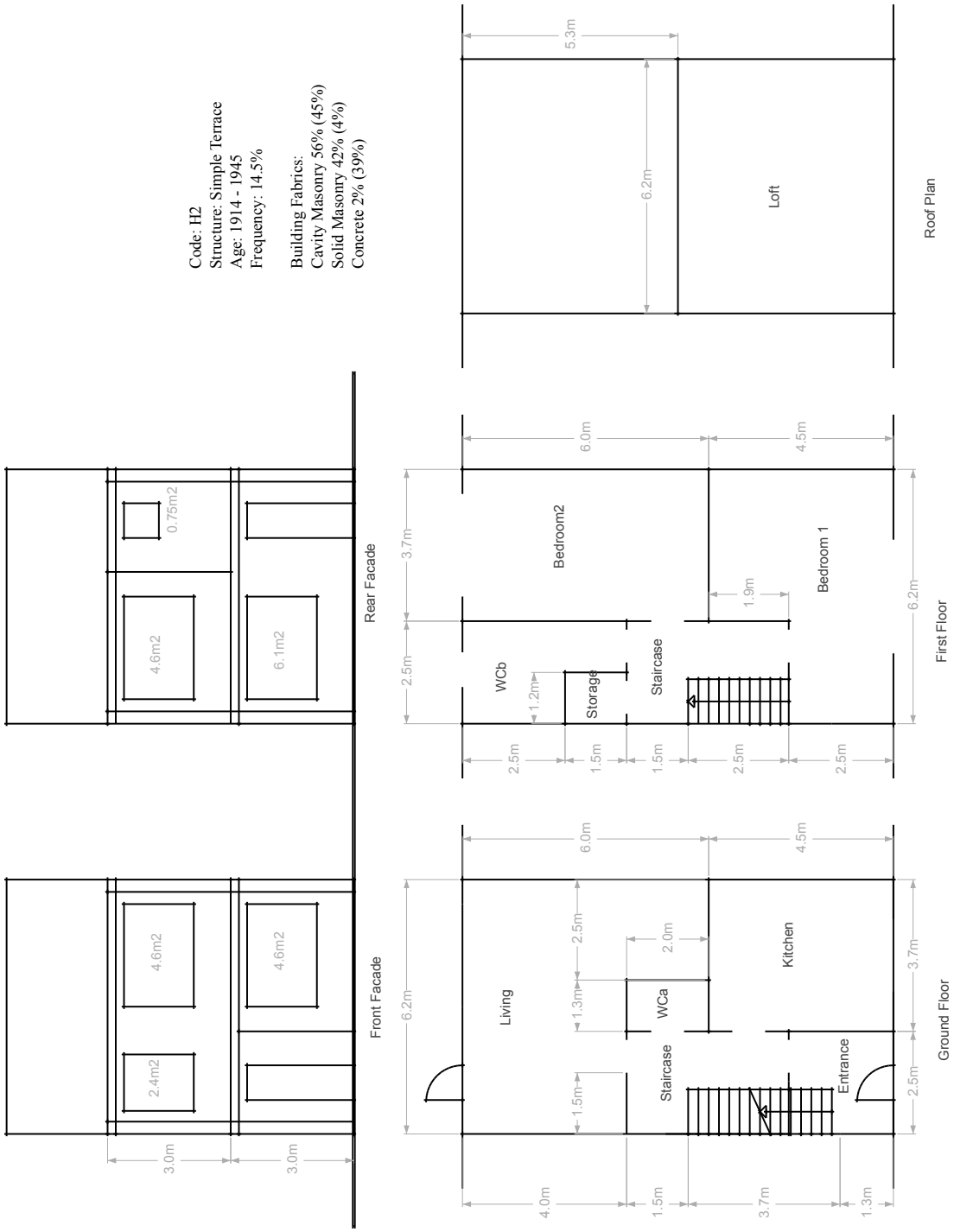
Code: H2
Structure: Simple Terrace
Age: 1914 - 1945
Frequency: 14.5%
Building Fabrics:
Cavity Masonry 56% (45%)
Solid Masonry 42% (4%)
Concrete 2% (39%)
Roof Plan
Loft
5.3m
6.2m
First Floor
Bedroom2
Bedroom 1
WCb
Storage
Staircase
6.0m
4.5m
3.7m
2.5m
1.2m
1.9m
1.5m
Ground Floor
Living
WCa
Kitchen
Staircase
Entrance
2.0m
1.3m
4.0m
3.7m
Rear Facade
Front Facade
0.75m2
4.6m2
6.1m2
2.4m2
3.0m

H03

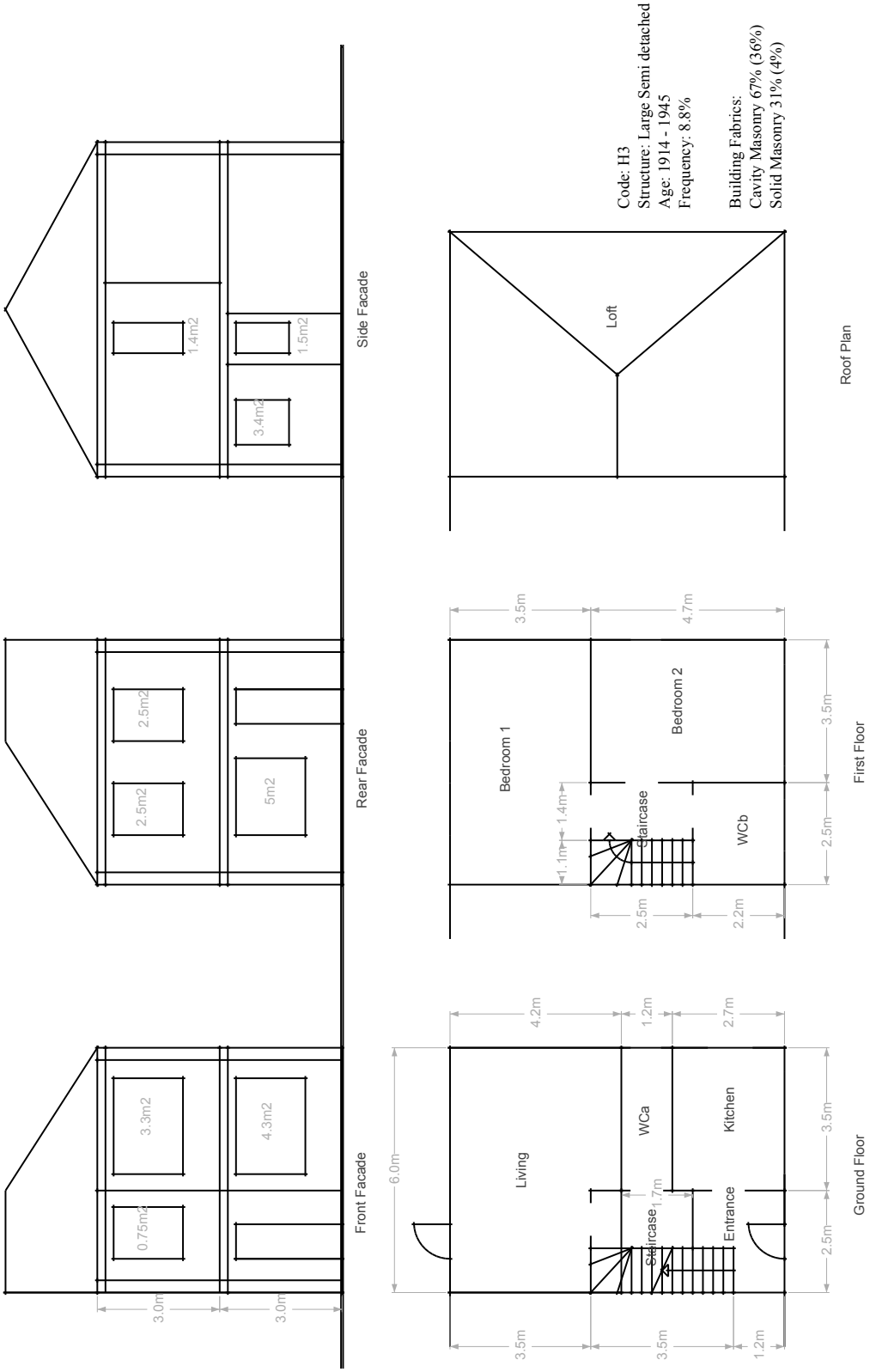
Code: H3
Structure: Large Semi detached
Age: 1914 - 1945
Frequency: 8.8%
Building Fabrics:
Cavity Masonry 67% (36%)
Solid Masonry 31% (4%)
Side Facade
Rear Facade
Front Facade
1.4m2
1.5m2
3.4m2
2.5m2
2.5m2
5m2
3.3m2
4.3m2
0.75m2
3.0m
3.0m
Loft
Roof Plan
3.5m
4.7m
Bedroom 1
Bedroom 2
Staircase
WCb
1.4m
1.1m
2.5m
2.2m
3.5m
2.5m
First Floor
4.2m
1.2m
2.7m
6.0m
Living
WCa
Kitchen
Staircase
1.7m
Entrance
3.5m
2.5m
3.5m
3.5m
1.2m
Ground Floor

H04


Code: H4
Structure: Purpose Built
Age: 1960 - 1979
Frequency: 5.7%
Building Fabrics:
Cavity Masonry 66% (37%)
Solid Masonry 5% (19%)
Concrete 28% (12%)
2.5m2
3.5m2
Front Facade
1.9m2
1.9m2
2.8m
Rear Facade
2.5m
1.9m
3.4m
WCa
Entrance
Kitchen
Bedroom 1
Living
3.5m
4.3m
Typical Floorplan

H05

Code: H5
Structure: Simple Terrace
Age: 1902 - 1913
Frequency: 5.5%

Building Fabrics:
Cavity Masonry 16% (16%)
Solid Masonry 84% (2%)

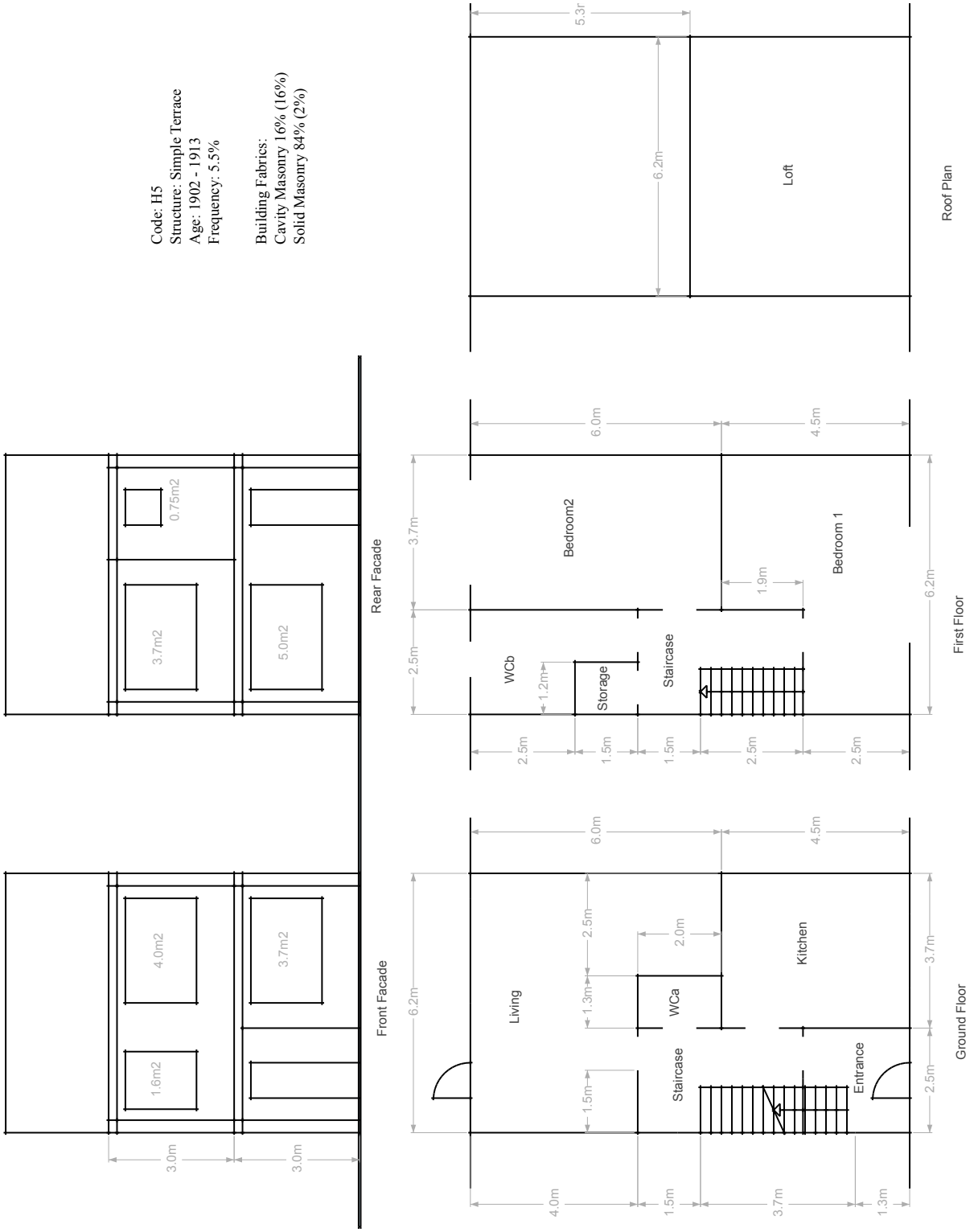

H06

Code: H6
Structure: Purpose Built
Age: 1946 - 1959
Frequency: 4.7%

Building Fabrics:
Cavity Masonry 59% (34%)
Solid Masonry 15% (9%)
Concrete 26% (14%)

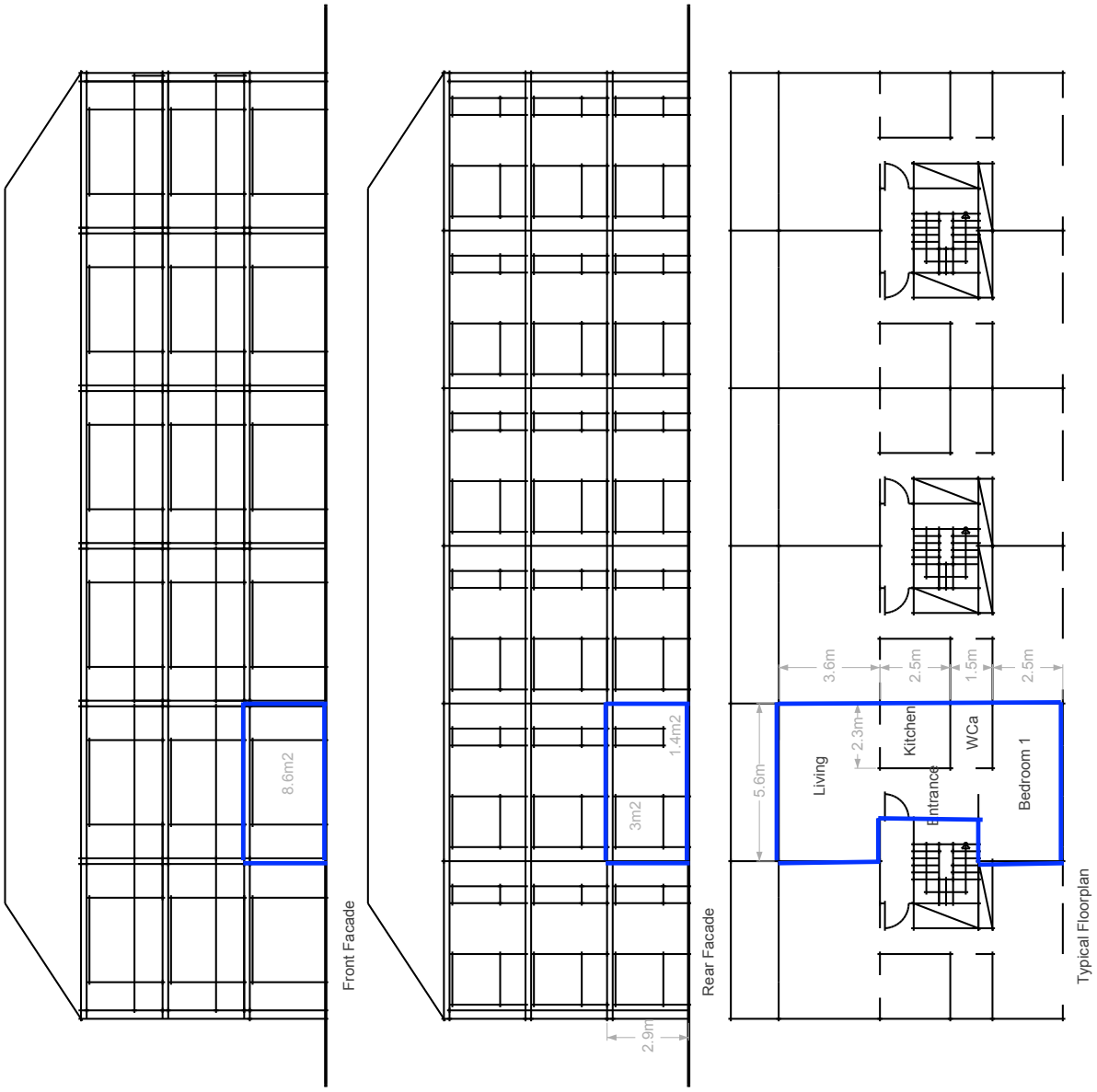

H07


Code: H7
Structure: Purpose Built
Age: 1980 - 2008
Frequency: 3.6%
Building Fabrics:
Cavity Masonry 89% (54%)
Solid Masonry 2% (69%)
Concrete 6% (42%)
2.5m2
3.5m2
Front Facade
1.9m2
1.9m2
Rear Facade
2.8m
2.5m
1.9m
3.4m
WCa
Entrance
Kitchen
Bedroom 1
Living
2.5m
4.5m
3.5m
4.3m
Typical Floorplan

H08

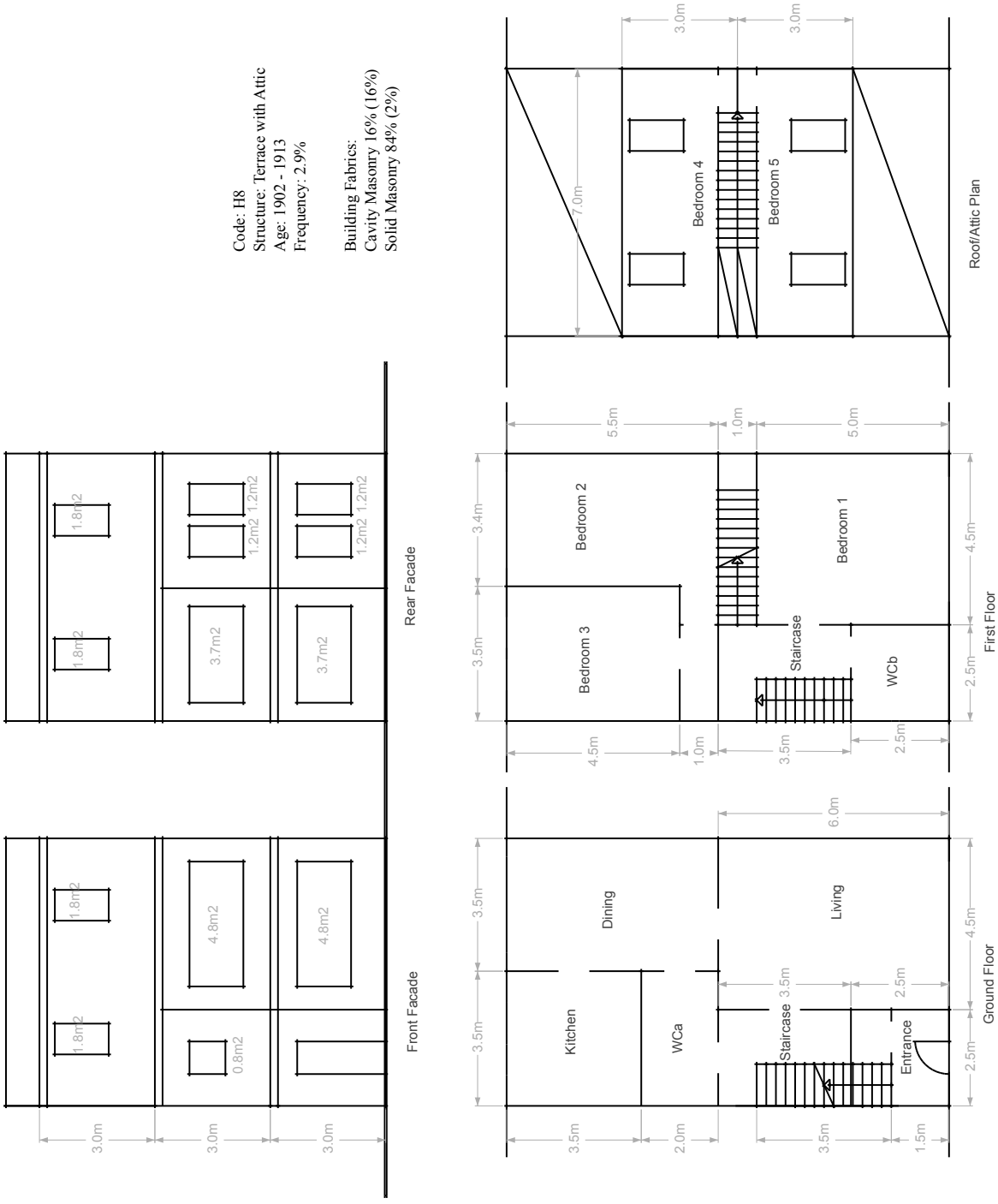
Code: H8
Structure: Terrace with Attic
Age: 1902 - 1913
Frequency: 2.9%
Building Fabrics:
Cavity Masonry 16% (16%)
Solid Masonry 84% (2%)
Front Facade
Rear Facade
Roof/Attic Plan
First Floor
Ground Floor
Bedroom 4
Bedroom 5
Bedroom 2
Bedroom 3
Bedroom 1
Staircase
WCb
Kitchen
Dining
WCa
Living
Entrance
1.8m2
3.7m2
4.8m2
0.8m2
1.2m2
3.0m
7.0m
5.5m
1.0m
5.0m
3.4m
3.5m
4.5m
2.5m
6.0m
2.0m
1.5m

H09

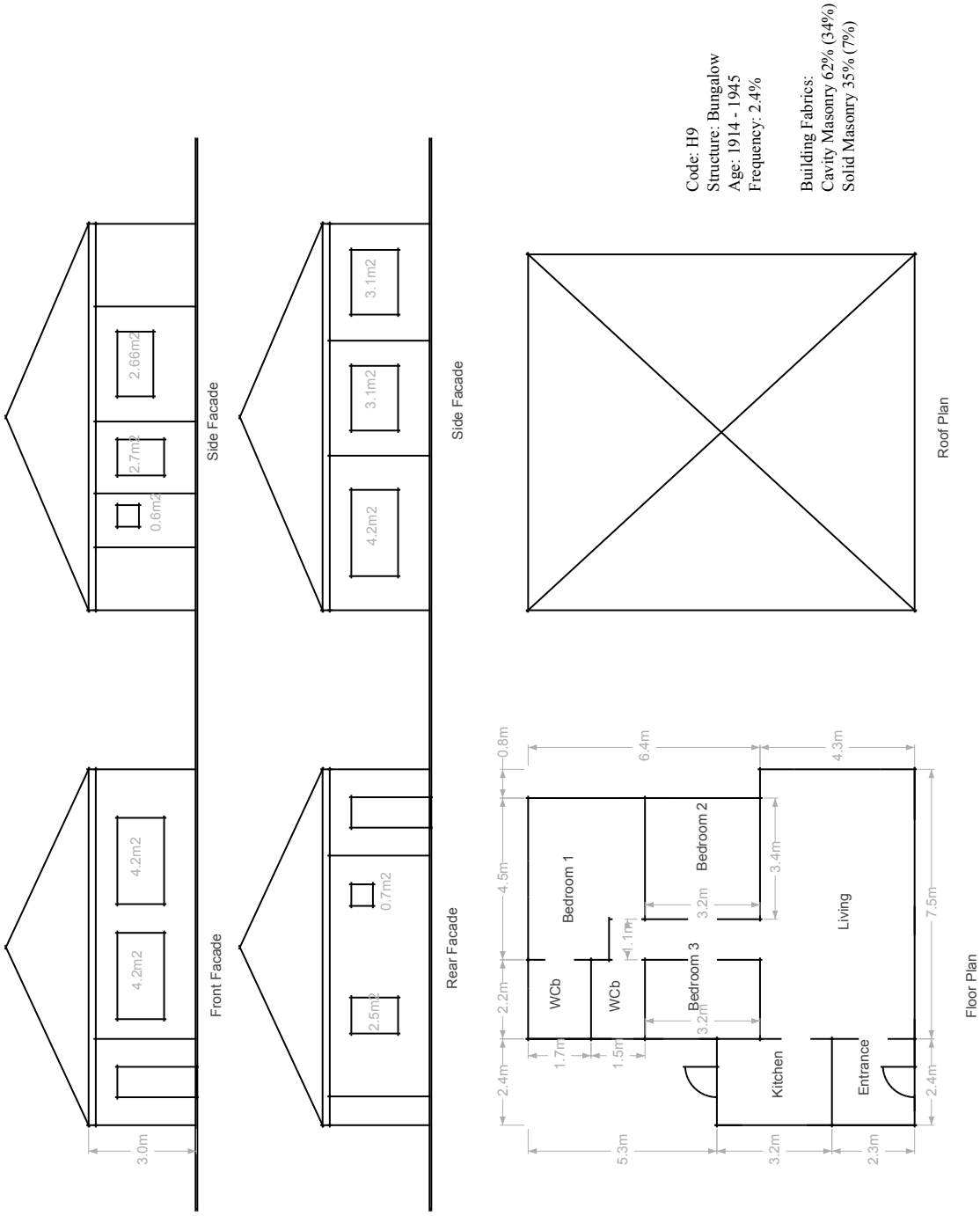
Code: H9
Structure: Bungalow
Age: 1914 - 1945
Frequency: 2.4%
Building Fabrics:
Cavity Masonry 62% (34%)
Solid Masonry 35% (7%)
Front Facade
Side Facade
Rear Facade
Side Facade
Roof Plan
Floor Plan
4.2m2
4.2m2
2.66m2
2.7m2
0.6m2
3.1m2
3.1m2
4.2m2
0.7m2
2.5m2
3.0m
0.8m
6.4m
4.3m
4.5m
2.2m
2.4m
5.3m
1.7m
1.5m
3.2m
3.2m
3.4m
7.5m
2.4m
2.3m
Bedroom 1
Bedroom 2
Bedroom 3
WCb
WCb
Kitchen
Living
Entrance

H10

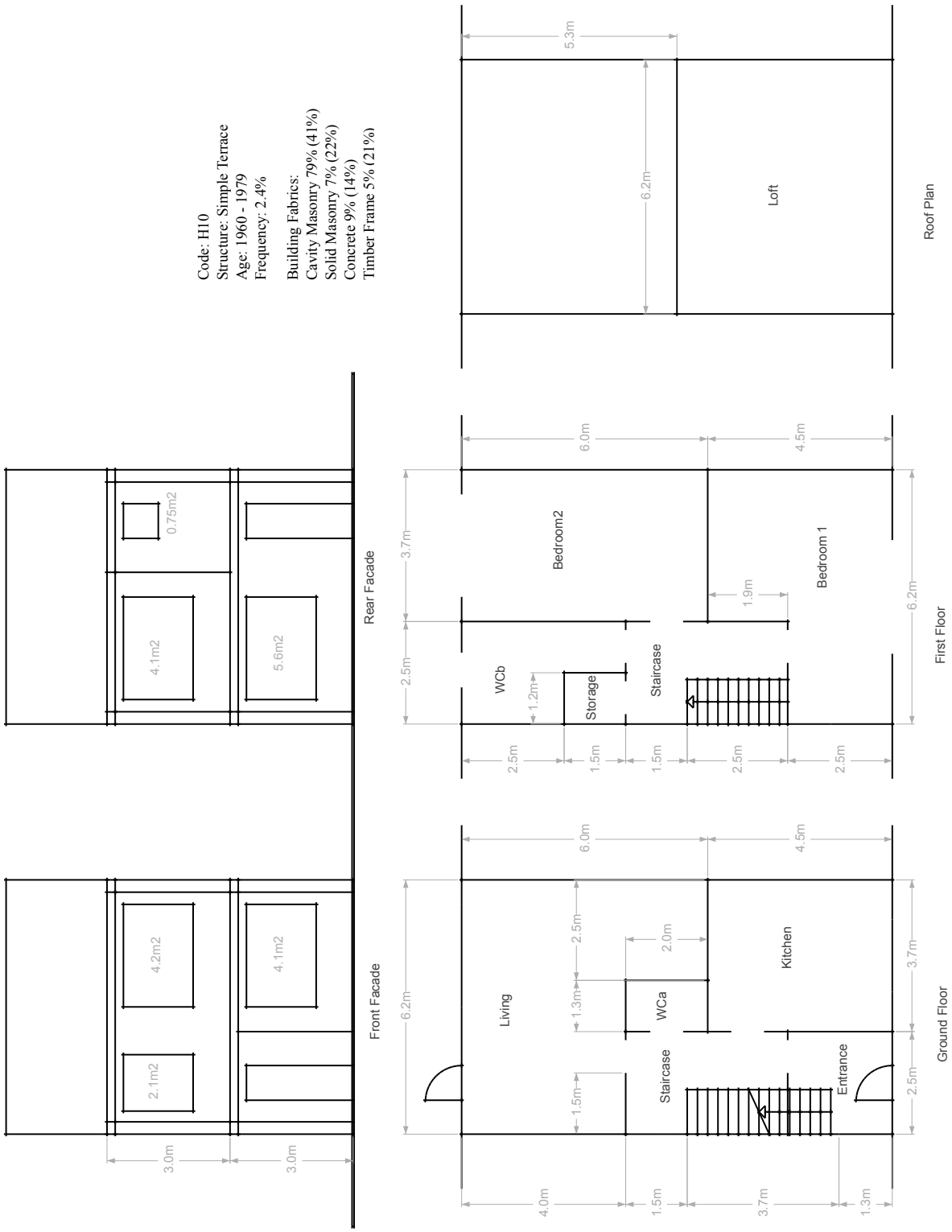
Code: H10
Structure: Simple Terrace
Age: 1960 - 1979
Frequency: 2.4%
Building Fabrics:
Cavity Masonry 79% (41%)
Solid Masonry 7% (22%)
Concrete 9% (14%)
Timber Frame 5% (21%)
Rear Facade
0.75m2
4.1m2
5.6m2
Front Facade
4.2m2
4.1m2
2.1m2
3.0m
3.0m
Roof Plan
5.3m
6.2m
Loft
First Floor
6.0m
4.5m
3.7m
2.5m
Bedroom2
Bedroom 1
1.9m
6.2m
WCb
1.2m
Storage
Staircase
2.5m
1.5m
1.5m
2.5m
2.5m
Ground Floor
6.0m
4.5m
6.2m
Living
2.5m
2.0m
Kitchen
3.7m
1.3m
WCa
Staircase
1.5m
Entrance
2.5m
4.0m
1.5m
3.7m
1.3m

H11

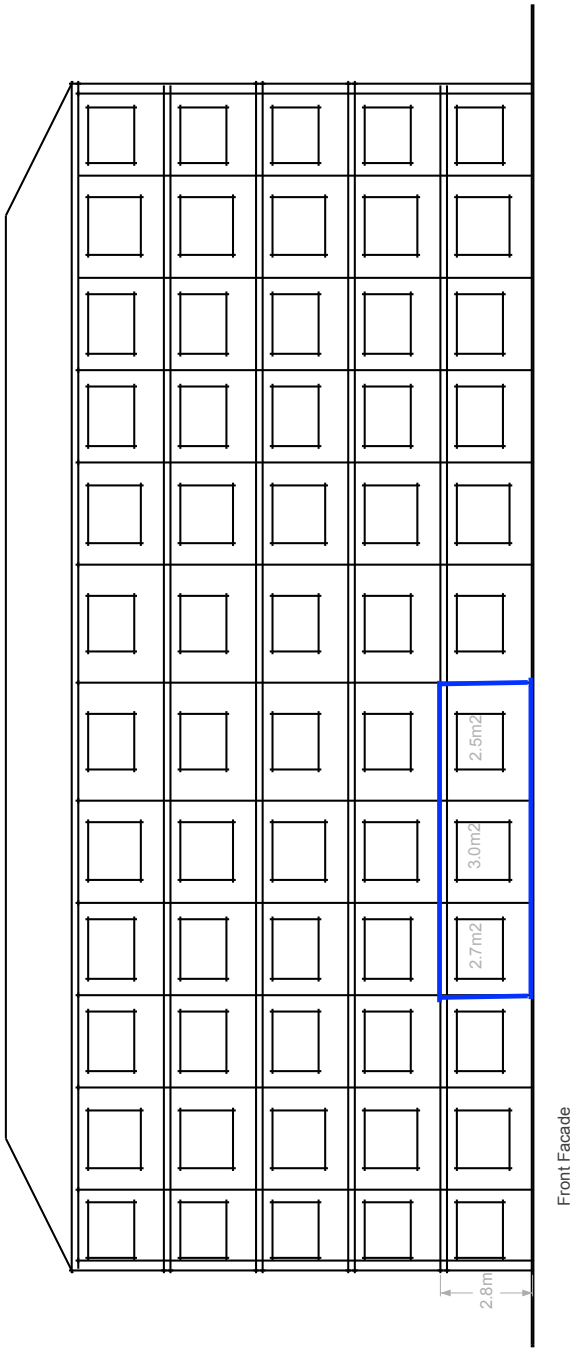

Code: H11
Structure: Purpose Built
Age: 1960 - 1979
Frequency: 2.3%

Building Fabrics:
Cavity Masonry 66% (37%)
Solid Masonry 5% (19%)
Concrete 28% (12%)

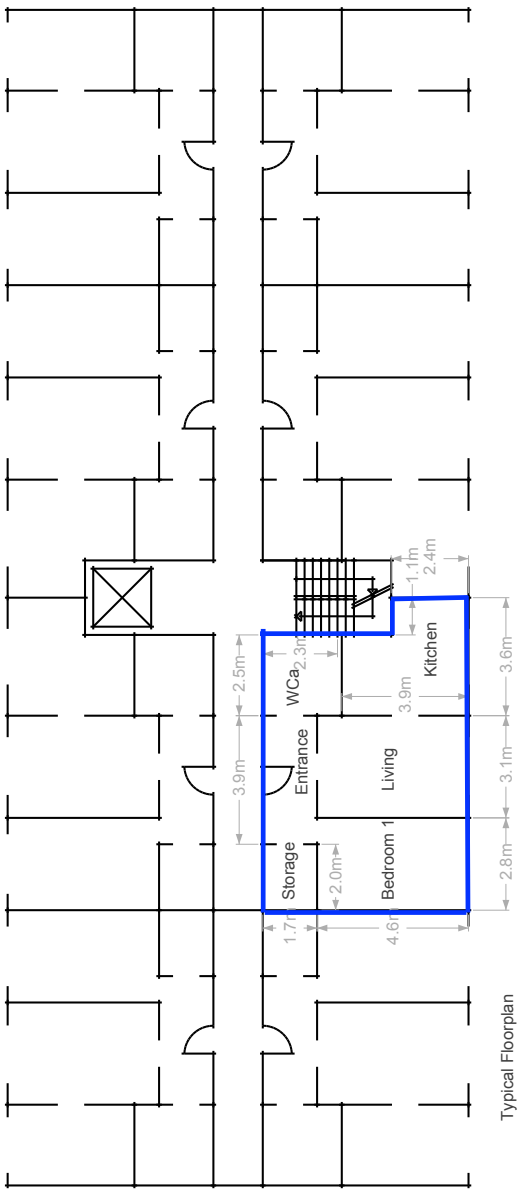

H12

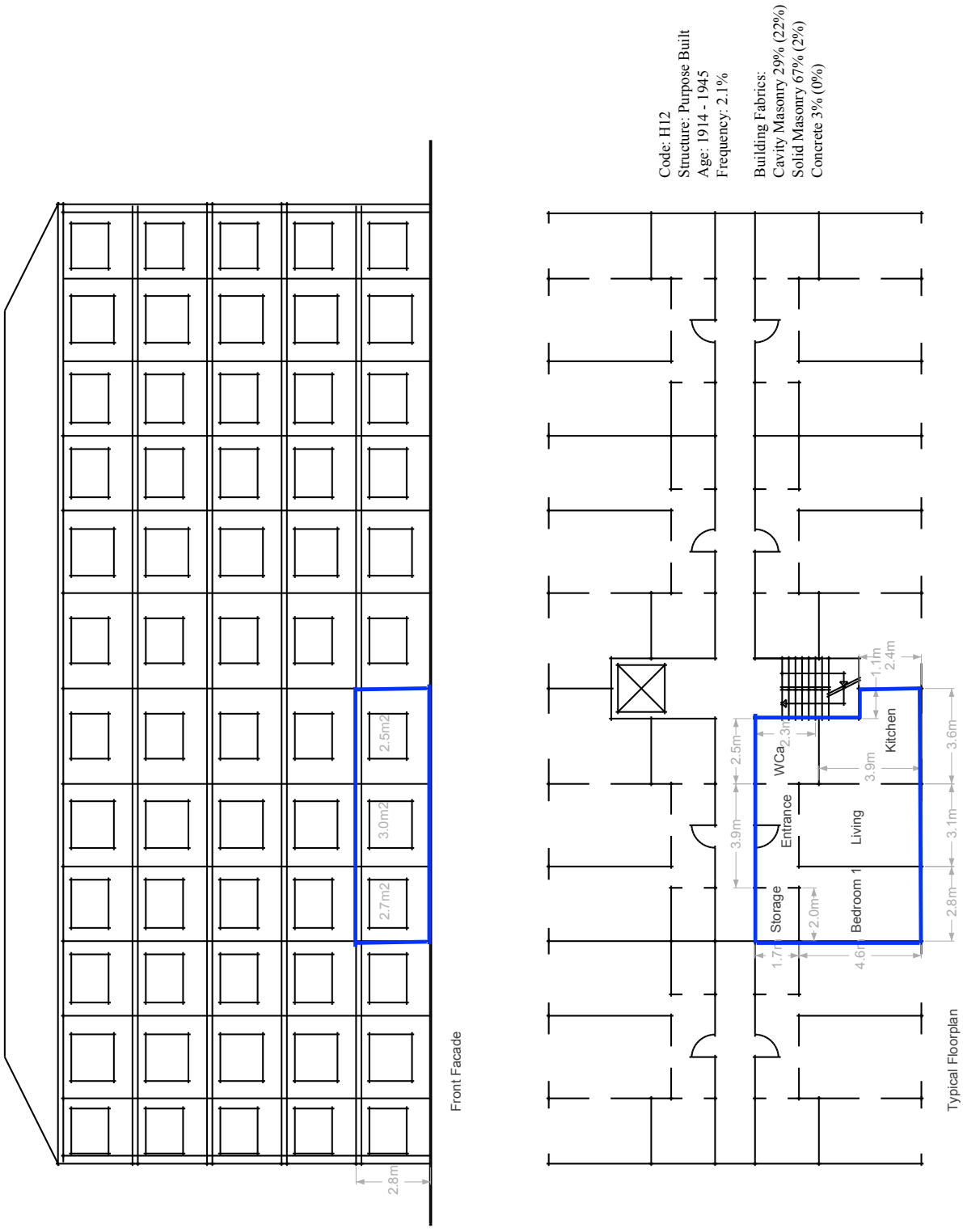
Code: H12
Structure: Purpose Built
Age: 1914 - 1945
Frequency: 2.1%
Building Fabrics:
Cavity Masonry 29% (22%)
Solid Masonry 67% (2%)
Concrete 3% (0%)
2.5m2
3.0m2
2.7m2
2.8m
Front Facade
WCa
Entrance
Storage
Living
Bedroom 1
Kitchen
2.5m
3.9m
2.0m
3.9m
1.1m
2.4m
3.6m
3.1m
2.8m
Typical Floorplan

H14

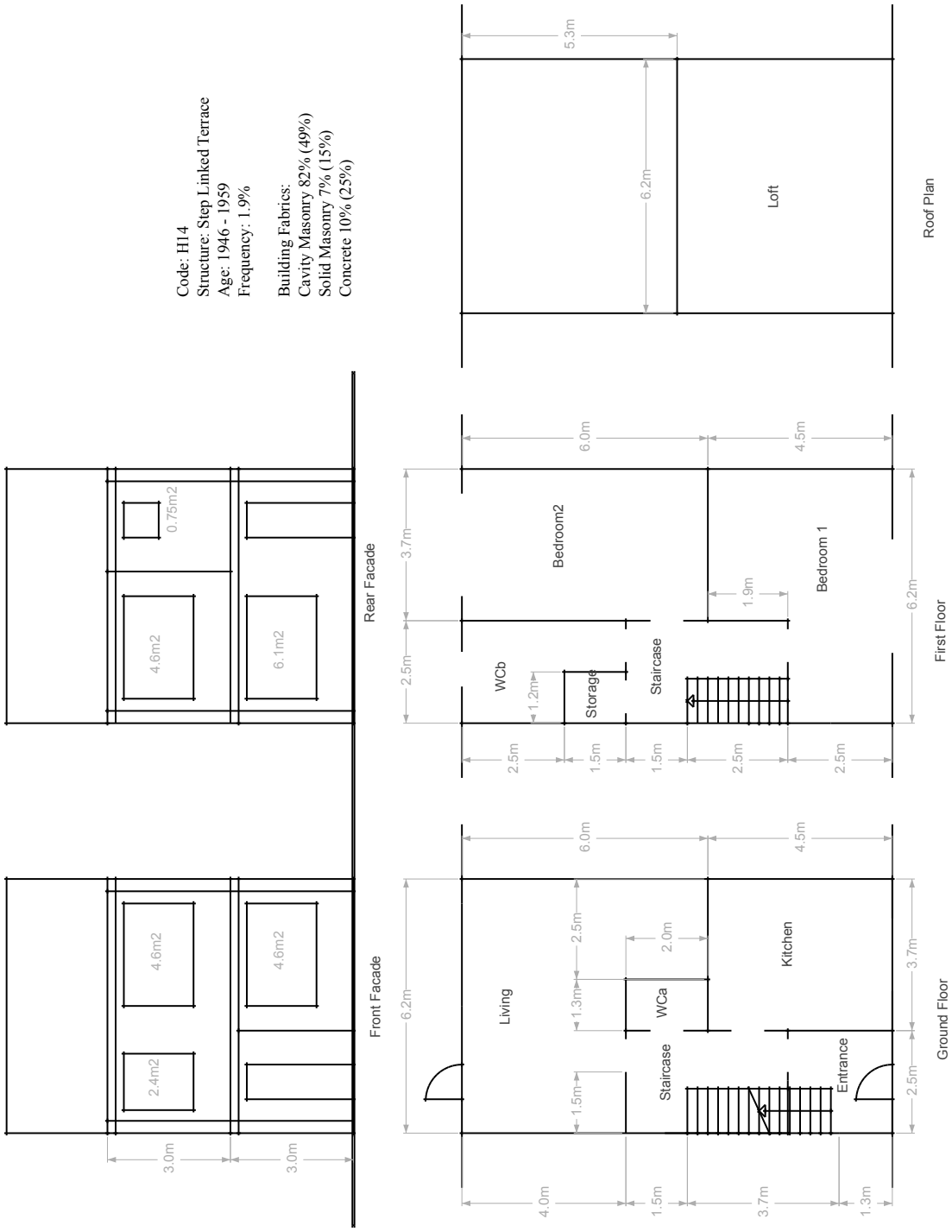
Code: H14
Structure: Step Linked Terrace
Age: 1946 - 1959
Frequency: 1.9%
Building Fabrics:
Cavity Masonry 82% (49%)
Solid Masonry 7% (15%)
Concrete 10% (25%)
Roof Plan
Loft
5.3m
6.2m
First Floor
Bedroom2
Bedroom 1
WCb
Storage
Staircase
6.0m
4.5m
3.7m
2.5m
1.2m
1.9m
Ground Floor
Living
WCa
Kitchen
Staircase
Entrance
2.0m
1.3m
1.5m
4.0m
3.7m
Rear Facade
Front Facade
0.75m2
4.6m2
6.1m2
2.4m2
3.0m

H15

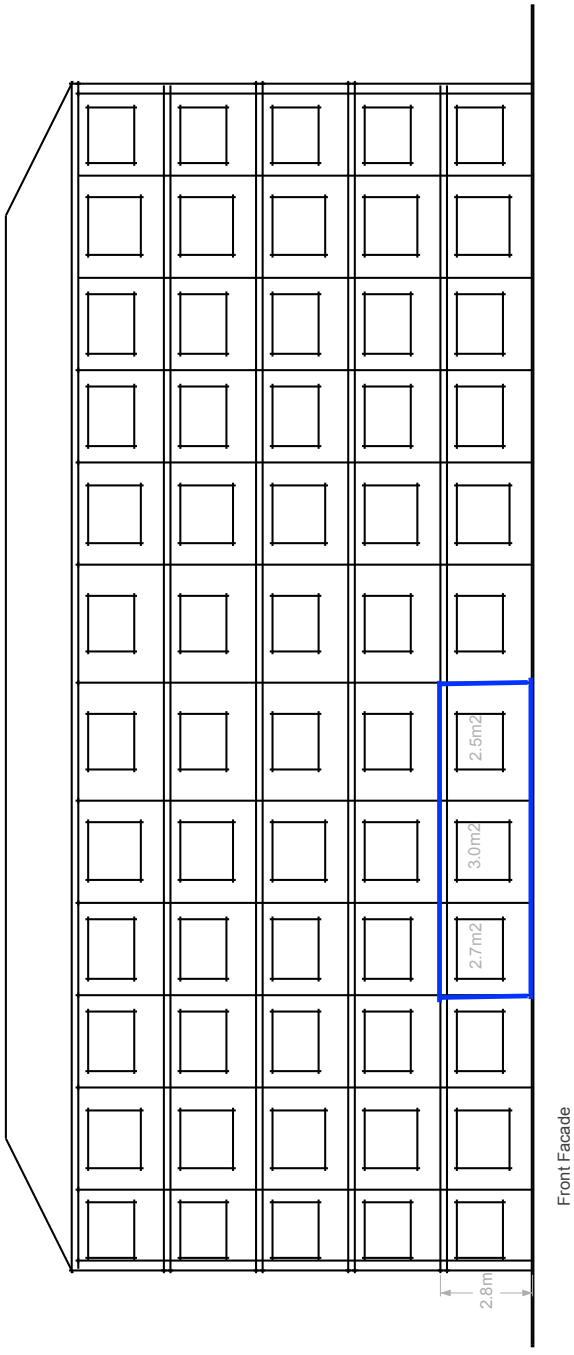

Code: H15
Structure: Purpose Built
Age: 1946 - 1959
Frequency: 1.8%

Building Fabrics:
Cavity Masonry 59% (34%)
Solid Masonry 15% (9%)
Concrete 26% (14%)

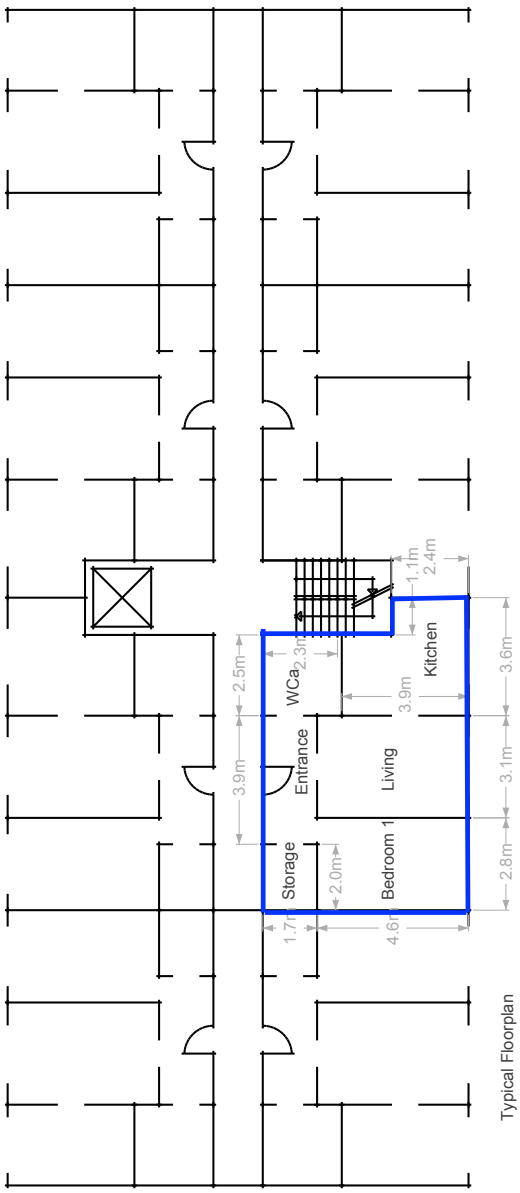

Appendix B

Materials Information

		Isotherm		Liquid Transport				Water Vapour Diffusion Resistance		Moisture Dependent Thermal Conductivity	
Roughness	Rough	RH	Water Content	Water Content	$D_{suction}$	Water Content	$D_{redistribution}$	RH	Resistance	Water Content	Thermal Conductivity
Conductivity {W/m-K}	0.14	0	0.00E+00	0	0.00E+00	0	0.00E+00	0	8.3	0	1.40E-01
Density {kg/m^3}	600	0.5	5.3E+00	3.5	2.00E-10	3.5	2.50E-10			770	7.62E-01
Specific Heat {J/kg-K}	850	0.8	1.07E+01	47	3.70E-09	47	4.00E-10				
Thermal Absorptance	0.9	0.93	2.60E+01	375	6.50E-09	375	1.55E-09				
Solar Absorptance	0.7	0.964	1.71E+02	423	2.50E-08	423	4.00E-09				
Visible Absorptance	0.7	0.99	3.57E+02	470	2.70E-07	470	4.00E-09				
Porosity	0.72	0.995	3.91E+02								
Initial Water (kg/kg)	1.78E-02	0.999	4.05E+02								
		1	4.70E+02								

Table B.1: AAC

		Isotherm		Liquid Transport				Water Vapour Diffusion Resistance		Moisture Dependent Thermal Conductivity	
Roughness	Rough	RH	Water Content	Water Content	$D_{suction}$	Water Content	$D_{redistribution}$	RH	Resistance	Water Content	Thermal Conductivity
Conductivity {W/m-K}	0.02485	0	0	0	0.00E+00	0.00E+00	0.00E+00	0.00E+00	1.00E+00	0.00E+00	2.49E-02
Density {kg/m^3}	1.204	1	0.017285								
Specific Heat {J/kg-K}	1004										
Thermal Absorptance	0.9										
Solar Absorptance	0.7										
Visible Absorptance	0.7										
Porosity	1										
Initial Water (kg/kg)	0.01										

Table B.2: Air Gap

		Isotherm		Liquid Transport				Water Vapour Diffusion Resistance		Moisture Dependent Thermal Conductivity	
Roughness	Rough	RH	Water Content	Water Content	$D_{suction}$	Water Content	$D_{redistribution}$	RH	Resistance	Water Content	Thermal Conductivity
Conductivity {W/m-K}	0.6	0	0.00E+00	0	0.00E+00	0	0.00E+00	0	10	0	6.00E-01
Density {kg/m^3}	1900	0.1	5.50E-01	10	1.50E-10	10	1.50E-10			240	1.74E+00
Specific Heat {J/kg-K}	850	0.2	1.23E+00	190	1.70E-06	190	1.70E-08				
Thermal Absorptance	0.9	0.3	2.11E+00								
Solar Absorptance	0.7	0.4	3.26E+00								
Visible Absorptance	0.7	0.5	4.84E+00								
Porosity	0.24	0.55	5.89E+00								
Initial Water (kg/kg)	0.001	0.6	7.17E+00								
		0.65	8.80E+00								
		0.7	1.09E+01								
		0.75	1.38E+01								
		0.8	1.80E+01								
		0.85	2.45E+01								
		0.9	3.62E+01								
		0.91	3.98E+01								
		0.92	4.39E+01								
		0.93	4.90E+01								
		0.94	5.52E+01								
		0.95	6.31E+01								
		0.96	7.33E+01								
		0.97	8.71E+01								
		0.98	1.07E+02								
		0.99	1.37E+02								
		1	1.90E+02								

Table B.3: Brick

		Isotherm		Liquid Transport				Water Vapour Diffusion Resistance		Moisture Dependent Thermal Conductivity	
Roughness	Rough	RH	Water Content	Water Content	$D_{suction}$	Water Content	$D_{redistribution}$	RH	Resistance	Water Content	Thermal Conductivity
Conductivity {W/m-K}	1.6	0	0	0	0	0	0	0	180	0	1.6
Density {kg/m^3}	2300	0.05	27	72	7.41E-11	72	7.41E-12			180	2.602
Specific Heat {J/kg-K}	850	0.1	32	85	2.53E-10	85	2.53E-11				
Thermal Absorptance	0.9	0.15	34	100	1.01E-09	100	1.01E-10				
Solar Absorptance	0.7	0.2	35	118	1.28E-09	118	1.28E-10				
Visible Absorptance	0.7	0.3	37								
Porosity	0.18	0.4	40								
Initial Water (kg/kg)	0.01	0.5	48								
		0.6	58								
		0.7	72								
		0.8	85								
		0.9	100								
		0.95	118								
		1	150								

Table B.4: Concrete

		Isotherm		Liquid Transport				Water Vapour Diffusion Resistance		Moisture Dependent Thermal Conductivity	
Roughness	Rough	RH	Water Content	Water Content	$D_{suction}$	Water Content	$D_{redistribution}$	RH	Resistance	Water Content	Thermal Conductivity
Conductivity {W/m-K}	0.071	0	0	0	0.00E+00	0	0.00E+00	0	1.3	0	0.071
Density {kg/m^3}	60	0.5	1.81E+00	800	1.00E-10	800	1.00E-11			10	0.070879
Specific Heat {J/kg-K}	850	0.8	3.04E+00	900	1.00E-10	900	1.00E-11			20	0.070879
Thermal Absorptance	0.9	0.9	5.1E+00	950	5.00E-07	950	5.00E-08			50	0.070879
Solar Absorptance	0.7	0.95	7.05E+00	980	3.30E-06	980	3.30E-07			100	0.070879
Visible Absorptance	0.7	0.99	9.43E+00							628.4	0.2458
Porosity	0.98	0.995	20.303E+00							937.3	0.514352
Initial Water (kg/kg)	0.01	0.9995	6.28E+02							980	0.561
		0.99995	9.37E+02								
		1.0	980								

Table B.5: Glass Fibre

		Isotherm		Liquid Transport				Water Vapour Diffusion Resistance		Moisture Dependent Thermal Conductivity	
Roughness	Rough	RH	Water Content	Water Content	$D_{suction}$	Water Content	$D_{redistribution}$	RH	Resistance	Water Content	Thermal Conductivity
Conductivity {W/m-K}	0.2	0	0	0	0	0	0	0	8.3	0	0.2
Density {kg/m^3}	850	0.5	3.6	60	0.000000003	60	3.00E-09			650	1.424
Specific Heat {J/kg-K}	850	0.65	5.2	100	1.00E-07	100	8.00E-09				
Thermal Absorptance	0.9	0.8	6.3	160	1.00E-07	160	8.00E-09				
Solar Absorptance	0.6	0.9	11	240	1.20E-07	240	1.30E-08				
Visible Absorptance	0.7	0.93	17	320	2.20E-07	320	1.00E-07				
Porosity	0.65	0.95	19	360	6.00E-07	360	3.00E-07				
Initial Water (kg/kg)	0.2	0.99	113	380	9.00E-07	380	7.00E-07				
		0.995	124	400	4.50E-06	400	1.00E-06				
		0.999	328								
		0.9995	378								
		1	400								

Table B.6: Gypsum

		Isotherm		Liquid Transport				Water Vapour Diffusion Resistance		Moisture Dependent Thermal Conductivity	
Roughness	Rough	RH	Water Content	Water Content	$D_{suction}$	Water Content	$D_{redistribution}$	RH	Resistance	Water Content	Thermal Conductivity
Conductivity {W/m-K}	0.2	0	0	0	0	0	0	0	8.3	0	0.2
Density {kg/m^3}	850	0.5	3.6	60	3.00E-09	60	3.00E-09			650	1.424
Specific Heat {J/kg-K}	850	0.65	5.2	100	1.00E-07	100	8.00E-09				
Thermal Absorptance	0.9	0.8	6.3	160	1.00E-07	160	8.00E-09				
Solar Absorptance	0.6	0.9	11	240	1.20E-07	240	1.30E-08				
Visible Absorptance	0.7	0.93	17	320	2.20E-07	320	1.00E-07				
Porosity	0.65	0.95	19	360	6.00E-07	360	3.00E-07				
Initial Water (kg/kg)	0.2	0.99	113	380	9.00E-07	380	7.00E-07				
		0.995	124	400	4.50E-06	400	1.00E-06				
		0.999	328								
		0.9995	378								
		1	400								

Table B.7: Plasterboard

		Isotherm		Liquid Transport				Water Vapour Diffusion Resistance		Moisture Dependent Thermal Conductivity	
Roughness	Rough	RH	Water Content	Water Content	$D_{suction}$	Water Content	$D_{redistribution}$	RH	Resistance	Water Content	Thermal Conductivity
Conductivity {W/m-K}	0.23	0	0	0	0	0	0	0	130	0	0.09
Density {kg/m^3}	455	0.2	30	20	3.2E-13	20	3.2E-13			730	0.278
Specific Heat {J/kg-K}	1500	0.5	45	600	9.2E-12	600	9.2E-12				
Thermal Absorptance	0.9	0.65	57								
Solar Absorptance	0.7	0.8	80								
Visible Absorptance	0.7	0.9	100								
Porosity	0.73	0.96	125								
Initial Water (kg/kg)	0.05	0.99	330								
		0.996	350								
		0.999	390								
		0.9996	430								
		0.9999	510								
		1	600								

Table B.8: Spruce

Appendix C

Drying of Wall Profiles

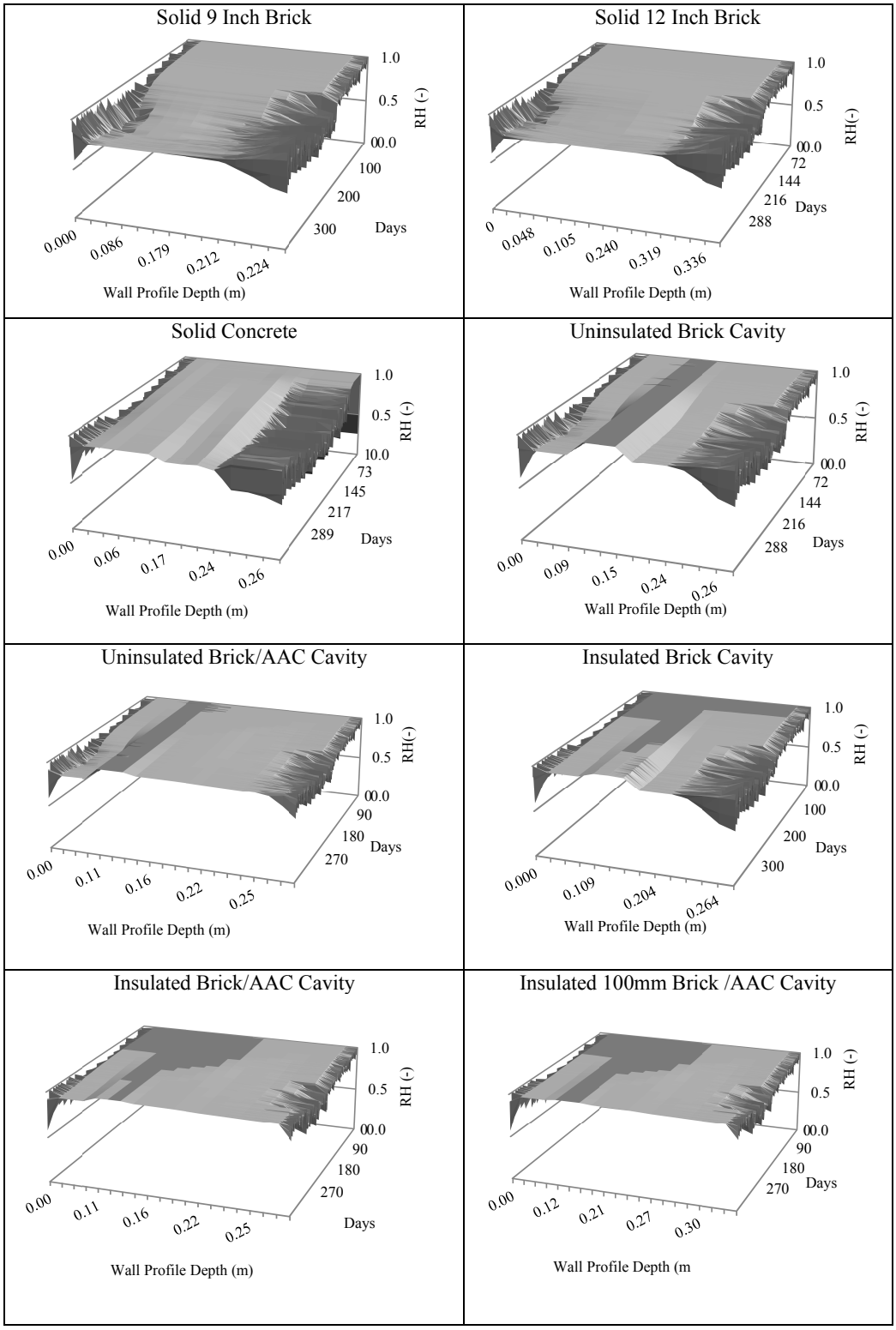

Figure C.1: RH across the profile of naturally drying walls

Appendix D

Drying Dwellings - Windows Open

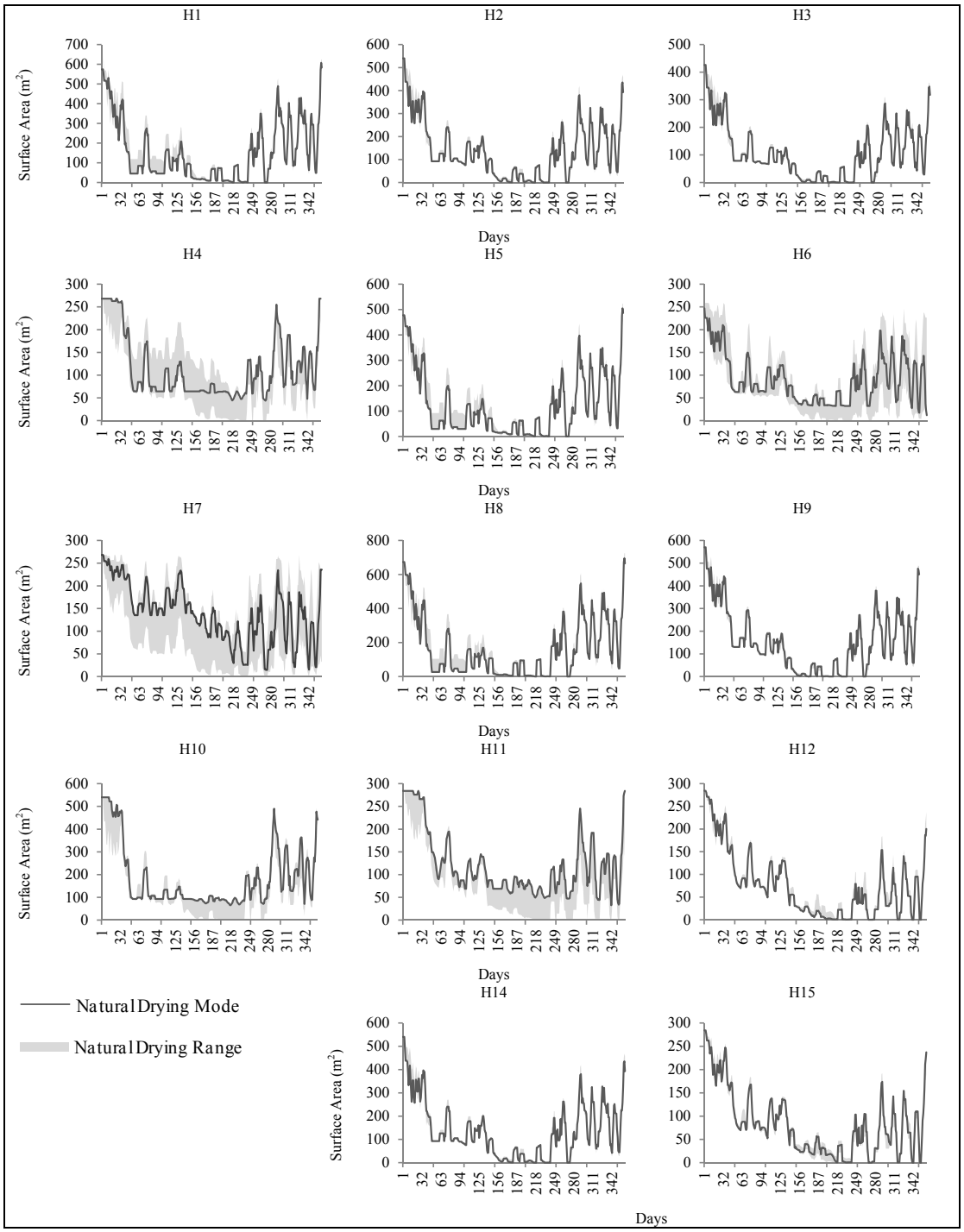

Figure D.1: *A. versicolor*

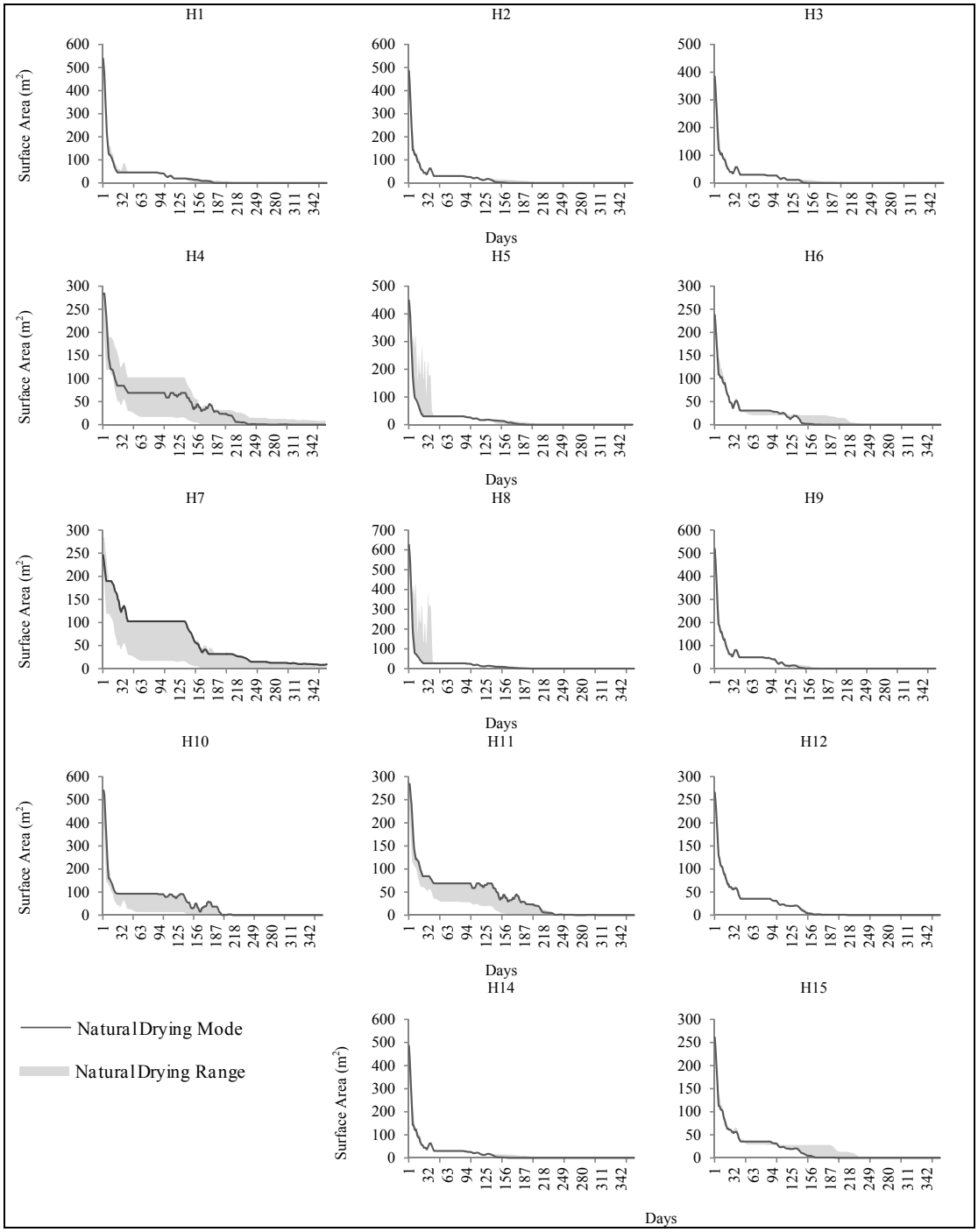

Figure D.2: *S. chartarum*

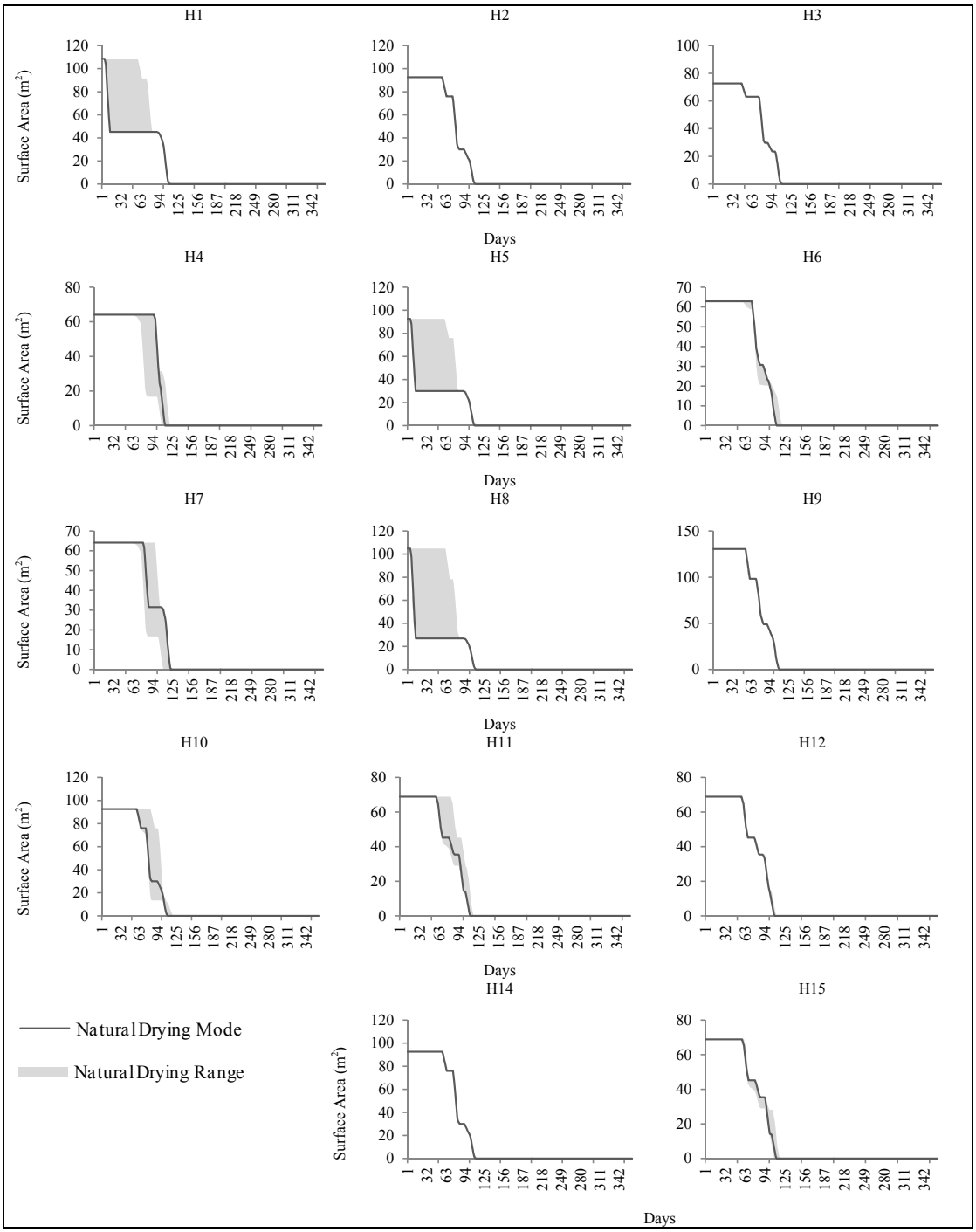

Figure D.3: *E. coli*

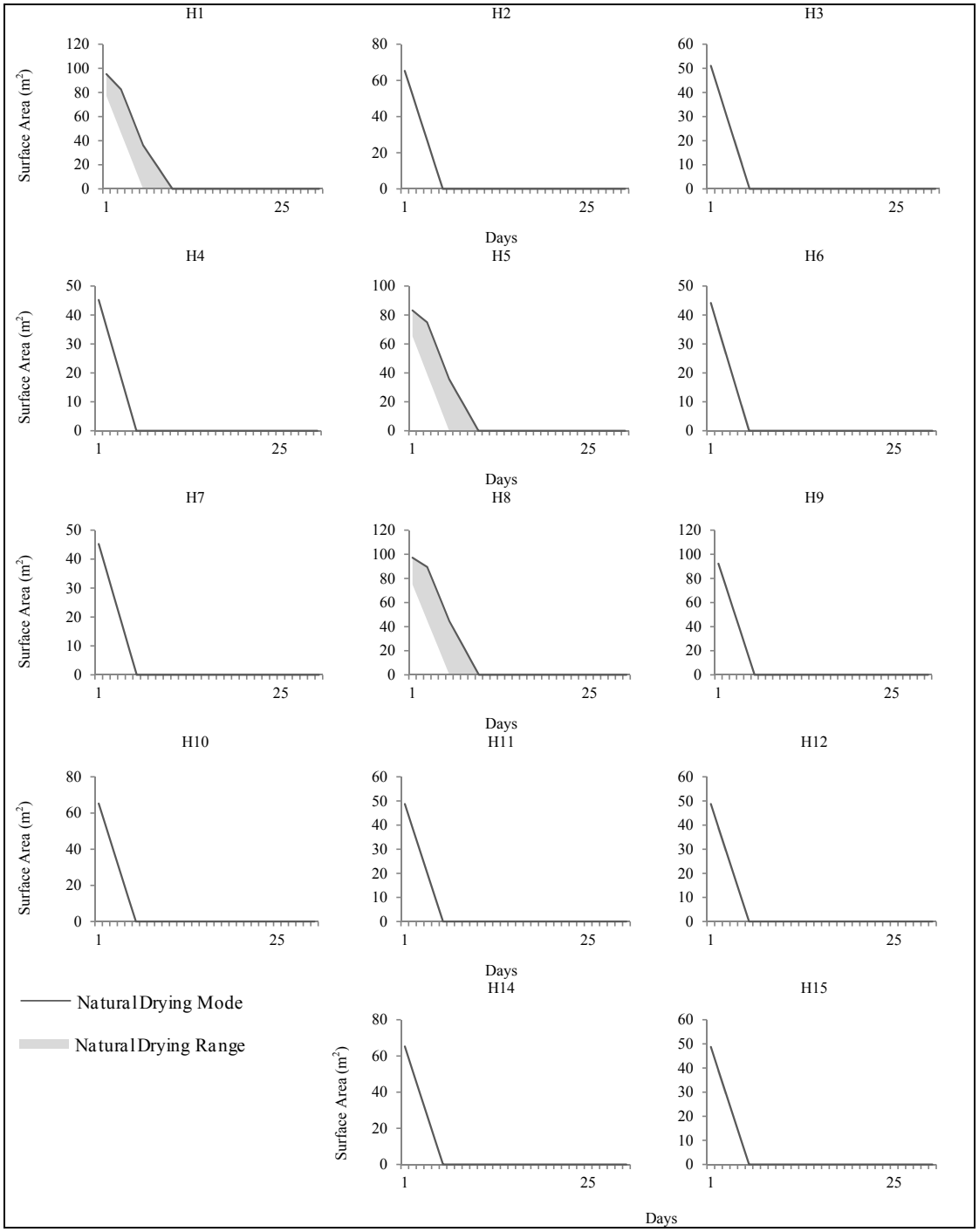

Figure D.4: *Salmonella*

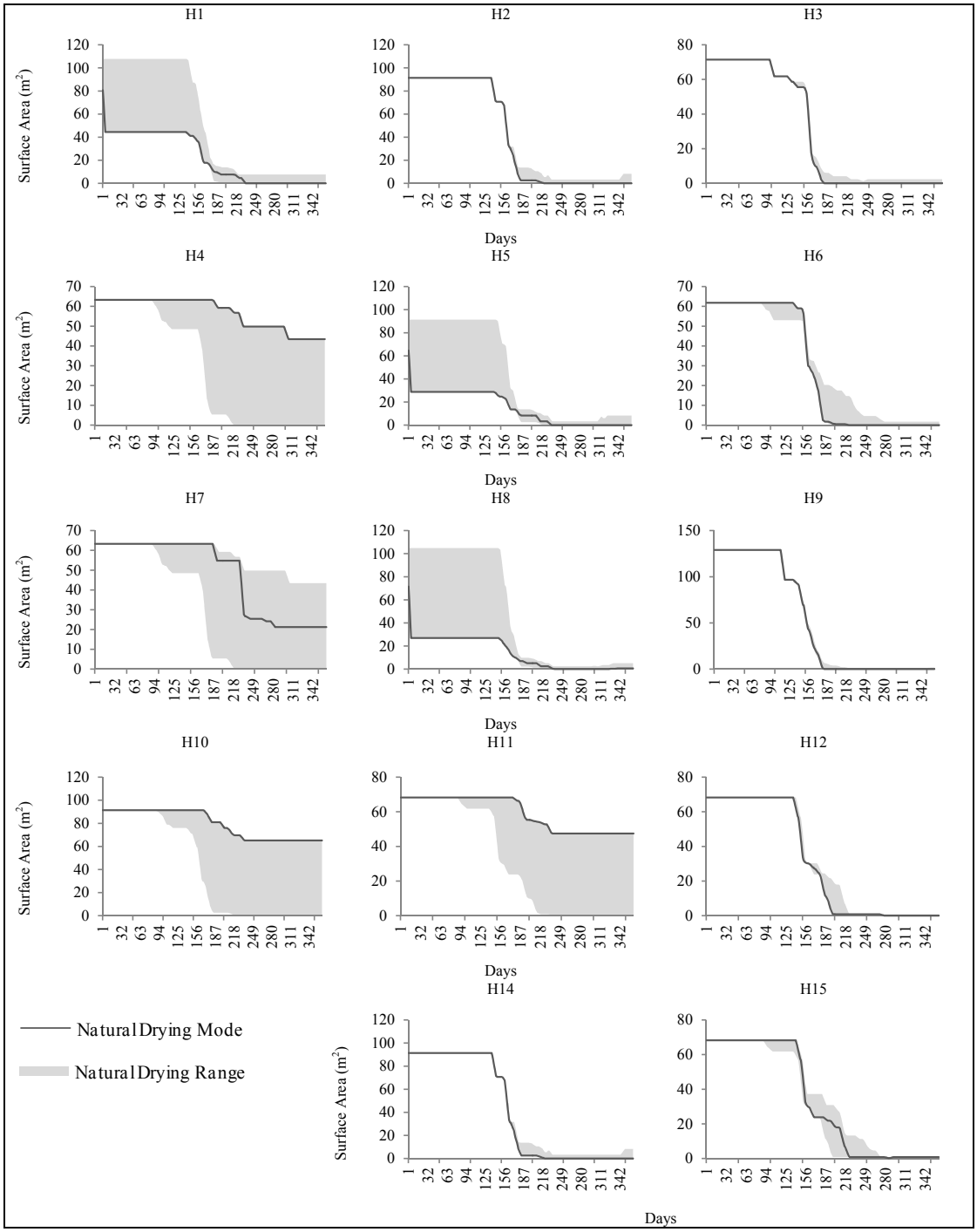

Figure D.5: *Listeria*

Appendix E

Drying Dwellings - Abandoned

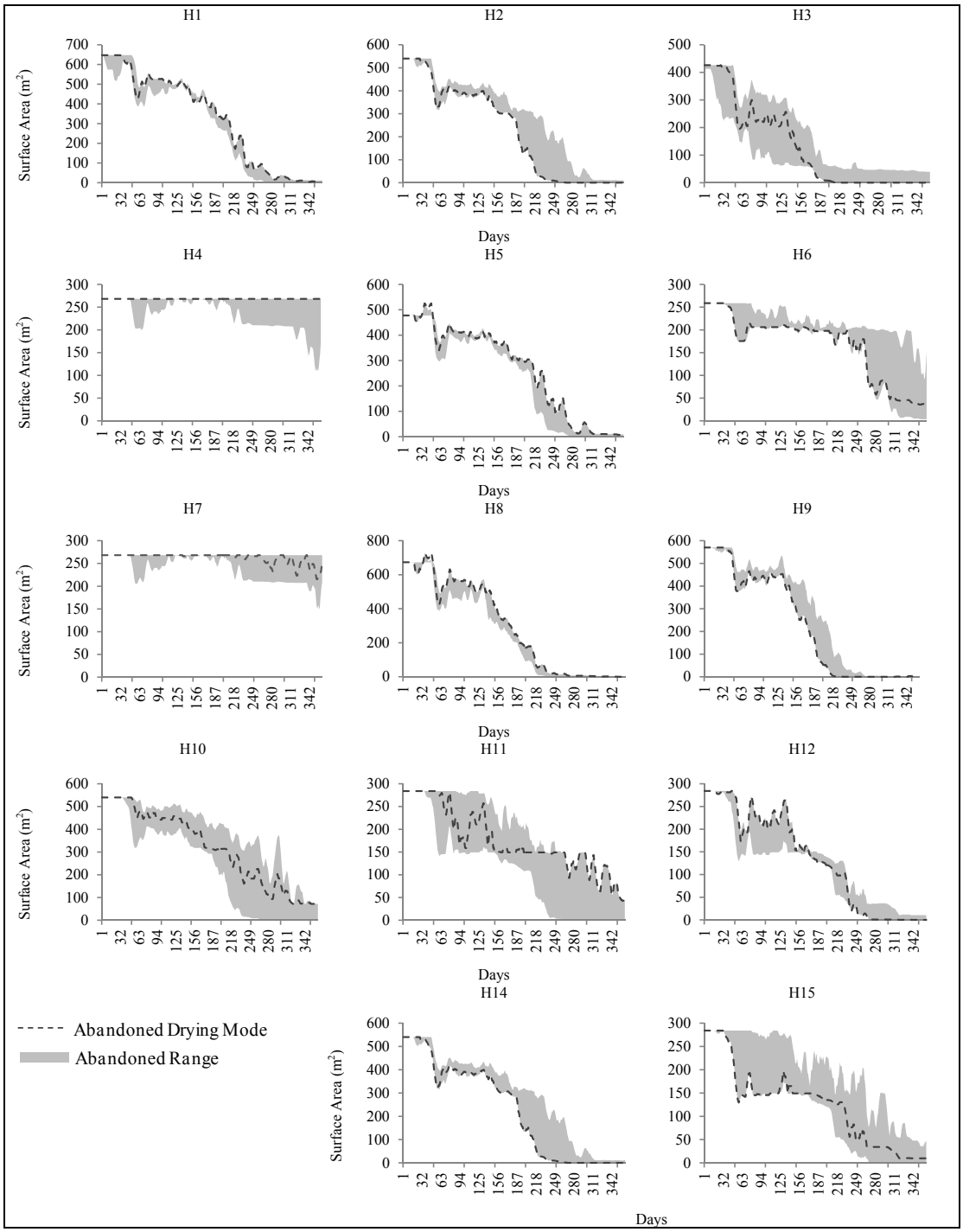

Figure E.1: *A. versicolor*

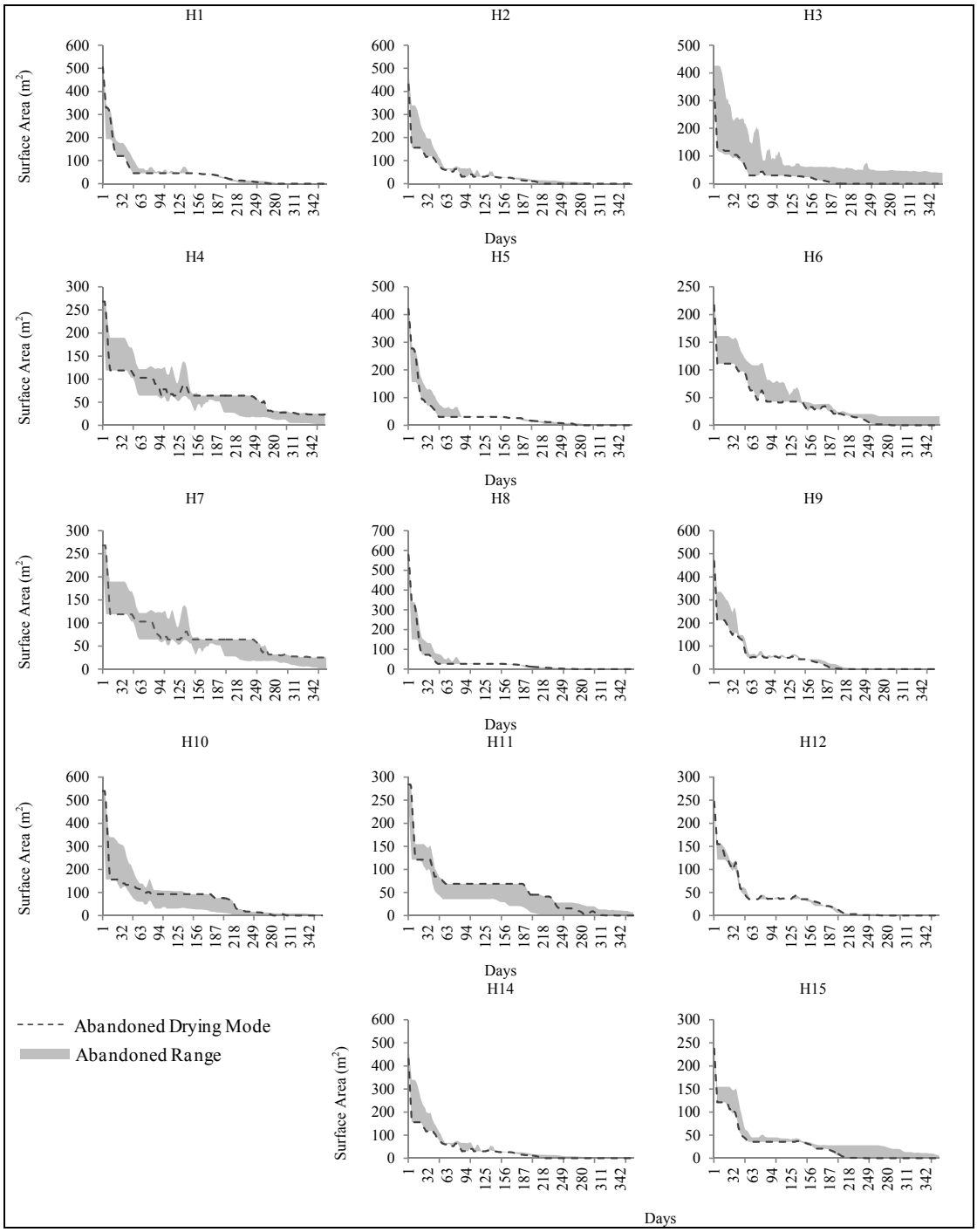

Figure E.2: *S. chartarum*

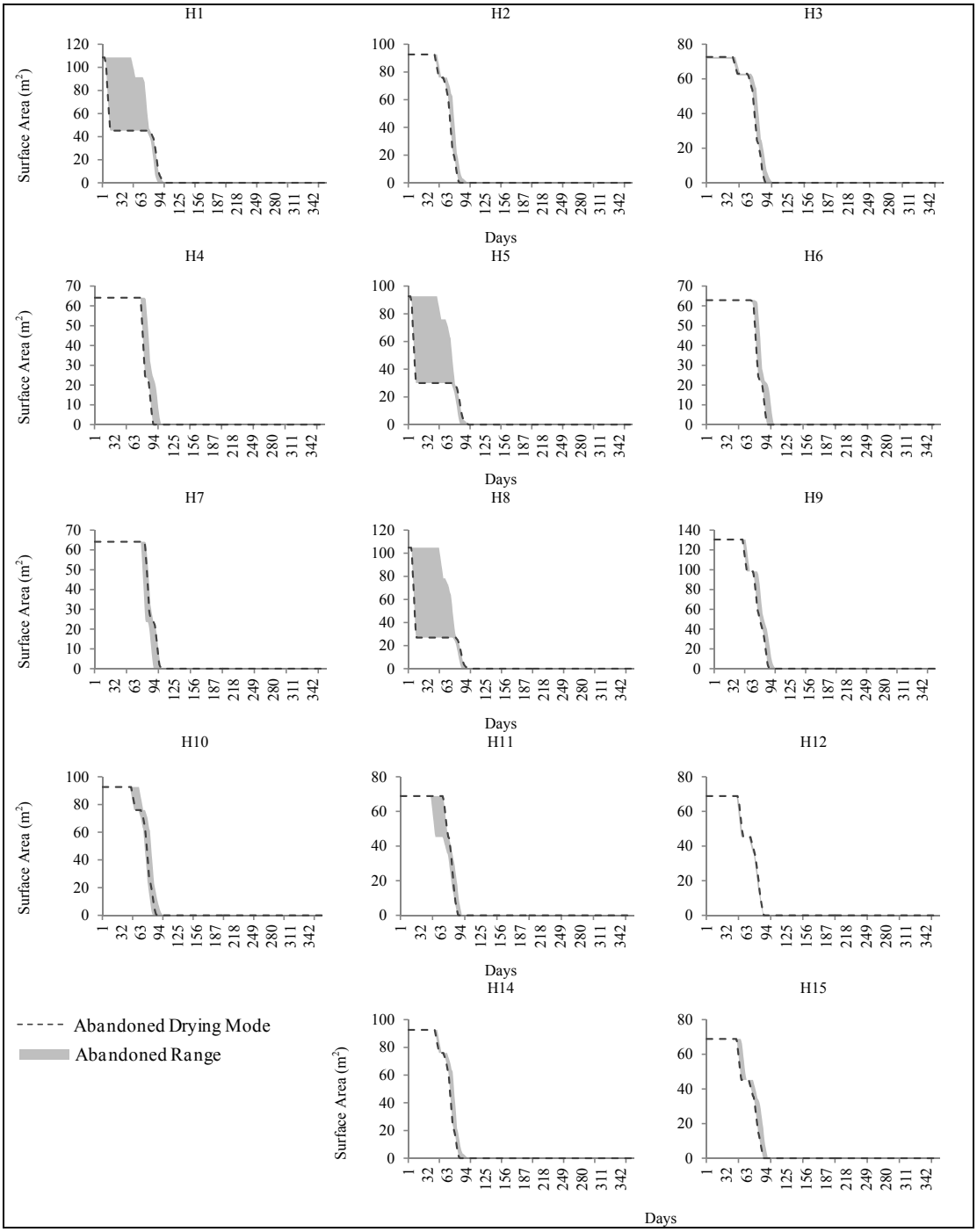

Figure E.3: *E. coli*

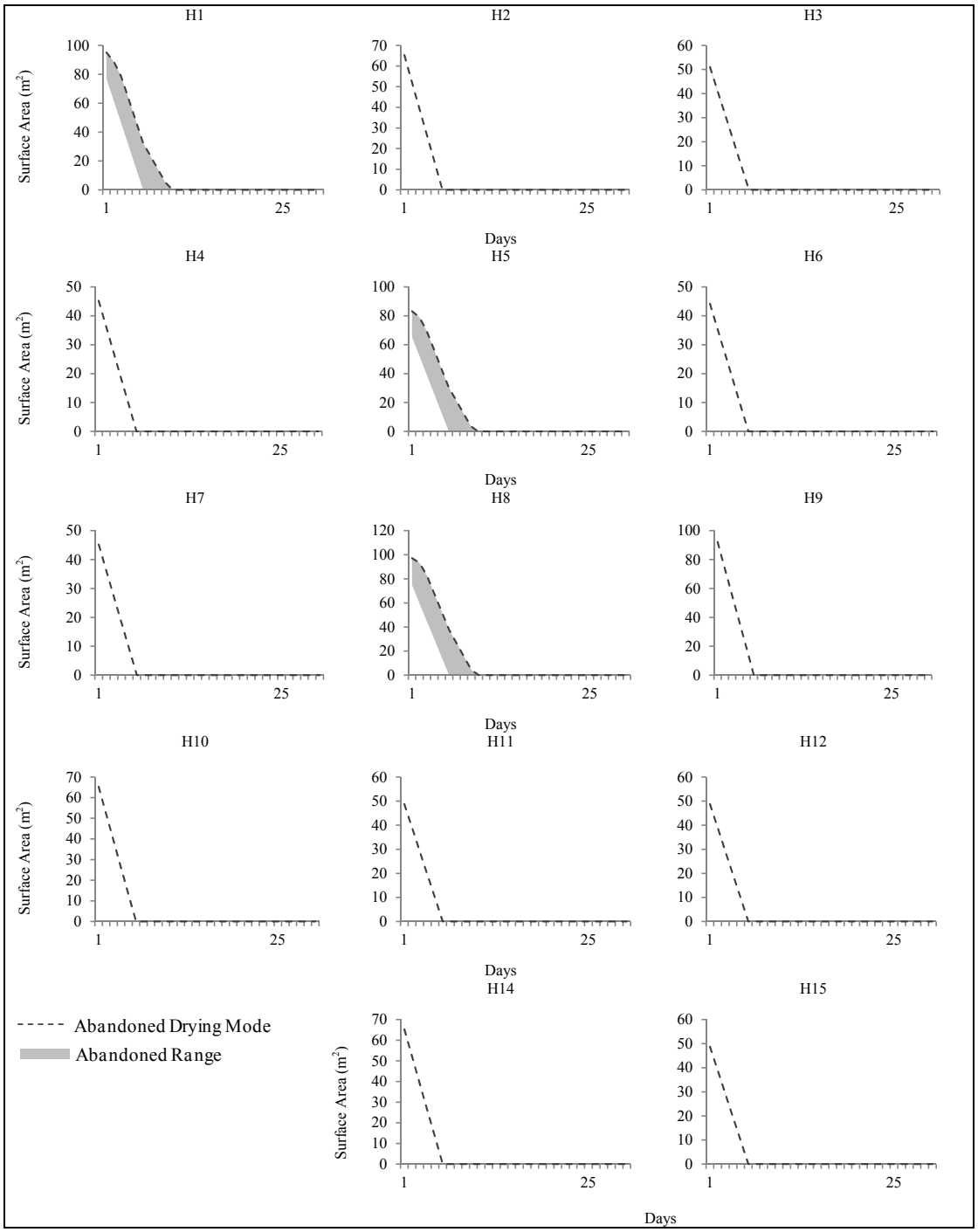

Figure E.4: *Salmonella*

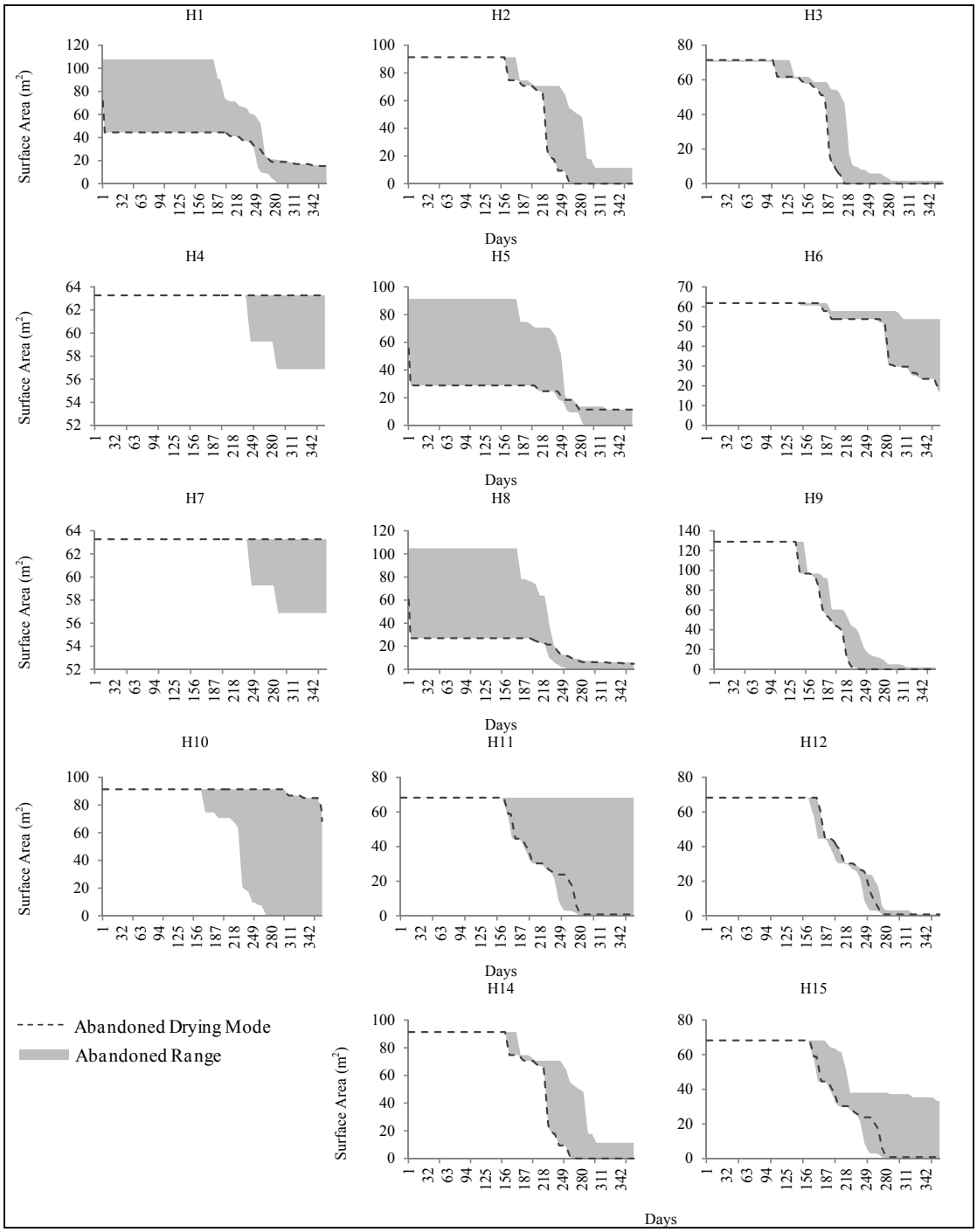

Figure E.5: *Listeria*

Appendix F

Drying Dwellings - Windows Open and Central Heating On

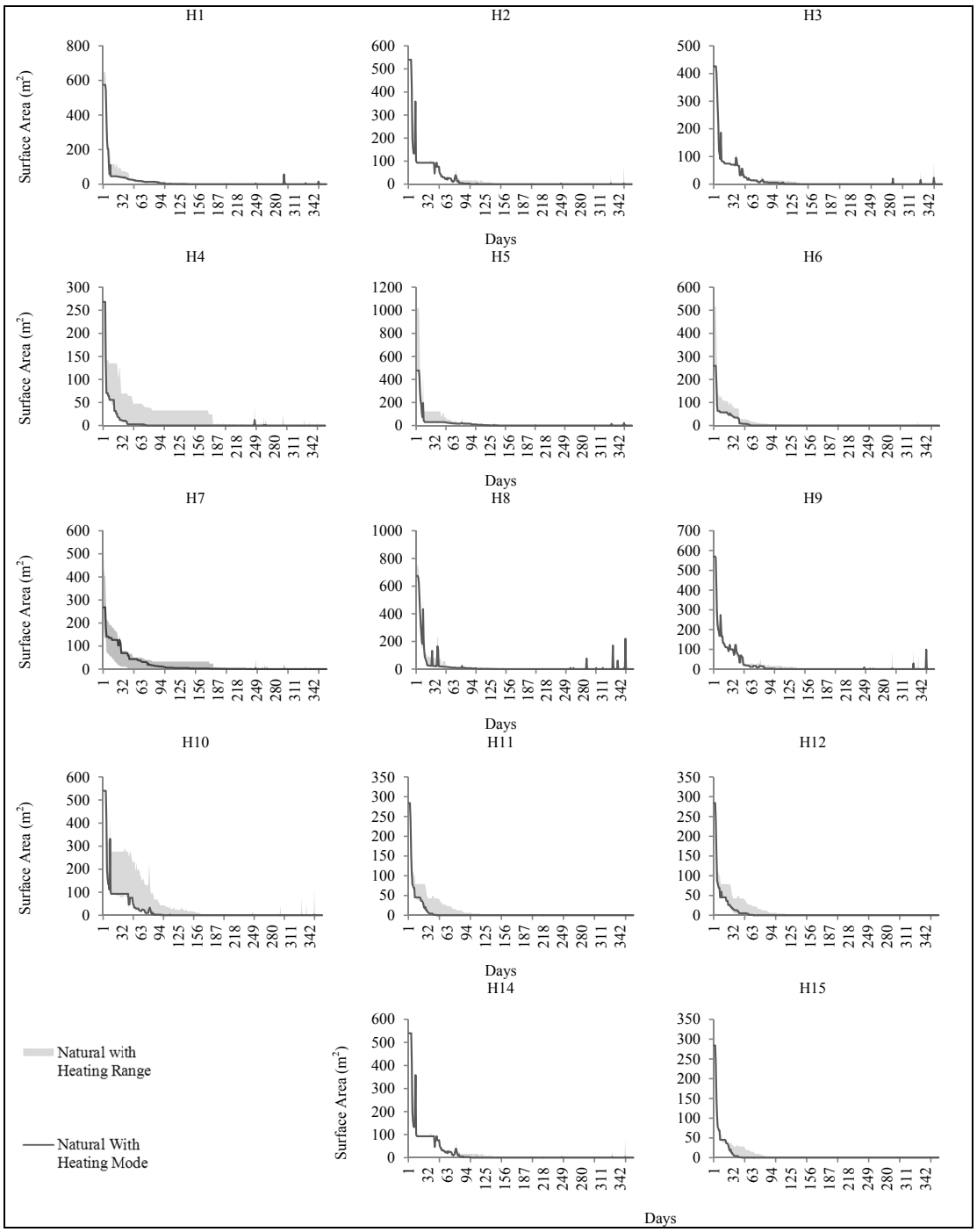

Figure F.1: *A. versicolor*

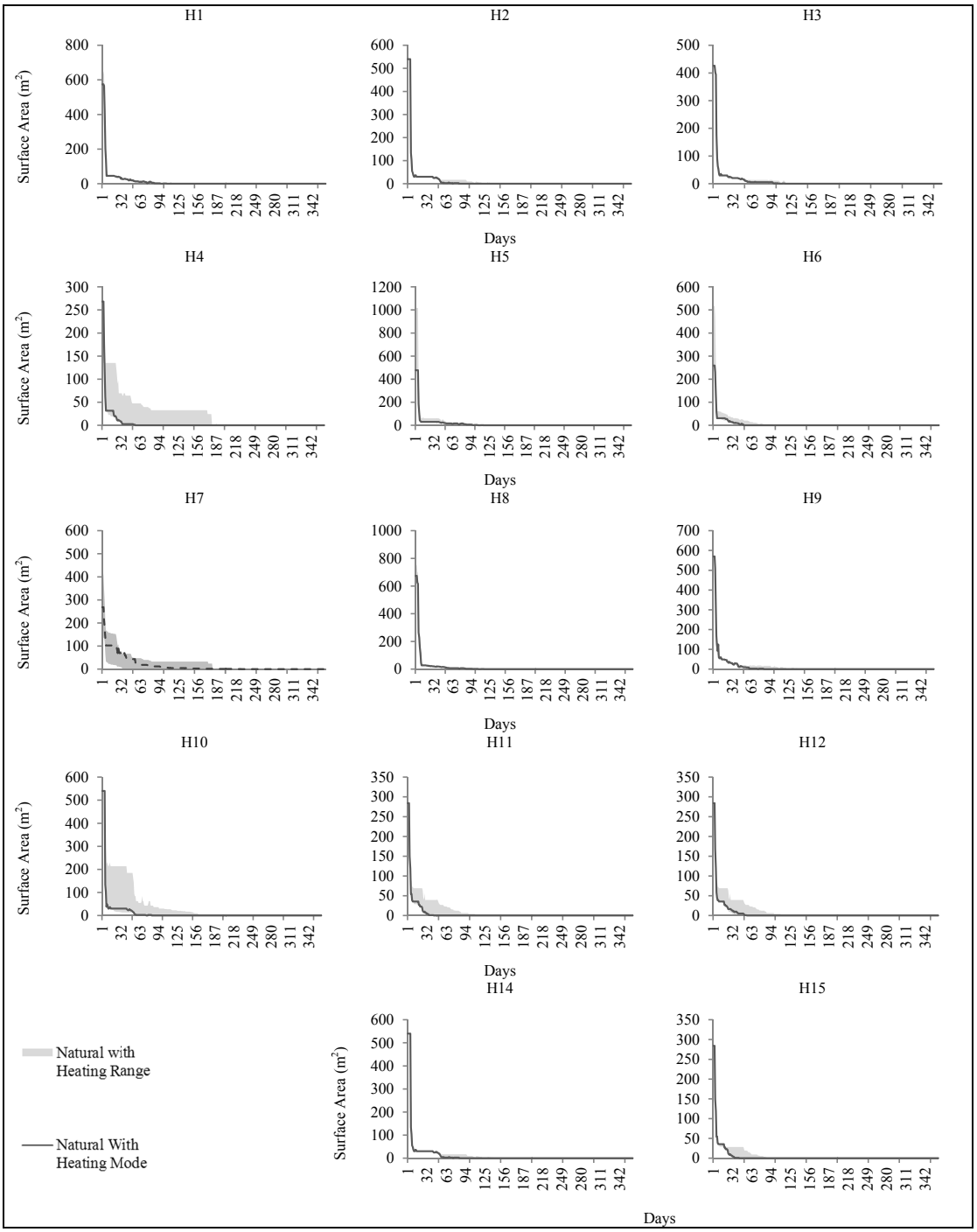

Figure F.2: *S. chartarum*

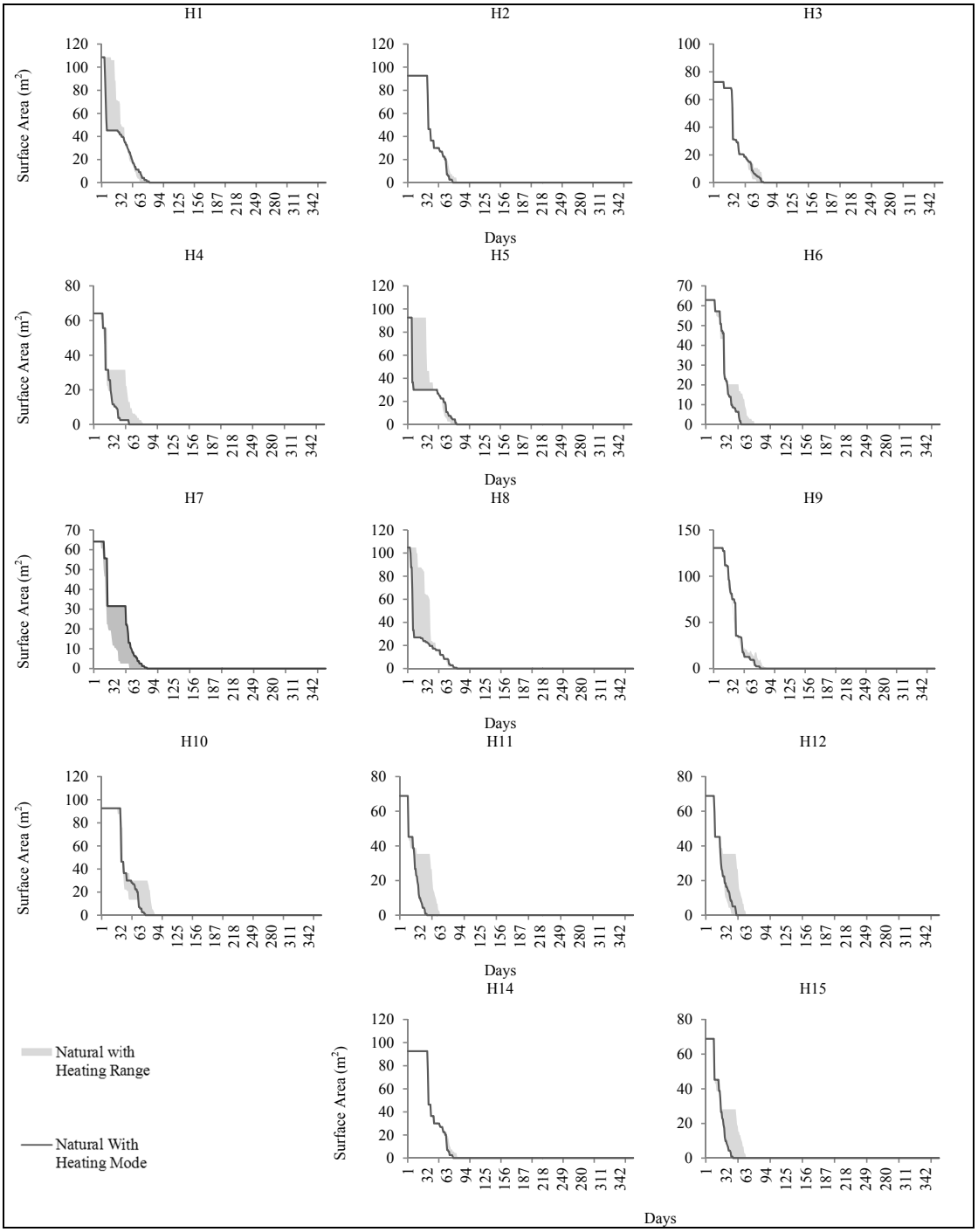

Figure F.3: *E. coli*

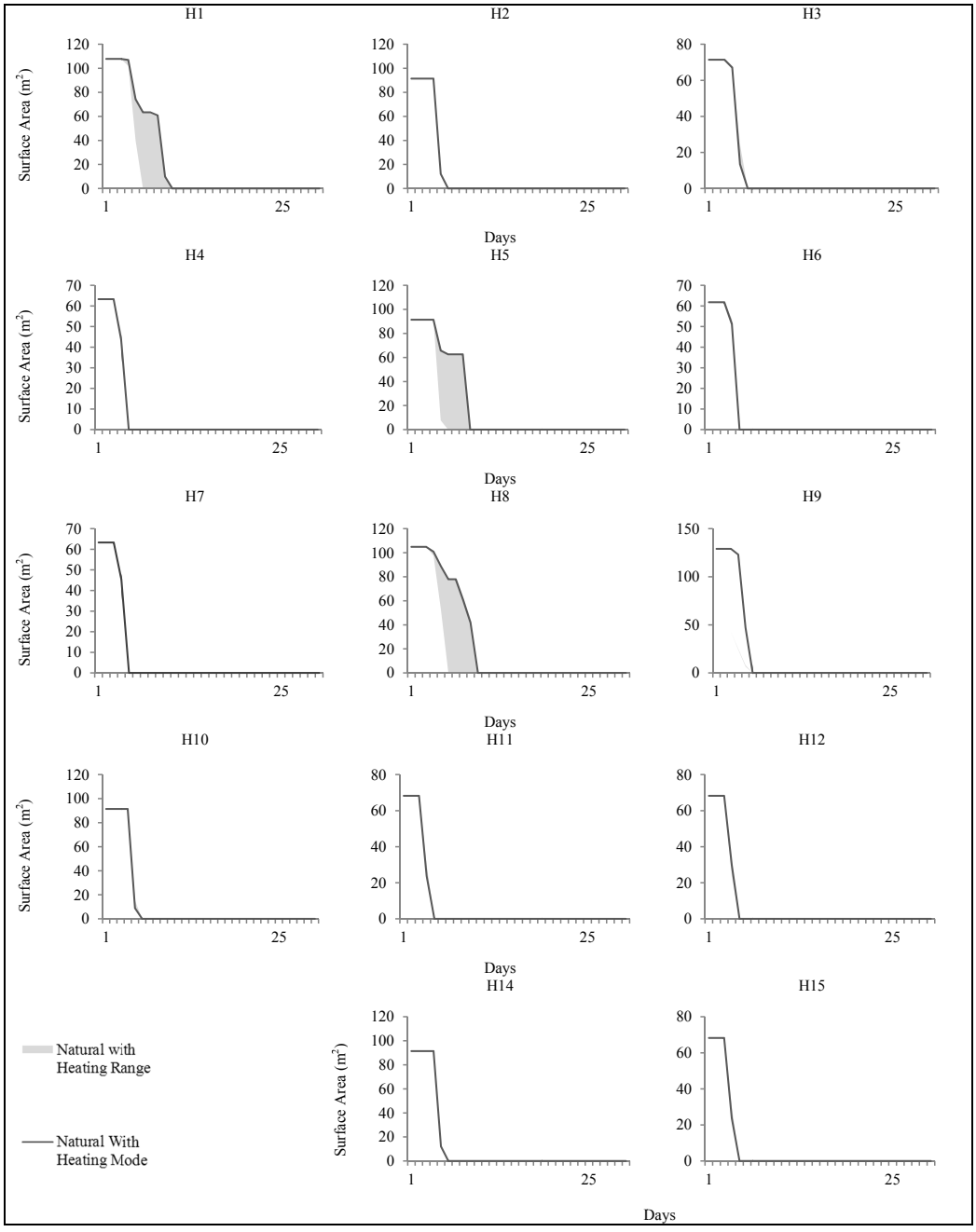

Figure F.4: *Salmonella*

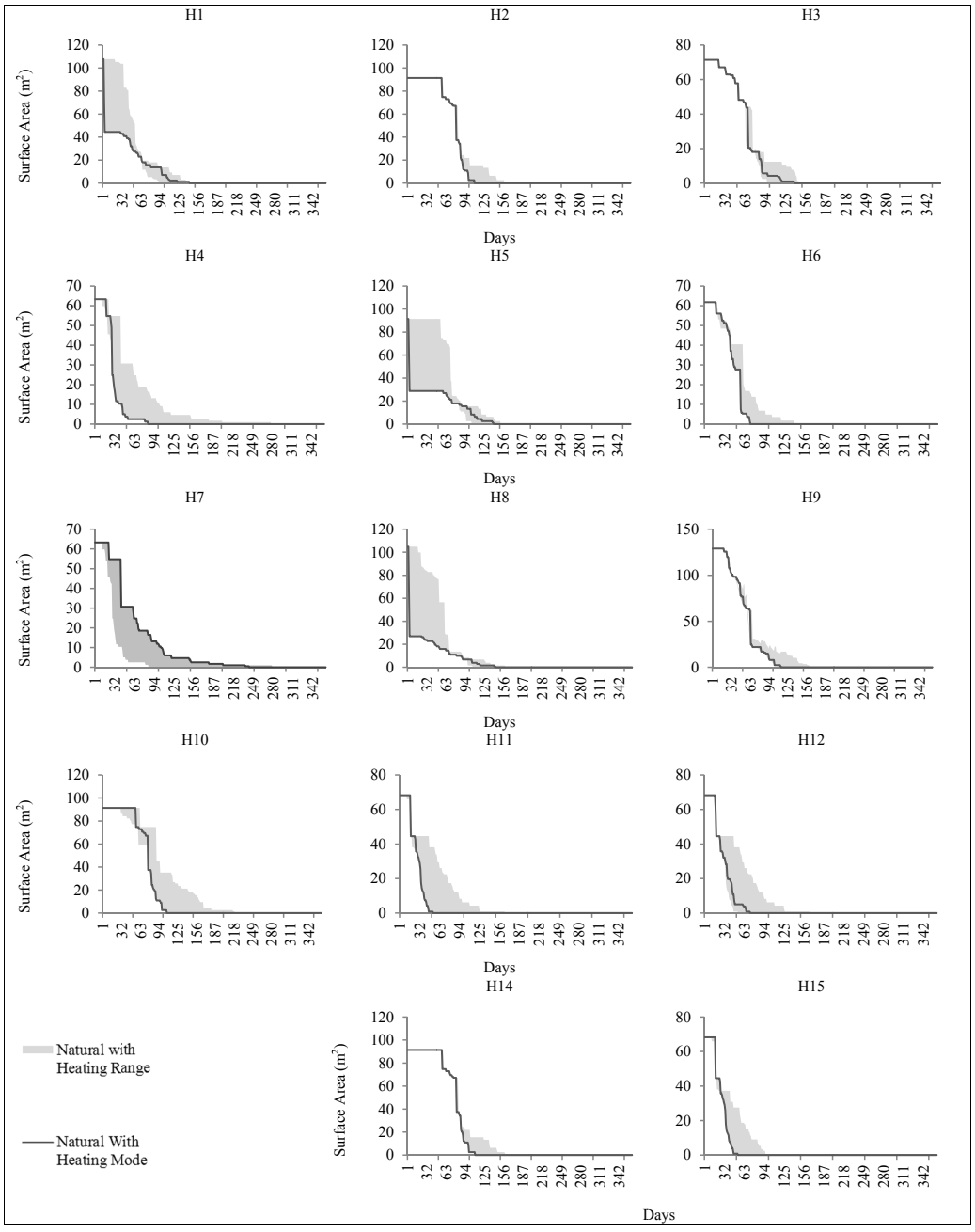

Figure F.5: *Listeria*

Appendix G

Walls Drying with Forced Heating

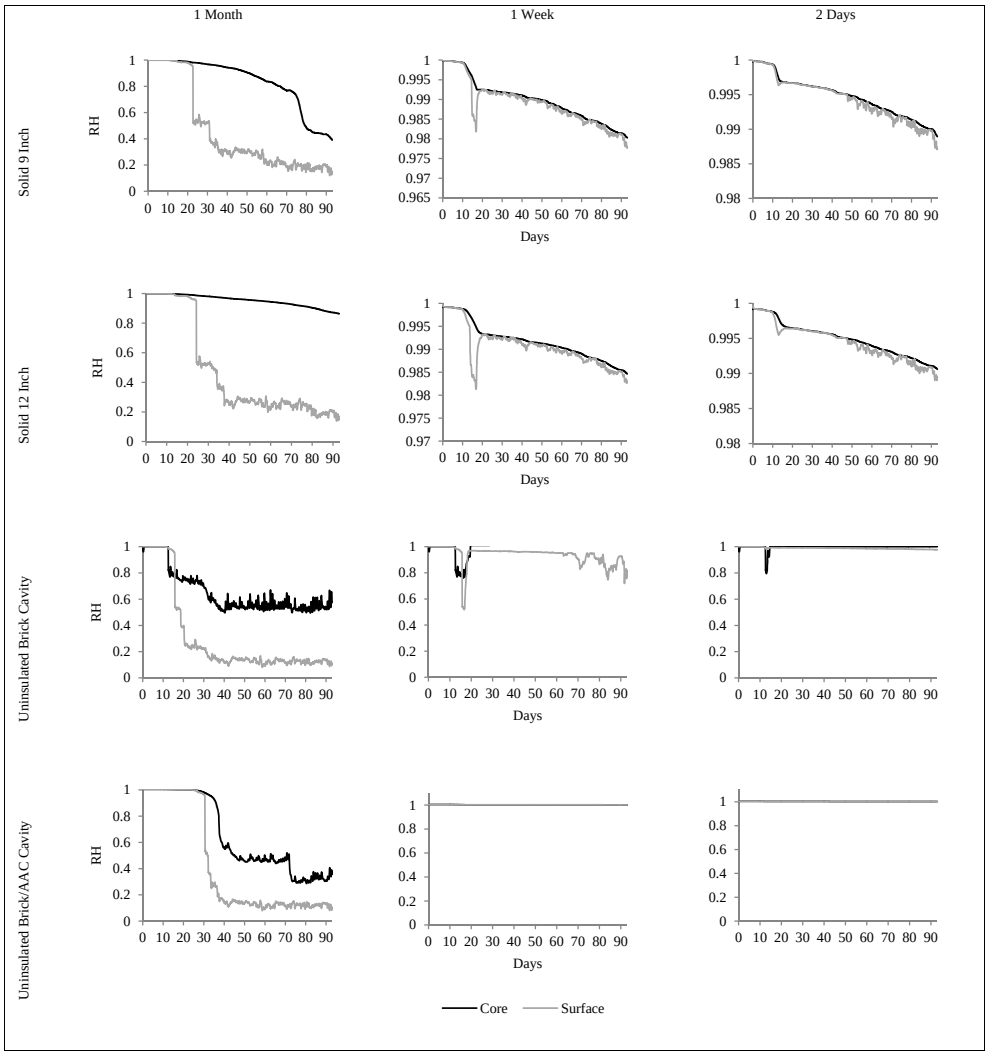
1 Month
1 Week
2 Days
Solid 9 Inch
Solid 12 Inch
Uninsulated Brick Cavity
Uninsulated Brick/AAC Cavity
RH
Days
Core
Surface

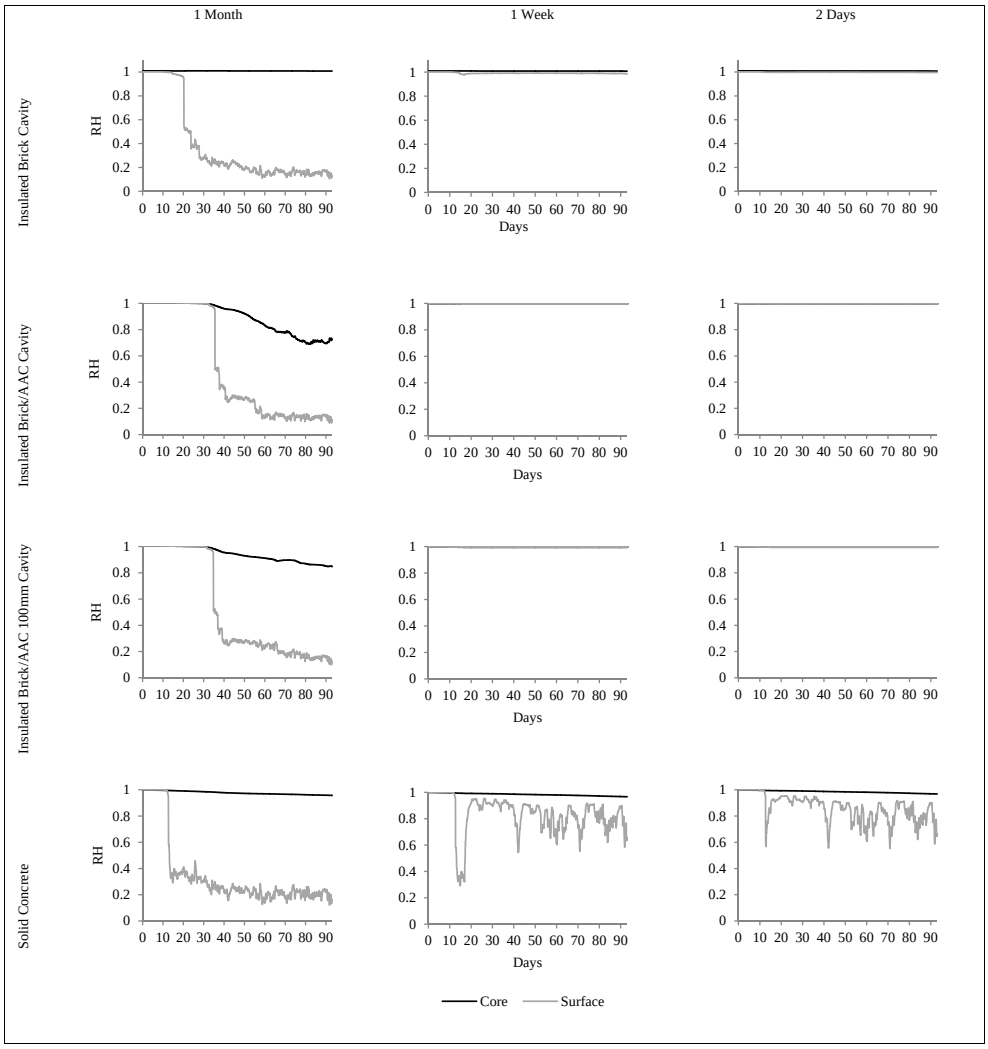
1 Month
1 Week
2 Days
Insulated Brick Cavity
Insulated Brick/AAC Cavity
Insulated Brick/AAC 100mm Cavity
Solid Concrete
RH
Days
Core
Surface

Appendix H

Duration of Contaminant Risk on Internal Surfaces for Natural Ventilation

Dwelling	Wall	*A. versicolor*	*S. chartarum*	*E. coli*	*Salmonella*	*Listeria*
H01	Solid Brick Wall & Suspended Wooden Floor	4826	4322	2666	242	5594
H02	Uninsulated Brick/Brick Cavity	4322	3866	2666	146	5306
	Insulated Brick/Brick Cavity	5618	5330	2762	146	10000
H03	Uninsulated Brick/Brick Cavity	3890	3410	2642	146	4370
	Insulated Brick/Brick Cavity	5258	4994	2762	146	5810
H04	Uninsulated Brick/AAC Cavity	10000	5618	2738	146	10000
	Insulated Brick/AAC Cavity	10000	6530	2762	146	10000
H05	Solid Brick Wall & Suspended Wooden Floor	5114	4466	2642	242	5594
H06	Uninsulated Brick/Brick Cavity	4586	3914	2690	146	5354
	Insulated Brick/Brick Cavity	6266	5594	2786	146	10000
H07	Uninsulated Brick/AAC Cavity	10000	5618	2738	146	10000
	Insulated Brick/AAC Cavity	10000	6530	2762	146	10000
H08	Solid Brick Wall & Suspended Wooden Floor	5186	4754	2690	242	5690
H09	Uninsulated Brick/Brick Cavity	4130	3602	2642	146	4370
	Insulated Brick/Brick Cavity	5234	4826	2738	146	5642
H10	Uninsulated Brick/AAC Cavity	10000	3890	2714	146	10000
	Insulated Brick/AAC Cavity	10000	6506	2762	146	10000
H11	Uninsulated Brick/AAC Cavity	10000	6506	2762	146	10000
	Insulated Brick/AAC Cavity	10000	7706	2786	146	10000
H12	Solid Brick Wall	5594	5186	2618	146	6674
H14	Uninsulated Brick/Brick Cavity	4322	3866	2666	146	5306
	Insulated Brick/Brick Cavity	5618	5330	2762	146	10000
H15	Uninsulated Brick/Brick Cavity	5234	4754	2690	146	6842
	Insulated Brick/Brick Cavity	6530	5906	2762	146	10000

Table H.1: Drying times.

Appendix I

Drying Behaviour of Modal Wall Types for Different Flood Heights

A. versicolor

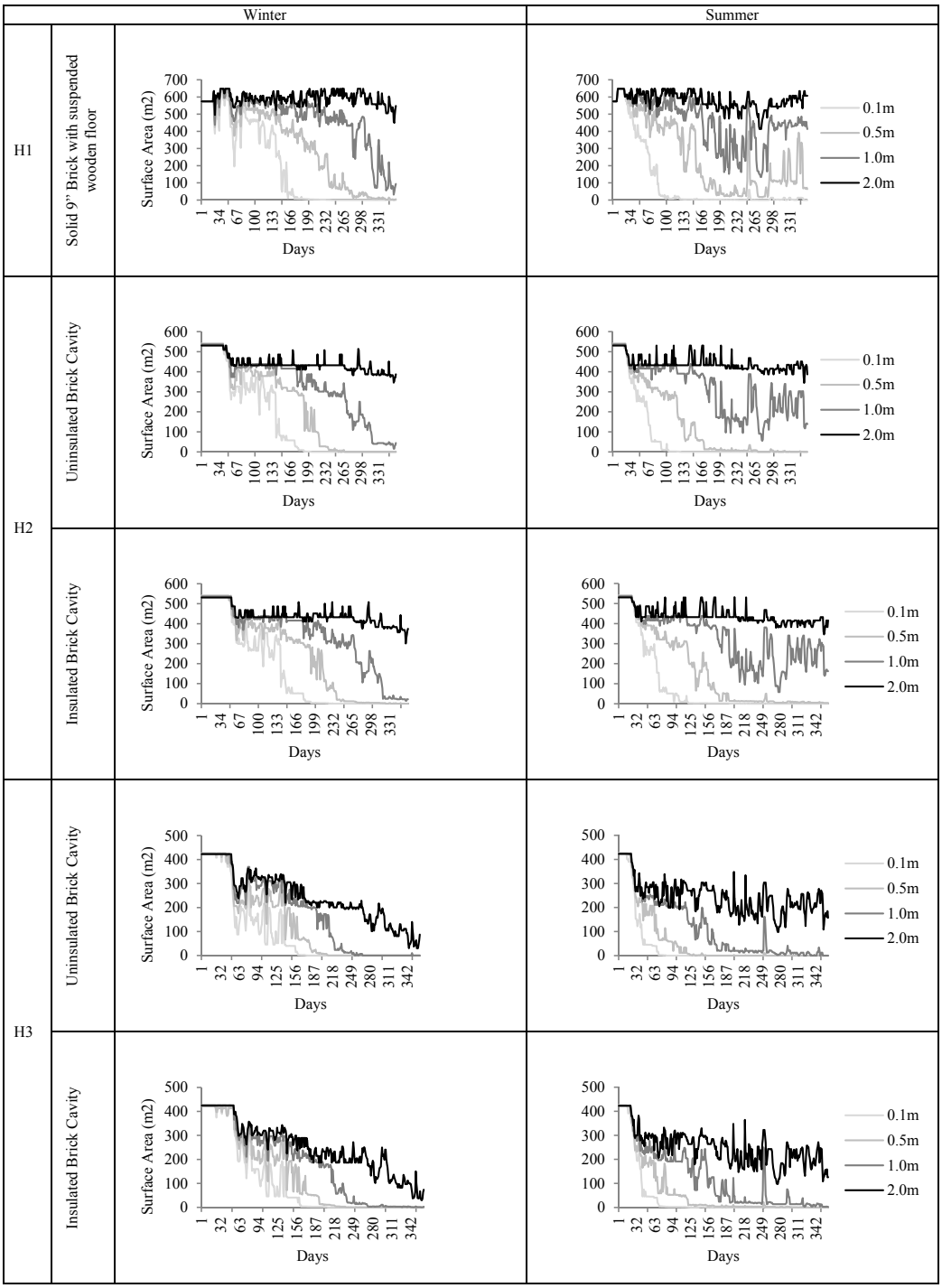

A. versicolor continued...

		Winter	Summer
H4	Uninsulated Brick Cavity	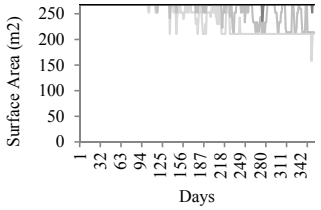	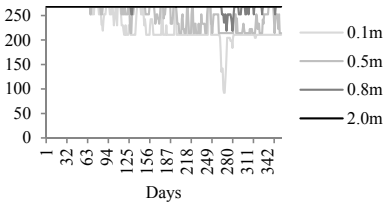
	Insulated Brick Cavity	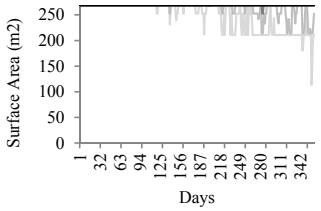	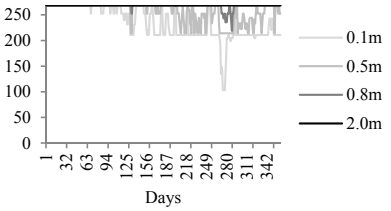
H5	Solid 9" Brick with suspended wooden floor	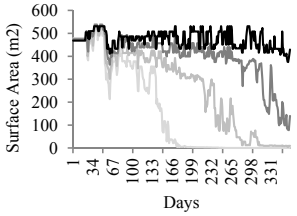	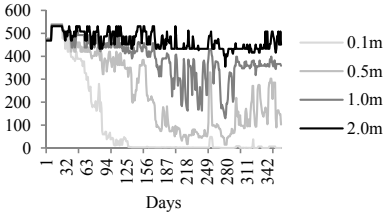
H6	Uninsulated Brick Cavity	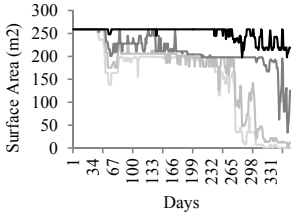	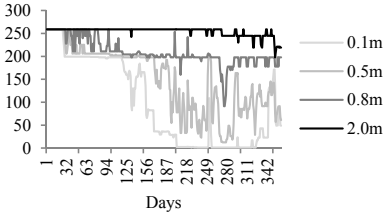
	Insulated Brick Cavity	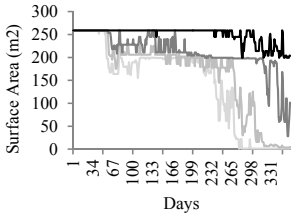	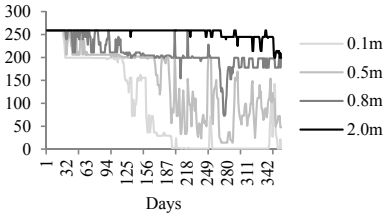

A. versicolor continued...

		Winter	Summer
H7	Uninsulated Brick/AAC Cavity	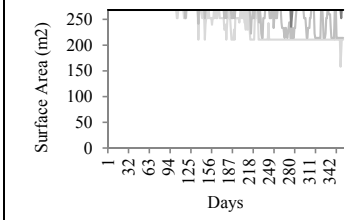	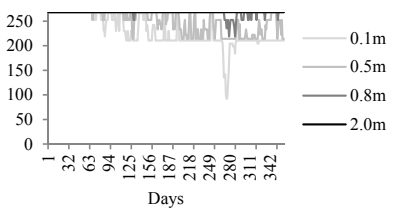
	Insulated Brick/AAC Cavity	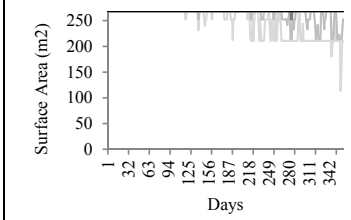	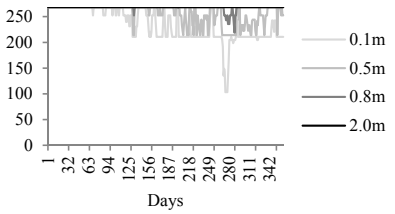
H8	Solid 9" Brick with suspended wooden floor	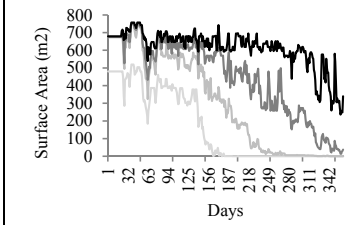	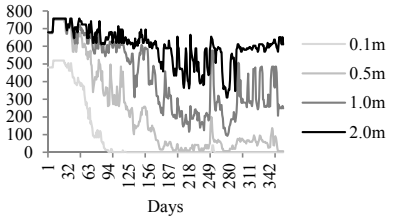
H9	Uninsulated Brick Cavity	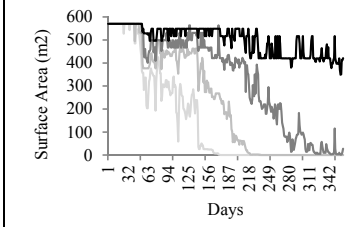	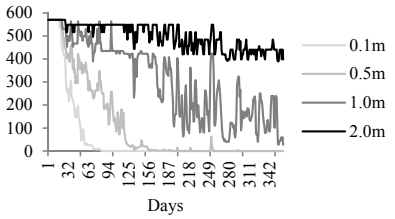
	Insulated Brick Cavity	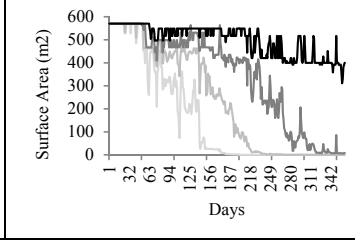	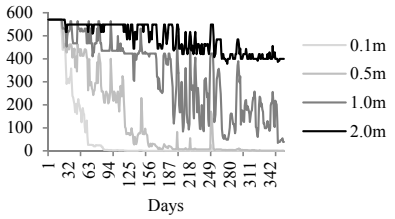

A. versicolor continued...

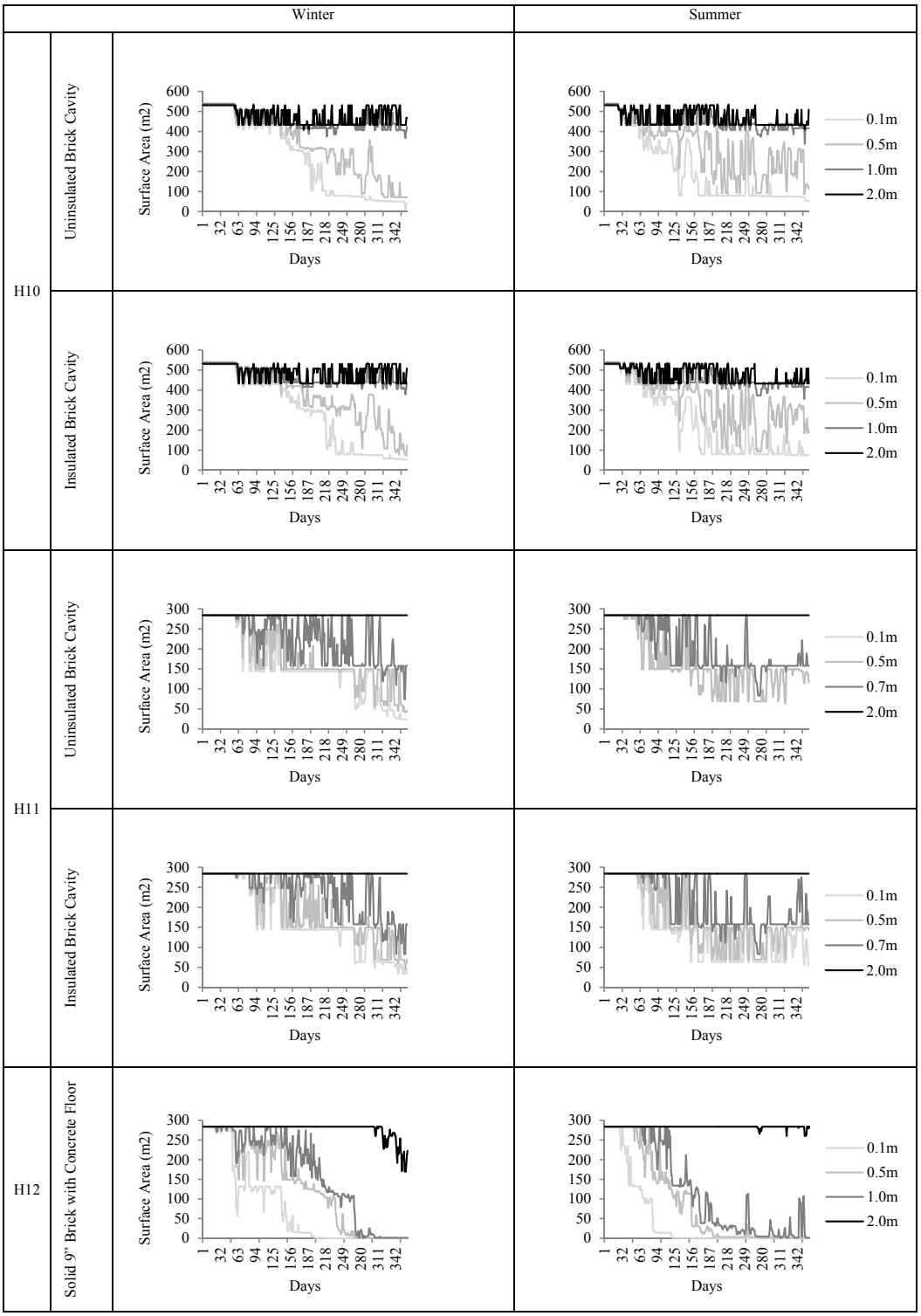

A. versicolor continued...

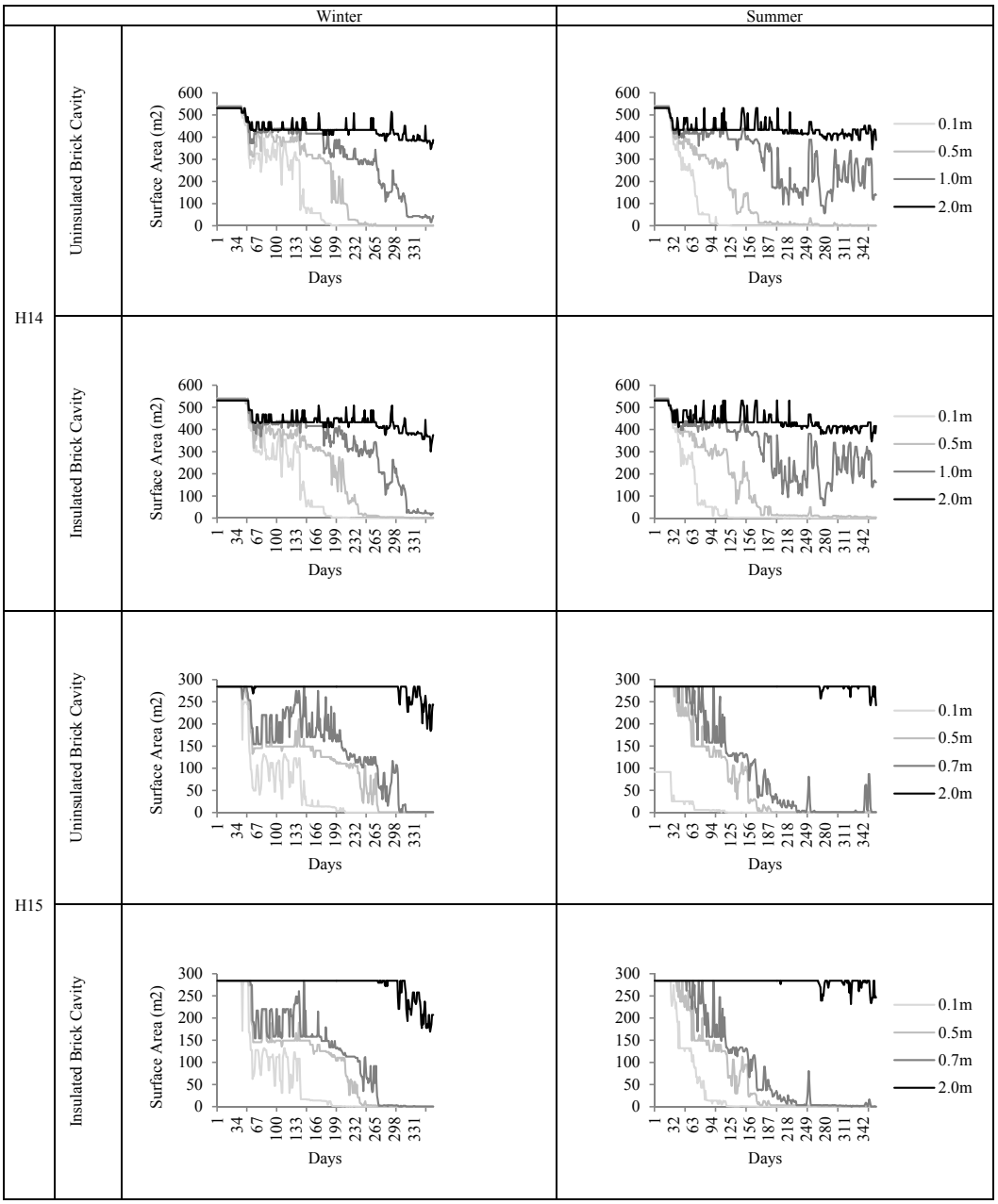

S. chartarum

		Winter	Summer
H1	Solid 9" Brick with suspended wooden floor	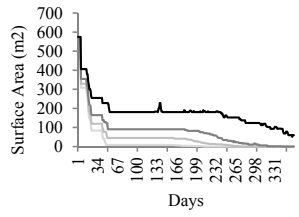	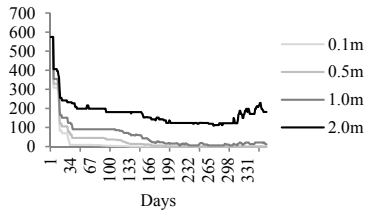
H2	Uninsulated Brick Cavity	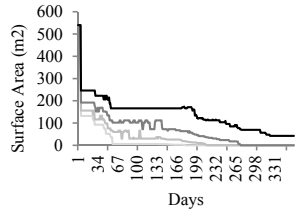	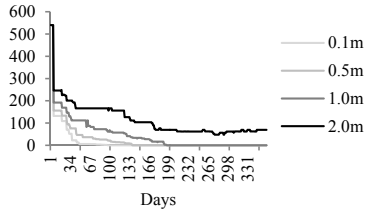
	Insulated Brick Cavity	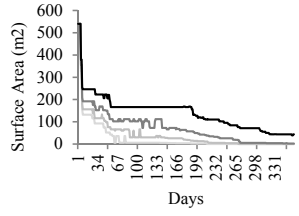	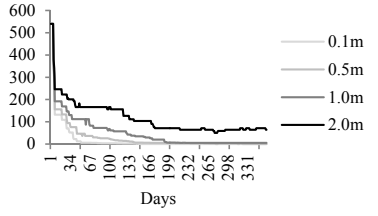
H3	Uninsulated Brick Cavity	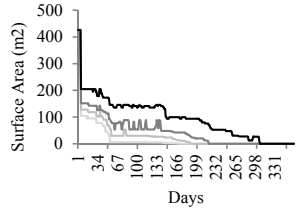	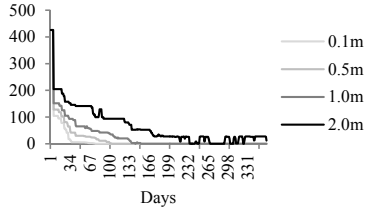
	Insulated Brick Cavity	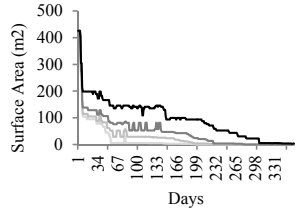	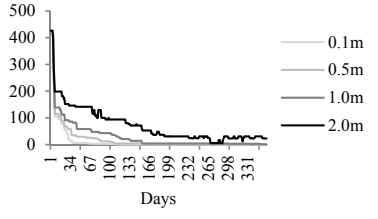

S. chartarum continued...

		Winter	Summer
H4	Uninsulated Brick Cavity	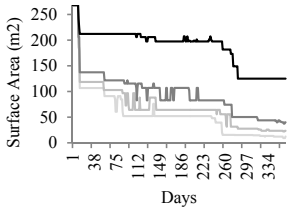	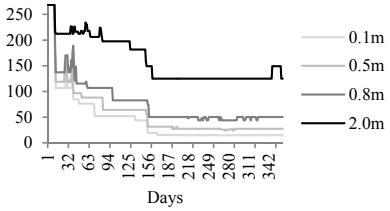
	Insulated Brick Cavity	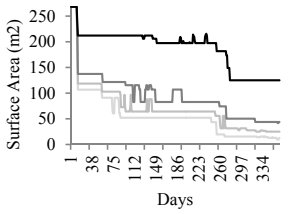	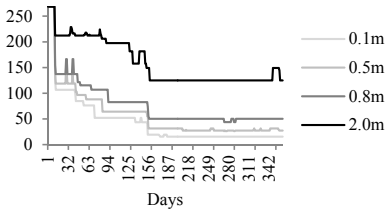
H5	Solid 9" Brick with suspended wooden floor	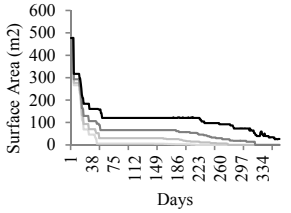	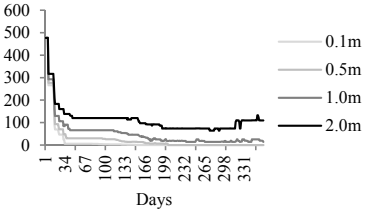
H6	Uninsulated Brick Cavity	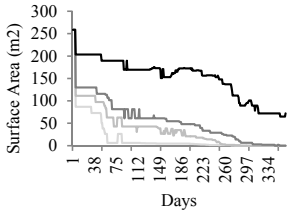	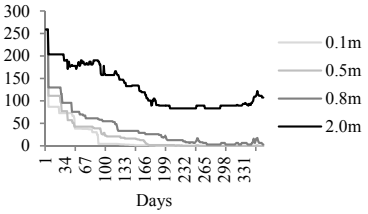
	Insulated Brick Cavity	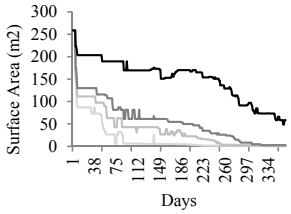	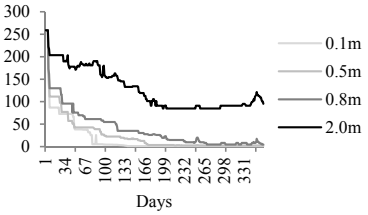

S. chartarum continued...

		Winter	Summer
H7	Uninsulated Brick/AAC Cavity	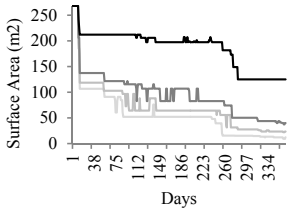	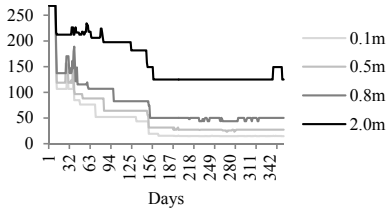
	Insulated Brick/AAC Cavity	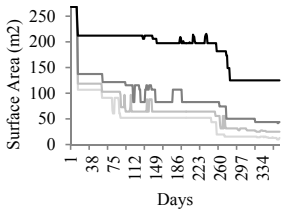	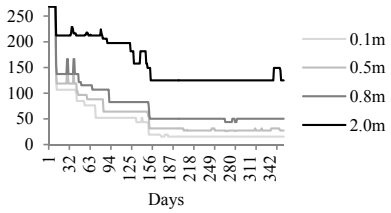
H8	Solid 9" Brick with suspended wooden floor	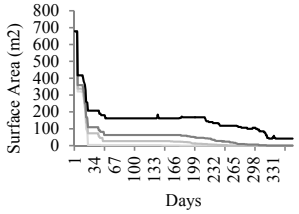	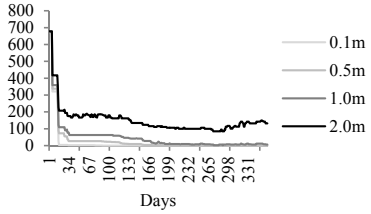
H9	Uninsulated Brick Cavity	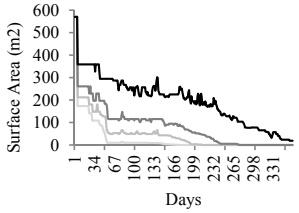	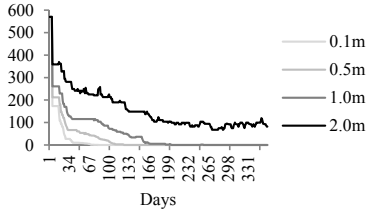
	Insulated Brick Cavity	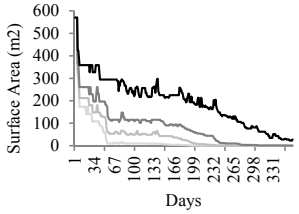	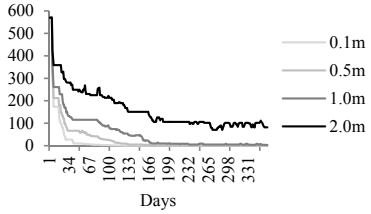

S. chartarum continued...

		Winter	Summer
H10	Uninsulated Brick Cavity	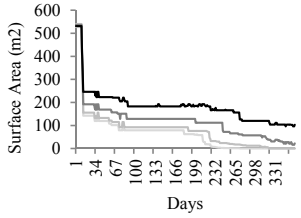	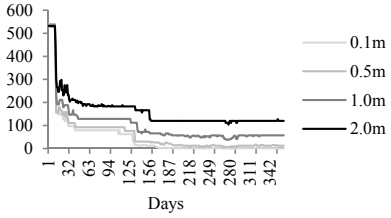
	Insulated Brick Cavity	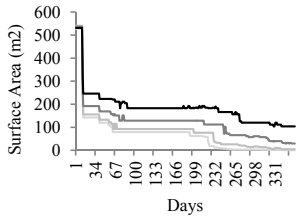	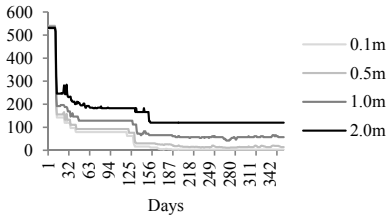
H11	Uninsulated Brick Cavity	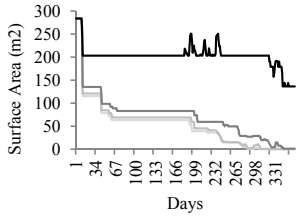	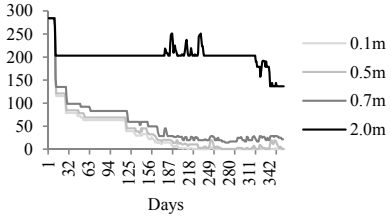
	Insulated Brick Cavity	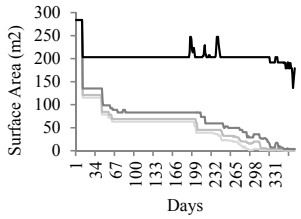	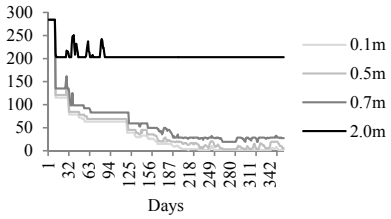
H12	Solid 9" Brick with Concrete Floor	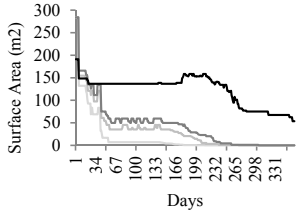	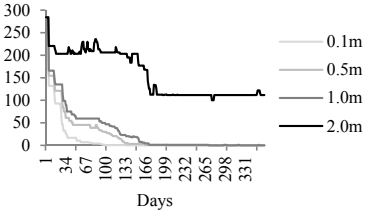

S. chartarum continued...

		Winter	Summer
H14	Uninsulated Brick Cavity	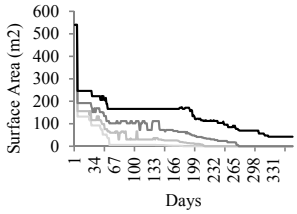	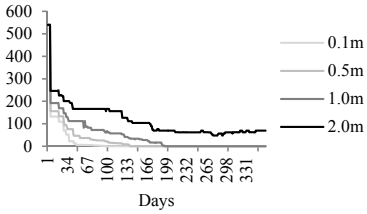
	Insulated Brick Cavity	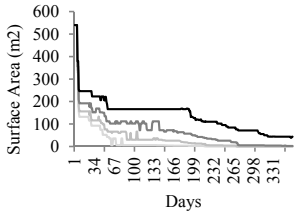	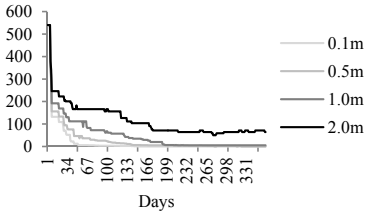
H15	Uninsulated Brick Cavity	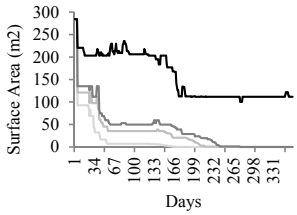	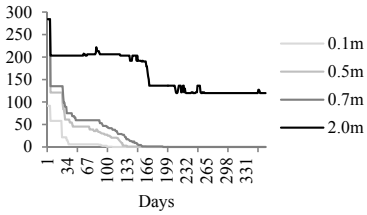
	Insulated Brick Cavity	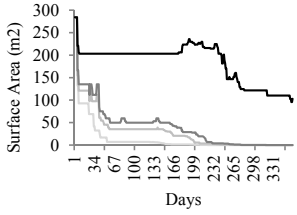	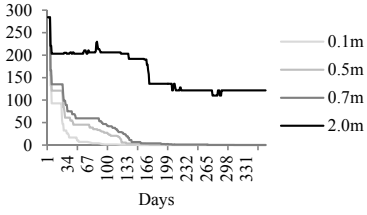

E. coli

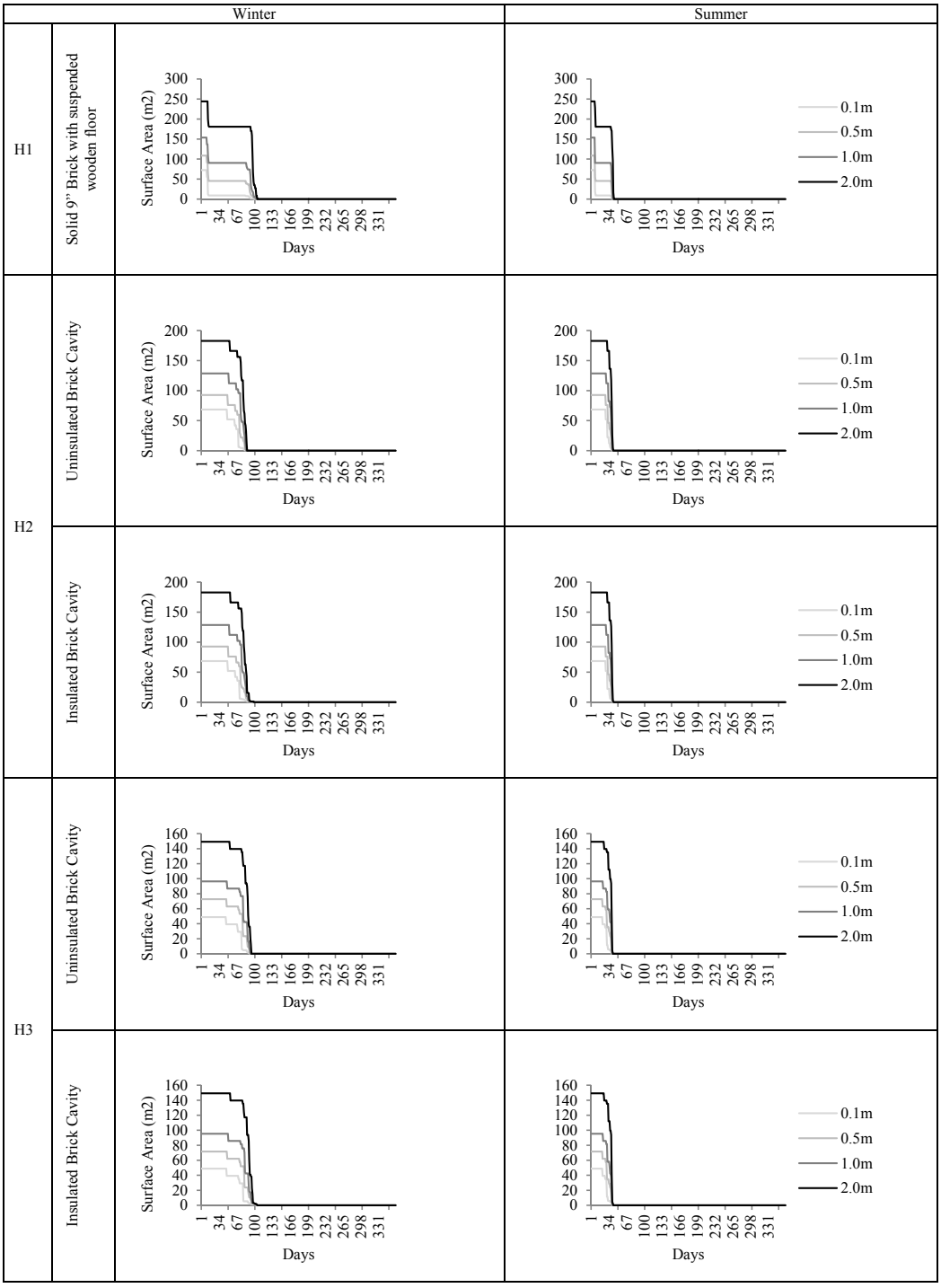
Winter
Summer
H1
Solid 9'' Brick with suspended wooden floor
H2
Uninsulated Brick Cavity
Insulated Brick Cavity
H3
Uninsulated Brick Cavity
Insulated Brick Cavity
Surface Area (m2)
Days
0.1m
0.5m
1.0m
2.0m

E. coli continued...

		Winter	Summer
H4	Uninsulated Brick Cavity	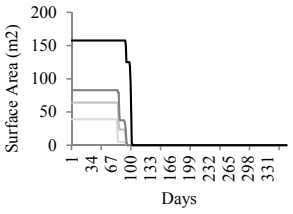	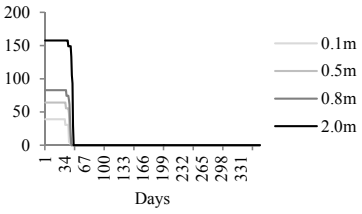
	Insulated Brick Cavity	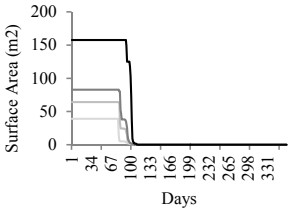	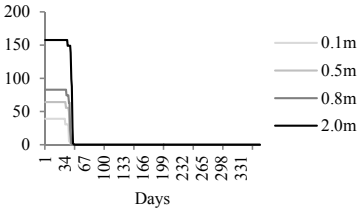
H5	Solid 9" Brick with suspended wooden floor	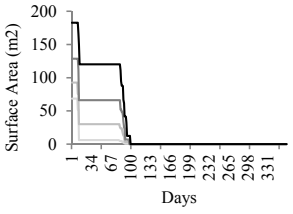	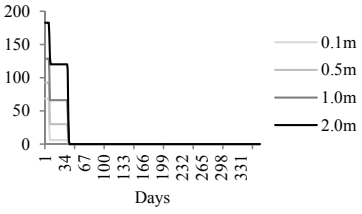
H6	Uninsulated Brick Cavity	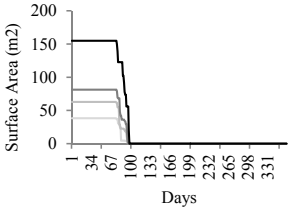	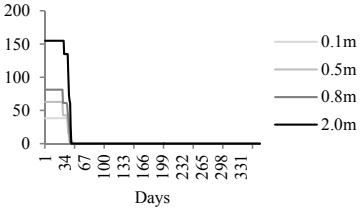
	Insulated Brick Cavity	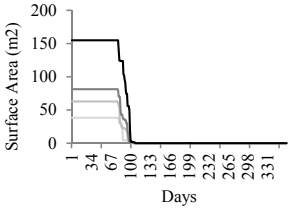	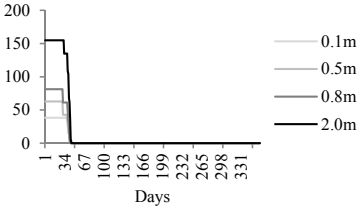

E. coli continued...

		Winter	Summer
H7	Uninsulated Brick/AAC Cavity	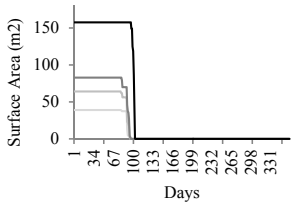	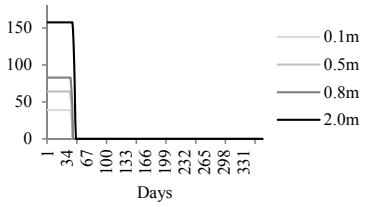
	Insulated Brick/AAC Cavity	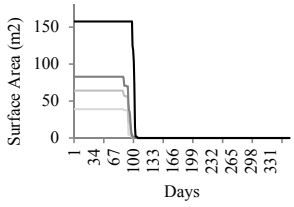	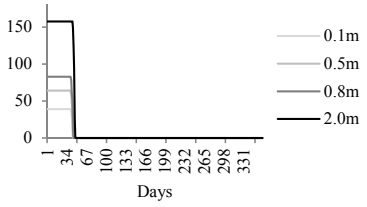
H8	Solid 9" Brick with suspended wooden floor	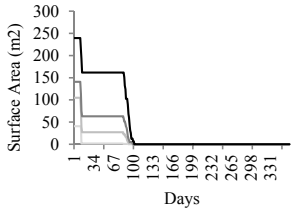	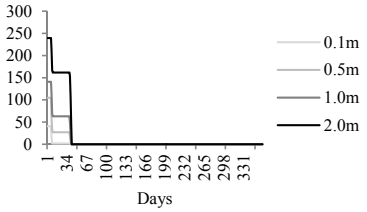
H9	Uninsulated Brick Cavity	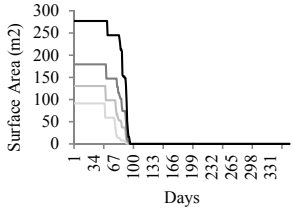	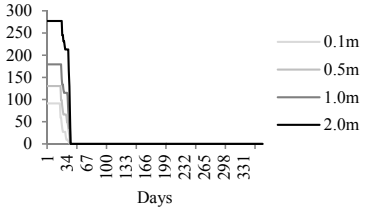
	Insulated Brick Cavity	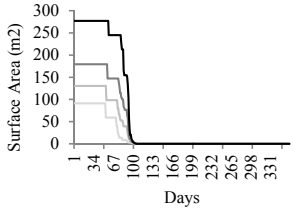	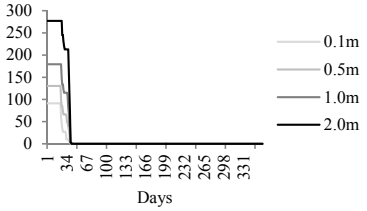

E. coli continued...

		Winter	Summer
H10	Uninsulated Brick Cavity	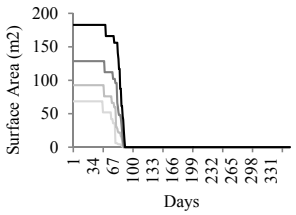	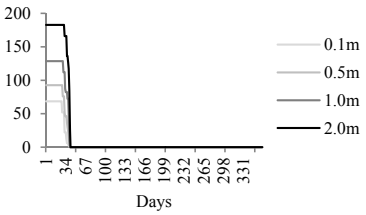
	Insulated Brick Cavity	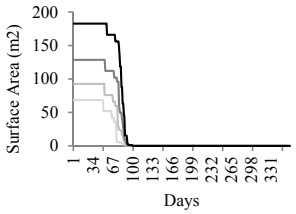	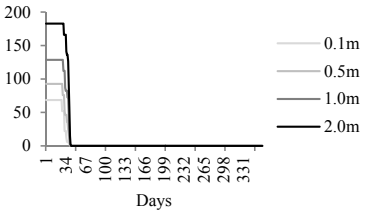
H11	Uninsulated Brick Cavity	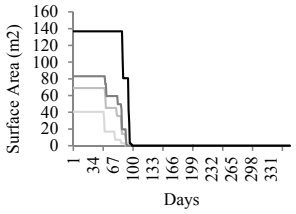	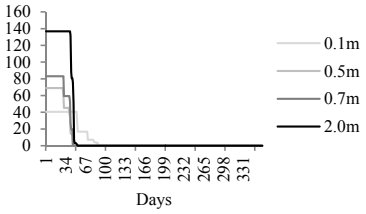
	Insulated Brick Cavity	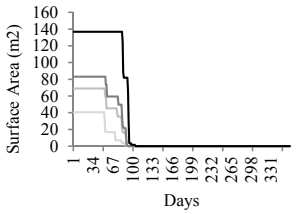	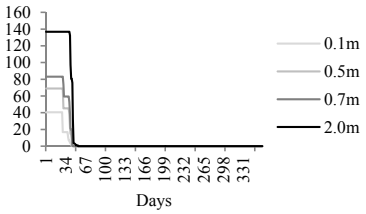
H12	Solid 9" Brick with Concrete Floor	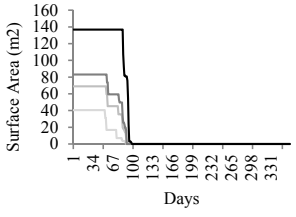	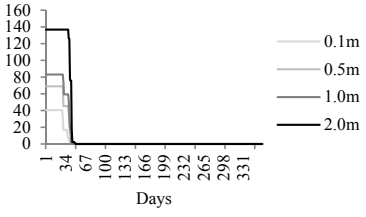

E. coli continued...

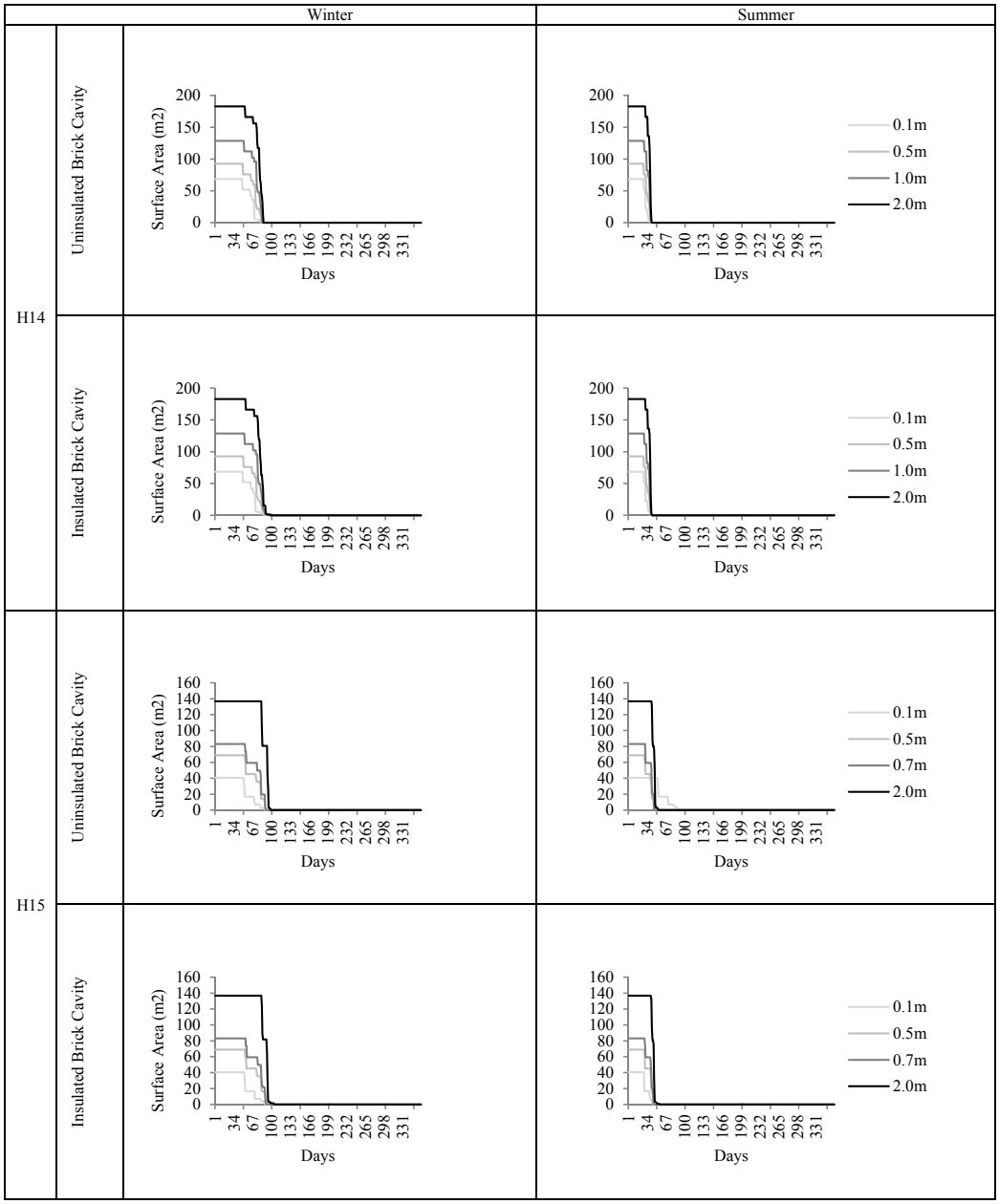

Salmonella

		Winter	Summer
H1	Solid 9" Brick with suspended wooden floor	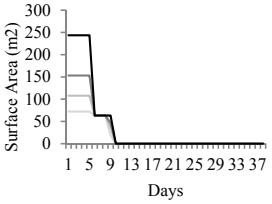	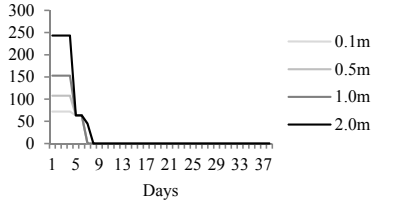
H2	Uninsulated Brick Cavity	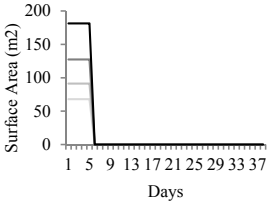	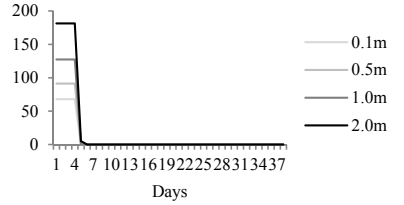
	Insulated Brick Cavity	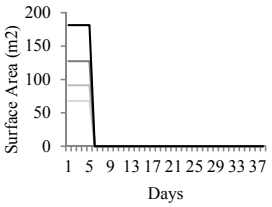	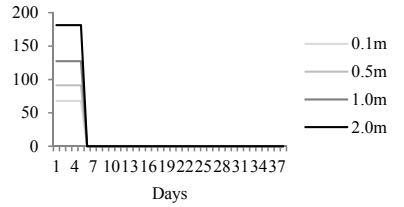
H3	Uninsulated Brick Cavity	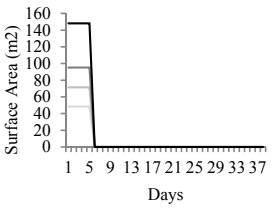	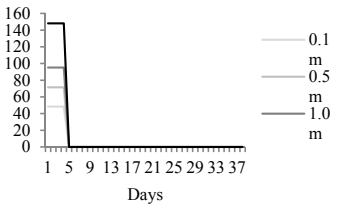
	Insulated Brick Cavity	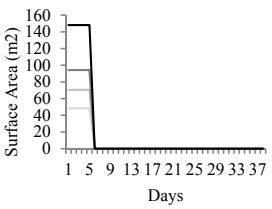	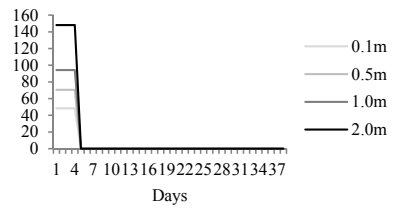

Salmonella continued...

		Winter	Summer
H4	Uninsulated Brick Cavity	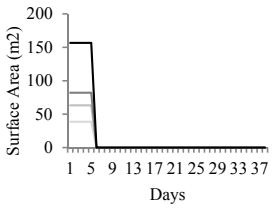	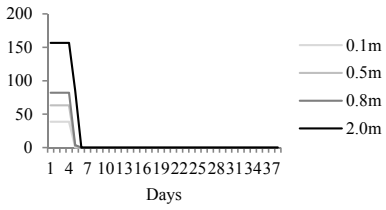
	Insulated Brick Cavity	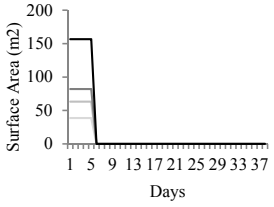	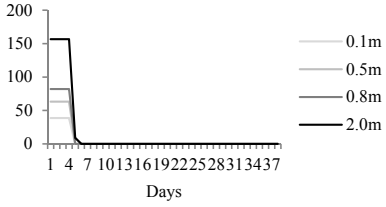
H5	Solid 9" Brick with suspended wooden floor	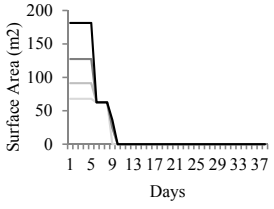	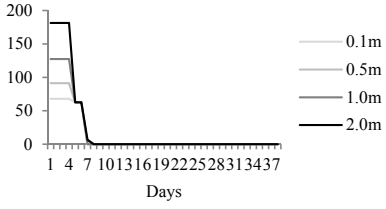
H6	Uninsulated Brick Cavity	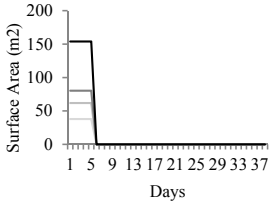	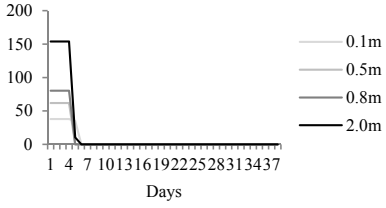
	Insulated Brick Cavity	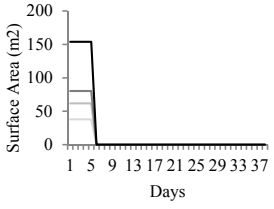	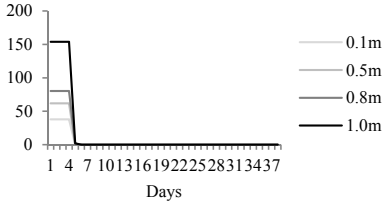

Salmonella continued...

		Winter	Summer
H7	Uninsulated Brick/AAC Cavity	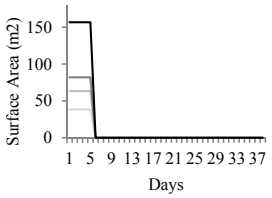	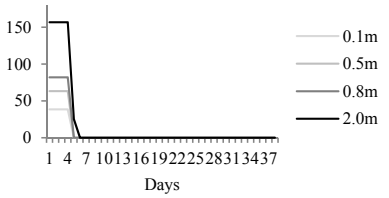
	Insulated Brick/AAC Cavity	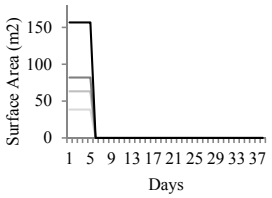	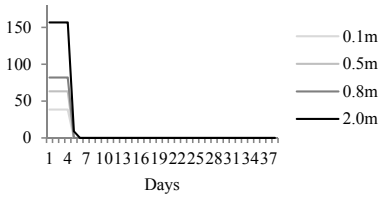
H8	Solid 9" Brick with suspended wooden floor	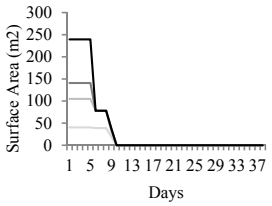	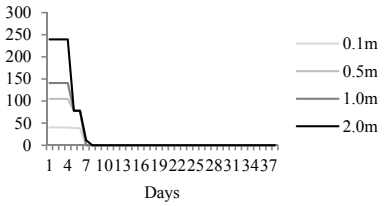
H9	Uninsulated Brick Cavity	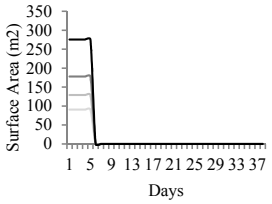	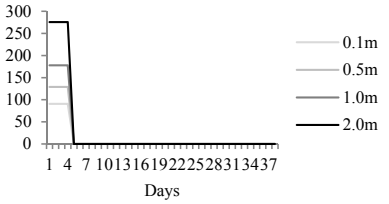
	Insulated Brick Cavity	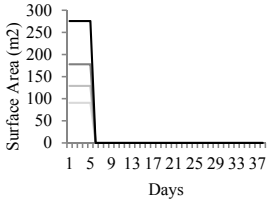	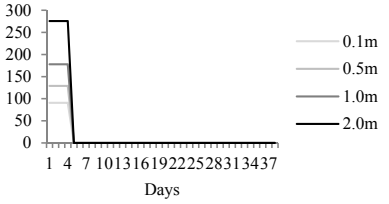

Salmonella continued...

		Winter	Summer
H10	Uninsulated Brick Cavity	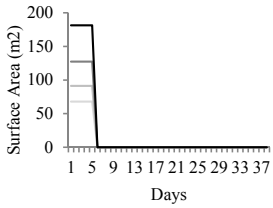	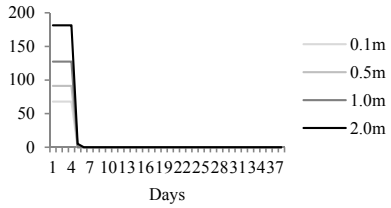
	Insulated Brick Cavity	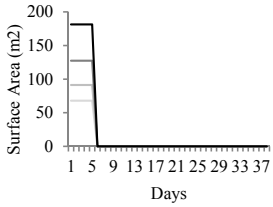	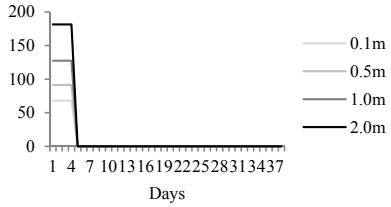
H11	Uninsulated Brick Cavity	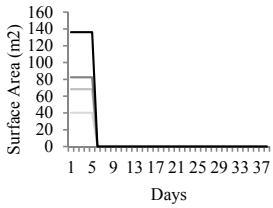	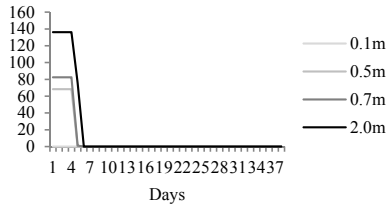
	Insulated Brick Cavity	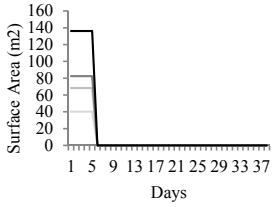	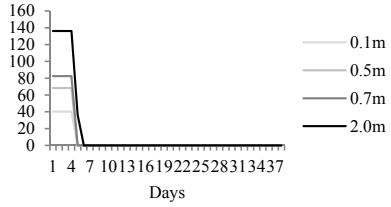
H12	Solid 9" Brick with Concrete Floor	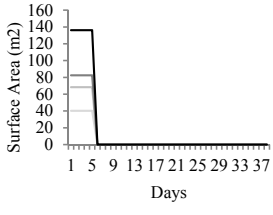	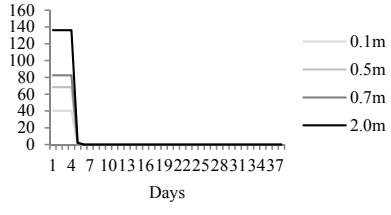

Salmonella continued...

		Winter	Summer
H14	Uninsulated Brick Cavity	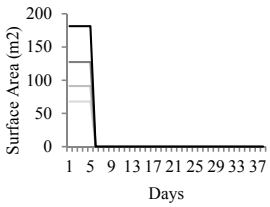	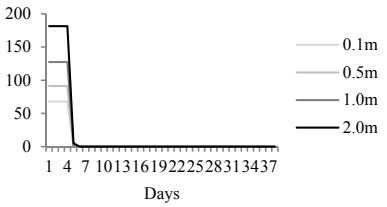
	Insulated Brick Cavity	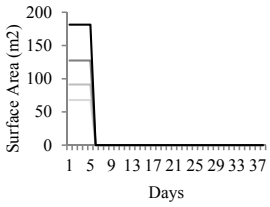	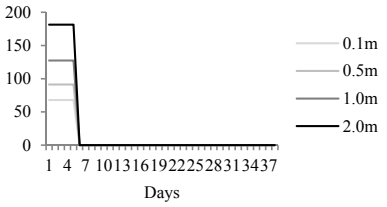
H15	Uninsulated Brick Cavity	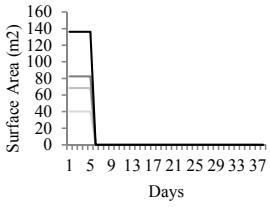	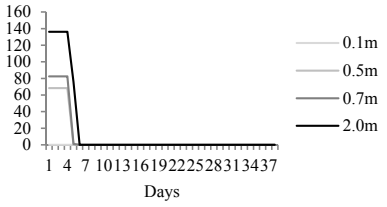
	Insulated Brick Cavity	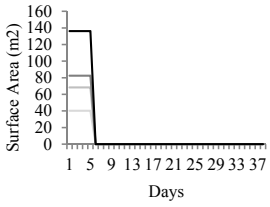	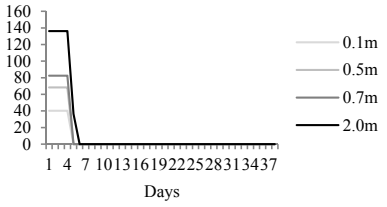

Listeria

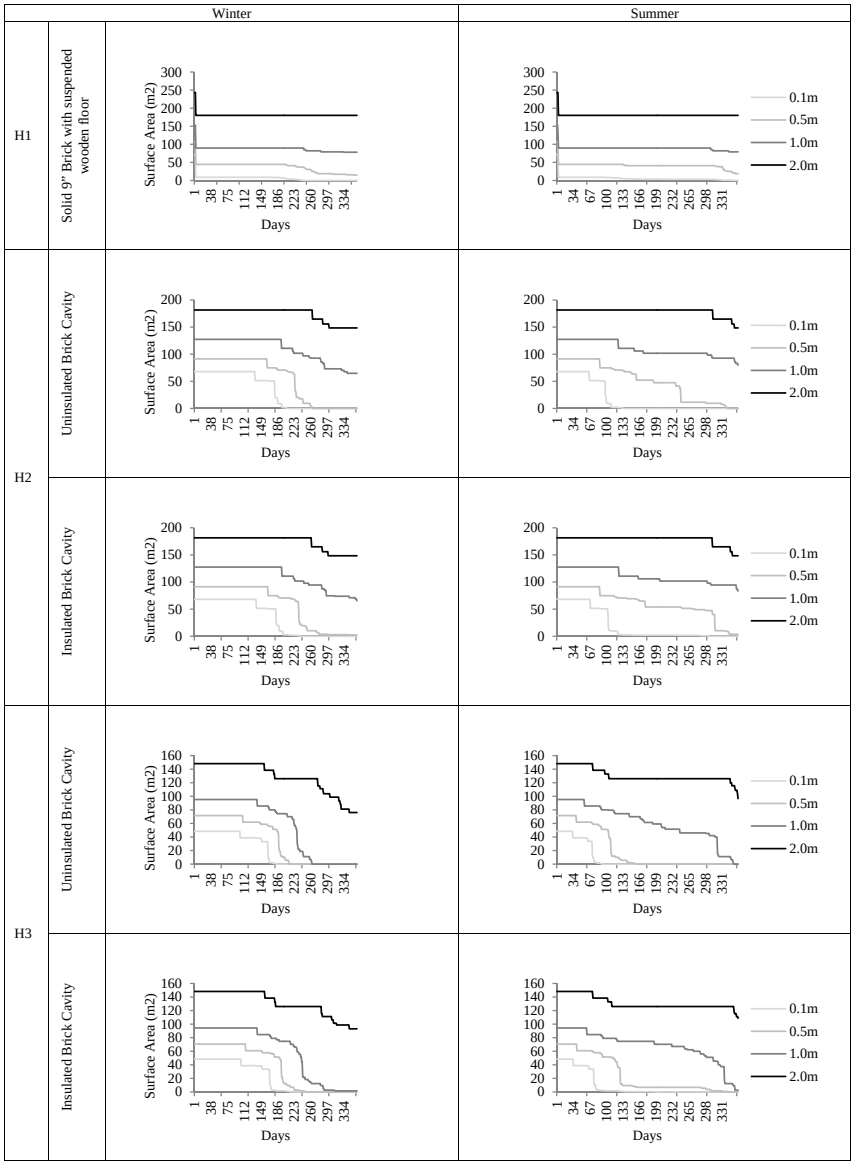
Winter
Summer
H1
Solid 9" Brick with suspended wooden floor
H2
Uninsulated Brick Cavity
Insulated Brick Cavity
H3
Uninsulated Brick Cavity
Insulated Brick Cavity
Surface Area (m2)
Days
0.1m
0.5m
1.0m
2.0m

Listeria continued...

		Winter	Summer
H4	Uninsulated Brick Cavity	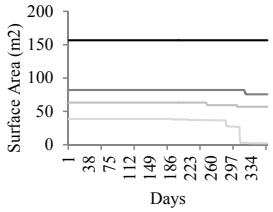	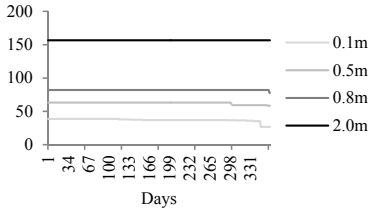
	Insulated Brick Cavity	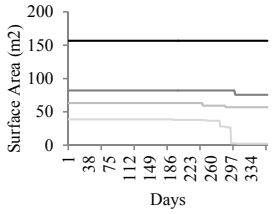	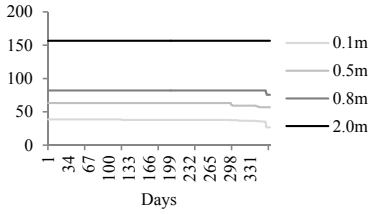
H5	Solid 9" Brick with suspended wooden floor	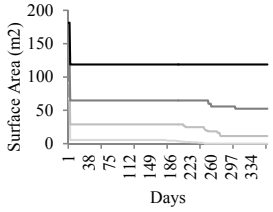	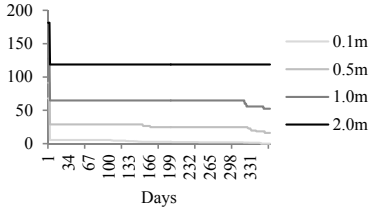
H6	Uninsulated Brick Cavity	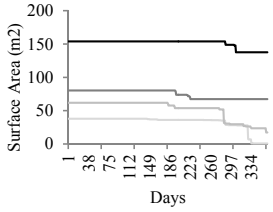	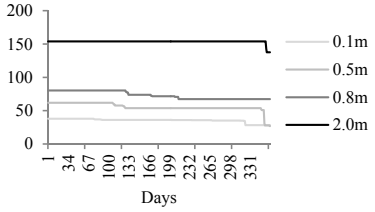
	Insulated Brick Cavity	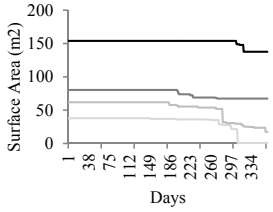	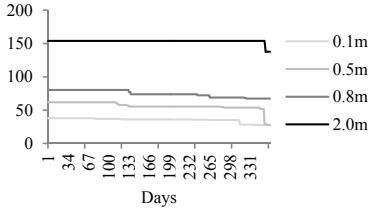

Listeria continued...

		Winter	Summer
H7	Uninsulated Brick/AAC Cavity	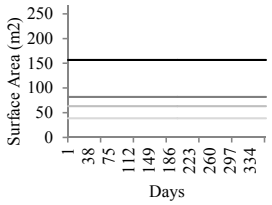	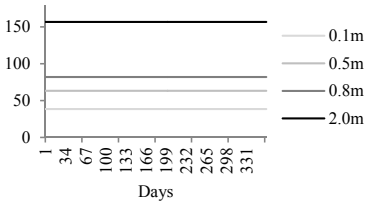
	Insulated Brick/AAC Cavity	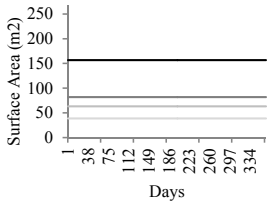	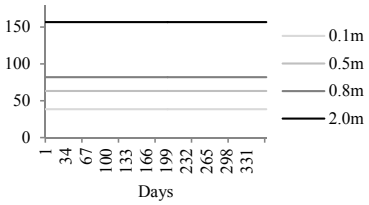
H8	Solid 9" Brick with suspended wooden floor	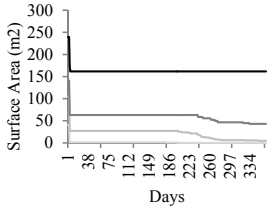	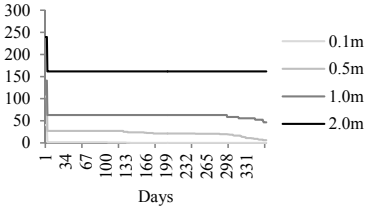
H9	Uninsulated Brick Cavity	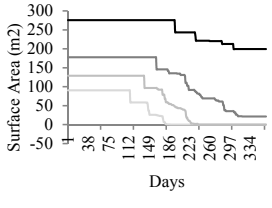	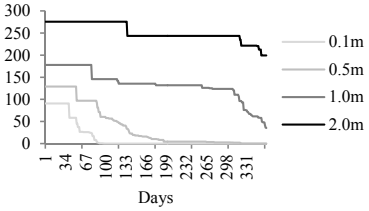
	Insulated Brick Cavity	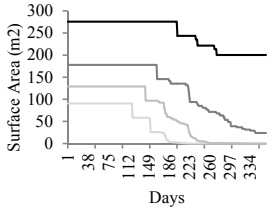	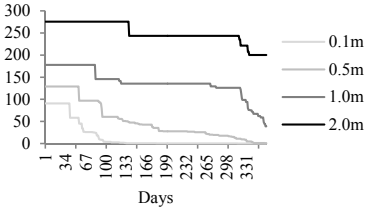

Listeria continued...

		Winter	Summer
H10	Uninsulated Brick Cavity	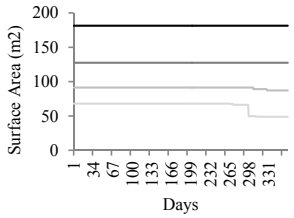	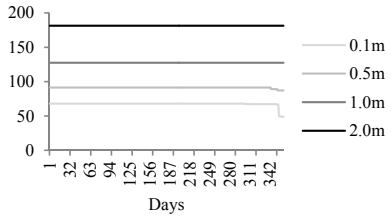
	Insulated Brick Cavity	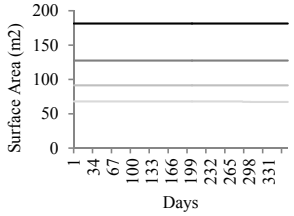	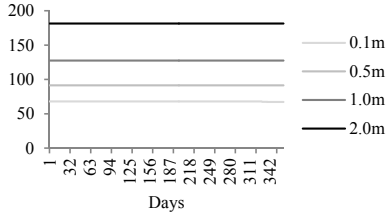
H11	Uninsulated Brick Cavity	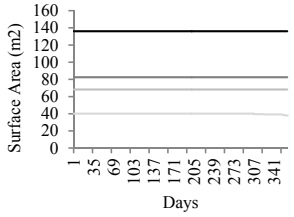	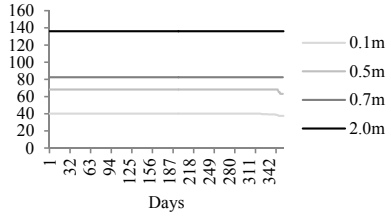
	Insulated Brick Cavity	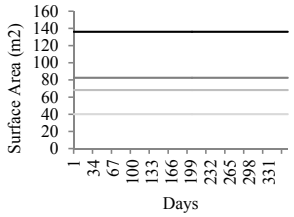	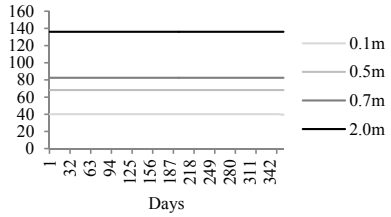
H12	Solid 9" Brick with Concrete Floor	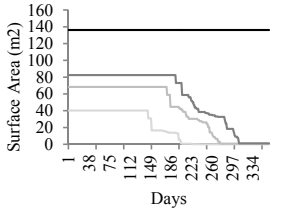	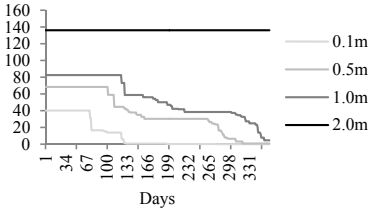

Listeria continued...

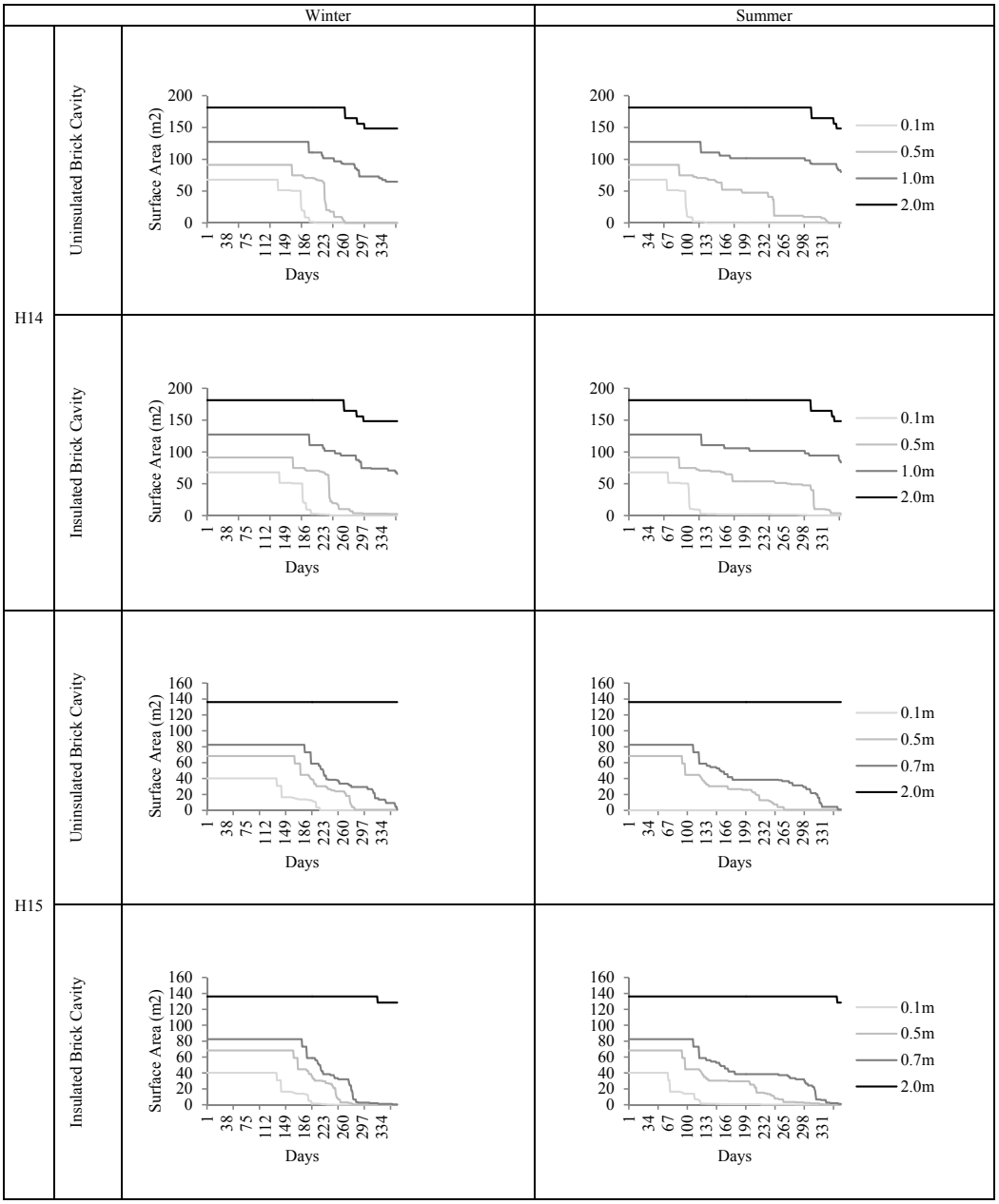

Appendix J

Depth-Drying Curve Parameters and Fits

-

Dwelling	Wall	a	b	c	d	f	g	r-square	RMSE
H01	Pre19299InchSolidBrick	5.73E+02 [5.68939E+02, 5.76721E+02]	3.30E+00 [3.12742E+00, 3.47174E+00]	-3.13E-02 [-3.26931E-02, -2.99608E-02]	6.32E+00 [6.02916E+00, 6.61877E+00]	- -	-1.00E01 [-1.00000E01, -1.00000E01]	9.55E-01	4.97E+01
H02	Uninsulated	4.61E+02 [4.56564E+02, 4.64900E+02]	3.24E+00 [3.04823E+00, 3.43313E+00]	-3.02E-02 [-3.16765E-02, -2.87824E-02]	4.53E+00 [4.29970E+00, 4.75573E+00]	- -	-1.00E-01 [-1.00000E01, -1.00000E-01]	9.41E-01	4.72E+01
	Insulated	4.65E+02 [4.61132E+02, 4.69707E+02]	3.14E+00 [2.95127E+00, 3.32678E+00]	-2.90E-02 [-3.03507E-02, -2.75802E-02]	4.39E+00 [4.16697E+00, 4.61411E+00]	- -	-1.00E01 [-1.00000E01, -1.00000E-01]	9.38E-01	4.84E+01
H03	Uninsulated	4.93E+02 [4.67740E+02, 5.18669E+02]	1.73E+00 [1.49347E+00, 1.97255E+00]	-2.39E-02 [-2.54857E-02, -2.22786E-02]	3.79E-02 [-4.67876E-02, 1.22501E-01]	7.26E-03 [6.87861E-03, 7.90001E-03]	-1.00E01 [-1.00000E01, -1.00000E01]	9.10E-01	4.58E+01
	Insulated	4.93E+02 [4.67740E+02, 5.18669E+02]	1.73E+00 [1.49347E+00, 1.97255E+00]	-2.39E-02 [-2.54857E-02, -2.22786E-02]	3.79E-02 [-4.67876E-02, 1.22501E-01]	7.26E-03 [6.87861E-03, 7.90001E-03]	-1.00E01 [-1.00000E01, -1.00000E01]	9.10E-01	4.08E+01
H04	Uninsulated AAC	2.71E+02 [2.69943E+02, 2.72005E+02]	2.93E+00 [2.80545E+00, 3.04652E+00]	-6.78E-03 [-7.19491E-03, -6.36936E-03]	2.62E+00 [2.32253E+00, 2.90850E+00]	- -	-1.00E01 [-1.00000E01, -1.00000E01]	7.94E-01	9.90E+00
	Insulated AAC	2.71E+02 [2.69943E+02, 2.72005E+02]	2.93E+00 [2.80545E+00, 3.04652E+00]	-6.78E-03 [-7.19491E-03, -6.36936E-03]	2.62E+00 [2.32253E+00, 2.90850E+00]	- -	-1.00E01 [-1.00000E01, -1.00000E01]	7.94E-01	9.90E+00
H05	Pre19299InchSolidBrick	4.61E+02 [4.57477E+02, 4.63736E+02]	3.42E+00 [3.23152E+00, 3.61197E+00]	-3.20E-02 [-3.35406E-02, -3.05379E-02]	7.08E+00 [6.73751E+00, 7.42085E+00]	- -	-1.00E01 [-1.00000E01, -1.00000E01]	9.48E-01	4.22E+01
H06	Uninsulated	2.34E+02 [2.32198E+02, 2.36336E+02]	6.24E+00 [5.79515E+00, 6.68273E+00]	-2.72E-02 [-2.90021E-02, -2.53951E-02]	3.61E+00 [3.31593E+00, 3.90443E+00]	- -	-1.00E01 [-1.00000E01, -1.00000E01]	8.33E-01	2.86E+01
	Insulated	2.34E+02 [2.32670E+02, 2.36357E+02]	6.24E+00 [8.51413E+00, 9.69314E+00]	-2.72E-02 [-4.32558E-02, -3.81137E-02]	3.61E+00 -	- [1.59366E-02, 1.84084E-02]	-1.00E01 [-1.00000E01, -1.00000E01]	8.33E-01	2.96E+01
H07	Uninsulated AAC	2.71E+02 [2.69943E+02, 2.72005E+02]	2.93E+00 [2.80545E+00, 3.04652E+00]	-6.78E-03 [-7.19491E-03, -6.36936E-03]	2.62E+00 [2.32253E+00, 2.90850E+00]	- -	-1.00E01 [-1.00000E01, -1.00000E01]	7.94E-01	9.90E+00
	Insulated AAC	2.71E+02 [2.69943E+02, 2.72005E+02]	2.93E+00 [2.80545E+00, 3.04652E+00]	-6.78E-03 [-7.19491E-03, -6.36936E-03]	2.62E+00 [2.32253E+00, 2.90850E+00]	- -	-1.00E01 [-1.00000E01, -1.00000E01]	7.94E-01	9.90E+00
H08	Pre19299InchSolidBrick	6.33E+02 [6.23722E+02, 6.42145E+02]	4.35E-01 [3.15223E-01, 5.53848E-01]	-2.17E-02 [-2.31479E-02, -2.02110E-02]	5.45E+00 [5.07677E+00, 5.81466E+00]	- -	-1.00E01 [-1.00000E01, -1.00000E01]	9.41E-01	6.46E+01
H09	Uninsulated	5.20E+02 [5.15314E+02, 5.23830E+02]	2.91E+00 [2.73819E+00, 3.07911E+00]	-3.69E-02 [-3.85529E-02, -3.52878E-02]	5.69E+00 [5.44575E+00, 5.93021E+00]	- -	-1.00E01 [-1.00000E01, -1.00000E01]	9.58E-01	4.83E+01
	Insulated	5.28E+02 [5.24220E+02, 5.32531E+02]	3.16E+00 [2.97696E+00, 3.33833E+00]	-3.35E-02 [-3.49071E-02, -3.21110E-02]	4.45E+00 [4.13199E+00, 4.77653E+00]	7.16E-04 [-1.73861E-04, 1.60565E-03]	-1.00E01 [-1.00000E01, -1.00000E01]	9.61E-01	4.49E+01
H10	Uninsulated AAC	4.83E+02 [4.79198E+02, 4.87226E+02]	2.93E+00 [2.73686E+00, 3.11369E+00]	-1.90E-02 [-1.99921E-02, -1.80300E-02]	4.56E+00 [4.31807E+00, 4.80245E+00]	- -	-1.00E01 [-1.00000E01, -1.00000E01]	8.79E-01	5.17E+01
	Insulated AAC	4.83E+02 [4.79198E+02, 4.87226E+02]	2.93E+00 [2.73686E+00, 3.11369E+00]	-1.90E-02 [-1.99921E-02, -1.80300E-02]	4.56E+00 [4.31807E+00, 4.80245E+00]	- -	-1.00E01 [-1.00000E01, -1.00000E01]	8.79E-01	5.17E+01
H11	Uninsulated	2.96E+02 [2.91796E+02, 2.99378E+02]	1.42E+00 [1.32612E+00, 1.51962E+00]	-8.93E-03 [-9.34992E-03, -8.50214E-03]	1.94E+00 [1.81777E+00, 2.06656E+00]	- -	-1.00E01 [-1.00000E01, -1.00000E01]	8.63E-01	2.70E+01
	Insulated	2.96E+02 [2.91796E+02, 2.99378E+02]	1.42E+00 [1.32612E+00, 1.51962E+00]	-8.93E-03 [-9.34992E-03, -8.50214E-03]	1.94E+00 [1.81777E+00, 2.06656E+00]	- -	-1.00E01 [-1.00000E01, -1.00000E01]	8.63E-01	2.70E+01
H12	9InchSolidBrick	2.81E+02 [2.78342E+02, 2.82998E+02]	1.76E+00 [1.62137E+00, 1.88985E+00]	-2.39E-02 [-2.48420E-02, -2.29048E-02]	5.94E+00 [5.56815E+00, 6.31701E+00]	-5.41E-03 [-6.45812E-03, -4.35695E-03]	-1.00E01 [-1.00000E01, -1.00000E01]	9.57E-01	2.45E+01
H14	Uninsulated	4.65E+02 [4.61132E+02, 4.69707E+02]	3.14E+00 [2.95127E+00, 3.32678E+00]	-2.90E-02 [-3.03507E-02, -2.75802E-02]	4.39E+00 [4.16697E+00, 4.61411E+00]	- -	-1.00E-01 [-1.00000E01, -1.00000E01]	9.38E-01	4.84E+01
	Insulated	4.93E+02 [4.67740E+02, 5.18669E+02]	1.73E+00 [1.49347E+00, 1.97255E+00]	-2.39E-02 [-2.54857E-02, -2.22786E-02]	3.79E-02 [-4.67876E-02, 1.22501E-01]	7.26E-03 [6.87861E-03, 7.90001E-03]	-1.00E01 [-1.00000E01, -1.00000E01]	9.10E-01	4.58E+01
H15	Uninsulated	2.96E+02 [2.91796E+02, 2.99378E+02]	1.42E+00 [1.32612E+00, 1.51962E+00]	-8.93E-03 [-9.34992E-03, -8.50214E-03]	1.94E+00 [1.81777E+00, 2.06656E+00]	- -	-1.00E01 [-1.00000E01, -1.00000E01]	8.63E-01	2.70E+01
	Insulated	2.96E+02 [2.91796E+02, 2.99378E+02]	1.42E+00 [1.32612E+00, 1.51962E+00]	-8.93E-03 [-9.34992E-03, -8.50214E-03]	1.94E+00 [1.81777E+00, 2.06656E+00]	- -	-1.00E01 [-1.00000E01, -1.00000E01]	8.63E-01	2.70E+01

Table J.1: *A. versicolor* - Winter

Dwelling	Wall	Summer							
		a	b	c	d	f	g	r-square	RMSE
H01	Pre19299InchSolidBrick	5.78E+02 [5.68579E+02, 5.88031E+02]	1.71E-01 [2.32922E-02, 3.18590E-01]	-1.60E-02 [-1.72947E-02, -1.46736E-02]	4.77E+00 [4.38655E+00, 5.14466E+00]	- -	-1.00E01 [-1.00000E01, -1.00000E01]	8.13E-01	1.04E+02
H02	Uninsulated	4.58E+02 [4.50259E+02, 4.65287E+02]	6.73E-01 [5.20538E-01, 8.25250E-01]	-2.46E-02 [-2.63782E-02, -2.27669E-02]	4.87E+00 [4.50031E+00, 5.23026E+00]	- -	-1.00E-01 [-1.00000E01, -1.00000E-01]	8.63E-01	7.35E+01
	Insulated	4.58E+02 [4.50259E+02, 4.65287E+02]	6.73E-01 [5.20538E-01, 8.25250E-01]	-2.46E-02 [-2.63782E-02, -2.27669E-02]	4.87E+00 [4.50031E+00, 5.23026E+00]	- -	-1.00E01 [-1.00000E01, -1.00000E-01]	8.63E-01	7.35E+01
H03	Uninsulated	9.79E+02 [9.45390E+02, 1.01213E+03]	- -	-3.42E-02 [-3.54417E-02, -3.30409E-02]	-2.88E-01 [-3.23494E-01, -2.51857E-01]	1.57E-02 [1.50839E-02, 1.63234E-02]	-1.00E01 [-1.00000E01, -1.00000E01]	8.37E-01	1.09E+02
	Insulated	9.38E+02 [9.05388E+02, 9.70624E+02]	- -	-3.15E-02 [-3.26528E-02, -3.04206E-02]	-2.24E-01 [-2.61887E-01, -1.86350E-01]	1.42E-02 [1.36529E-02, 1.48174E-02]	-1.00E01 [-1.00000E01, -1.00000E01]	8.94E-01	4.36E+01
H04	Uninsulated AAC	2.70E+02 [2.68865E+02, 2.71325E+02]	2.89E+00 [2.72675E+00, 3.06154E+00]	-8.82E-03 [-9.61146E-03, -8.03770E-03]	3.42E+00 [3.14420E+00, 3.69425E+00]	- -	-1.00E01 [-1.00000E01, -1.00000E01]	6.23E-01	1.39E+01
	Insulated AAC	2.70E+02 [2.68865E+02, 2.71325E+02]	2.89E+00 [2.72675E+00, 3.06154E+00]	-8.82E-03 [-9.61146E-03, -8.03770E-03]	3.42E+00 [3.14420E+00, 3.69425E+00]	- -	-1.00E01 [-1.00000E01, -1.00000E01]	6.23E-01	1.39E+01
H05	Pre19299InchSolidBrick	4.65E+02 [4.61158E+02, 4.69691E+02]	2.04E+00 [1.86119E+00, 2.22733E+00]	-4.13E-02 [-4.38737E-02, -3.88080E-02]	8.64E+00 [8.12533E+00, 9.16428E+00]	- -	-1.00E01 [-1.00000E01, -1.00000E01]	9.46E-01	4.96E+01
H06	Uninsulated	2.48E+02 [2.44847E+02, 2.51105E+02]	1.27E+00 [1.12291E+00, 1.41411E+00]	-1.39E-02 [-1.48071E-02, -1.30044E-02]	4.43E+00 [4.12919E+00, 4.72550E+00]	- -	-1.00E01 [-1.00000E01, -1.00000E01]	8.08E-01	3.49E+01
	Insulated	2.48E+02 [2.44536E+02, 2.50626E+02]	1.33E+00 [1.17943E+00, 1.47635E+00]	-1.50E-02 [-1.59128E-02, -1.40445E-02]	4.74E+00 [4.43269E+00, 5.04686E+00]	- -	-1.00E01 [-1.00000E01, -1.00000E01]	8.42E-01	3.49E+01
H07	Uninsulated AAC	2.70E+02 [2.68865E+02, 2.71325E+02]	2.89E+00 [2.72675E+00, 3.06154E+00]	-8.82E-03 [-9.61146E-03, -8.03770E-03]	3.42E+00 [3.14420E+00, 3.69425E+00]	- -	-1.00E01 [-1.00000E01, -1.00000E01]	6.23E-01	1.39E+01
	Insulated AAC	2.70E+02 [2.68865E+02, 2.71325E+02]	2.89E+00 [2.72675E+00, 3.06154E+00]	-8.82E-03 [-9.61146E-03, -8.03770E-03]	3.42E+00 [3.14420E+00, 3.69425E+00]	- -	-1.00E01 [-1.00000E01, -1.00000E01]	6.23E-01	1.39E+01
H08	Pre19299InchSolidBrick	6.60E+02 [6.52201E+02, 6.68423E+02]	1.24E+00 [1.11043E+00, 1.36951E+00]	-3.36E-02 [-3.53773E-02, -3.17407E-02]	4.45E+00 [4.21653E+00, 4.68607E+00]	- -	-1.00E01 [-1.00000E01, -1.00000E01]	9.43E-01	6.80E+01
H09	Uninsulated	5.81E+02 [5.73839E+02, 5.87254E+02]	1.30E+00 [1.14577E+00, 1.45464E+00]	-3.22E-02 [-3.42515E-02, -3.01991E-02]	6.24E+00 [5.83766E+00, 6.64298E+00]	- -	-1.00E01 [-1.00000E01, -1.00000E01]	8.93E-01	7.40E+01
	Insulated	5.20E+02 [5.11383E+02, 5.27736E+02]	2.17E-01 [9.49236E-02, 3.39709E-01]	-2.37E-02 [-2.52823E-02, -2.21187E-02]	4.61E+00 [4.31539E+00, 4.90277E+00]	- -	-1.00E01 [-1.00000E01, -1.00000E01]	8.90E-01	7.38E+01
H10	Uninsulated AAC	4.74E+02 [4.68576E+02, 4.78566E+02]	1.19E+00 [1.06746E+00, 1.31668E+00]	-1.18E-02 [-1.25189E-02, -1.11284E-02]	4.18E+00 [3.93641E+00, 4.42295E+00]	- -	-1.00E01 [-1.00000E01, -1.00000E01]	8.35E-01	5.83E+01
	Insulated AAC	4.74E+02 [4.68576E+02, 4.78566E+02]	1.19E+00 [1.06746E+00, 1.31668E+00]	-1.18E-02 [-1.25189E-02, -1.11284E-02]	4.18E+00 [3.93641E+00, 4.42295E+00]	- -	-1.00E01 [-1.00000E01, -1.00000E01]	8.35E-01	5.83E+01
H11	Uninsulated	2.96E+02 [2.91796E+02, 2.99378E+02]	1.42E+00 [1.32612E+00, 1.51962E+00]	-8.93E-03 [-9.34992E-03, -8.50214E-03]	1.94E+00 [1.81777E+00, 2.06656E+00]	- -	-1.00E01 [-1.00000E01, -1.00000E01]	8.63E-01	2.70E+01
	Insulated	2.96E+02 [2.91796E+02, 2.99378E+02]	1.42E+00 [1.32612E+00, 1.51962E+00]	-8.93E-03 [-9.34992E-03, -8.50214E-03]	1.94E+00 [1.81777E+00, 2.06656E+00]	- -	-1.00E01 [-1.00000E01, -1.00000E01]	8.63E-01	2.70E+01
H12	9InchSolidBrick	2.86E+02 [2.84090E+02, 2.88642E+02]	1.18E+00 [1.07970E+00, 1.28351E+00]	-4.05E-02 [-4.22832E-02, -3.87312E-02]	7.26E+00 [6.95388E+00, 7.57131E+00]	- -	-1.00E01 [-1.00000E01, -1.00000E01]	9.79E-01	1.84E+01
H14	Uninsulated	4.58E+02 [4.50259E+02, 4.65287E+02]	6.73E-01 [5.20538E-01, 8.25250E-01]	-2.46E-02 [-2.63782E-02, -2.27669E-02]	4.87E+00 [4.50031E+00, 5.23026E+00]	- -	-1.00E-01 [-1.00000E01, -1.00000E01]	8.63E-01	7.35E+01
	Insulated	9.79E+02 [9.45390E+02, 1.01213E+03]	- -	-3.42E-02 [-3.54417E-02, -3.30409E-02]	-2.88E-01 [-3.23494E-01, -2.51857E-01]	1.57E-02 [1.50839E-02, 1.63234E-02]	-1.00E01 [-1.00000E01, -1.00000E01]	8.37E-01	1.09E+02
H15	Uninsulated	2.96E+02 [2.91796E+02, 2.99378E+02]	1.42E+00 [1.32612E+00, 1.51962E+00]	-8.93E-03 [-9.34992E-03, -8.50214E-03]	1.94E+00 [1.81777E+00, 2.06656E+00]	- -	-1.00E01 [-1.00000E01, -1.00000E01]	8.63E-01	2.70E+01
	Insulated	2.96E+02 [2.91796E+02, 2.99378E+02]	1.42E+00 [1.32612E+00, 1.51962E+00]	-8.93E-03 [-9.34992E-03, -8.50214E-03]	1.94E+00 [1.81777E+00, 2.06656E+00]	- -	-1.00E01 [-1.00000E01, -1.00000E01]	8.63E-01	2.70E+01

Table J.2: *A. versicolor* - Summer

Dwelling	Wall	Winter							
		a	b	c	d	f	g	r-square	RMSE
H01	Pre19299InchSolidBrick	1.90E+02 [1.88256E+02, 1.92647E+02]	-2.97E+00 [-3.12325E+00, -2.82260E+00]	-4.41E-03 [-5.14210E-03, -3.67648E-03]	4.25E+00 [4.07624E+00, 4.41691E+00]	-6.08E-03 [-6.66900E-03, -5.48310E-03]	-1.00E01 [-1.00000E01, -1.00000E01]	8.49E-01	4.27E+01
H02	Uninsulated	5.53E+02 [5.37333E+02, 5.69630E+02]	- -	-1.54E-02 [-1.61486E-02, -1.46114E-02]	- -	5.67E-03 [5.27510E-03, 6.05644E-03]	-1.00E-01 [-1.00000E01, -1.00000E-01]	6.82E-01	5.51E+01
	Insulated	5.53E+02 [5.37333E+02, 5.69630E+02]	- -	-1.54E-02 [-1.61486E-02, -1.46114E-02]	- -	5.67E-03 [5.27510E-03, 6.05644E-03]	-1.00E01 [-1.00000E01, -1.00000E-01]	6.82E-01	5.51E+01
H03	Uninsulated	4.86E+02 [4.60267E+02, 5.12592E+02]	- -	-4.56E-02 [-4.81161E-02, -4.30792E-02]	5.49E-03 [-5.74397E-02, 6.84217E-02]	1.83E-02 [1.69342E-02, 1.96174E-02]	-1.00E01 [-1.00000E01, -1.00000E01]	8.15E-01	3.04E+01
	Insulated	4.96E+02 [4.82839E+02, 5.09046E+02]	- -	-4.77E-02 [-5.01081E-02, -4.53372E-02]	- -	1.93E-02 [1.81822E-02, 2.05147E-02]	-1.00E01 [-1.00000E01, -1.00000E01]	8.17E-01	3.04E+01
H04	Uninsulated AAC	235.6979413 [2.28301E+02, 2.43095E+02]	-0.708740031 [-8.08158E-01, -6.09322E-01]	-0.011665604 [-1.24165E-02, -1.09147E-02]	1.908574941 [1.70559E+00, 2.11156E+00]	0.001770456 [1.12677E-03, 2.41414E-03]	-1.00E01 [-1.00000E01, -1.00000E01]	0.862783089	24.88283468
	Insulated AAC	2.36E+02 [2.28301E+02, 2.43095E+02]	-7.09E-01 [-8.08158E-01, -6.09322E-01]	-1.17E-02 [-1.24165E-02, -1.09147E-02]	1.91E+00 [1.70559E+00, 2.11156E+00]	1.77E-03 [1.12677E-03, 2.41414E-03]	-1.00E01 [-1.00000E01, -1.00000E01]	8.63E-01	2.28E+01
H05	Pre19299InchSolidBrick	1.03E+03 [9.85815E+02, 1.07299E+03]	- -	-8.48E-02 [-8.88304E-02, -8.08461E-02]	-5.86E-01 [-6.24482E-01, -5.46766E-01]	3.97E-02 [3.76740E-02, 4.16915E-02]	-1.00E01 [-1.00000E01, -1.00000E01]	8.42E-01	3.41E+01
H06	Uninsulated	2.12E+02 [2.05457E+02, 2.18923E+02]	- -	-2.16E-02 [-2.22929E-02, -2.08146E-02]	1.48E+00 [1.31754E+00, 1.64022E+00]	5.76E-03 [5.26836E-03, 6.24275E-03]	-1.00E01 [-1.00000E01, -1.00000E01]	9.26E-01	1.84E+01
	Insulated	2.19E+02 [2.11647E+02, 2.26233E+02]	- -	-2.09E-02 [-2.16081E-02, -2.02680E-02]	1.36E+00 [1.20617E+00, 1.50776E+00]	5.65E-03 [5.17013E-03, 6.13479E-03]	-1.00E01 [-1.00000E01, -1.00000E01]	9.29E-01	1.79E+01
H07	Uninsulated AAC	2.28E+02 [2.21268E+02, 2.34324E+02]	- -	-8.84E-03 [-9.03028E-03, -8.64221E-03]	1.26E+00 [1.12276E+00, 1.39422E+00]	1.36E-03 [9.84067E-04, 1.72999E-03]	-1.00E01 [-1.00000E01, -1.00000E01]	9.41E-01	1.48E+01
	Insulated AAC	2.28E+02 [2.21268E+02, 2.34324E+02]	- -	-8.84E-03 [-9.03028E-03, -8.64221E-03]	1.26E+00 [1.12276E+00, 1.39422E+00]	1.36E-03 [9.84067E-04, 1.72999E-03]	-1.00E01 [-1.00000E01, -1.00000E01]	9.41E-01	1.48E+01
H08	Pre19299InchSolidBrick	1.84E+02 [1.76796E+02, 1.91333E+02]	- -	-2.09E-02 [-2.30769E-02, -1.87018E-02]	2.77E+00 [2.43220E+00, 3.10891E+00]	- -	-1.00E01 [-1.00000E01, -1.00000E01]	6.58E-01	4.79E+01
H09	Uninsulated	4.36E+02 [4.16251E+02, 4.56082E+02]	- -	-4.83E-02 [-4.99683E-02, -4.65895E-02]	3.87E-01 [3.20586E-01, 4.52910E-01]	2.00E-02 [1.90338E-02, 2.08764E-02]	-1.00E01 [-1.00000E01, -1.00000E01]	9.38E-01	2.03E+01
	Insulated	4.36E+02 [4.16251E+02, 4.56082E+02]	- -	-4.83E-02 [-4.99683E-02, -4.65895E-02]	3.87E-01 [3.20586E-01, 4.52910E-01]	2.00E-02 [1.90338E-02, 2.08764E-02]	-1.00E01 [-1.00000E01, -1.00000E01]	9.38E-01	2.03E+01
H10	Uninsulated AAC	5.52E+02 [5.36374E+02, 5.67614E+02]	- -	-3.67E-02 [-3.86760E-02, -3.47958E-02]	- -	1.52E-02 [1.42804E-02, 1.61718E-02]	-1.00E01 [-1.00000E01, -1.00000E01]	7.81E-01	4.12E+01
	Insulated AAC	5.75E+02 [5.58802E+02, 5.90258E+02]	- -	-3.74E-02 [-3.92990E-02, -3.54775E-02]	- -	1.54E-02 [1.44566E-02, 1.63203E-02]	-1.00E01 [-1.00000E01, -1.00000E01]	7.91E-01	4.09E+01
H11	Uninsulated AAC	2.26E+02 [2.20024E+02, 2.31719E+02]	-4.64E-01 [-5.51212E-01, -3.77108E-01]	-1.00E-02 [-1.06473E-02, -9.34391E-03]	2.31E+00 [2.16960E+00, 2.44529E+00]	0.00E+00 [0.00000E+00, 0.00000E+00]	-1.00E01 [-1.00000E01, -1.00000E01]	8.47E-01	3.05E+01
	Insulated AAC	2.26E+02 [2.20024E+02, 2.31719E+02]	-4.64E-01 [-5.51212E-01, -3.77108E-01]	-1.00E-02 [-1.06473E-02, -9.34391E-03]	2.31E+00 [2.16960E+00, 2.44529E+00]	0.00E+00 [0.00000E+00, 0.00000E+00]	-1.00E01 [-1.00000E01, -1.00000E01]	8.47E-01	3.05E+01
H12	9InchSolidBrick	2.31E+02 [2.25049E+02, 2.37319E+02]	3.07E-01 [1.65250E-01, 4.49624E-01]	-4.42E-02 [-4.72431E-02, -4.11184E-02]	1.83E+00 [1.59924E+00, 2.06180E+00]	1.59E-02 [1.45159E-02, 1.73662E-02]	-1.00E01 [-1.00000E01, -1.00000E01]	9.24E-01	2.29E+01
H14	Uninsulated	5.53E+02 [5.37333E+02, 5.69630E+02]	- -	-1.54E-02 [-1.61486E-02, -1.46114E-02]	- -	5.67E-03 [5.27510E-03, 6.05644E-03]	-1.00E-01 [-1.00000E01, -1.00000E01]	6.82E-01	5.51E+01
	Insulated	4.86E+02 [4.60267E+02, 5.12592E+02]	- -	-4.56E-02 [-4.81161E-02, -4.30792E-02]	5.49E-03 [-5.74397E-02, 6.84217E-02]	1.83E-02 [1.69342E-02, 1.96174E-02]	-1.00E01 [-1.00000E01, -1.00000E01]	8.15E-01	3.04E+01
H15	Uninsulated AAC	2.24E+02 [2.16270E+02, 2.31013E+02]	-1.16E+00 [-1.24942E+00, -1.07116E+00]	-1.27E-02 [-1.35738E-02, -1.17681E-02]	2.28E+00 [2.13762E+00, 2.42179E+00]	0.00E+00 -	-1.00E01 [-1.00000E01, -1.00000E01]	9.22E-01	2.67E+01
	Insulated AAC	2.29E+02 [2.22487E+02, 2.35030E+02]	2.84E-02 [-1.06592E-01, 1.63485E-01]	-4.15E-02 [-4.44099E-02, -3.85869E-02]	1.88E+00 [1.64150E+00, 2.11499E+00]	- [1.37954E-02, 1.65473E-02]	-1.00E01 [-1.00000E01, -1.00000E01]	8.65E-01	2.20E+01

Table J.3: *S. chartarum* - Winter

Dwelling	Wall	Summer							
		a	b	c	d	f	g	r-square	RMSE
H01	Pre19299InchSolidBrick	2.25E+02 [2.12984E+02, 2.36756E+02]	-1.51E+00 [-1.66648E+00, -1.34998E+00]	-1.12E-02 [-1.24738E-02, -9.83886E-03]	2.45E+00 [2.20995E+00, 2.68659E+00]	- -	-1.00E01 [-1.00000E01, -1.00000E01]	7.25E-01	4.41E+01
H02	Uninsulated	6.26E+02 [6.04941E+02, 6.47054E+02]	- -	-2.70E-02 [-2.86641E-02, -2.53888E-02]	0.00E+00 [0.00000E+00, 0.00000E+00]	1.04E-02 [1.54309E-02, 1.77990E-02]	-1.00E-01 [-1.00000E01, -1.00000E-01]	6.66E-01	5.94E+01
	Insulated	6.26E+02 [6.04941E+02, 6.47054E+02]	- -	-2.70E-02 [-2.86641E-02, -2.53888E-02]	0.00E+00 [0.00000E+00, 0.00000E+00]	1.04E-02 [1.54309E-02, 1.77990E-02]	-1.00E01 [-1.00000E01, -1.00000E-01]	6.66E-01	5.94E+01
H03	Uninsulated	2.59E+02 [2.50818E+02, 2.68160E+02]	- -	-5.03E-02 [-5.17045E-02, -4.89910E-02]	5.47E-01 [4.90763E-01, 6.02314E-01]	1.72E-02 [1.64063E-02, 1.80258E-02]	-1.00E01 [-1.00000E01, -1.00000E01]	9.61E-01	8.77E+00
	Insulated	2.59E+02 [2.50818E+02, 2.68160E+02]	- -	-5.03E-02 [-5.17045E-02, -4.89910E-02]	5.47E-01 [4.90763E-01, 6.02314E-01]	1.72E-02 [1.64063E-02, 1.80258E-02]	-1.00E01 [-1.00000E01, -1.00000E01]	9.61E-01	8.77E+00
H04	Uninsulated AAC	205.3951251 [1.99075E+02, 2.11716E+02]	-0.886470051 [-9.72455E-01, -8.00485E-01]	-0.010917457 [-1.16479E-02, -1.01870E-02]	2.151372504 [2.02663E+00, 2.27611E+00]	- -	-1.00E01 [-1.00000E01, -1.00000E01]	0.862783089	24.88283468
	Insulated AAC	2.05E+02 [2.77319E+02, 3.03720E+02]	-8.86E-01 [-1.95934E+00, -1.60791E+00]	-1.09E-02 [-2.48299E-02, -2.30500E-02]	2.15E+00 [4.07443E-01, 5.81428E-01]	0.00E+00 [9.12956E-03, 1.02120E-02]	-1.00E01 [-1.00000E01, -1.00000E01]	8.63E-01	2.28E+01
H05	Pre19299InchSolidBrick	1.22E+02 [1.19080E+02, 1.24617E+02]	-1.97E+00 [-2.06212E+00, -1.88349E+00]	-1.03E-02 [-1.09796E-02, -9.61798E-03]	2.96E+00 [2.81575E+00, 3.09485E+00]	- -	-1.00E01 [-1.00000E01, -1.00000E01]	6.21E-01	3.66E+01
H06	Uninsulated	3.09E+02 [2.96574E+02, 3.21636E+02]	- -	-3.45E-02 [-3.57491E-02, -3.31766E-02]	2.96E-01 [2.35865E-01, 3.55932E-01]	1.45E-02 [1.37934E-02, 1.51978E-02]	-1.00E01 [-1.00000E01, -1.00000E01]	9.21E-01	1.73E+01
	Insulated	3.21E+02 [3.08477E+02, 3.33740E+02]	- -	-3.54E-02 [-3.66703E-02, -3.40654E-02]	2.47E-01 [1.91608E-01, 3.03019E-01]	1.50E-02 [1.43278E-02, 1.57357E-02]	-1.00E01 [-1.00000E01, -1.00000E01]	9.22E-01	1.72E+01
H07	Uninsulated AAC	2.43E+02 [2.33285E+02, 2.53264E+02]	- -	-1.24E-02 [-1.27943E-02, -1.20777E-02]	8.10E-01 [6.94497E-01, 9.25396E-01]	3.56E-03 [3.16358E-03, 3.95041E-03]	-1.00E01 [-1.00000E01, -1.00000E01]	9.17E-01	1.73E+01
	Insulated AAC	2.43E+02 [2.33285E+02, 2.53264E+02]	- -	-1.24E-02 [-1.27943E-02, -1.20777E-02]	8.10E-01 [6.94497E-01, 9.25396E-01]	3.56E-03 [3.16358E-03, 3.95041E-03]	-1.00E01 [-1.00000E01, -1.00000E01]	9.17E-01	1.73E+01
H08	Pre19299InchSolidBrick	2.11E+02 [2.06776E+02, 2.15867E+02]	-2.63E+00 [-2.68409E+00, -2.58304E+00]	-1.03E-02 [-1.07452E-02, -9.92619E-03]	2.46E+00 [2.40087E+00, 2.52910E+00]	- -	-1.00E01 [-1.00000E01, -1.00000E01]	6.39E-01	4.64E+01
H09	Uninsulated	1.07E+03 [1.02570E+03, 1.11601E+03]	- -	-9.97E-02 [-1.04159E-01, -9.51672E-02]	-3.48E-01 [-3.85904E-01, -3.09667E-01]	4.65E-02 [4.42259E-02, 4.87567E-02]	-1.00E01 [-1.00000E01, -1.00000E01]	8.92E-01	3.43E+01
	Insulated	6.82E+06 [2.51870E+02, 2.62303E+02]	-9.00E-01 [-1.03354E+00, -7.66161E-01]	-4.13E-02 [-4.68146E-02, -3.57426E-02]	4.00E+00 [3.72671E+00, 4.27275E+00]	-7.97E-02 [-8.74917E-02, -7.20001E-02]	-1.00E01 [-1.00000E01, -1.00000E01]	9.52E-01	1.13E+01
H10	Uninsulated AAC	3.31E+02 [3.19425E+02, 3.43008E+02]	- -	-3.75E-02 [-3.85830E-02, -3.64073E-02]	3.62E-01 [3.09798E-01, 4.13529E-01]	1.46E-02 [1.39766E-02, 1.52008E-02]	-1.00E01 [-1.00000E01, -1.00000E01]	9.50E-01	1.36E+01
	Insulated AAC	3.31E+02 [3.19425E+02, 3.43008E+02]	- -	-3.75E-02 [-3.85830E-02, -3.64073E-02]	3.62E-01 [3.09798E-01, 4.13529E-01]	1.46E-02 [1.39766E-02, 1.52008E-02]	-1.00E01 [-1.00000E01, -1.00000E01]	9.50E-01	1.36E+01
H11	Uninsulated AAC	2.16E+02 [2.11585E+02, 2.19673E+02]	-1.25E+00 [-1.33208E+00, -1.16514E+00]	-1.17E-02 [-1.24677E-02, -1.09579E-02]	3.23E+00 [3.06212E+00, 3.40778E+00]	- -	-1.00E01 [-1.00000E01, -1.00000E01]	8.99E-01	2.48E+01
	Insulated AAC	2.16E+02 [2.11585E+02, 2.19673E+02]	-1.25E+00 [-1.33208E+00, -1.16514E+00]	-1.17E-02 [-1.24677E-02, -1.09579E-02]	3.23E+00 [3.06212E+00, 3.40778E+00]	- -	-1.00E01 [-1.00000E01, -1.00000E01]	8.99E-01	2.48E+01
H12	9InchSolidBrick	4.29E+02 [4.13108E+02, 4.44291E+02]	- -	-5.57E-02 [-5.76592E-02, -5.36607E-02]	1.12E-01 [6.79828E-02, 1.56093E-01]	2.56E-02 [2.45800E-02, 2.66414E-02]	-1.00E01 [-1.00000E01, -1.00000E01]	9.48E-01	1.73E+01
H14	Uninsulated	6.26E+02 [6.04941E+02, 6.47054E+02]	- -	-2.70E-02 [-2.86641E-02, -2.53888E-02]	0.00E+00 [0.00000E+00, 0.00000E+00]	1.04E-02 [1.54309E-02, 1.77990E-02]	-1.00E-01 [-1.00000E01, -1.00000E01]	6.66E-01	5.94E+01
	Insulated	2.59E+02 [2.50818E+02, 2.68160E+02]	- -	-5.03E-02 [-5.17045E-02, -4.89910E-02]	5.47E-01 [4.90763E-01, 6.02314E-01]	1.72E-02 [1.64063E-02, 1.80258E-02]	-1.00E01 [-1.00000E01, -1.00000E01]	9.61E-01	8.77E+00
H15	Uninsulated AAC	2.49E+02 [2.37284E+02, 2.61473E+02]	- -	-4.68E-02 [-4.85671E-02, -4.50517E-02]	9.81E-01 [8.27516E-01, 1.13498E+00]	1.99E-02 [1.89904E-02, 2.08627E-02]	-1.00E01 [-1.00000E01, -1.00000E01]	9.46E-01	1.72E+01
	Insulated AAC	2.49E+02 [2.37284E+02, 2.61473E+02]	- -	-4.68E-02 [-4.85671E-02, -4.50517E-02]	9.81E-01 [8.27516E-01, 1.13498E+00]	1.99E-02 [1.89904E-02, 2.08627E-02]	-1.00E01 [-1.00000E01, -1.00000E01]	9.46E-01	1.72E+01

Table J.4: *S. chartarum* - Summer

Appendix K

Vulnerable Locations in London

Figure K.1:

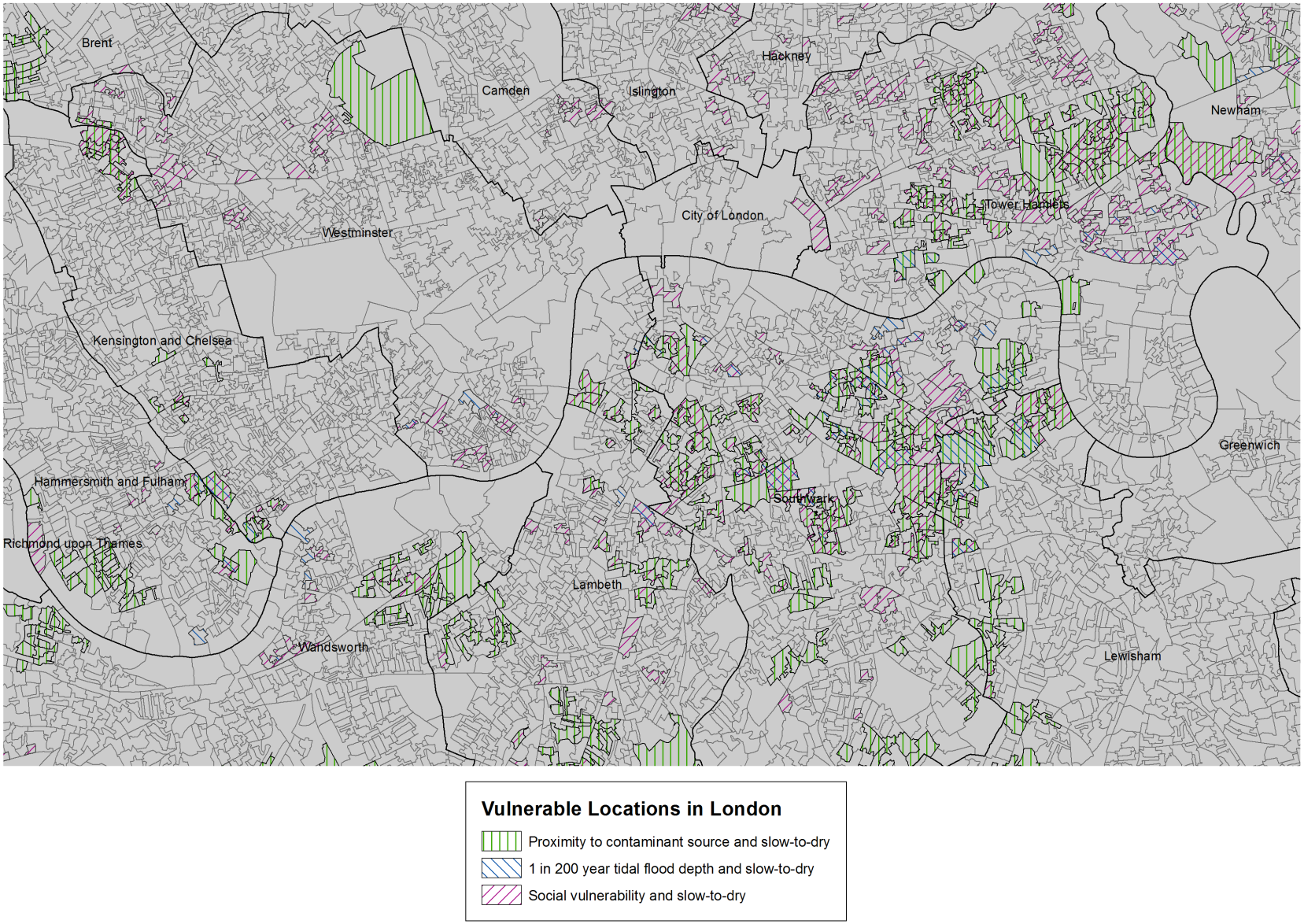
Brent
Camden
Islington
Hackney
Newham
City of London
Tower Hamlets
Westminster
Kensington and Chelsea
Greenwich
Hammersmith and Fulham
Southwark
Richmond upon Thames
Lambeth
Wandsworth
Lewisham
Vulnerable Locations in London
Proximity to contaminant source and slow-to-dry
1 in 200 year tidal flood depth and slow-to-dry
Social vulnerability and slow-to-dry